Analysis of SEDS proteins and their cognate PBPs in Streptomyces coelicolor.

Mistry, Bhavesh V

Analysis of SEDS proteins and their cognate PBPs in *Streptomyces coelicolor*

by

BHAVESH V. MISTRY

A thesis submitted to the School of Medicine, Swansea University in candidature of the degree of Doctor of Philosophy

Swansea University
Prifysgol Abertawe

Institute of Life Sciences, School of Medicine
Swansea University
September 2008

न हि ज्ञानेन सदृशम् पवित्रमिह विद्यते।
तत्स्वयं योगसंसिद्धिः कालेनात्मनि विन्दति॥
— भगवद्गीता ४-३८

"On earth, there is no purifier as great as knowledge;
He who has attained purity of heart through a prolonged practice of karmayoga automatically sees the light of truth in the self in course of time."
— bhagavadgītā 4-38

नरस्य आभरणं रूपं रूपस्य आभरणं गुणः।
गुणस्य आभरणं ज्ञानं ज्ञानस्य आभरणं क्षमा॥

The ornament of man is beauty, the ornament of beauty is guṇās (~good qualitites).
Knowledge adorns good qualities, and forgiveness is the ornament of knowledge.

Acknowledgements

Doing research and writing a thesis in a foreign country are the processes that require not only hard work but a lot of support from family, supervisor, colleagues and friends. Therefore, I would like to express my deepest gratitude to all those who helped me and contributed directly or indirectly to the accomplishment of this research.

Words are not enough to express my thanks and deepest gratitude to my respected supervisor, ***Prof. Paul J. Dyson*** *for providing me such a great opportunity to work on this project as a part of his research group and supporting me in every ways to complete this research successfully. Without his help this work would not have been possible. I am very appreciative of him being patient and generous with his precious time and valuable advice. I have been very fortunate to have such a kind, supportive and generous supervisor. I am most thankful to* ***Dr. Ricardo Del Sol*** *for teaching me molecular biology and always being there to solve difficulties, to discuss findings and achievements. His great research experience, thorough knowledge, encouragement and enthusiasm gave me a confidence and courage to carry out successful research. I will never forget what you have done make this work successful. I would also like to thank* ***Mr. Meirwyn Evans*** *and* ***Mrs. Sue Fielding*** *for their valuable help. I wish to thank all my present and previous lab-mates,* ***Lorena, Lindsay, Simon, Matt, Paola, Sandra, Greg, Amy*** *and* ***Abbas*** *for being friendly and making a homely and creative environment in the lab. I would also like to thank* ***Mrs. Eileen Waters*** *for allowing me to use her printer to print this thesis. It has been a great honour and a pleasure working with* ***Prof. Paul J. Dyson*** *and his research group.*

I also like to thank all my friends in Swansea for creating homely and sociable environment. My special thanks to the members of ***MSU Microbiotech alumni*** *for providing some of the valuable references.*

Last but not least, I would like to thank ***School of Medicine, Swansea University,*** *for providing excellent facilities and a great academic environment for research.*

I would like to dedicate this thesis to my parents, ***Vishnubhai P. Mistry*** *and* ***Kailashben V. Mistry,*** *my uncle,* ***Dr. Kishor P. Mistry*** *and my aunt,* ***Dr. Varsha Shah*** *because without their support and love I would have never accomplished this work. I am most grateful to my uncle,* ***Dr. Kishor P. Mistry,*** *for his financial support without which it was impossible to come to UK and pursue my academic career.*

This study was supported by grants from the European Commission and the BBSRC.

- Bhavesh V. Mistry

Abstract

The *rodA* and *ftsW* genes encode polytopic membrane proteins that are essential for bacterial cell elongation and division, respectively. These genes are highly conserved among bacteria with a peptidoglycan cell wall and belong to the SEDS ("shape, elongation, division, and sporulation") gene family. Each SEDS gene is invariably linked with a cognate class B high-molecular weight penicillin-binding protein (HMW PBP) gene. Four such pairs of genes are found in the genome of filamentous differentiating *Streptomyces coelicolor*. This study focused on characterization of four SEDS genes [*SCO2085 (ftsW), SCO2607 (sfr), SCO3846 (rodA)* and *SCO5302 (rodA2)*] and *SCO2090 (ftsI)* and *SCO2608 (pbp2)* [cognate HMW PBP genes of *ftsW* and *sfr*, respectively]. Computational analysis of each SEDS gene locus revealed that each gene is a part of specific gene cluster. Construction of disruption mutants of each SEDS gene revealed that *ftsW, sfr* and *rodA2* are dispensable for growth and survival of *S. coelioclor*, whereas *rodA* is essential. Mutation of *sfr* or *rodA2* did not cause gross changes to growth and septation of the organism. However, the mutation in *sfr* made the spores susceptible to heat, SDS and cell wall specific antibiotics. Similar effects were observed in the *pbp2* (cognate HMW PBP gene of *sfr*) disrupted mutant. The susceptibility of the spores of *sfr* and *pbp2* mutants to such a physical and chemical stress implies an important role of these genes in spore wall synthesis. Disruption of either *ftsW* or the cognate *ftsI* gene blocked the formation of sporulation septation in aerial hyphae. The inability of spiral polymers of FtsZ to reorganize into rings in aerial hyphae of these mutants indicates an early pivotal role of an FtsW-FtsI complex in cell division. Mutants of *ftsQ* were also unable to sporulate and the cytological analysis of this mutant showed that it was blocked at a later stage in cell division, during septum closure. Analysis of FtsZ distribution in *ftsQ* mutant aerial hyphae revealed that concerted assembly of the complete divisome was not required for Z ring stabilization in this mutant. Complete cross-wall formation in the vegetative hyphae of all three *fts* mutants imply that the typical bacterial divisome functions specifically during non-essential sporulation septation. Thus, it provides a unique opportunity to investigate the function and dependencies of individual components of the divisome *in vivo*.

ABBREVIATIONS

A	Adenine
ADP	Adenosine Diphosphate
AFM	Atomic Force Microscopy
ATP	Adenosine Triphosphate
bp	Base pair(s)
C	Cytosine
CIAP	Calf Intestinal Alkaline Phosphatase
DMSO	Dimethyl sulfoxide
DNA	Deoxyribose nucleic acid
dNTP	Deoxynucleoside Triphosphate
EDTA	Ethylene Diamine Tetraacetic acid
EGFP	Enhanced Green Fluorescent Protein
g	Gram(s)
G	Guanine
h	Hour(s)
HMW	High Molecular Weight
IPTG	Isopropyl-*β-D*-thiogalactoside
Kbp	Kilobase pair(s)
kDa	Kilodalton(s)
L or l	Litre
Mb	Megabase(s)
MIC	Minimum Inhibitory Concentration
min	Minute(s)
MW	Molecular weight
μ	Micro
ORF	Open Reading Frame

PCR	Polymerase Chain Reaction
PBP(s)	Penicillin Binding Protein(s)
rpm	Revolutions per minute
s	Second(s)
SDS	Sodium Dodecyl Sulphate
SEDS	Shape, Elongation, Division and Sporulation
T	Thymine
TBE	Tris Borate EDTA
TEM	Transmission Electron Microscopy
TES	*N*-tris(hydroxymethyl)-*2*-aminoethanesulphonic acid
TMH	Transmembrane Helix
Tris	Tris(hydroxymethyl)amino-methane
UV	Ultraviolet light
V	Volt(s)
W	Watt(s)
X-gal	5-bromo-4-chloro-3-indolyl-β-*D*-galactoside

CONTENTS

Chapter - 1

Introduction

Streptomyces coelicolor is a representative of gram-positive, soil-dwelling, filamentous streptomycetes that are responsible for producing a vast variety of secondary metabolites including a number of medicinally important antibiotics. It exhibits a complex multicellular life cycle with morphologically and physiologically differentiated vegetative mycelium and spore forming aerial hyphae. Both morphological and physiological processes are tightly regulated spatially and temporally during the developmental cycle. One of the interesting features of *S. coelicolor* is the drastic changes that occur in growth and cell division during the developmental cycle. The availability of complete genome sequences of several *Streptomyces* spp., including *S. coelicolor,* has had an important impact on understanding the developmental aspects of *Streptomyces*.

In rod-shaped unicellular bacteria, such as *Escherichia coli, Bacillus subtilis* and *Mycobacterium tuberculosis*, cell elongation and division processes involve a highly organized and dynamic assembly of different regulatory and structural proteins (eg. FtsZ, PBPs, MreB, FtsW and RodA), many of which are highly conserved among bacteria. During cell elongation in rod shaped bacteria, new cell wall material is intercalated in the lateral wall [an exception is *M. tuberculosis* and other actinomycetes where new cell wall synthesis occurs at the poles (Hett and Rubin, 2008; Letek *et al.*, 2008)]. Cell division in rod-shaped bacteria occurs by binary fission, where the parental cell divides into two daughter cells by the formation of a division septum in the middle of the cell. The first stage of cell division is the assembly of the tubulin-like protein FtsZ in a ring like structure at the division site. In subsequent steps several membrane-associated proteins localize to form a divisome complex which mediates the septum formation. Assembly of the Z ring is controlled by several negative and positive regulators. The division process is tightly coordinated with chromosomal replication.

Unlike unicellular bacteria, multicellular filamentous *Streptomyces* display two types of cell division: vegetative septa produced by occasional cross-wall formation in vegetative mycelium and regularly spaced synchronous multiple sporulation septa in aerial hyphae. This chapter provides a general description of *Streptomyces* biology with emphasis on the *S. coelicolor* developmental cycle and also explains all the aspects of cell division in rod shaped bacteria in relation to growth and development in *Streptomyces.*

1.1 General Features and Systematics of *Streptomyces*

1.1.1 *Actinobacteria*

Streptomyces belongs to a class *Actinobacteria* that represents a large group of gram-positive bacteria with a high guanine plus cytosine (G+C) contents in their genomes within the domain *Bacteria* (Stackebrandt *et al.*, 1997). The G+C base composition of their chromosome ranges from 51 mol% in some *Corynebacteria* to more than 70 mol% in streptomycetes. An exception to this is the DNA of an obligate pathogen *Tropheryma whipplei*, with less than 50 mol% G+C content. *Actinobacteria* exhibit diverse morphologies, from simple coccoid (e.g. *Micrococcus*) to complex, multicellular, highly differentiated mycelium (e.g. *Streptomyces*). The habitats of *Actinobacteria* are exceedingly varied and include pathogens like *Mycobacterium tuberculosis, Mycobacterium leprae* and *Corynebacterium diphtherae*; soil bacteria such as *Streptomyces* spp. and marine inhabitants like *Salinispora* spp. (Ventura *et al.*, 2007). This class also includes physiologically and metabolically diverse bacteria producing varieties of extracellular enzymes and secondary metabolites (Sanglier *et al.*, 1993a; Sanglier *et al.*, 1993b).

Early classification of *Actinobacteria* was based on morphological, biochemical and physiological characteristics of an organism (Embley and Stackebrandt, 1994). However, the rich diversities of their characteristics have made actinomycete classification vulnerable to frequent changes and created confusions in the study of their evolution. In recent years the classification systems have changed fundamentally by incorporation of molecular biological characteristics in prokaryotic systematics (Fox *et al.*, 1977). The classification system of actinomycetes, based on 16S rRNA gene sequence analysis has placed the organisms in the framework of phylogenetic relationships that provided basis for classification and also allowed the investigation of evolution of actinomycetes. The 16S rRNA gene sequence comparison has shown the presence of 35 families and 130 genera in the class *Actinobacteria* (Fig. 1.1) (Ventura *et al.*, 2007). The deepest and most ancient branch within *Actinobacteria* is bifidobacteria. The divergence of actinomycetes from other bacteria is so ancient that it is difficult to identify phylogenetically the closest ancestor of *Actinobacteria* with confidence by 16S rRNA gene sequence analysis (Embley and Stackebrandt, 1994).

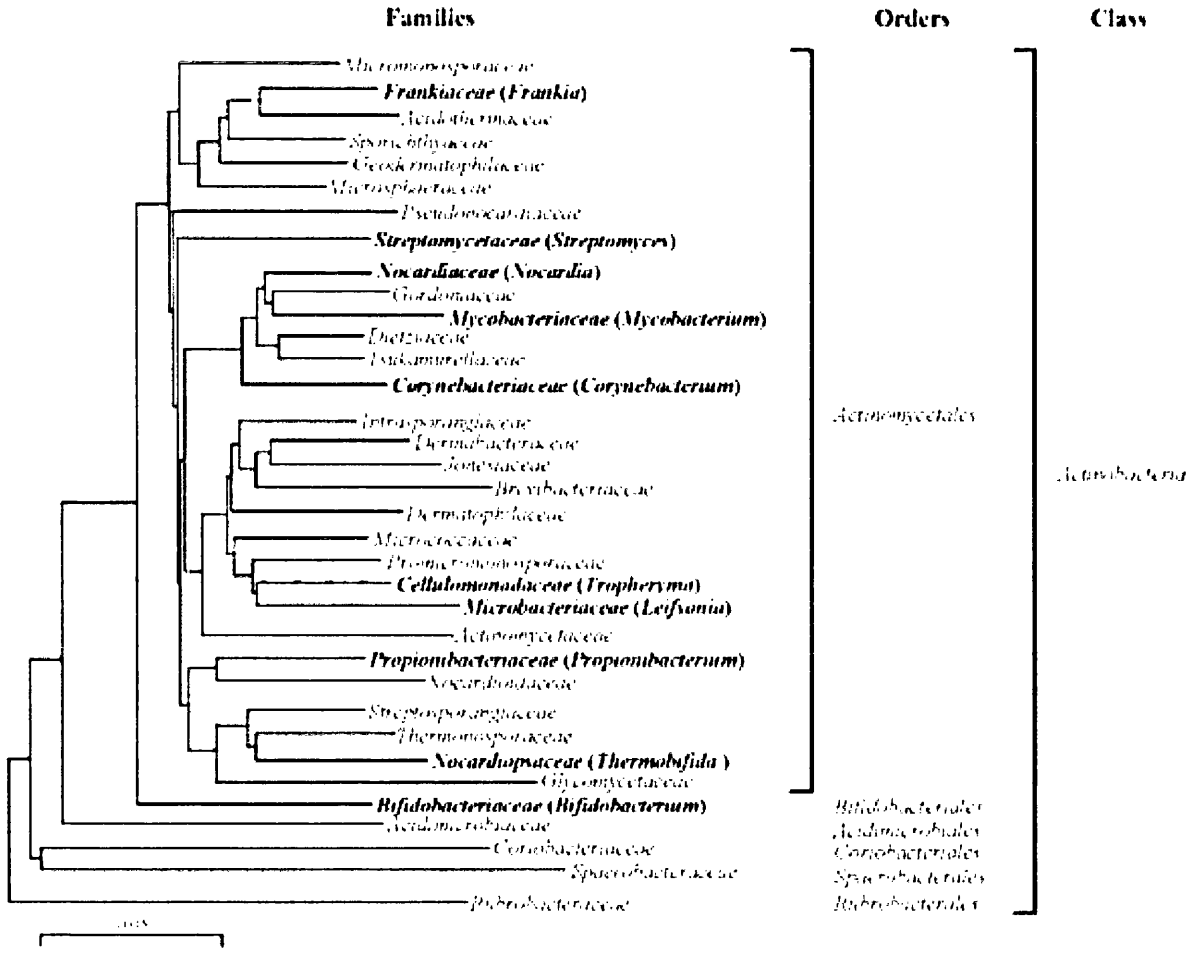

Figure 1.1: Phylogenetic tree of *Actinobacteria* showing the presence of six orders and 35 families based upon 16S rRNA gene sequence comparison. Families containing members subjected to complete genome sequencing at the time of writing are presented in bold letters. The scale bar represents 5 nucleotide substitutions per 100 nucleotides (Ventura *et al.*, 2007).

1.1.2 *Streptomyces*

Waksman and Henrici (1943) coined the name of the genus "*Streptomyces*" (twisted- or chain-like fungus). On the basis of morphology and cell wall chemotype the genus is classified within the family *Streptomycetaceae* (Fig.1.1), which includes bacteria that exhibit a mycelial, spore-forming habit (Embley and Stackebrandt, 1994). Over 500 species are described within the genus *Streptomyces* by Bergey's Manual. In the past streptomycetes were classified as fungi because of the features such as mycelial structure and spore forming aerial hyphae. However, the following characteristics have

firmly placed them under bacterial domain: cell wall composition, sensitivity to anti-bacterial antibiotics and lack of nuclear membrane (Hopwood, 1999). Streptomycete colonies on agar media tend to be tough, leathery in appearance and frequently pigmented (Fig. 1.2) (Frobisher *et al.*, 1974). Unlike unicellular bacteria, streptomycetes grow as distinct clumps or pellets in liquid culture (Brock *et al.*, 1994). Their peptidoglycan cell wall contains LL-diaminopimelic acid (LL-DAP) and glycine (Lechevalier and Lechevalier, 1970). In addition to these traits the acyl type of the muramyl residues in the cell wall peptidoglycans is acetyl (Uchida and Seino, 1997).

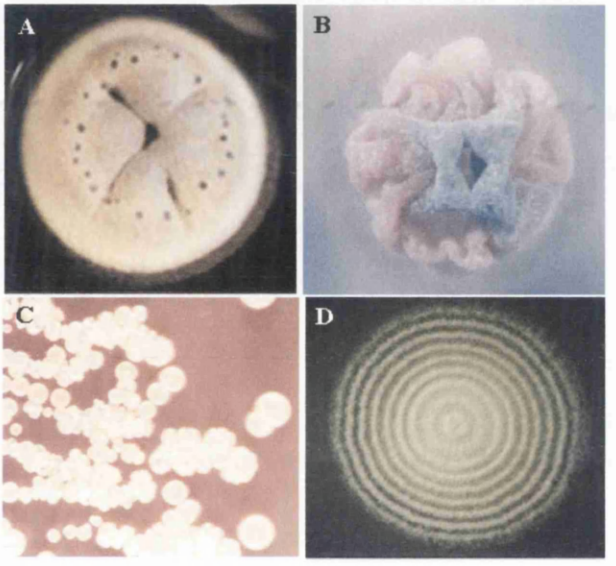

Figure 1.2: Colonies of different *Streptomyces* species. (A) *S. coelicolor* with drops of blue antibiotic actinorhodin. (B) *S. coelicolor* producing blue antibiotic actinorhodin and red antibiotic undecylprodigiosin. (C) *S. griseus* and (D) *S. levoris* colony showing concentric rings of aerial mycelium. Source of Figures: (A) and (D)- diploma thesis (Stockman, 2007), (B)- www.astbury.leeds.ac.uk/gallery/Sco01.JPG, and (C)- http://www.britannica.com/eb/art-96594/Streptomyces-griseus-bacteria.

The genus *Streptomyces* is one of the most extensively investigated groups of bacteria due to their special features. One of the important features is their extreme abundance in soil and capacity to utilize a wide variety of carbon compounds by producing many diverse hydrolytic extracellular enzymes (Kieser *et al.*, 2000). A second striking property of streptomycetes is the extent to which they produce secondary metabolites such as antibiotics and immunosuppresscents. Finally they exhibit developmental complexity during their life cycle (Chater, 1998).

Systematic analysis of *Streptomyces* using different methods revealed that they form a monophyletic clade with considerable diversity (Anderson and Wellington, 2001; Embley and Stackebrandt, 1994). Numerical taxonomic study of *Streptomyces* and related genera using 475 strains and 139 phenotypic characteristics detected 19 major, 40 minor and 18 single strain clusters (Williams *et al.*, 1983). Revision of the numerical classification system using many more strains (over 800) and phenotypic characters (over 300) established similar major clusters (Kampfer *et al.*, 1991). Sequence analysis of 16S rRNA genes also maintained major cluster groups as defined by Williams *et al.* (Anderson and Wellington, 2001). One of the most studied organism of this genus, *Streptomyces coelicolor*, was classified under major cluster 1A and minor group 21 by both genotypic and phenotypic analysis (Anderson and Wellington, 2001; Kataoka *et al.*, 1997; Williams *et al.*, 1983).

1.2 Ecology of *Streptomyces*

Streptomycetes are numerous and widely distributed in nature. They are primarily soil organisms but also found in a variety of other habitats such as composts, fresh waters and deep-sea deposits (Colquhoun *et al.*, 1998; Colquhoun *et al.*, 2000; Johnston and Cross, 1976; Kieser *et al.*, 2000; Lacey, 1973; Moran *et al.*, 1995). Most *Streptomyces* species are saprophytes and play an important role in soil fertility by degrading a wide range of simple and complex organic materials such as starch, cellulose, hemicellulose, lignin and chitin (McCarthy and Williams, 1992). The characteristic earthy odour of moist soil is due to metabolites called geosmins produced by *Streptomyces* spp. (Gerber and Lechevalier, 1965; Jiang *et al.*, 2006). Alkaline and neutral soils are more favourable for *Streptomyces* development (Alexander, 1997).

Soil is a highly complex and unstable environment. There are constant changes in chemical, physical and biological properties of the soil in space and time. To sustain in such a variable and complex environment, streptomycetes have adapted several strategies. Being non-motile organisms, they undergo rapid proliferation and sporulation cycles to maintain their populations. Another adaptation to overcome such environmental stresses is their ability to secrete different hydrolytic enzymes, which metabolize recalcitrant molecules. Antibiotic production, in coordination with

morphological development also inhibits the growth of other microorganisms and defends their food source (Challis and Hopwood, 2003). Thus, these adaptations make *Streptomyces* one of the most successful competitors in nature.

Although, classically *Streptomyces* species are free-living saprophytes some species are shown to colonize the rhizosphere of plant roots and plant tissues in a symbiotic relationship (Castillo *et al.*, 2002; Tokala *et al.*, 2002). Very few medically important species of *Streptomyces* have been reported. The only human pathogen known is *S. somaliensis*, a causative agent of actinomycetoma. It is a chronic subcutaneous infection, occurs in many parts of world, particularly with tropical or subtropical climate such as Sudan (Fahal and Hassan, 1992; Quintana *et al.*, 2008). Other *Streptomyces* species isolated from humans include *S. violaceoruber, S. griseus, S. rimosus, S. albus* and *S. lavendulae* (McNeil and Brown, 1994). Among the plant pathogens, *S. scabies* and *S. acidiscabies* are well known examples of potato scab disease-causing streptomycetes (Doering-Saad *et al.*, 1992). Another economically important plant disease is sweet potato soil pox (or rot) caused by *S. ipomoea* (Zhang *et al.*, 2003). A few other plant pathogens reported are: *S. parvulus*, *S. sparsogenes* and *S. flavovirens* (Kieser *et al.*, 2000).

1.3 Life cycle of *Streptomyces*

One of the major features of streptomycetes is their complex developmental life cycle. They form highly structured multicellular colonies composed of physiologically distinct cells (Fig. 1.3) (Chater, 1993, 1998). The major stages of the *Streptomyces* life cycle are shown in Figure 1.4. The developmental cycle initiates with spore germination, producing one or two germ tubes under favourable environmental conditions. These germ tubes elongate by apical growth (Daniel and Errington, 2003; Flardh, 2003a, 2003b) and branch repeatedly giving rise to infrequently septated vegetative (substrate) mycelium with multi-genomic compartments. The vegetative mycelium grows attached to its substrate, forming an intricate network of hyphae that penetrates the medium solubilizing organic compounds by the action of extracellular hydrolytic enzymes. Such a densely-packed filamentous growth allows full utilization of all nutrients present in the soil, and also enables the streptomycetes to colonize on solid substrates more efficiently than other non-motile, unicellular microorganisms. As

a colony grows nutrients start depleting from the medium. After two or three days due to nutrient limitation or other environmental stress, specialized branches emerge from the substrate mycelium. These special branches represent the reproductive aerial mycelium that grows vertically, upwards into the air (Chater, 1993, 1998). At the onset

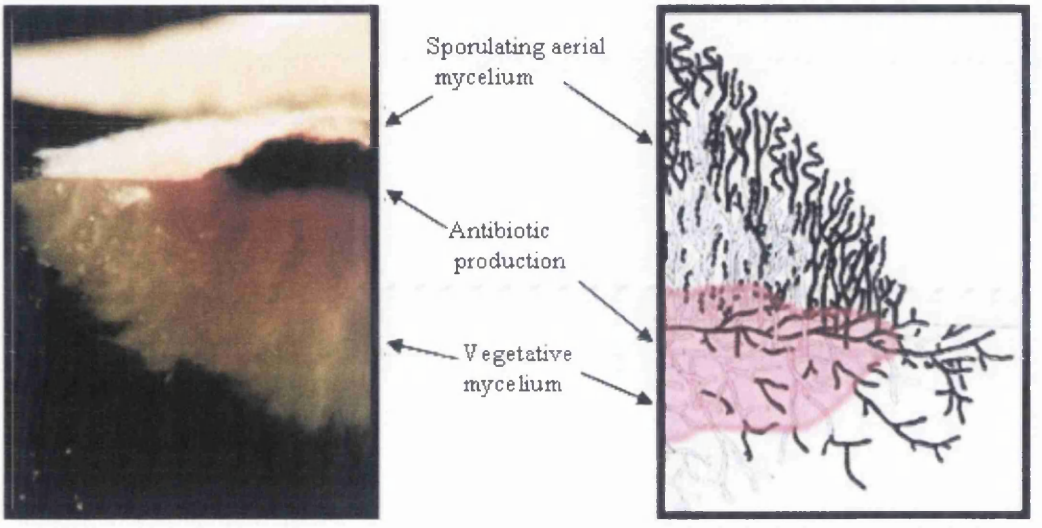

Figure 1.3: Complex multicellular colony of *Streptomyces*. (A) Photograph of vertical sections through a *S. coelicolor* colony growing on agar. (B) Diagrammatic representation of complex architecture of streptomycetes colony. Antibiotic production in the lower part of the colony can protect the nutrients released from dead cells (white) so that they can support aerial growth and sporulation. Living cells are shown as black. (Chater, 2006)

of differentiation, a small hydrophobic surfactant protein (SapB in *S. coelicolor*) secreted from the colony surface allows aerial hyphae to break the surface tension of the aqueous environment and consequently helps them grow into the air (Claessen *et al.*, 2006; Willey *et al.*, 1991). Coordinated with morphological change, a colony also under goes physiological changes like increased production of extracellular enzymes, synthesis of antibiotics and other secondary metabolites (Champness, 1988). Since the

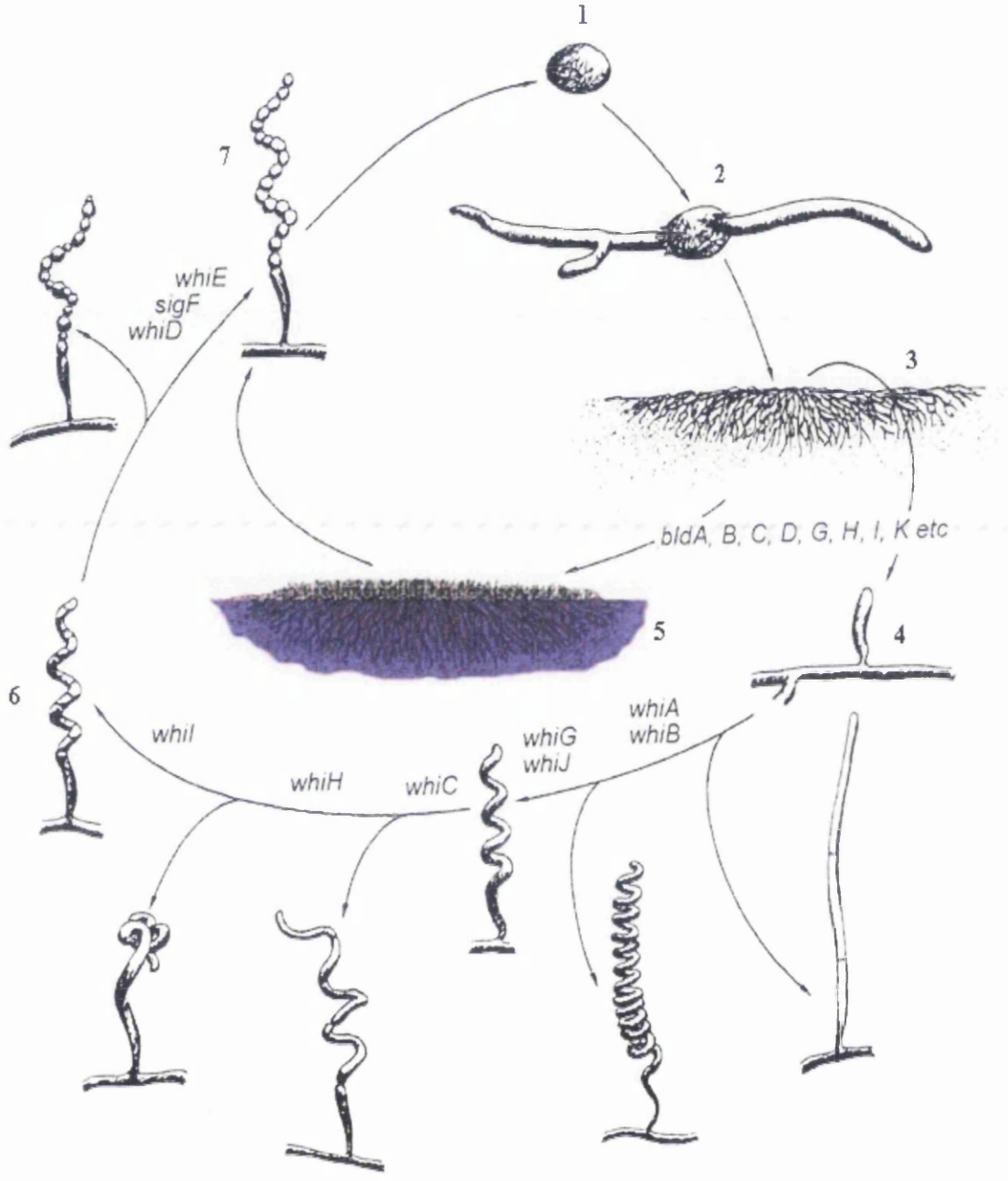

Figure 1.4: Diagrammatic representation of the *Streptomyces* life cycle. Under favourable conditions, a spore (1) germinates (2) and extends into a complex network of vegetative mycelium by apical growth and repeated branching (3). Due to environmental stress, under the regulation of *bld* cascade, reproductive aerial hyphae emerge from the colony surface in coordination with secondary metabolite production (4 and 5). Regulated by *whi* genes, aerial hyphae undergo multiple septation to form chains of unigenomic compartments (6) which, finally, metamorphose in to tick-walled spore chains (7). Side arrows before the genes show the phenotype of respective mutants blocked at different stages during aerial hyphae maturation. (Kieser *et al.*, 2000)

aerial mycelium grows on nutrient-depleted medium, necessary nutrients required for the development of aerial mycelium are provided by degeneration of vegetative mycelium (Mendez *et al.*, 1985; Miguelez *et al.*, 2000; Nicieza *et al.*, 1999). Two types of degenerative events occur during development of *Streptomyces*: (1) autolysis and (2) physiological cell death (Miguelez *et al.*, 1999). Autolytic hyphal death is characterized by early degradation of the cell wall by uncontrolled murein hydrolases. It is usually very rapid and affects few hyphae in the colony. Autolysis results in rupture of plasma membranes and the release of cellular contents to the extracellular medium. Physiological hyphal death occurs in a progressive manner by degradation of intracellular components and takes a longer time. It occurs in most hyphae. In physiological death the integrity of the plasma membrane and cell wall is maintained for a long time and there is little or no leakage of cellular contents to the extracellular medium. This minimizes the risk of adjoining cells being exposed to potentially harmful substances and aids utilization of degraded cellular contents by cells without disturbing the general organization of the colony. Physiologically dead hyphae can also provide mechanical support for aerial hyphae to develop far from the surface of the culture medium. At the vulnerable stage of vegetative hyphal lysis and aerial development, antibiotics are secreted in the medium to protect nutrients from other micro-organisms.

Aerial hyphae development is regulated by a number of *bld* genes (for bald, meaning unable to form aerial hyphae) encoding regulatory proteins (except *bldA* which encodes a tRNA) (Kelemen and Buttner, 1998; Lawlor *et al.*, 1987). Mutants of various *bld* genes show lack of aerial hyphae formation. In addition to a block in differentiation, *bld* mutations prevent antibiotic production, and cause a defect in carbon catabolite repression and in cell-cell signalling (Kelemen and Buttner, 1998). As the maturation of aerial hyphae take place, the apical compartment of individual aerial hyphae forms a spiral syncytium containing multiple copies of the genome. At this stage growth of aerial hyphae stops and they undergo multiple septation which give rise to chains of unigenomic pre-spore compartments. Finally the hyphae bearing pre-spore compartments metamorphose into thick-walled, pigmented spores. Spore formation is controlled by at least eight regulatory genes known as *whi* genes (*whiA,B,D,E,G,J,H,I*), for white aerial mycelial phenotype (Chater and Chandra, 2006; Kieser *et al.*, 2000). The characteristic grey spore pigment of *S. coelicolor* is a polyketide-derived aromatic compound and specified by the *whiE* gene that encodes a polyketide synthase (Kelemen

et al., 1998; Shen *et al.*, 1999). Several changes in cell properties have been observed during reproductive growth. Vegetative mycelium growing in moist substrates have a hydrophilic cell surface, whereas the aerial hyphae and spores are surrounded by a hydrophobic layer (Del Sol *et al.*, 2007; Elliot *et al.*, 2003; Wildermuth *et al.*, 1971). As the aerial hyphae and spores grow in a non-aqueous environment, the hydrophobic sheath protects them from dehydration. Distinct from the substrate mycelium, the aerial hyphae are thicker and usually unbranched. The growth of aerial hyphae, away from the surface, into the air places the spores in a favourable position for easy dispersal by wind, insects or animals, thus solving the problem of population survival raised by the immobility of the vegetative mycelium.

1.4 Physiology of *Streptomyces*

Streptomyces species are considered exceptionally well endowed to cope with physiological changes that occur in soil ecosystems. Nutrient levels and high number of microbial competitors in the soil ecosystems reflect their diverse physiological behaviour. As in other organisms, the complex life cycle of streptomycetes is a result of two major processes; a primary metabolism responsible for growth and viability and secondary metabolism in co-ordination with morphological differentiation to cope with different environmental (physical, chemical and biological) stresses.

1.4.1 Primary Metabolism

The detailed studies of different primary metabolism pathways of *Streptomyces* revealed interesting similarities to and differences from other bacterial systems. The main source of nutrients in the soil is plant derived material therefore it is going to be rich in carbon compounds while poor in nitrogen and phosphate compounds. Due to the variety and richness of carbon compounds in soil, *Streptomyces* have adopted different carbohydrate catabolic pathways like glycerol, galactose, cellulose and chitin catabolism pathways (Hodgson, 2000). For efficient utilization of carbon sources, these carbohydrate catabolic pathways are inducible and often subjected to carbon catabolite repression (CCR) (Angell *et al.*, 1994; Champness, 1988; Kwakman and Postma, 1994).

In contrast to other gram-negative and low G+C gram-positive bacteria where the cAMP-dependent glucose-phosphotransferase system (glucose-PTS) plays a central role in CCR, in *Streptomyces* ATP-dependent glucose kinase (GlkA) plays a key role in CCR (Kieser *et al.*, 2000). The *glkA* mutants of *S. coelicolor* are not able to utilize glucose and are resistant to the non-metabolizable glucose analog 2-deoxyglucose. In these mutants glucose repression of different genes involved in the utilization of alternative carbon sources is relieved (Angell *et al.*, 1994; Kwakman and Postma, 1994). Another example of CCR is the glucose-dependent phenotype of most bald mutants of *S. coelicolor* (Champness, 1988). The *bld* mutants are unable to form aerial hyphae when grown on glucose containing medium but form aerial hyphae when grown on other carbon sources like mannitol. This suggests that they are defective in glucose repression and therefore unable to sense environmental signals necessary for triggering morphological differentiation.

Streptomycetes use glutamate synthase (GS) and glutamate: 2-oxoglutarate transaminase (GOGAT) as main pathways for nitrogen assimilation (Fisher, 1992; Kieser *et al.*, 2000). The GS pathway is energetically more costly because it requires ATP to assimilate ammonia into glutamate, but it operates at low ammonia concentrations (Fisher, 1992). The presence of both GS and GOGAT pathways in *Streptomyces* species explains the nitrogen limiting nature of soil ecosystem.

Most of the amino acid biosynthesis and catabolic pathways are similar to those found in other bacteria. An exception of amino acid catabolism is arginine, which is catabolised via γ-guanidinobutyramide and γ-guannidinobutyrate (Kieser *et al.*, 2000). Synthesis of tyrosine is via arogenate instead of hydroxyphenylpyruvate (Keller *et al.*, 1985). About half of the amino acid catabolic pathways are constitutive and the global carbon and nitrogen catabolite repression is rare. Feed-back inhibition of amino acid biosynthesis pathways is uncommon (Hood *et al.*, 1992; Hu *et al.*, 1999; Kendrick and Wheelis, 1982; Kroening and Kendrick, 1987). Such a constitutive nature of biosynthesis and catabolism of amino acids may be explained by the oligotrophic nature of soil, where chemical, physical and biological changes occur constantly. Thus, the absence of regulatory mechanisms seems to be an adaptation to compete in the soil ecosystem.

1.4.2 Secondary Metabolism

Actinomycetes and in particular *Streptomyces* species are remarkable in producing a variety of novel secondary metabolites, compounds that are secondary to the growth and maintenance of the producing organism, with a wide range of biological activities such as antibacterial agents, antifungal agents, antihelminthic agents, herbicides, antitumor agents, immunosuppressants and enzyme inhibitors (Paradkar *et al.*, 2003; Sanglier *et al.*, 1993a; Sanglier *et al.*, 1993b; Watve *et al.*, 2001). Over 10000 bioactive compounds are produced by various species of actinomycetes, out of which 8700 are antibiotics. The most frequent producers, the *Streptomyces* species produces 7600 bioactive compounds (74% of all actinomycetes), while other actinomycetes produce 2500 bioactive compounds (26% of all actinomycetes) (Berdy, 2005). The capacity of streptomycetes to produce such a large number of secondary metabolites is also explained by analysis of three completely sequenced genomes from the genus *Streptomyces*. The genome sequence of *S. coelicolor, S. avermitilis* and *S. griseus* revealed 23, 30 and 34 gene clusters for biosynthesis of secondary metabolites, respectively (Bentley *et al.*, 2002; Ikeda *et al.*, 2003; Ohnishi *et al.*, 2008).

Unlike primary metabolism, secondary metabolism in streptomycetes is well studied due to their biological and economical importance. Secondary metabolism is tightly regulated and generally coincides with, or slightly precedes, morphological differentiation in *Streptomyces*. The relationship of physiological and morphological differentiation has been well recognized through experimental observations of different mutants affecting developmental (morphological and/or physiological) process(es) in some *Streptomyces* species. Both secondary metabolism and morphological differentiation are triggered by various physiological and environmental stresses (physical, chemical and biological) and regulated by variety of common and pathway specific regulatory genes or substances. The best studied examples of morphological and physiological regulations are *bld* mutants of *S. coelicolor*, which are defective in both antibiotic production and aerial hyphae formation (Chater, 1993; Pope *et al.*, 1996; White and Bibb, 1997).

Another example of pleiotropic regulators of morphological and physiological differentiation is γ-butyrolactones, produced by many *Streptomyces* species (Eritt *et al.*, 1982; Horinouchi and Beppu, 1992a, 1992b; Takano, 2006). The γ-butyrolactones exert

their effects by modulating the repressor activity of γ-butyrolactones-receptor proteins which are repressors of chemical and morphological differentiation. A-factor (2*R*-isocapryloyl-3*R*-hydroxymethyl-4-butanolide) of *S. griseus* is the most characterized γ-butyrolactone and is required for both antibiotic (streptomycin and grixazone) production and morphological differentiation (Horinouchi, 2002). It is produced just before the onset of streptomycin production and disappears before streptomycin is at its maximum level (Bibb, 2005; Horinouchi, 2002). The role of A-factor in regulation of streptomycin production has been largely resolved (Distler *et al.*, 1992; Vujaklija *et al.*, 1991). The A-factor binds to its receptor protein ArpA and releases the latter from the promoter region of the *adpA* gene encoding a transcriptional activator protein (AdpA). AdpA then binds to the promoters of the *strR* gene encoding a pathway-specific transcriptional activator for streptomycin synthesis (Fig. 1.5) and other genes required for morphological and physiological differentiation.

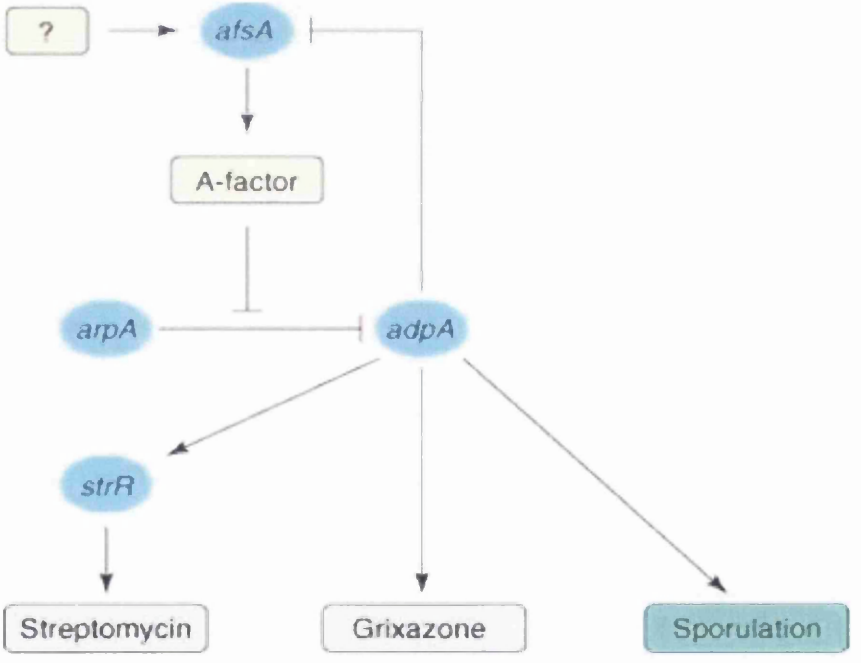

Figure 1.5: The A-factor regulatory cascade of *S. griseus*. Some unknown signal(s) (shown as '?') trigger A-factor synthesis, mediated in some manner by AfsA. At a critical concentration A-factor binds and releases the A-factor receptor protein (ArpA) from the promoter region of transcriptional activator encoding gene *adpA*. AdpA then binds to promoter regions of many genes required for morphological and physiological differentiation. For streptomycin biosynthesis AdpA activates the *strR* gene encoding the pathway-specific transcriptional activator for other streptomycin biosynthesis genes (Bibb, 2005).

In contrast to A-factor, most γ-butyrolactones found in other streptomycetes appear to be involved only in regulation of secondary metabolism. Some examples of γ-butyrolactones produced by other streptomycetes are shown in Table 1.1. A series of virginiae butanolides (VBs) A to E control virginiamycin production in *S. virginiae*, IM-2 controls production of showdomycin and minimycin in *S. lavendulae*, a regulatory factor controls both morphological and anthracycline biosynthesis in *S. bikiniensis* and *S. cyaneofuscatus*. Recently, three A-factor homologues (SCB1, SCB2 and SCB3) have been determined in *S. coelicolor*. The most abundant is SCB1 (*S. coelicolor* butanolide 1), which stimulates actinorhodin and undecylprodigiosin biosynthesis (Bibb, 2005; Horinouchi, 2002; Takano, 2006).

Table 1.1: Chemical structures of γ-butyrolactones from *Streptomyces* species (Horinouchi, 2002).

Chemical structure of γ-butyrolactone	Producing organism	Biological activity
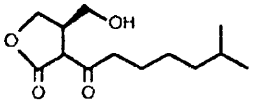 A-factor	*S. griseus*	Streptomycin Grixazone Sporulation
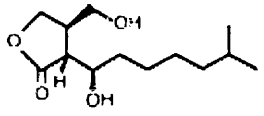 SCB1 [(2*R*,3*R*,1′*R*)-2-(1′-hydroxy-6-methylheptyl)-3-hydroxymethylbutanolide]	*S. coelicolor*	Actinorhodin Undecylprodigiosin
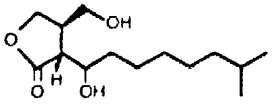	*S. bikiniensis*, *S. cyaneofuscatus*	Anthracycline Morphological differentiation
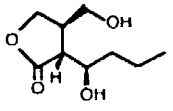 IM-2 [(2R,3R,1′R)-2-1′-hydroxybutyl-3-hydroxymethyl γ-butanolide]	*S. lavendulae*	Showdomycin Minimycin
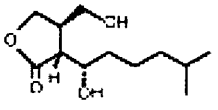 VB virginiae butanolides	*S. virginiae*	Virginiamycin

In addition to positive regulation of secondary metabolism, secondary metabolite synthesis is also subject to metabolite repression and/or inhibition by readily utilised carbon, nitrogen and phosphorous sources (Bibb, 2005; Chakraburtty and Bibb, 1997; Martin, 2004).

1.5 *Streptomyces* Genetics

Streptomyces genetics has been one of the major subjects of research for more than 50 years, focusing mainly on different aspects of developmental cycle and secondary metabolism. Sir David A. Hopwood is a pioneer in the *Streptomyces* genetics. For a PhD research project on *Streptomyces* genetics at Cambridge University, he selected a blue pigment producing *S. coelicolor* (Hopwood, 1999). The first genetic map of *S. coelicolor* was constructed by analyzing auxotrophic and antibiotic mutants and published in the late 1950s. It had six genes distributed into two linkage groups. The number of mapped gene increased gradually with the development of genetic tools. Soon scientists in different part of the world started assembling genetic maps for other species of *Streptomyces,* such as *S. ambofaciens, S. griseus, S. lividans, S. venezuelae* and *S. clavuligeurs,* using easily scorable phenotypic markers like auxotrophy, antibiotic resistance or morphological differences (Paradkar *et al.*, 2003). Kieser *et al.* in 1992 published a detailed genetic map combined with a physical map of *S. coelicolor* that contained more than 170 loci on the map. Pulse field gel electrophoresis (PFGE) analysis of the genomes of different *Streptomysis* species, including *S. coelicolor* and *S. lividans*, revealed that the chromosome of these organisms is linear possessing defined ends or telomeres (Leblond *et al.*, 1993; Paradkar *et al.*, 2003). Subsequent genome sequencing has also confirmed the linearity of the chromosomes (Bentley *et al.*, 2002; Ikeda *et al.*, 2003; Ohnishi *et al.*, 2008; Omura *et al.*, 2001). Linearity of *Streptomyces* chromosome is thought to have originated by single-crossover recombination between an initially circular chromosome and a linear plasmid (Chen, 1996; Ventura *et al.*, 2007; Volff and Altenbuchner, 1998). The chromosomal ends consist of terminal inverted repeats (TIRs) that are covalently bound to a protein known as terminal protein at free 5′ ends (Bao and Cohen, 2001; Wang *et al.*, 1999; Yang *et al.*, 2002; Yang and Losick, 2001). It is also proposed that the terminal proteins may anchor the DNA to the

membrane during chromosome replication and cell division (Bao and Cohen, 2001). The size of TIRs varies drastically depending upon the species (Table 1.2) (Bentley *et al.*, 2002; Ikeda *et al.*, 2003; Ohnishi *et al.*, 2008; Ventura *et al.*, 2007).

With the advancement in sequencing techniques, genomes of four *Streptomyces* species have been completely sequenced and published or made available online. The species whose complete genome sequences available are: *S. coelicolor, S. avermitilis, S. griseus* and *S. scabies* (Bentley *et al.*, 2002; Ikeda *et al.*, 2003; Ohnishi *et al.*, 2008). *Streptomyces* chromosomes range from around 8 Mb to 10 Mb in size and are very large compared to the chromosomes of unicellular bacteria such as *Escherichia coli* and *Bacillus subtilis,* which are about half the size in both DNA content and number of genes. In fact the number of predicted genes in *Streptomyces* genome is higher than that of a simple eukaryote *Saccharomyces cerevisiae*, which contains 6,203 recognized genes (Table 1.2) (Bentley *et al.*, 2002; Ikeda *et al.*, 2003; Ohnishi *et al.*, 2008). Depending upon the distribution of different types of genes the *Streptomyces* chromosomes are divided into two regions: a central core region that contains unconditionally essential genes such as those for cell division, DNA replication, transcription, translation and amino acid biosynthesis; and a pair of arms coding for non-essential genes such as secondary metabolites, hydrolytic enzymes and gas vesicle proteins. The replication of linear *Streptomyces* chromosomes is initiated from a fairly centrally located replication origin *(OriC)* rich in DnaA box sequences and proceeds bidirectionally towards the telomeres leaving a terminal single stranded gap on the discontinuous strand after removal of the last RNA primer. The terminal gap is filled by an unusual mechanism that includes priming from covalently bound terminal proteins (Bao and Cohen, 2001).

Global sequence comparison of *S. coelicolor, S. avermitilis* and *S. griseus* showed remarkable conservation of the internal core region of each chromosome with regards to sequence and orthologue distribution. The chromosomal arms are less conserved among these three chromosomes. It was found that the three species of streptomyces mentioned above share 3039 orthologues genes among them (Ohnishi *et al.*, 2008). Similar analysis using *S. coelicolor, S. avermitilis, S. scabies* and *S. venezuelae* genomes showed 3,566 conserved genes among the four species (Ventura *et al.*, 2007).

Table 1.2: General features of the chromosomes of four *Streptomyces* species

Fearutes	*S. coelicolor* A3(2)[a]	*S. avermitilis*[b]	*S. griseus*[c]	*S. scabies*[d]
Size (bp)	8,667,507	9,025,608	8,545,929	10,148,695
G+C content (%)	72.12	70.7	72.2	71.45
Coding density (%)	88.9	86.3	88.1	NA
Terminal inverted repeat (TIR)	21,653	174	132,910	NA
Protein-coding genes	7,825	7,581	7,138	NA
Average gene length (bp)	991	1,027	1,055	NA

References:- [a] Bently *et al.*, 2002; [b] http://avermitilis.ls.kitasato-u.ac.jp/;
[c] Ohnishi *et al.*, 2008; [d] http://www.sanger.ac.uk/Projects/S_scabies
NA: Data Not Available

In addition to chromosomal DNA, most of the *Streptomyces* species also contain plasmids that are either integrating in the chromosome or non-integrating. Non-integrating plasmids occur as linear or circular forms. Most of the plasmids are self-transmissible fertility factors and contain neither antibiotic resistance genes nor biosynthesis genes (an exception is the *S. coelicolor* SCP1 plasmid which contains methylenomycin resistance and biosynthesis genes). The size of linear plasmids range from 10 to 600 kb and they have TIRs carrying covalently bound terminal proteins at the 5′ end, similar to the chromosome. The replication mechanism of linear plasmids is also similar to the chromosomal DNA, starting at a centrally located replication origin and proceeding bidirectionally towards the ends. Examples of linear plasmids are pSLA2 from *S. rochei* and SCP1 from *S. coelicolor*. Circular plasmids are either low copy number or high copy number. Usually the larger ones are low copy number (eg. SCP2 from *S. coelicolor*) and replicate by the theta mode, bidirectionally, while the smaller ones are tend to be high copy number (eg. pIJ101, 300 copies) and replicate by a rolling circle mechanism (sigma mode). Some circular plasmids have phage λ-like *int* (integrase) and *xis* (excisase) genes for site specific, non-mutagenic integration into highly conserved tRNA genes. Examples of integrated plasmids are SLP1 from *S. coelicolor* and pSAM2 from *S. ambofaciens* (Kieser *et al.*, 2000).

1.5.1 *Streptomyces coelicolor* A3(2)

S. coelicolor A3(2) is genetically the best characterized representative of the genus. As a model organism it exhibits all the main features of the genus *Streptomyces*. It has a complex multicellular lifecycle with differentiation into distinct aerial hyphae and spores (Fig. 1.4) (Kieser *et al.*, 2000). Morphological differentiation is coordinated with the production of species specific secondary metabolites. *S. coelicolor* produces several secondary metabolites of which four antibiotics are well characterized: blue pigmented diffusible actinorhodin; red pigmented mycelium bound undecylprodigiosin; non-pigmented methylenomycin and calcium-dependent antibiotic (CDA) (Bentley *et al.*, 2002; Chater, 1998; Kieser *et al.*, 2000).

The linear chromosome of *S. coelicolor* is 8,667,507 bp long with 72.12% of G+C content. It encodes 7,825 potential open reading frames (ORFs) where 965 (12.3% of the genome) are probable regulatory proteins, 614 (7.8%) are predicted transporters and 819 (10.5%) potentially secreted proteins. The core region containing essential genes appears to extend from around 1.5 Mb to 6.4 Mb and accounts for approximately half of the chromosome (Bentley *et al.*, 2002). The left and right arms encoding non-essential genes are ~1.5 Mb and ~2.3 Mb in length, respectively. The centrally located origin of replication (*OriC*) maps near *dnaA* and *gyrB* genes encoding the replication initiation protein and DNA gyrase, respectively. The *OriC* region consists of 19 conseved DnaA boxes and contains slightly higher A-T rich sequences, characteristic of bacterial replication origins (Paradkar *et al.*, 2003).

S. coelicolor A3(2) has three plasmids, SCP1, SCP2 and SLP1. SCP1 is a 350 kb linear plasmid with genes for the biosynthesis of and resistance to methylenomycin. SCP2 is a 30 kb low copy number self replicating circular plasmid. It replicates bidirectionally by theta mode. SLP1 is a 17.2 kb integrated plasmid containing phage λ-like *int* and *xis* genes for site-specific, non-mutagenic integration into highly conserved chromosomal tRNA genes (Kieser *et al.*, 2000).

1.6 Molecular Basis of Morphogenesis in *Streptomyces*

The complex multicellular architecture of a streptomycete colony is the result of a developmentally controlled complex intercellular communication system. The

growing colony of *Streptomyces* experiences environmental stress through some signal(s). This stress signal(s) initiates the developmental program. Much of our understanding about the complex development of *Streptomyces* is based on characterization of *S. coelicolor* developmental mutants (Chater and Chandra, 2006). The developmental mutants of *S. coelicolor* are divided in to two major classes: bald (*bld*) mutants that fail to produce aerial hyphae, resulting in a smooth and shiny appearance of the colony (Kelemen and Buttner, 1998; Merrick, 1976) and white (*whi*) mutants, which produce aerial hyphae but cannot form mature grey spores (Chater, 1972; Flardh *et al.*, 1999). Most of these mutants are affected in genes with regulatory properties.

1.6.1 Erection of Aerial Hyphae – The *bld* Cascade

Regulation of aerial hyphae formation is a complex process. In *S. coelicolor*, the differentiation of vegetative mycelium into aerial hyphae is regulated by *bld* genes and mutations in *bld* genes result in failure to raise aerial hyphae in a conditionally dependent manner (Kelemen and Buttner, 1998). In addition to the lack of differentiation, *bld* mutants are also blocked in antibiotic production and are affected in carbon catabolite repression and the cell-cell signalling system of the organism, suggesting the inability of *bld* mutants to respond to environmental stress (Champness, 1988; Chater, 2006; Pope *et al.*, 1996).

Extensive research on different aspects of *S. coelicolor* development resulted in the identification and characterization of many *bld* genes (Table 1.3) whose products control various developmentally regulated events. The best characterized of the *bld* cascade genes is *bldA* gene, which encodes the only tRNA that can efficiently translate the rare leucine codon, UUA without G or C residues (Lawlor *et al.*, 1987; Leskiw *et al.*, 1991a; Leskiw *et al.*, 1991b). This is the rarest codon in streptomycete genomes and only 2 to 3% of genes in any one streptomycete contain a TTA codon (Chater and Chandra, 2006, 2008). Although non-essential for growth, the role of this rare leucyl tRNA in different aspects of secondary metabolism and morphological differentiation as a translational regulator has been revealed by the phenotypes of *bldA* mutants in diverse streptomycetes (Kataoka *et al.*, 1999; Kwak *et al.*, 1996; Lawlor *et al.*, 1987; Leskiw *et al.*, 1991b). The temporal accumulation of active form of *bldA* tRNA at the onset of

morphological and physiological differentiation also supports the role of *bldA* tRNA during early stages of colony differentiation in *Streptomyces* (Kataoka *et al.*, 1999; Leskiw *et al.*, 1993; Trepanier *et al.*, 1997). The biosynthesis of the antibiotics actinorhodin (blue) and undecylprodigiosin (red) is *bldA* dependent and is activated by the pathway-specific activator genes *act*II-orfIV and *redZ*, both containing TTA codons (Fernandez-Moreno *et al.*, 1991; White and Bibb, 1997). The role of the *bldA* gene in aerial hyphae formation came from the study of the *adpA* gene found in different *Streptomyces* species, which contains a TTA codon and encodes an AraC-like transcriptional regulator (Chater and Horinouchi, 2003; Kwak *et al.*, 1996; Nguyen *et al.*, 2003; Takano *et al.*, 2003). Unlike in *S. griseus,* where the *adpA* gene is involved both in antibiotic production and morphological differentiation, the orthologue of *S. coelicolor* does not have an apparent role in regulating antibiotic production and its transcription does not depend on the host's γ-butyrolactone signalling system (Horinouchi, 2002; Kato *et al.*, 2005; Takano *et al.*, 2003). Later, complementation analysis of a *S. coelicolor bldH* mutant with the *adpA* gene and sequence analysis of the *S. coelicolor adpA* gene showed that the *adpA* and *bldH* genes are the same (Nguyen *et al.*, 2003; Takano *et al.*, 2003). *bldB* and *bldD* encode putative transcription factors of 99 and 167 amino acid residues, respectively (Elliot *et al.*, 1998; Pope *et al.*, 1998). Unlike, most *bld* mutants, which can restore their developmental phenotype when grown on minimal medium containing a poor carbon source like mannitol, a *bldB* mutant remains both morphologically and physiologically defective, failing to sporulate or produce antibiotics, regardless of carbon source (Champness, 1988; Merrick, 1976; Pope *et al.*, 1996). BldD, a small DNA binding protein, exhibits autorepressor activity and also represses promoters of two developmentally important sigma factor encoding genes, *bldN* and *whiG* (Elliot and Leskiw, 1999; Elliot *et al.*, 2001). *bldN* encodes an extracytoplasmic function (ECF) sigma factor, which is required to transcribe the *bldM* gene (Bibb *et al.*, 2000). The BldM protein is a response regulator of the FixJ subfamily proteins required for aerial growth (Molle and Buttner, 2000). Interestingly, some *bldM* and *bldN* mutants showed a white phenotype, suggesting that both gene products have addition roles in later development of aerial hyphae (Bibb *et al.*, 2000; Molle and Buttner, 2000; Ryding *et al.*, 1999). *bldC* encodes a small DNA binding protein related to the MerR family of transcriptional activators (Hunt *et al.*, 2005). *bldG* gene encodes an anti-anti-sigma factor, a member of a protein family found exclusively in gram-

positive bacteria, which may regulate the activity of several sigma factors during development (Bignell *et al.*, 2000; Bignell *et al.*, 2003). *bldK* is a complex locus and encodes homologs of the subunits of the oligopeptide-permease, which is inferred by the resistance of a *bldK* mutant to the toxic tripeptide bialaphos (Nodwell *et al.*, 1996). *bldJ (bld261)* is required for the production of an extracellular oligopeptide, which functions as a signalling molecule (Nodwell and Losick, 1998).

Table 1.3: Genes discovered through the analysis of bald mutants of *S. coelicolor*

Gene	Gene product	Function	Reference(s)
bldA	UUA leucyl tRNA	Translation of rare TTA codons	(Lawlor *et al.*, 1987; Leskiw *et al.*, 1991a)
bldB	Small DNA binding protein	Putative transcription factor	(Eccleston *et al.*, 2002; Pope *et al.*, 1998)
bldC	DNA binding protein	Member of MerR family of transcription regulators	(Hunt *et al.*, 2005; Merrick, 1976)
bldD	Small DNA binding protein	Transcription regulator (Repressor protein)	(Elliot *et al.*, 1998; Elliot *et al.*, 2001)
bldG	Like ant-anti sigma factor	Unknown	(Bignell *et al.*, 2000; Champness, 1988)
bldH (=adpA)	Activator/repressor family protein	Unknown	(Nguyen *et al.*, 2003; Takano *et al.*, 2003)
bldI	Unknown	Unknown	(Harasym *et al.*, 1990; Leskiw and Mah, 1995)
bldJ (=bld261)	Unknown	Required for production of signal 1, an extracellular oligopeptide in *bld* signalling cascade	(Nodwell and Losick, 1998)
bldK	Oligopeptide permease	Oligopeptide importer	(Nodwell *et al.*, 1996)
bldL	Unknown	Unknown	(Nodwell *et al.*, 1999)
bldM (=whiK)	Orphan response regulator	Activation of the *chp* genes that encodes chaplin proteins	(Molle and Buttner, 2000)
bldN (=whiN)	Extracytoplasmic function (ECF) sigma factor	Require for transcription of one of two promoters of *bldM*	(Bibb *et al.*, 2000)
ramR	Response regulator (Related to NarL/FixJ family proteins)	Activation of the *ramCSAB* operon transcription	(Kodani *et al.*, 2004; Ma and Kendall, 1994)
ramS	SapB precursor protein	Precursor protein of SapB, a biological surfactant	(Kodani *et al.*, 2004; Ma and Kendall, 1994)
ramA/B	ABC transporters	Probable exporter of SapB	(Kodani *et al.*, 2004; Ma and Kendall, 1994)
ramC	Membrane associated lantibiotic processing protein	Post-translational modification of *rams* gene product to produce SapB	(Kodani *et al.*, 2004; Ma and Kendall, 1994)
chpA-H	Chaplins (coelicolor hydrophobic aerial proteins)	Biological surfactants	(Claessen *et al.*, 2003; Elliot *et al.*, 2003)
osaB	Response regulator	Unknown	(Bishop *et al.*, 2004)

An important feature of *bld* mutants is that they exhibit extracellular complementation (Willey *et al.*, 1991; Willey *et al.*, 1993). This complementation apparently results from the diffusion of substances from one strain (donor) to another (recipient) when grown in close proximity to each other on certain rich media. The pattern of complementation observed among different *bld* mutants is always unidirectional and constitutes a hierarchical pattern of different mutant classes: *bldJ<bldK/L<bldA/H<bldG<bldC<bldD/M/ram*, where each mutant can rescue the developmental defect in all the mutants to the left but not to the right. Those mutants which are in the same complementation group (e.g. *bldA* and *bldH*) do not interact with each other and display the same pattern of complementation. This sequential complementation is interpreted as an intercellular signalling pathway involving as many as five extracellular signals, which ultimately leading to synthesis of SapB (Fig. 1.6) (Chater, 1998; Kelemen and Buttner, 1998). Interestingly, *bldB, bldI* and *bldN* mutants do not fit into the proposed hierarchical signalling cascade (Bibb *et al.*, 2000; Willey *et al.*, 1993). The phenotype of most *bld* mutants depend on the growth medium, and many of them can restore aerial mycelium formation and sporulation (but not antibiotic production) when grown on minimal medium with mannitol as a carbon source instead of glucose (Willey *et al.*, 1991).

The defects in the aerial hyphae formation of *bld* mutants can be relieved by the exogenous application of purified SapB (spore associated protein B) (Willey *et al.*, 1993; Willey *et al.*, 2006). However, the aerial hyphae formed by SapB rescued *bld* mutants do not resemble wild type aerial hyphae and do not undergo sporulation (Tillotson *et al.*, 1998; Willey *et al.*, 1993). SapB is a small secreted lantibiotic-like lanthionine containing hydrophobic peptide, that functions as a biological surfactant releasing the surface tension at the air-water interface, thereby allowing the hyphae to escape the aqueous milieu of the colony surface and grow upright (Kodani *et al.*, 2004; Tillotson *et al.*, 1998). Unlike most lantibiotics, SapB does not appear to have antibiotic activity. It was shown that SC3 hydrophobin from the fungus *Schizophyllum commune* and streptofactin (SapT, a lantibiotic-like structure similar to SapB) from *Streptomyces tendae*, can restore the capacity of *S. coelicolor* and *S. tendae* bald mutants to erect aerial structures (Tillotson *et al.*, 1998). These observations further imply that the role of the hydrophobic peptide as a surfactant, rather than as a signalling molecule. All the *bld* mutants, except *bldM* and *bldN*, fail to produce and secrete SapB, which suggests

that SapB production is dependent on *bld* genes (Willey *et al.*, 1991). Although *bld* mutants fail to synthesize SapB, there is yet no evidence of a direct connection between any *bld* gene products and SapB production.

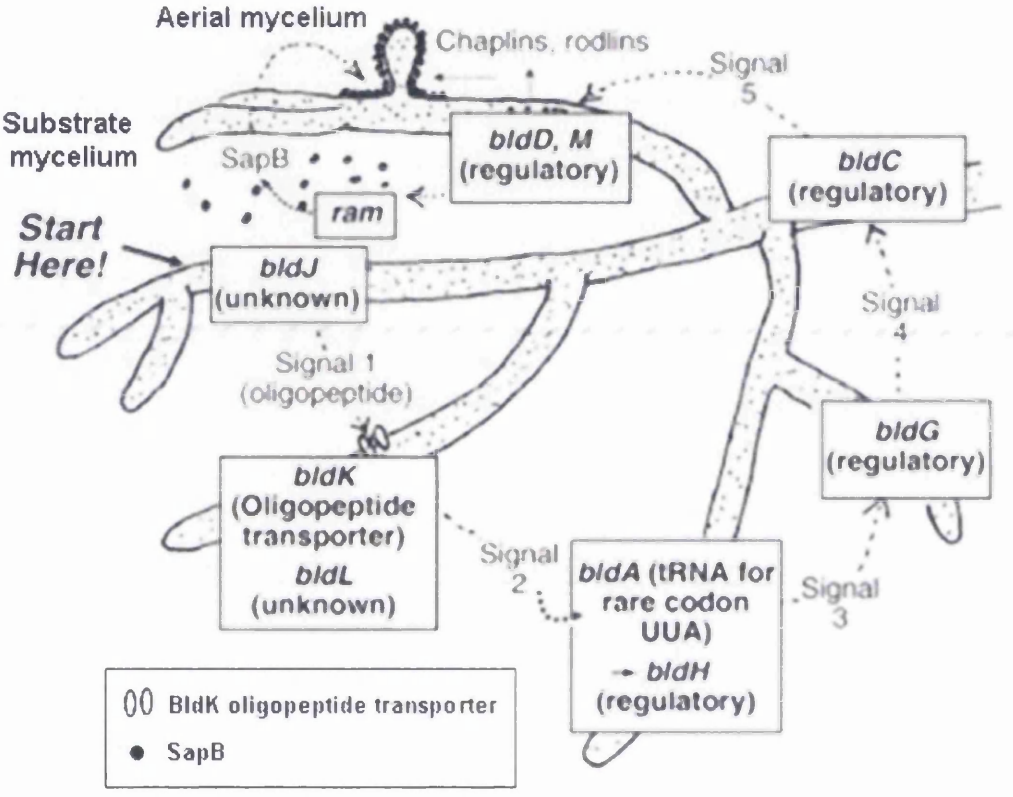

Figure 1.6: Diagrammatic representation of the *S. coelicolor* extracellular signalling pathway leading to aerial hyphae formation involving *bld* genes. After reaching an appropriate nutritional and developmental stage, the substrate mycelium produces signal 1 in a *bldJ* dependent manner. Signal 1 is taken up by the BldK oligopeptide permease, which subsequently triggers synthesis and release of signal 2 and so on, leading to the eventual *bldD* dependent production of SapB and other potential morphogens, which leads to the growth of aerial mycelium. (Chater and Chandra, 2006)

SapB is derived by post-translational modification from the product of the *ramS* gene, a member of the *ram* (rapid aerial mycelium) gene cluster (Kodani *et al.*, 2004; Ma and Kendall, 1994). The *ram* gene cluster consists of the *ramCSAB* operon and the divergently expressed *ramR*. Overexpression of the *ram* cluster accelerates the formation of aerial hyphae in wild-type strains, and deletion of *ramR, ramC* or *ramS*

results in a reduced ability to raise aerial structures (Ma and Kendall, 1994). *ramS* is predicted to encode a 42 amino acid peptide. This 42 amino acid peptide is predicted to be modified by the product of *ramC* gene to yield an active form of 21 amino acid SapB peptide. RamC is membrane-associated protein, that showed homology of its amino terminal and carboxy terminal domains with serine/threonine kinases and lantibiotic processing protein, respectively (Hudson *et al.*, 2002; Kodani *et al.*, 2004). *ramA* and *ramB* encode components of an ABC transporter probably invoelved in SapB export. RamR is a response regulator-like protein of NarL/FixJ subgroup that activates the transcription of the *ramCSAB* operon by binding to the *ramC* promoter (Ma and Kendall, 1994; Nguyen *et al.*, 2002). Interestingly, the production of SapB in wild type *S. coelicolor* appears to be media-dependent, as it is produced on rich media but not on minimal media (Willey *et al.*, 1991). Ueda and co-workers identified the *ram* orthologous gene cluster in *S. griseus,* termed as *amf* (aerial mycelium formation), which is composed of *amfT (ramC), amfS (ramS), amfA (ramB), amfB (ramA),* and *amfR (ramR)* (Ueda *et al.*, 1993). Unlike the *S. coelicolor ramR*, its *S. griseus* orthologue, *amfR* contains a TTA codon and is also a member of the AdpA regulon in the A-factor regulatory cascade (Yamazaki *et al.*, 2003b). The medium dependent phenotype of most of the *bld* mutants, conditional production of SapB and extracellular complementation cascade suggest that the checkpoint controls involving *bld* genes are by-passed in certain nutritionally less- favourable conditions, and that another morphogenetic protein then carries out the surfactant role of SapB (Claessen *et al.*, 2006; Kelemen and Buttner, 1998).

Another gene cluster of contiguously cotranscribed developmental genes has been discovered recently, that is regulated by *ramR* gene product and modulates both aerial hyphae formation and sporulation (San Paolo *et al.*, 2006). The cluster consists of four *ramR*-activated genes (*ragABKR*), which forms an operon and encode two subunits of an ABC transporter *(ragA and ragB)*, a putative histidine kinase *(ragK)* and a response regulator *(ragR,* a *ramR* paralogue*)*. The *ragABKR null* mutant was able to synthesize SapB and erect aerial hyphae; however, these hyphae were unusually branched, reminiscent of substrate hyphae and subsequent stages of differentiation, septation and sporogenesis were delayed. Extracellular complementation and epistasis analyses in which *ragK* and *ragR* or an activated mutant allele of *ragR* were overexpressed in *bld* and *ram* mutants revealed that the *rag* operon triggered the

sporulation program of *S. coelicolor* by activating a SapB-independent pathway downstream of RamR (San Paolo *et al.*, 2006).

Chaplins (coelicolor hydrophobic aerial proteins), a family of secreted proteins, also play a important role in surface hydorphobicity and consequently, in development of aerial hyphae (Claessen *et al.*, 2003; Elliot *et al.*, 2003). Together with rodlins, chaplins appear to form a hydrophobic sheath on the surface of aerial hyphae and spores (Claessen *et al.*, 2004; Elliot and Talbot, 2004). There are eight chaplin proteins (ChpA–H) in *S. coelicolor,* all sharing a highly conserved, hydrophobic domain of ~40 amino acids, termed the 'chaplin domain'. ChpD–H are short proteins made up of a single chaplin domain, while ChpA–C are much longer, having two amino terminal chaplin domains (Claessen *et al.*, 2003; Elliot *et al.*, 2003; Elliot and Talbot, 2004). The chaplin genes have been identified only in sporulating actinomycetes such as *S. coelicolor, S. avermitilis* and *Thermobifida fusca*, and have not been observed in non-sporulating actinomycetes such as *Mycobacterium tuberculosis* and *Corynebacterium diphtheriae* (Elliot and Talbot, 2004). Deletion of a single chaplin gene has no detectable effect on colony morphology. The loss of as few as four of the eight chaplin genes (two long and two short) results in delays in aerial hyphae formation and sporulation, while deletion of all eight results in an extremely severe defect in aerial hyphae formation with the loss of surface hydrophobicity (Claessen *et al.*, 2004; Elliot *et al.*, 2003). Unlike most *bld* mutants, the phenotype of chaplin deletion strains is unconditional. The mutant with all eight genes deleted fails to form aerial hyphae regardless of media composition (Claessen *et al.*, 2004; Elliot *et al.*, 2003). As in the case of SapB, chaplins are not expressed in *bld* mutants grown on rich media, suggesting the regulatory role of *bld* genes in the expression of chaplin genes (Elliot *et al.*, 2003). So far no information is available regarding the upstream regulation of chaplin genes. The chaplins also appear to be very surface-active, and are capable of reducing surface tension of water dramatically (Capstick *et al.*, 2007; Claessen *et al.*, 2003). The pathway controlling the expression of the chaplin and rodlin genes is called the sky pathway (Claessen *et al.*, 2006). Recently, the functional interplay between SapB and the chaplins to enable growth of aerial hyphae has been demonstrated, where the chaplins are key contributors to the 'SapB-independent' pathway of aerial hyphae formation on minimal medium, but both chaplins and SapB are required for normal aerial hyphae formation on rich medium (Capstick *et al.*, 2007).

1.6.2 Metamorphosis of Aerial Hyphae into Spores – The *whi* Genes

Once the aerial hyphae have formed, the apical region of the hyphae forms a spiral syncytium, containing tens of genome copies per hyphae, which undergoes multiple septation and gives rise to chain of unigenomic compartments which, metamorphose into thick-walled grey spores (Fig. 1.4). Several genes function significantly during this sporulation stage and play such important roles that mutations in these genes disrupt sporulation of aerial hyphae (Table 1.4 and Fig. 1.4). Such developmental mutants have been isolated in the extensively studied organism *S. coelicolor* on the basis of their inability to form mature grey pigmented spores. These mutants are called *whi* mutants, as they retain white aerial hyphae even after prolonged incubation (Chater, 1972; Hopwood *et al.*, 1970). On the basis of the effect of mutations on particular stages of sporulation, the *whi* genes are divided into 'early' and 'late' sporulation genes. Mutants with the defects in early genes fail to form unigenomic compartments, whereas late *whi* genes mutants produce recognizable spores that are defective in pigmentation or irregular in size (Chater, 2000).

Six early *whi* genes (*whiA, B, G, H, I* and *J*) have been identified and characterized (Chater, 1972, 2000). Three (*whiG, H* and *I*) of the six early *whi* genes encode members of well know families of proteins, while the other three (*whiA, B* and *J*) encode proteins that do not closely resemble any well characterized protein families. *whiG* gene is the first gene in the *whi* gene regulatory cascade and it encodes an RNA polymerase sigma factor (σ^{WhiG}), a homologue of motility sigma factors required for the formation of the flagella and the chemotaxis systems in motile unicellular bacteria (Chater, 1989, 2000; Tan *et al.*, 1998). The crucial role of WhiG in committing aerial hyphae to sporulate is evident from the *whiG* mutant phenotype, which has long, straight aerial hyphae with few vegetative-like septa, and overexpression of *whiG* results in abnormal sporulation (Chater, 1989; Flardh *et al.*, 1999). *whiG* is repressed by BldD, the only example of a regulatory link between *bld* and *whi* genes (Elliot *et al.*, 2001). However, the mechanism of *whiG* gene regulation is not clear. Although, σ^{WhiG} is transcribed more or less constantly throughout the lifecycle, it seems to be active only during the beginning of the sporulation process. σ^{WhiG} transcribes two 'early' *whiH* and *whiI* genes (Ainsa *et al.*, 1999; Ryding *et al.*, 1998). Homologues of WhiG have been

identified in *S. avermitilis, S. griseocarnum* and *S. aureofaciens* (Kormanec *et al.*, 1994; Omura *et al.*, 2001; Soliveri *et al.*, 1993).

Table 1.4: Regulatory genes affecting sporulation in *S. coelicolor.*

Genes	Product	Reference(s)
Early *whi* genes		
whiA	Unknown (conserved among gram-positive bacteria)	(Ainsa *et al.*, 2000)
whiB	Small putative DNA binding protein (specific to actinomycetes)	(Molle *et al.*, 2000; Soliveri *et al.*, 1992)
whiG	Sigma factor (similar to σ^{FliA} of *E. coli*)	(Chater, 1989; Tan *et al.*, 1998)
whiH	GntR-like regulatory protein	(Ryding *et al.*, 1998)
whiI	Response regulator	(Ainsa *et al.*, 1999)
whiJ	Small protein with lambda repressor-like DNA binding domain	(Chater and Chandra, 2006)
Late *whi* genes		
whiD	WhiB-like protein	(Molle *et al.*, 2000)
whiE	Type II polyketide synthases	(Davis and Chater, 1990; Kelemen *et al.*, 1998)
whiL	Unknown	(Ryding *et al.*, 1999)
whiM	Unknown	(Ryding *et al.*, 1999)
whiO	Unknown	(Ryding *et al.*, 1999)
Other genes		
ssgA-G	Unknown [members of SsgA-like proteins (SALPs) family]	(Noens *et al.*, 2005)
sigF	RNA polymerase sigma factor	(Potuckova *et al.*, 1995)
crgA	Unknown (Small membrane protein)	(Del Sol *et al.*, 2003; Del Sol *et al.*, 2006)
smeA	Unknown (small membrane protein)	(Ausmees *et al.*, 2007)
sff	Unknown (member of SpoIIIE/FtsK-like protein family)	(Ausmees *et al.*, 2007)

The next step in the sporulation process, a coordinated cessation of aerial hyphae growth, is proposed to be mediated by *whiA* and *whiB* gene products. *whiA, whiB* and *whiAB* double mutants have abnormally long and curly aerial hyphae that completely lack sporulation septa (Chater, 1975; Flardh *et al.*, 1999). *whiA* encodes a protein of unknown function which appears to be conserved among gram-positive bacteria whose genome sequence is known (Ainsa *et al.*, 2000). *whiB* encodes a small putative DNA-binding protein of unknown function that belongs to the Wbl (WhiB-like) family of transcription factors found exclusively in actinomycetes (Soliveri *et al.*, 2000). This family of proteins has four highly conserved cysteine residues. There are ten genes encoding WhiB-like proteins in *S. coelicolor* genome, which also includes the 'late' sporulation gene *whiD* (Molle *et al.*, 2000; Soliveri *et al.*, 2000). A *whiB* mutant of *S. aureofaciens* has a similar phenotype and the *whiB* orthologue in *Mycobacterium smegmatis*, *whmD*, has been shown to play an essential role in septation and cell division (Gomez and Bishai, 2000; Kormanec *et al.*, 1998). The expression of *whiA* and *whiB* genes in *S. coelicolor* is developmentally controlled and strongly up-regulated at the time of aerial hyphae growth. The developmentally controlled expression of *whiA* and *whiB* appears to be largely independent of σ^{WhiG} (Ainsa *et al.*, 2000; Soliveri *et al.*, 1992).

The *whiH* gene encodes a protein that is related to the GntR family of repressors containing a helix–turn–helix DNA-binding motif (Ryding *et al.*, 1998). Disruption mutants of *whiH* produce loosely coiled aerial hyphae with occasional sporulation septa, condensed and abnormally partitioned DNA (Flardh *et al.*, 1999). The colonies of *whiH* mutants are pale grey, while those of *whiG, whiA* and *whiB* mutants remain pure white. The spore-like features and synthesis of grey pigment in *whiH* mutants suggest that *whiG, whiA* and *whiB* are epistatic to *whiH.* It also suggests that there is a weak expression of *whiE*, a gene responsible for grey pigment production, in *whiH* mutants in contrast to no expression in *whiG, whiA* and *whiB* mutants (Flardh *et al.*, 1999; Ryding *et al.*, 1998). WhiH appears to induce the strong developmentally controlled *ftsZp2* promoter to bring about sporulation septation (Flardh *et al.*, 2000).

The *whiI* gene encodes a response regulator protein that belong to so-called two-component response regulator systems (Ainsa *et al.*, 1999). Similar to typical response regulators, it has a conserved N-terminal phosphorylation pocket and α-helical DNA-binding region near its C-terminus. However, the phosphorylation pocket of WhiI

lacks certain highly conserved and functionally important amino acid residues needed for phosphorylation and there is no recognizable kinase gene next to *whiI,* suggesting that WhiI may function in a phosphorylation-independent manner (Ainsa *et al.*, 1999; Tian *et al.*, 2007). The phenotype of the *whiI* mutants is similar to that of a *whiH* mutant; loosely coiled aerial hyphae with no spores, although there is a lack of DNA condensation similar to *whiG, whiA* and *whiB* mutants (Ainsa *et al.*, 1999; Flardh *et al.*, 1999). Expression of *whiH* and *whiI* is σ^{WhiG} dependent, and both show some autoregulatory activity. There is also evidence of cross-regulation between *whiH* and *whiI*, repressing each others expression (Ainsa *et al.*, 1999; Ryding *et al.*, 1998). *whiJ* mutants are pale grey and produce low numbers of apparently normal spore chains (Ryding *et al.*, 1999). The product of *whiJ* has a lambda repressor-like DNA-binding domain at its N-terminus and is a member of a *Streptomyces* specific protein family (Chater and Chandra, 2006).

Among the late sporulation genes, *whiD* encodes a protein containing an oxygen-sensitive 4Fe-4S cluster and is a member of the WhiB-like family of putative transcription factors (Jakimowicz *et al.*, 2005). A *whiD* mutant forms spores that are highly irregular in size and shape, extremely variable in spore cell wall deposition and prone to lysis (Chater, 1972; McVittie, 1974). *whiE* is a complex locus and contains a cluster of eight genes, most of which encode homologues of enzymes involved in aromatic polyketide biosynthesis (Davis and Chater, 1990). The *whiE* genes form two divergently transcribed units which are switched on only during sporulation. Promoters of both transcription units are dependent on all the early *whi* genes, and only one of the promoters that is reading into *orfVIII* is also dependent on the late sporulation-specific SigF sigma factor (Kelemen *et al.*, 1998). *whiE* mutants lack in grey pigment production but do not appear to be morphologically defective in sporulation (Chater, 1972; Davis and Chater, 1990; McVittie, 1974). The *whiL, whiM,* and *whiO* loci are not well characterized. Mutants of *whiL* showed long curved and straight spores; disruption of *whiM* or *whiO* showed undifferentiated aerial hyphae with rare spore chains (Ryding *et al.*, 1999).

1.6.3 Other Genes Influencing Aerial Hyphae Development

In more recent years, several important new loci or gene families of developmental genes have been discovered (Table 1.4). One such family of genes is the *ssgA*-like genes that encode members of SsgA-like proteins (SALPs) family, a group of novel developmental regulators found exclusively in sporulating actinomycetes (van Wezel and Vijgenboom, 2004). The model strain *S. coelicolor* contains seven paralogues (SsgA-G) each involved in a specific step in the sporulation process, from initiation of sporulation septa to the autolytic cleavage of spore wall peptidoglycan. While SsgA and SsgB are essential for sporulation-specific cell division in *S. coelicolor*, SsgC–G are responsible for correct DNA segregation/condensation (SsgC), spore wall synthesis (SsgD), autolytic spore separation (SsgE, SsgF) or exact septum localization (SsgG) (Noens *et al.*, 2005). There are six SALPs in *S. avermitilis* (van Wezel and Vijgenboom, 2004). Among the seven SALPs of *S. coelicolor,* SsgA (a small acidic peptide) is the best studied protein and was first identified as an effecter of cell division in *Streptomyces griseus* (Kawamoto and Ensign, 1995). *ssgA* mutants of *S. coelicolor* and *S. griseus* produce normal vegetative septa but are defective in sporulation, however some viable spores are formed on mannitol containing media (Jiang and Kendrick, 2000). *ssgA* is strongly expressed at the onset of sporulation in submerged culture of *S. griseus*, whereas there is no expression of *ssgA* in liquid grown *S. coelicolor* culture (Kawamoto *et al.*, 1997; van Wezel *et al.*, 2000a; van Wezel *et al.*, 2000b). Also there is a difference in the regulation of *ssgA* in two *Streptomyces* species. In *S. griseus* the transcription of *ssgA* is controlled by AdpA (a transcriptional activator in the A-factor regulatory cascade), while in *S. coelicolor* it is regulated by upstream-located *ssgR* (an *iclR*-type regulatory gene) in a *whi*-independent mannar (Traag *et al.*, 2004; Yamazaki *et al.*, 2003a). Transcription of both *ssgA* and *ssgR* is developmentally regulated in *S. coelicolor* and activated towards the onset of sporulation (Traag *et al.*, 2004). Overexpression of SsgA in liquid grown cultures of *S. coelicolor* and *S. griseus* resulted in mycelial fragmentation and highly increased septation, suggesting the activating role of SsgA in sporulation specific septation (Kawamoto *et al.*, 1997; van Wezel *et al.*, 2000a). The septa in an SsgA-overexpressing culture of *S. coelicolor* were extremely thick and irregular (van Wezel *et al.*, 2000a). *In vivo* localization studies of SsgA showed that it localizes dynamically during development of aerial hyphae and most

likely marks the sites where changes in local cell-wall morphogenesis are required, especially in septum formation and germination (Noens *et al.*, 2007).

Another gene encoding a member of SALPs is *ssgB*. It is also essential for sporulation as the deletion mutant failed to sporulate and produced significantly large white colonies with increased production of actinorhodin (Keijser *et al.*, 2003; Kormanec and Sevcikova, 2002). Expression of SsgB is associated with aerial hyphae formation and it depends upon *sigH* (σ^H), a stress-response sigma factor, essential for sporulation in *S. coelicolor* (Kormanec and Sevcikova, 2002).

sigF encodes an RNA polymerase sigma factor (σ^F) required for the late stages of sporulation (Potuckova *et al.*, 1995). The *sigF* mutant produced small, irregular and thin walled spores with uncondensed chromosomes, and the spores were sensitive to detergents. *sigF* expression appeared to be regulated at the level of transcription and expressed transiently when sporulation septa were observed in the aerial hyphae. Transcription of *sigF* depends upon all six of the early whi genes (Kelemen *et al.*, 1996; Potuckova *et al.*, 1995). One of the promoters of *whiE* genes is dependent on σ^F (Kelemen *et al.*, 1998).

A whole genome microarray comparison approach in *S. coelicolor* detected a number of previously unrecognized sporulation genes such as *smeA* and *sffA* (Ausmees *et al.*, 2007). *smeA* encodes a small membrane protein while *sffA* encodes a member of the SpoIIIE/FtsK-like protein family. Mutational analysis of *smeA* and *sffA* genes revealed that they are involved in late sporulation processes like division septum placement, chromosome segregation and condensation, spore wall maturation, spore pigmentation and spore separation. Transcription of both the genes occurs at the onset of sporulation division just after Z-ring formation. Expression of the *smeA* promoter is dependent on the products of all the *whi* genes (Ausmees *et al.*, 2007).

The *crgA* gene is a representative of a well conserved family of genes among actinomycetes encoding a small membrane protein that plays a role in coordinating growth and cell division during the reproductive growth (Del Sol *et al.*, 2003). Disruption of *crgA* in *S. coelicolor* resulted in early growth of aerial hyphae and increased production of actinorhodin, whereas overexpression of *crgA* blocked sporulation septation. In *S. avermitilis*, *crgA* mutants failed to form sporulation septa (Del Sol *et al.*, 2003). Expression of CrgA is also developmentally controlled and

maximally expressed at the time of differentiation. It has been shown that CrgA may have important role in Z-ring formation (Del Sol *et al.*, 2006).

The members of the basic cell division machinery, the Fts proteins, have also been studied in *S. coelicolor* and has been shown to play important roles in development by affecting cell division in the organism (McCormick *et al.*, 1994; McCormick and Losick, 1996). Fts proteins so far studied in *S. coelicolor* will be discussed separately later in the chapter.

1.7 Cell Division in Unicellular Bacteria

Cell division is one of the most fundamental processes of the biological system and is essential for the propagation of all living organisms. In bacteria, cell division involves duplication of the cell contents and formation of a septum by ingrowth of the cytoplasmic membrane and cell wall resulting into two daughter cells. The seemingly simple process of bacterial cell division is in fact a complex and tightly regulated mechanism, in both space and time. The cell division process is best characterized in *Escherichia coli* and *Bacillus subtilis*. In *E. coli* there are at least 15 proteins (FtsZ, FtsA, ZipA, ZapA, FtsE, FtsX, FtsK, FtsQ, FtsB, FtsL, FtsW, FtsI, FtsN, AmiC and EnvC) known to be recruited at the site of septum formation during the cell division process (Table 1.5) (Bernhardt and de Boer, 2004; Weiss, 2004). Out of 15 proteins, 10 proteins (FtsZ, FtsA, ZipA, FtsK, FtsQ, FtsB, FtsL, FtsW, FtsI, and FtsN) are essential for cell division (Goehring and Beckwith, 2005; Vicente and Rico, 2006). Many of these essential proteins are attractive targets for antibacterial drug discovery. Homologues of most of the *E. coli* division proteins, which include FtsZ, FtsA, ZipA (a possible functional homologue of *B. subtilis* EzrA), FtsL, FtsB (DivIC in *B. subtilis*), FtsQ (DivIB in *B. subtilis*), FtsW (YlaO in *B. subtilis*), and FtsI (Pbp2B in *B. subtilis*) are present in *B. subtilis* (Table 1.5) (Errington *et al.*, 2003). Many genes encoding the cell division proteins in *E. coli* and *B. subtilis* have been identified by the isolation of conditional mutants that were devoid of division septa and formed filaments at the

Table 1.5: Cell division proteins of *E. coli* and *B. subtilis* (Ebersbach *et al.*, 2008; Errington *et al.*, 2003; Goehring and Beckwith, 2005; Harry *et al.*, 2006).

***E. coli* Protein**	**Homologue in *B. subtilis***	**Product**	**Function**
Early division (Z-ring associated) proteins			
FtsZ	**FtsZ**	Tubulin homologue	Z-ring scaffold formation
FtsA	FtsA	Actin superfamily member	Z-ring stabilization, recruitment of late division proteins
ZipA	NP	Unknown	Z-ring stabilization
ZapA	ZapA	Unknown	Positive regulator of Z-ring formation
ZapB	?	Unknown, Homodimeric anti-parallel coiled-coil protein	Z-ring assembly
?	EzrA	Unknown	Negative regulator of Z-ring assembly
Late division proteins			
FtsE	FtsE	Similar to ABC transporter	Unknown
FtsX	?	Similar to ABC transporter	Unknown
FtsK	SpoIIIE^{S}	Unknown	Chromosome segregation
FtsQ	DivIB	Unknown	Unknown
FtsL	**FtsL**	Contain putative leucine zipper coiled-coil regions	Unknown
FtsB (formerly YgbQ)	**DivIC**	Unknown	Unknown
FtsW	**FtsW**^{N} (YlaO)	Polytopic membrane protein of SEDS family	Probably in recruitment of cognate PBPs
FtsI	Pbp2B &	Division specific transpeptidase	Septal cell wall synthesis
FtsN	NP	Contains murein binding domain	Unknown
AmiC	?	Amidase	Daughter cell separation
EnvC	?	Lipoprotein murein hydrolytic activity	Daughter cell separation
NP	SepF (=YlmF)	Unknown	Unknown, FtsZ interacting protein
Z- ring positioning			
MinC	MinC	Unknown	FtsZ polymerization inhibitor
MinD	MinD	ParA family ATPase	Min oscillator (*E. coli*), Localization of MinC at the cell poles (*B. subtilis*)
MinE	NP	Unknown	Topological regulator of Min system
NP	**DivIVA**	Unknown	Topological specificity of Min system
SlmA	Noc^{F}	Unknown	Negative regulator of FtsZ assembly, prevents Z ring formation over nucleoid (Nucleoid occlusion)
SulA	YneA^{F}	Unknown	Negative regulator of FtsZ assembly indused by SOS response

NP: Not Present; ?: Other homologues may exist; ^{F} Functional homologue (structurally unrelated); ^{N} Function is not verified yet; ^{S} Sporulation Specific and not required for vegetative septation; Essential proteins indicated in bold letters.

nonpermissive temperature; hence the genes have been named *fts,* for ***f****ilamentous* ***t****emperature* ***s****ensitive* phenotype. Comparison of the cell division genes across several bacterial genomes revealed that many of the genes are well conserved among bacteria, suggesting the presence of some universal machinery and mechanism for bacterial cell

division. However, some genes are missing or some additional genes are found in some groups of bacteria (eg. *ftsW* homologues in *E. coli* and *B.subtilis,* absence of *ftsA* and *zipA* from actinobacterial species), indicating diversity of bacterial cell envelopes, shapes and life cycle (Nikolaichik and Donachie, 2000). Many of the division genes are grouped together along with the genes encoding peptidoglycan synthesis enzymes in the genomes of several bacteria including *E. coli* and *B. subtilis,* forming a cluster of genes known as **d**ivision **c**ell **w**all (*dcw*) cluster (Vicente *et al.*, 1998). The presence of this well organized gene cluster suggests that there is some specific regulatory mechanism for the coordinated expression of the cell division and cell wall synthesis genes.

The first apparent step in cell division is the formation of a Z ring by polymerization of FtsZ protein in a GTP-dependent fashion, at the site of future septum exactly in the middle of the cell (Erickson *et al.*, 1996; Romberg and Levin, 2003). This Z ring marks the site of division and provides a scaffold for the recruitment of subsequent division proteins. The complex formed by the localization of division proteins including the Z ring at the midcell is known as the divisome, which drives the cell division process. The precise functions of many of these divisome proteins are not fully understood. However their functions involve (1) assisting and stabilizing Z ring assembly (FtsA, ZipA, ZapA), (2) coordinating septation with chromosome segregation (FtsK), (3) recruiting and stabilizing the late divisome proteins at the division site, (4) synthesis of the peptidoglycan cell wall (FtsI, FtsW) and (5) hydrolysis of peptidoglycan to separate daughter cells (AmiC, EnvC) (Errington *et al.*, 2003; Harry *et al.*, 2006).

1.7.1 Divisome proteins and their assembly

FtsZ, the first known protein to localize at the cell division site, is a structural homologue of eukaryotic tubulin (Erickson, 1995). It is the best conserved cell division protein in nearly all bacteria, archaea and some eukaryotic organelles (Harry *et al.*, 2006). Like tubulin, FtsZ binds and hydrolyzes GTP (Romberg and Levin, 2003). In the presence of GTP, it reversibly assembles into dynamic filamentous structures *in vitro* that are analogous to tubulin polymers, suggesting the possible cytoskeletal function of FtsZ (Mukherjee *et al.*, 1993; Mukherjee and Lutkenhaus, 1998). FtsZ-GFP fusion and immunofluorescence microscopy revealed that assembly of the Z ring at the midcell

results from reorganization of an FtsZ helix (Anderson *et al.*, 2004; Stricker *et al.*, 2002; Thanedar and Margolin, 2004).

One of the early recruited proteins to the Z ring is the cytoplasmic protein FtsA (Fig. 1.7). Its sequence and structure are similar to the ATPase superfamily of proteins that contains actin, sugar kinase and the Hsp70 family of heat shock proteins (Bork *et al.*, 1992). FtsA is believed to support the formation and stabilization of Z rings by interacting directly with the C-terminus of FtsZ, as demonstrated by yeast two-hybrid interaction studies (Di Lallo *et al.*, 2003; Din *et al.*, 1998; Ma *et al.*, 1996; Yan *et al.*, 2000). In *E. coli* FtsA is an essential protein while in *B. subtilis*, although an *ftsA* mutant displays a highly filamentous phenotype, it is not essential (Harry *et al.*, 2006).

The second early recruited protein, ZipA (for Fts**Z** interacting protein **A**), in *E. coli* divisome assembly is a membrane protein with an unusual N-terminal membrane anchor and a large C-terminal cytoplasmic domain (Errington *et al.*, 2003). Although ZipA is essential for division in *E. coli*, it is a poorly conserved protein, found only in the γ-proteobacteria (Margolin, 2000). ZipA directly interacts with FtsZ and localizes to the Z ring in an FtsZ-dependent, FtsA-independent manner (Hale and de Boer, 1997, 1999). Although, FtsA and ZipA are needed for septal constriction, a Z ring is formed in the presence of either ZipA or FtsA but not in the absence both proteins, suggesting some redundant role of these proteins in Z ring assembly (Pichoff and Lutkenhaus, 2002). No ZipA homologue is found in *B. subtilis* (Margolin, 2000). Recently, a new protein SepF (YlmF), has been identified as an FtsZ interacting protein in *B. subtilis* and shown to localize at the site of cell division in FtsZ dependent manner (Hamoen *et al.*, 2006; Ishikawa *et al.*, 2006).

The EzrA protein, identified as a negative regulator in *B. subtilis* is a transmembrane protein, topologically similar to ZipA protein (Levin *et al.*, 1999). It is conserved in several gram-positive bacteria with low genomic content of G+C nucleotides (Levin *et al.*, 1999). EzrA is distributed evenly throughout the plasma membrane and concentrates at the cytokinetic ring in an FtsZ-dependent manner during cell division (Levin *et al.*, 1999). Loss of EzrA results in the formation of multiple Z rings, located at the middle as well as at the poles (Levin *et al.*, 1999). It directly interacts with FtsZ *in vitro* to inhibit FtsZ polymerization (Haeusser *et al.*, 2004). Recently, it has been shown that the interaction between EzrA and FtsZ reduces the GTP-binding ability of FtsZ and also accelerates the rate of GTP hydrolysis by EzrA,

both of which are unfavorable for the polymerization of FtsZ (Chung *et al.*, 2007). EzrA has also been suggested to act as a positive regulator of cell division because a low level expression of EzrA partially inhibited cell division and resulted in a filamentous phenotype (Chung *et al.*, 2004).

The next proteins recruited to the division site, FtsE and FtsX, are related to the ABC transporter superfamily of proteins. They are known to interact with one another to form a complex and require FtsZ, FtsA and ZipA for their localization at the midcell (Schmidt *et al.*, 2004). ZapA, a **Z** ring **a**ssociated **p**rotein, is a widely conserved small cytoplasmic protein that is also believed to interact directly with FtsZ. It is not essential for cell division and not required for subsequent localization of downstream division proteins (Gueiros-Filho and Losick, 2002). Recently, a new FtsZ interacting protein, ZapB, has been identified that is required to maintain normal cell length and to promote Z ring assembly. It is a homodimeric coiled-coil protein and requires FtsZ but not FtsA, ZipA or FtsI for its localization at the division site (Ebersbach *et al.*, 2008). The function and position of ZapB in the divisome is not known.

FtsK is a large multifunctional polytopic membrane protein containing three distinct domains. In *E. coli*, the N-terminal domain and a central linker domain function in cell division while the C-terminal domain is an ATP-dependent translocase involved in chromosome separation (Begg *et al.*, 1995; Bigot *et al.*, 2004). It is fairly well conserved among bacteria (Margolin, 2000). FtsK requires FtsZ, FtsA and ZipA for its localization to the division site in *E. coli*. The FtsK homologue in *B. subtilis*, SpoIIIE, has been shown to be involved in chromosome segregation and membrane fusion only during sporulation (Liu *et al.*, 2006; Sharp and Pogliano, 2003; Wu and Errington, 1997).

In *E. coli*, three bitopic proteins FtsQ, FtsL and FtsB are recruited to the Z ring subsequent to the localization of FtsK (Weiss, 2004). Homologues of these proteins in *B. subtilis* are DivIB, FtsL and DivIC, respectively (Errington *et al.*, 2003). Topologically, these three proteins of both organisms are similar and contain a short N-terminal cytoplasmic region, a single transmembrane segment and a large C-terminal periplasmic domain. In both the organisms the proteins are believed to form a complex prior to their localization to division site (Buddelmeijer and Beckwith, 2004; Chen *et al.*, 1999; Chen and Beckwith, 2001; Daniel *et al.*, 2006). In *E. coli*, FtsQ is essential for survival while its *B. subtilis* homologue, DivIB is essential only for cell survival at high

temperatures (Katis *et al.*, 2000). FtsQ relies on FtsZ, FtsA, ZipA and FtsK for its localization to the Z ring (Chen and Beckwith, 2001). Recently, structural and mutational analysis of *E. coli* FtsQ and *B. subtilis* DivIB have identified three functional subdomains (α, β and γ in *B. subtilis*) in their large periplasmic domain that are involved in interaction with many cell divisome proteins, thus suggesting their role in recruitment and stabilization of other division proteins (D'Ulisse *et al.*, 2007; Robson and King, 2006; van den Ent *et al.*, 2008; Wadsworth *et al.*, 2008). FtsL and FtsB (DivIC in *B. subtilis*) are also essential for viability in their respective organisms (*E. coli* and *B. subtilis*) (Daniel *et al.*, 1998; Guzman *et al.*, 1992; Levin and Losick, 1994). Periplasmic domains of FtsL, FtsB and DivIC contain putative leucine zipper coiled-coil motifs that are usually involved in protein-protein interactions (Buddelmeijer *et al.*, 2002; Daniel and Errington, 2000; Ghigo and Beckwith, 2000). In *B. subtilis* it has been shown that four proteins, FtsL, DivIC, DivIB, and PBP 2B, are interdependent for assembly. This contrasts with the mainly linear assembly pathway for the equivalent proteins in *E. coli* (Errington *et al.*, 2003).

Subsequent to FtsQ, FtsL and FtsB complex localization in *E. coli*, FtsW and FtsI (PBP3) proteins are recruited to the divisome site (Vicente and Rico, 2006; Vicente *et al.*, 2006). These proteins are believed to interact prior to their localization to Z ring (Goehring *et al.*, 2006). FtsW is a member of a large family of polytopic membrane proteins involved in determining cell **s**hape, **e**longation, **d**ivision and **s**porulation (SEDS) (Henriques *et al.*, 1998; Ikeda *et al.*, 1989). It is a highly conserved protein. The precise role of FtsW is not clear; however it is proposed to recruit FtsI protein (Mercer and Weiss, 2002). Previously, interaction between FtsW and FtsZ has been suggested in *E. coli,* but no further evidence has been reported (Boyle *et al.*, 1997). Another member of the SEDS family proteins found in *E. coli* is RodA, which is involved in cell elongation. In *B. subtilis*, there are three SEDS proteins: sproulation specific, SpoVE, required for cortex formation; RodA, involved in elongation; and FtsW (YlaO) a functional homologue of *E. coli* FtsW (Errington *et al.*, 2003; Henriques *et al.*, 1992; Henriques *et al.*, 1998). FtsI (PBP3), in *E. coli* and its homologue, PBP 2B, in *B. subtilis* are class B penicillin-binding proteins (PBPs) with transpeptidase activity (Daniel *et al.*, 2000; Errington *et al.*, 2003; Harry *et al.*, 2006). Both, FtsI and PBP 2B are involved in septum specific peptidoglycane synthesis (Harry *et al.*, 2006).

Localization of FtsI requires FtsZ, FtsA, FtsQ, FtsW and FtsL (Mercer and Weiss, 2002; Weiss *et al.*, 1999).

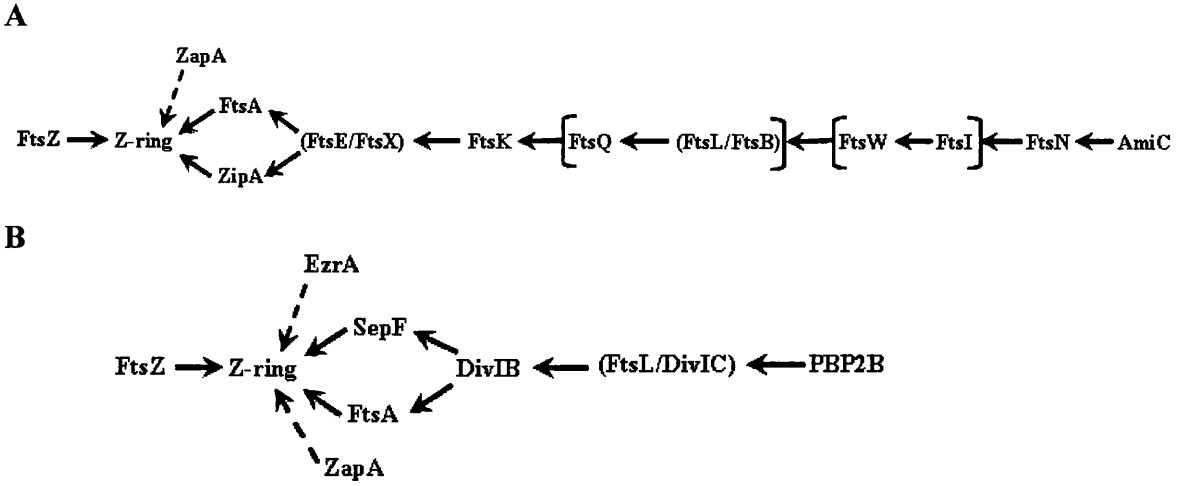

Figure 1.7: Divisome assembly pathway in *E. coli* and *B. subtilis*. (A) In *E. coli* a proto-ring is formed by interaction between three proteins (FtsZ, FtsA and ZipA) assembling on the cytoplasmic membrane, that is followed by the addition of FtsK to form the cytoplasmic ring. At a late assembly stage additional elements forming a periplasmic connector (FtsQ, FtsB and FtsL) and the proteins of the ring involved in manufacturing septal peptidoglycan (FtsW and FtsI) are added, followed by FtsN, as a ring protruding into the periplasm and connecting with the peptidoglycan layer. FtsL and FtsB, presented in small bracket can contact with each other independently of the FtsQ prior to forming a complex (present in big bracket) with FtsQ. (B) In *B. subtilis* the divisome assembles in a much more concerted manner. Similar to *E. coli* proto-ring is formed by interaction of FtsZ, FtsA, SepF and EzrA. Once the Z ring has formed the late recruited proteins (DivIB, FtsL, DivIC and PBP 2P) are localized interdependently, forming the divisome. Dashed arrows indicate that a protein is not required for downstream recruitment but is involved in forming or stabilizing the Z ring. In *B. subtilis* there is not apparent homologue of FtsN and the FtsK homologue (SpoIIIE) is not required for division. (Errington *et al.*, 2003; Goehring *et al.*, 2006; Harry *et al.*, 2006)

FtsN is the last bitopic membrane protein known to localize at the division site in *E. coli* (Addinall *et al.*, 1997). It is a poorly conserved protein being found only in enteric bacteria and *Haemophilus* spp. (Errington *et al.*, 2003). The localization of FtsN is dependent on FtsZ, FtsA, FtsI and FtsQ (Addinall *et al.*, 1997). The function of FtsN is unknown. However, it shows limited sequence similarity to cell wall amidases,

suggesting a possible role in cell wall hydrolysis (Errington *et al.*, 2003). Finally, two periplasmic proteins AmiC and EnvC are recruited to *E. coli* division ring (Bernhardt and de Boer, 2003, 2004). The localization of AmiC is dependent on FtsN. AmiC is an N-acetylmuramoyl-L-alanine amidase that specifically degrades the septal cell wall and allows the separation of two daughter cells (Bernhardt and de Boer, 2003). EnvC has been shown to have murein hydrolase activity, suggesting its role in daughter cell separation (Bernhardt and de Boer, 2004).

For many years the recruitment pathway of divisome proteins in *E. coli* was predicted to be in a strict linear order (Buddelmeijer and Beckwith, 2002). However, recent studies suggest that assembly of *E. coli* divisome proteins (especially late proteins) involve the formation of complexes, which are assembled in a hierarchical manner (Fig. 1.7A) (Aarsman *et al.*, 2005; Goehring *et al.*, 2005; Goehring *et al.*, 2006). Thus, during Z ring assembly a proto-ring is first formed by concerted assembly of FtsZ, FtsA and ZipA. FtsK is recruited to proto-ring to form a cytoplasmic ring. Later, a complex of three proteins, FtsQ, FtsL and FtsB, is incorporated to the cytoplasmic ring, which acts as a connecter between the cytoplasmic ring and late recruited proteins. Subsequently, FtsW and FtsI proteins involved in septal peptidoglycan synthesis are added. Finally, FtsN is recruited connecting the ring with peptidoglycan (Goehring *et al.*, 2006; Vicente and Rico, 2006).

In contrast to *E. coli* divisome assembly, many divisome proteins (DivIB, DivIC, FtsL PBP 2B and possibly FtsW) of *B. subtilis* are completely interdependent on one another for assembly at the division site (Errington *et al.*, 2003). Assembly of all these proteins is prevented by mutating or depleting just one of the proteins (Errington *et al.*, 2003).

1.7.2 Asymmetric Septation during Sporulation

In addition to midcell division, *B. subtilis* undergoes asymmetric septation during its sporulation cycle that is regulated by the complex regulatory cascade of sporulation specific proteins (Levin and Grossman, 1998; Piggot and Hilbert, 2004). Sporulation sepation takes place by relocalization of the Z-ring from its midcell position to polar sites through a spiral intermediate (Ben-Yehuda and Losick, 2002). This

migration of the Z-ring from the middle position to the cell poles is initiated by the activity of SpoIIE, which is expressed under Spo0A control (Barak and Youngman, 1996; Khvorova *et al.*, 1998). SpoIIE is a polytopic membrane protein with its central domain involved in oligomerization and in interaction with FtsZ (Lucet *et al.*, 2000). Fluorescence microscopy of a SpoIIE-GFP fusion showed localization at the asymmetric septum in the form of a ring (Arigoni *et al.*, 1995). A probable role of SpoIIE in sporulation septation is activation of bipolar Z ring formation and/or stabilization of the rings once formed. It is also believed to serve as a membrane anchor for the Z ring, similar to ZipA in *E. coli* cell division (Barak and Wilkinson, 2007). After the formation of the FtsZ and SpoIIE ring, all the division machinery, responsible for mid cell division, is assembled at the cell poles (Barak and Wilkinson, 2007). The assembly pathway of both vegetative and sporulation division proteins appears to be similar (Barak and Wilkinson, 2007). Although sporulation septation resembles vegetative septation, the mechanism regulating accurate positioning of the division machinery during sporulation is unclear.

1.7.3 Spatial Control of Z-ring Positioning

In bacterial cell division, control of timing and placement of the septum is an important process, which is attained primarily by regulating Z ring assembly. There are two well known mechanisms responsible for accurate positioning of the Z ring in *E. coli* and *B. subtilis*: the Min system that specifically prevents asymmetric septation during vegetative growth and nucleoid occlusion that inhibits Z ring assembly at the midcell (Fig. 1.8) (Barak and Wilkinson, 2007; Errington *et al.*, 2003; Harry *et al.*, 2006; Margolin, 2001; Rothfield *et al.*, 2005).

(I) The Min System

The Min system consists of three proteins, MinC, MinD and MinE that are encoded by the *minCDE* locus in *E. coli* as well as in many other bacteria (Margolin, 2001). MinC and MinD form a complex, MinCD, which acts as a non-specific inhibitor of Z ring assembly at all potential division sites in the cell (de Boer *et al.*, 1989). MinC

interacts directly with FtsZ and inhibits FtsZ polymerization, while MinD, a membrane-associated ATPase, is required for concentrating MinC at the membrane of cell poles (Hu and Lutkenhaus, 1999; Marston and Errington, 1999; Wang *et al.*, 1999). MinE imparts topological specificity to MinCD by preventing the localization of MinCD at the midcell, where MinE localizes, in an FtsZ-independent manner, as a ring adjacent to the midcell septation site (Raskin and de Boer, 1997). The Min system in *E. coli* is highly dynamic and oscillates very rapidly, with pole to pole oscillation of MinCD and somewhat restricted side to side oscillation of the MinE ring about the midcell (Fig. 1.8A). Thus, MinE sweeps the MinCD complex from one pole to the other in a periodic

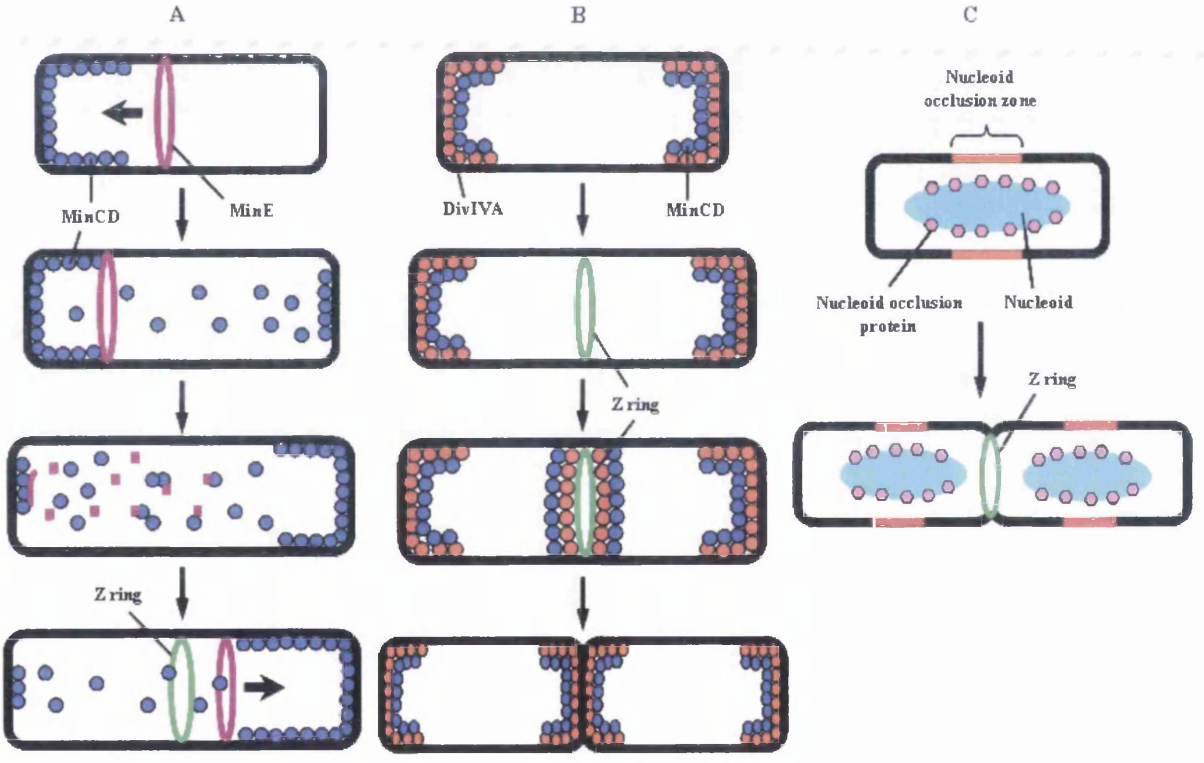

Figure 1.8: The Min system and nucleoid occlusion system in *E. coli* and *B. subtilis*. (A) In *E. coli*, MinE (violet) acts as a topological regulator of MinCD division inhibitor complex (blue) by sweeping the complex from one pole to other. (B) In *B. subtilis*, DivIV (red) directs the MinCD division inhibitor complex (blue) to the cell poles, allowing Z ring formation to occur only at the midcell position. Once the Z ring (green) and the divisome are assembled, DivIVA recruits the MinCD complex to midcell. After completion of division, DivIVA retains MinCD at the poles to inhibit the division at the poles in subsequent cycle. (C) In the nucleoid occlusion system of both the bacteria, nucleoid occlusion proteins (Noc or SlmA, small pink ovals), associated with the nucleoid form a nucleoid occlusion zone (red line) in the vicinity of nucleoid (light blue) and block the cell division. (Harry *et al.*, 2006; Rothfield *et al.*, 2005)

manner. Oscillation of MinCD depends on MinE, and the midcell localization of MinE depends on MinD (Errington *et al.*, 2003; Hu and Lutkenhaus, 1999; Raskin and de Boer, 1999). Recently, it has been shown that the dynamic nature of Min protein distribution occurs in the form of long helical arrangements instead of assembly and disassembly at the cell membrane near each poles (Rothfield *et al.*, 2005; Shih *et al.*, 2003). In *B. subtilis*, homologues of MinC and MinD are present but there is no MinE (Barak and Wilkinson, 2007; Harry *et al.*, 2006). As in *E. coli*, MinCD acts as a division inhibitor by preventing Z ring assembly (Fig. 1.8B) (Marston and Errington, 1999). The function of MinE in topological control of MinCD activity is provided by a non-homologues protein, DivIVA (Cha and Stewart, 1997; Edwards and Errington, 1997; Marston and Errington, 1999; Rothfield *et al.*, 2005). It is a cytoplasmic protein containing an α-helical coiled-coil domain whose homologues are found in gram-positive bacteria (Muchova *et al.*, 2002; Rigden *et al.*, 2008). DivIVA is stably associated with the membrane at the cell poles and localizes MinCD to the poles probably by a direct interaction with MinD (Barak and Wilkinson, 2007; Rothfield *et al.*, 2005). In contrast to *E. coli* MinCD, there is no oscillation of this complex in *B. subtilis.* Another difference with the *B. subtilis* Min system is that MinCD and DivIVA are also recruited to the Z ring after it forms, where they stay attached to the ring until after cell division (Barak and Wilkinson, 2007; Harry *et al.*, 2006; Rothfield *et al.*, 2005). A second function of DivIVA in *B. subtilis* has been suggested by analysis of *divIVA* mutants that produced prespore compartments devoid of DNA with a high frequency, indicating that DivIVA has a role in localizing or attaching the *oriC* region of the chromosome to the cell pole during sporulation (Errington, 2001; Thomaides *et al.*, 2001). The mechanism of DivIVA localization to the poles is not known.

(II) Nucleoid Occlusion

The second negative regulation of cell division occurs in nonpolar regions, where centrally located chromosomes (nucleoid) prevent the formation of a septum in their vicinity, a mechanism known as nucleoid occlusion (Fig. 1.8C) (Woldringh *et al.*, 1991). As with the Min system, nucleoid occlusion occurs at the level of Z ring assembly in both *E. coli* and *B. subtilis* (Harry *et al.*, 2006). Recently, two genes, *noc* and *slmA*, that encode specific effectors responsible for nucleoid occlusion have been identified in *B. subtilis* and *E. coli,* respectively (Bernhardt and de Boer, 2005; Wu and

Errington, 2004). The proteins, Noc and SlmA, encoded by *noc* and *slmA* genes, respectively, are associated non-specifically with the chromosome (Bernhardt and de Boer, 2005; Wu and Errington, 2004). These proteins function by preventing FtsZ polymerization or accumulation in the vicinity of the nucleoid (Bernhardt and de Boer, 2005; Wu and Errington, 2004). Although, the two proteins perform similar function, Noc and SlmA belong to completely different families of DNA binding proteins and there is no significant sequence similarity between them (Barak and Wilkinson, 2007; Harry *et al.*, 2006).

1.8 Shape Determination in Bacteria

Over the course of the cell cycle, rod shaped bacteria such as *E. coli* and *B. subtilis* undergoes successive cycles of elongation and cell division. Cell elongation requires lateral extension of the murein sacculus by intercalation of new glycan strands into the pre-existing shell. When the cell acquires double the length of its original legth, elongation ceases and the division process commences where the cell switches to septal cell wall synthesis at the midcell position that will divide the cell into two daughter cells (Scheffers and Pinho, 2005). Genetic studies have identified a number of genes involved in cell shape determination. Some of these genes encode proteins involved in peptidoglycan synthesis and remodelling, such as penicillin binding proteins (PBPs), while other encode proteins that are members of bacterial cytoskeletal system like MreB and Mbl (Formstone and Errington, 2005; Scheffers and Pinho, 2005; Spratt, 1975; Tamaki *et al.*, 1980). However, the cell shape also depends on membrane bound shape determinants, such as RodA, MreC and MreD of unknown function (Carballido-Lopez and Formstone, 2007; Henriques *et al.*, 1998; Kruse *et al.*, 2005; Osborn and Rothfield, 2007).

The rod-shaped bacteria contain *mreBCD* genes organized as an operon that encode proteins required for cell shape determination (Figge *et al.*, 2004; Jones *et al.*, 2001; Kruse *et al.*, 2005; Leaver and Errington, 2005; Shih and Rothfield, 2006). In most of the bacteria *mre*-encoded proteins appear to be essential for viability (Carballido-Lopez, 2006; Kruse *et al.*, 2005; Leaver and Errington, 2005). The MreB protein is a prokaryotic actin homologue that forms a dynamic helical filamentous

structure just underneath the cytoplasmic membrane extending form one pole to the other (Cabeen and Jacobs-Wagner, 2005; Carballido-Lopez and Errington, 2003; Jones *et al.*, 2001). Some bacterial species, such as *E. coli, Caulobacter crescentus*, contain only one MreB, while others contain multiple copies of MreB-like proteins (Moller-Jensen and Lowe, 2005; Shih and Rothfield, 2006). For example, *B. subtilis* has three MreB homologues, MreB, Mbl (**MreB-l**ike) and MreBH (**MreB h**omologue), which colocalize and are able to interact with each other (Defeu Soufo and Graumann, 2006). Depletion of MreB or MreB homologues in *B. subtilis*, *E. coli*, and *C. crescentus* leads to loss of the normal rod shape, with the formation of spherical cells that finally undergo lysis (Figge *et al.*, 2004; Jones *et al.*, 2001; Kruse *et al.*, 2005). In *B. subtilis,* loss of *mbl* also results in extremely deformed cell morphologies with large bulges and irregular increase in cell width (Formstone and Errington, 2005; Jones *et al.*, 2001). Microscopic analysis, using fluorescent labelled vancomycin that binds to nascent peptidoglycan in gram-positive bacteria, showed helical pattern of murein synthesis over the cylindrical surface of the cell in *B. subtilis* and the cell wall synthesis was dependent on presence of Mbl (Daniel and Errington, 2003; Tiyanont *et al.*, 2006). The outer membrane in Gram-negative bacteria is not permeable to fluorescent vancomycin, however, studies of murein deposition in *E. coli* using an alternative technique, d-cysteine labelling, also revealed a coiled pattern of cell wall synthesis (de Pedro *et al.*, 1997; De Pedro *et al.*, 2003). *In situ* localization studies of GFP-tagged PBP2, a transpeptidase required for lateral cell wall synthesis, have shown a similar helical distribution pattern to that of MreB and Mbl (Den Blaauwen *et al.*, 2003; Divakaruni *et al.*, 2005; Dye *et al.*, 2005; Figge *et al.*, 2004). Localization of PBP2 in a helical pattern depends on MreB and MreC, indicating the important role of MreB and MreC in distribution of PBP2 across the cell (Divakaruni *et al.*, 2005; Figge *et al.*, 2004). In addition to control of cell shape, MreB has also been shown to involve in localization of specific proteins, which are implicated in chemotaxis, motility, secretion and virulence, to one or both the cell poles (Shih and Rothfield, 2006). The mechanism of polar targeting of these proteins by MreB is not known. Furthermore, the experimental evidences have also suggested the role of MreB in chromosome segregation (Gitai *et al.*, 2005; Kruse *et al.*, 2003). In *E. coli* and *C. crescentus*, MreB depletion affects the segregation of the replication origin and terminus regions of newly replicated chromosomes, resulting in multi-nucleated or anucleated or incompletely partitioned nucleoid cells (Gitai *et al.*, 2005; Kruse *et al.*,

2003; Shih and Rothfield, 2006). MreBH has been shown to have a specialized function in directing lateral cell wall hydrolysis by localizing the peptidoglycan hydrolase LytE in a helical structure over the cell cylinder (Carballido-Lopez *et al.*, 2006).

MreC is a bitopic membrane protein with a large periplasmic domain and MreD is an integral membrane protein (den Blaauwen *et al.*, 2008). Bacterial two-hybrid analyses have shown that MreC interacts with itself, presumably forming a dimer. It also interacts with MreB and with MreD, whereas MreB does not with MreD (Kruse *et al.*, 2005). The interaction of the three proteins is essential for lateral growth as depletion of each of these proteins is sufficient for spherical growth. Thus, MreC and MreD appear to act as a link between the MreB cytoskeleton and the cell wall biosynthesis machinery.

1.9 Role of SEDS Proteins and their cognate PBPs in Cell Wall Synthesis

The bacterial cell wall is composed of glycan polymers interconnected by peptide side chains via peptide bonds. Synthesis of peptidoglycan begins in the cytoplasm where peptidoglycan precursors, uridine diphosphate-N-acetylglucosamine (UDP-GlcNAc) and uridine diphosphate-N-acetylmuramyl-pentapeptide (UDP-MurNAc-pentapeptide) are synthesized. UDP-MurNAc-pentapeptide is linked to undecaprenyl phosphate to form lipid I intermediate at the cytoplasmic membrane. Then, N-acetylglucoseamine (GlcNAc) from UDP-GlcNAc is added to lipid I producing lipid II that is transported to periplasmic space across the membrane by some unknown mechanism, which could involve SEDS family proteins (Scheffers and Pinho, 2005). The final stage of cell wall synthesis takes place outside of the cytoplasmic membrane and involves polymerization of newly synthesized disaccharide pentapeptide units and incorporation into the growing peptidoglycan. This is mainly performed by penicillin-binding proteins (PBPs) which catalyze the transglycosylation and transpeptidation reactions responsible for the formation of the glycosidic and peptide bonds of peptidoglycan, respectively (Nanninga, 1998; Scheffers and Pinho, 2005). The two modes of cell wall synthesis, elongation and septation, in rod-shaped bacteria appear to be catalyzed by different protein complexes (Scheffers and Pinho, 2005).

Several components of cell wall synthesis complexes have been described above briefly. PBPs and SEDS family proteins are among the most intensely studied proteins from the cell wall synthesis complexes.

PBPs belong to the acyl serine transferase protein family that includes high molecular weight (HMW) PBPs, low molecular weight (LMW) PBPs and β-lactamases (Scheffers and Pinho, 2005). HMW PBPs are multidomain proteins composed of a cytoplasmic tail, a transmembrane anchor and two domains joined by a β- rich linker located on the outer surface of the cyotplasmic membrane where peptidoglycan synthesis takes place (Goffin and Ghuysen, 1998; Macheboeuf *et al.*, 2006; Sauvage *et al.*, 2008). Depending on the primary structure and the catalytic activity of their N-terminal domain, HMW PBPs are divided into two major classes, namely class A and class B (Goffin and Ghuysen, 1998; Sauvage *et al.*, 2008). Class A HMW PBPs (eg. PBP 1A and PBP 1B of *E. coli*) are bifunctional with both glycosyltransferase and transpeptidase activities, where transpeptidase activity is provided by the C-terminal domain and glycosyltransferase activity is provided by the N-terminal domain (Sauvage *et al.*, 2008; Scheffers and Pinho, 2005). Class B HMW PBPs, which includes PBP2 and PBP3 (FtsI) from *E. coli*, exhibit transpeptidase activity only, at their C-terminal domain (Sauvage *et al.*, 2008). The N-terminal domain of class B HMW PBPs is believed to act as a morphogenetic determinant by proper folding and stabilizing the penicillin-binding domain and interacting with other cell cycle proteins (den Blaauwen *et al.*, 2008; Nguyen-Disteche *et al.*, 1998).

LMW PBPs are monofunctional DD-peptidases, where most of them act as DD-carboxypeptidases, however, some exhibit transpeptidase or endopeptidase activity (Sauvage *et al.*, 2008; Scheffers and Pinho, 2005). As a whole LMW PBPs are frequently described with the general term of class C PBPs. Unlike HMW PBPs, LMW PBPs are not involved in peptidoglycan synthesis but help to modify the peptidoglycan by hydrolysis of carboxy-terminal D-alanyl-D-alanine peptide bond of pentapeptide sidechains (DD-carboxypeptidases), thus making the peptide side chains inaccessible for cross-linking or by breaking the peptide crosslinks that hold the glycan chains together (endopeptidases) (den Blaauwen *et al.*, 2008; Scheffers and Pinho, 2005). In *E. coli*, mutants lacking multiple LMW PBPs exhibited extensive and severe morphological aberrations, indicating the fundamental role for these proteins in regulating cell shape (den Blaauwen *et al.*, 2008; Nelson and Young, 2001).

As mentioned earlier, SEDS family proteins are polytopic membrane proteins that are involved in determination of cell shape, elongation, division and sporulation (Henriques *et al.*, 1998). Members of this protein family are present in all the bacteria that have a peptidoglycan cell wall (Henriques *et al.*, 1998). The gene encoding a member of the SEDS family proteins is frequently located close to the gene encoding a member of class B HMW PBPs and each SEDS protein appears to work in conjunction with a specific class B HMW PBP (Datta *et al.*, 2006; Hara *et al.*, 1997; Matsuzawa *et al.*, 1989; Mercer and Weiss, 2002). Examples of such pairs are RodA and PBP2, responsible for cell elongation and FtsW and FtsI (PBP3), responsible for cell division in *E. coli* (Hara *et al.*, 1997; Matsuzawa *et al.*, 1989; Mercer and Weiss, 2002; Tamaki *et al.*, 1980). FtsW in *E. coli* is required to recruit FtsI at the division site (Mercer and Weiss, 2002). In addition to its role in FtsI localization, it has been suggested that *E. coli* FtsW is required for Z ring stabilization, however, no further evidence of direct interaction between FtsW and FtsZ has been reported (Boyle *et al.*, 1997). Interestingly, interaction between FtsW and FtsZ of *M. tuberculosis* has been shown (Datta *et al.*, 2002; Datta *et al.*, 2006; Rajagopalan *et al.*, 2005). However, this interaction is mediated through a C-terminal extensions of FtsW and FtsZ, which are absent from the homologues of most other bacteria (Datta *et al.*, 2006; Harry *et al.*, 2006). FtsW of *M. tuberculosis* has also been shown to interact with FtsI (Datta *et al.*, 2006). Both proteins, PBP2 and RodA, are encoded by the *pbpA-rodA* operon in *E. coli* and mutations in *rodA* or *pbpA* or specific inactivation of PBP2 results in spherical growth, suggesting the specific role of both the proteins in cell elongation (Spratt, 1975; Tamaki *et al.*, 1980). Similarly, depletion of RodA in *B. subtilis* also caused formation of spherical cells that are eventually lysed (Henriques *et al.*, 1998). On the other hand, inactivation of FtsW or FtsI protein blocks cell division, resulting in filamentous morphology, indicating their involvement in septation specific cell wall synthesis (Boyle *et al.*, 1997). FtsW and RodA are essential for viability in most bacteria (Boyle *et al.*, 1997; Gerard *et al.*, 2002; Henriques *et al.*, 1998). In *B. subtilis,* another SEDS protein homologue, SpoVE, and its cognate class B PBP, SpoVD, are required during the sporulation process (Ikeda *et al.*, 1989; Joris *et al.*, 1990). Synthesis of the spore cortex was completely blocked in SpoVE mutants but there was no effect on vegetative growth (Henriques *et al.*, 1992). Disruption of SpoVD severely affected the spore cortex formation in the organism (Daniel *et al.*, 1994). Interestingly, the genes encoding

SpoVE and SpoVD are located in the *dcw* cluster of spore-forming bacteria, where *spoVE* occupies the position of *ftsW* in the cluster indicating the importance of coordinated expression of *dcw* genes for spore cortex synthesis (Henriques *et al.*, 1992; Real *et al.*, 2008).

The topologies of *E. coli, Streptococcus pneumoniae* and *M. tuberculosis* FtsW proteins and *B. subtilis* SpoVE protein have been determinted experimentally (Datta *et al.*, 2006; Gerard *et al.*, 2002; Lara and Ayala, 2002; Real *et al.*, 2008). All these proteins contain 10 transmembrane (TM) segments, a large extracytoplasmic loop (except *M. tuberculosis* FtsW) and N- and C- termini both located in the cytoplasm. Apart from localizing their cognate PBPs, other proposed functions of SEDS proteins are; (1) Z ring stabilization (Boyle *et al.*, 1997; Datta *et al.*, 2006); (2) to integrate signals between the cytoplasmic and periplasmic components of the division by linking them together (Margolin, 2000); (3) translocation of the lipid-linked peptidoglycan precursor through the cytoplasmic membrane (Pastoret *et al.*, 2004; Real *et al.*, 2008). Less is known about the mechanism of SEDS protein targeting to the specific location.

1.10 Growth and Division in *S. coelicolor*

Streptomycetes markedly differ from most other bacteria in their growth and division biology. Different aspects of growth and division in streptomycetes have been extensively studied for several years, using *S. coelicolor* as a model organism. Being mycelial prokaryotes, *S. coelicolor* and other actinomycetes grow asymmetrically by incorporation of new peptidoglycan material at the tip and sub-apical branching of hyphae to form branched mycelium (Flardh, 2003a, 2003b; Gray *et al.*, 1990; Schwedock *et al.*, 1997). In the feeding vegetative mycelium of *Streptomyces,* cross-wall formation is relatively infrequent forming multigenomic compartments. A sub-apical cell disconnected from the apical compartment by such a cross-wall formation can grow by creating a new lateral branch. The molecular basis of tip extension in *Streptomyces* remains unclear. Flardh in 2003 identified an essential component, DivIVA, of an apical protein complex required for tip extension in *S. coelicolor* (Table 1.6). Localization studies of a DivIVA-EGFP (Enhanced Green Fluorescent Protein)

Table 1.6: Cell division and cell wall synthesis related genes in *E. coli, B. subtilis* and *S. coelicolor.*

***E. coli* Gene**	**Homologue in *B. subtilis***	**Homologue in *S. coelicolor***
ftsZ	*ftsZ*	SCO2082 *(ftsZ)*
ftsA	*ftsA*	NP
zipA	*NP*	NP
zapA	*zapA*	NP
zapB	*?*	?
?	*ezrA*	NP
ftsE	*ftsE*	SCO2969 *(ftsE)*
ftsX	*?*	SCO2968 *(ftsX)*
ftsK	*spoIIIE*	SCO5750
ftsQ	*divIB*	SCO2083 *(ftsQ)*
ftsL	*ftsL*	SCO2091 *(ftsL)*
ftsB (formerly *ygbQ)*	*divIC*	SCO3095 *(divIVC)*
ftsW *rodA*	*dtsW (ylaO) & spoVE* *rodA*	SCO2085 *(ftsW)* SCO3846 SCO2607 *(sfr)* SCO5302
ftsI	*Pbp2B & spoVD*	SCO2090
ftsN	*NP*	NP
?	*sepF*	?
minC	*minC*	NP
minD	*minD*	SCO5006 SCO3557
minE	*NP*	NP
NP	*divIVA*	SCO2077 *(divIVA)*
mreB	*mreB* *mbl* *mreBH*	SCO2611 SCO2451
mreC	*mreC*	SCO2610
mreD	*mreD*	SCO2609

NP: Not Present; ?: Other homologues may exist

fusion showed distinctive localization of the protein at the hyphal tips and lateral branches. Partial depletion of the protein resulted in abnormal polar growth with curly hyphae and apical branching. Overexpression of the protein in preformed hyphae dramatically induced multiple branching and affected cell shape determination at the growing tips, consistent with a role in stimulating tip growth (Flardh, 2003a). Homologues of DivIVA are also found in other rod-shaped actinomycetes such as *M. tuberculosis*, *Corynebacterium glutamicum* and *Brevibacterium lactofermentum* that also grow by apical extension at both poles where the homologue of DivIVA in each respective organism localizes at the poles and is essential for viability (Kang *et al.*, 2008; Letek *et al.*, 2008; Ramos *et al.*, 2003). DivIVA in *C. glutamicum* has also been shown to interact with PBP1a, a HMW class A PBP, suggesting that DivIVA may

function in localizing peptidoglycan synthesis machinery at the cell poles (Valbuena *et al.*, 2007). As explained earlier, the DivIVA homologue in *B. subtilis* has completely different functions. In *B. subtilis*, DivIVA sequesters MinC and MinD at the cell poles, thus participating in the spatial regulation of cell division and in chromosome segregation during sporulation (Barak and Wilkinson, 2007; Thomaides *et al.*, 2001). Interestingly, all sequenced genomes of actinomycetes lack a *bona fide* Min system (Table1.6) (Flardh, 2003b).

Important proteins that direct lateral cell wall synthesis in non-actinomycete rod-shaped bacteria *B. subtilis* are prokaryotic actin homologues MreB and Mbl (Daniel and Errington, 2003). In *S. coelicolor* also there are two actin homologues, MreB and Mbl, which are highly conserved among streptomycetes (Table 1.6) (Mazza *et al.*, 2006; Noens, 2007). Unlike *B. subtilis*, they are nonessential for viability in *S. coelicolor*. Mutants of *mreB* and *mbl* produced spores with abnormal shapes that often germinated prematurely suggesting their role in spore wall synthesis thus maintaining the integrity of the spore wall (Mazza *et al.*, 2006; Noens, 2007). Overexpression of MreB resulted in growth impairment and lysis. Localization studies of MreB-EGFP using fluorescent microscopy showed diffuse fluorescence in vegetative hyphae, indicating its random distribution in vegetative hyphae. In contrast, during aerial growth MreB-EGFP localized to the septa of soprogenic aerial hyphae and subsequently underneath the cytoplasmic membrane of spores (Mazza *et al.*, 2006).

Streptomyces have at least two modes of cell division: (1) vegetative septation leading to crosswall formation in the substrate mycelium without detachment of the daughter cells and (2) developmentally regulated sporulation septation in sporogenic aerial hyphae resulting in unigenomic spore chains (Flardh, 2003b; Kwak *et al.*, 2001). Most of the proteins required for cell division are present in *Streptomyces*, suggesting that the basic mechanism of cell division is similar to that in most other bacteria (Table 1.6) (Flardh, 2003b; Hett and Rubin, 2008). In contrast to other unicellular bacteria such as *B. subtilis, E. coli* and *M. tuberculosis*, cell division in *Streptomyces* is not essential for growth and viability. Deletion mutants of *S. coelicolor ftsZ, ftsQ, ftsK, ftsL, divIC* and *ftsX* genes resulted in viable strains that are defective in different aspects of cell division (Bennett *et al.*, 2007; McCormick *et al.*, 1994; McCormick and Losick, 1996; Noens, 2007; Wang *et al.*, 2007). The *ftsZ* null mutant lacks cross walls in both vegetative and aerial hyphae resulting in typical white phenotype of non-sporulating

hyphae. Lack of cross wall formation in vegetative and aerial hyphae indicates that division process in both the stages may involve same basic cell division machinery (McCormick *et al.*, 1994). Similarly, *ftsQ* deletion mutant is also defective in cell division, although not as severe as *ftsZ* mutant (McCormick and Losick, 1996). FtsL and DivIC mutants are shown to be defective in constriction of division septum, a phenotype that is dependent on the growth medium (Bennett *et al.*, 2007). FtsK protein has been shown to be involved in chromosomal segregation during cell division (Wang *et al.*, 2007). A deletion mutant of *ftsK* produced aberrant colonies that were associated with large deletions from the chromosome. A FtsK-EGFP fusion localized at the sporulation septum after forming distinctive complexes, further supporting the role of FtsK in chromosome segregation (Wang *et al.*, 2007). FtsX, in conjunction with FtsE, is proposed to be involved in the last stage of cell division during autolytic separation of spores (Noens, 2007). Frequent branching close to the base of spore chain has been observed in *ftsX* mutants.

Assembly of Z rings during vegetative and sporulation requires developmental control of *ftsZ* transcription. Isolation of a missense mutation in *ftsZ* that specifically prevented sporulation septation suggests difference in Z-ring assembly during vegetative septation and sporulation septation (Grantcharova *et al.*, 2003). Three putative promoters, *ftsZ1p, ftsZ2p* and *ftsZ3p,* have been detected in the *ftsQ-ftsZ* intergenic region (Flardh *et al.*, 2000). Expression studies revealed that *ftsZ3p* promoter was expressed most intensively during early vegetative growth and its activity decreased gradually during development. On the other hand, promoter *ftsZ2p* was upregulated specifically during sporulating aerial hyphae. Upregulation of *ftsZ2p* promoter requires all the six early developmental regulatory genes (*whiA, B, G, H, I* and *J*), as there was no strong upregulation of *ftsZ2p* promoter in any of the six *whi* mutants. Expression of *ftsZ1p* remained constant and at low level throughout development (Flardh *et al.*, 2000). Similarly, two *ftsZ* promoters have been found in *S. griseus* whose expression patterns correspond to *ftsZ2p* and *ftsZ3p* promoters of *S. coelicolor* (Flardh *et al.*, 2000; Kwak *et al.*, 2001). As an early sporulation event, FtsZ first polymerizes into spirals that are subsequently reorganized into regularly-spaced stable Z rings in a synchronous manner along the sporogenic aerial hyphae (Grantcharova *et al.*, 2005; Schwedock *et al.*, 1997). The synchronous assembly of Z rings in aerial hyphae of *Streptomyces* is intriguing with respect to the absence of the Min system for spatial

regulation of Z ring formation. Nucleoid occlusion, which is responsible for preventing Z ring assembly in the vicinity of chromosome in *E. coli* and *B. subtilis*, appears to have little influence in *Streptomyces* (Flardh, 2003b; Schwedock *et al.*, 1997). It is also interesting to note that there are no apparent orthologs of FtsA, ZipA, ZapA, EzrA and SpoIIE, which are responsible for anchoring and stabilization of the Z ring in *E. coli* and *B. subtilis,* in *Streptomyces* (Table 1.6) (Flardh, 2003b; Harry *et al.*, 2006). The absence of these orthologs from the *Streptomyces* genome raise an important question of how the Z ring localizes and attaches to the membrane, and also suggests that some other protein of the divisome may have aquired these functions or there may be some new proteins involved in these processes, which are still to be investigated. The CrgA and SsgA proteins may function as negative and positive regulators of Z ring assembly, respectively, as overexpression of CrgA protein inhibits the Z ring assembly in aerial hyphae and overexpression of SsgA resulted in hyper-septation in both vegetative and aerial hyphae (Del Sol *et al.*, 2006; Noens *et al.*, 2005; van Wezel *et al.*, 2000b).

1.11 Aims and Objectives

The aim of this investigation is to understand the role of SEDS family proteins and their cognate PBPs during *S. coelicolor* division processes. In this study *S. coelicolor* M145, a prototrophic derivative of *S. coelicolor* A3(2) strain lacking its two plasmids SCP1 and SCP2, is used as a model organism. This organism is in many ways unique and interesting for studying growth and cell division. As is already discussed above, this mycelial organism grows by tip extension and undergoes two distinct types of cell division that are not essential for viability and take place in two different cell types formed during the course of the developmental cycle. Cell division in this organism is under tight control of and highly coordinated with fairly well understood yet complex regulatory mechanisms underlying morphological differentiation. The genes that have been shown to be involved in the assembly of FtsZ into a stable Z ring, a critical early stage for successful cytokinesis in bacteria like *E. coli* and *B. subtilis*, are absent from *Streptomyces*. They are in fact absent from almost all actinomycetes, including mycobacteria. Another important feature is the lack of Min system,

responsible for spatial and temporal regulation of Z ring assembly in *E. coli* and *B. subtilis*, from the *Streptomyces* genome. So far there is no information available about stabilization and regulation of Z rings in space and time during the developmental cycle of *S. coelicolor* or other actinomycetes. Thus, the molecular mechanisms linking the spatial and temporal regulation of cell division with morphological differentiation are also of interest to understand developmental biology of bacteria and should be useful for developing new antibacterial drugs targeting cell division.

As SEDS family proteins play an essentially important role in cell wall synthesis during different aspects of the bacterial life cycle, these proteins have become one of the major topics of research in bacterial growth and division. Publically available complete genome sequence of *S. coelicolor* has facilitated the identification of genes encoding SEDS proteins in this organism. Computational analysis of *S. coelicolor* SEDS protein sequences will provide some clue regarding their structure, function and phylogenetic relationship with different SEDS proteins from other bacteria. Mutation analysis of the genes encoding SEDS family proteins and their cognate PBPs in *S. coelicolor* will provide information about essentiality of the genes for growth and viability. Phenotypic and cytological characterization of the mutants will shed some light on the function of each protein during the complex life cycle of *S. coelicolor*. From the experimental evidence of this study and available information regarding cell division in *S. coelicolor*, we hope to get some more understanding about the growth and division processes in *Streptomyces*.

Chapter - 2

Materials and Methods

2.1 Bacterial strains

Bacterial strains used during this study are listed in Table 2.1.

Table 2.1: Bacterial strains

Strain	Genotype	Transposon insertion* (position in genome)	Source
Escherichia coli JM109	F' *traD36, proA*$^+$*B*$^+$, *lacI*^{q} *Δ(lacZ)M15 Δ(lac-proAB), supE44, gyrA96, recA1, relA1, endA1, thi, hsdR17*	NA	Promega Corp., (Yanisch-Perron *et al.*, 1985)
E. coli BW25113/pIJ790	*E. coli* K12 derivative: *lacI*^{q}, *rrnB, ΔlacZ, hsdR514, ΔaraBAD, ΔrhaBAD,* containing λ-RED recombination plasmid pIJ790	NA	(Datsenko and Wanner, 2000; Gust *et al.*, 2003)
E. coli ET12567 (pUZ8002)	*dam13*::Tn*9 dcm-6, hsdM, hsdR, recF143, zjj201* ::Tn*10, galK2, galT22, ara14, lacY1, xyl-5, leuB6, thi-1, tonA31, rpsL136, hisG4, tsx-78, mtlI, glnV44*, containing the non-transmissible *oriT* mobilizing plasmid pUZ8002	NA	(Flett *et al.*, 1997)
Streptomyces coelicolor M145	Prototrophic; SCP1$^-$, SCP2$^-$, Pgl$^+$	NA	(Kieser *et al.*, 2000)
DSCO3846-1::pSHRCI	M145::pSHRCI *rodA*::Tn*5062*	SCH69.1.E11 (4230660)	This study

* Details of each transposon insertion can be found at http://strepdb.streptomyces.org.uk; NA – Not applicable

Table 2.1: Bacterial strains (Continued)

Strain	Genotype	Transposon insertion* (position in genome)	Source
DSCO3846-2::pSHRCI	M145::pSHRCI *rodA*::Tn*5062*	SCH69.1.H03 (4231825)	This study
DSCO5302-1	M145 *rodA2*::Tn*5062*	SC6G9.1.D07 (5775697)	This study
DSCO5302-2	M145 *rodA2*::Tn*5062*	SC6G9.1.B07 (5774850)	This study
DSCO2607	M145 *sfr*::Tn*5062*	SCC88.2.H10 (2830098)	This study
DSCO2607-hyg^R	M145 *sfr*::Tn*5062-hyg*	SCC88.2.H10 (2830098)	This study
DSCO2611	M145 *mreB*::Tn*5062*	SCC88.1.B06 (2835672)	This study
DSCO5302-1/2607	M145 *rodA2*::Tn*5062*, *sfr*::Tn*5062-hyg*	SC6G9.1.D07 (5775697), SCC88.2.H10 (2830098)	This study
DSCO2608-1	M145 *SCO2608*::Tn*5062*	SCC88.1.C05 (2832285)	This study
DSCO2608-2	M145 *SCO2608*::Tn*5062*	SCC88.2.B04 (2831062)	This study
DSCO2606	M145 *SCO2606*::Tn*5062*	SCC88.2.H08 (2828769)	This study
DSCO2085-1	M145 *ftsW*::Tn*5062* (1)	SC4A10.2.H05 (2239002)	This study
DSCO2085-hyg^R	M145 *ftsW*::Tn*5062-hyg*	SC4A10.2.H05 (2239002)	This study
DSCO2085-2	M145 *ftsW*::Tn*5062* (2)	SC4A10.1.H10 (2238747)	This study
DSCO2085-3	M145 *ftsW*::Tn*5062* (3)	SC4A10.2.F03 (2238425)	This study
DSCO2085-4	M145 *ftsW*::Tn*5062* (4)	SC4A10.2.F08 (2238210)	This study
DSCO2085-5	M145 *ftsW*::Tn*5062* (5)	SC4A10.1.F05 (2237893)	This study
DSCO2085-6	M145 *ftsW*::Tn*5062* (6)	SC4A10.2.F05 (2238043)	This study
DSCO5302-1/2085	M145 *rodA2*::Tn*5062*, *ftsW*::Tn*5062-hyg*	SC6G9.1.D07 (5775697) SC4A10.2.H05 (2239002)	This study
DSCO2607-hyg^R/2085	M145 *sfr*::Tn*5062-hyg*, *ftsW*::Tn*5062*	SCC88.2.H10 (2830098) SC4A10.2.H05 (2239002)	This study
DSCO2090-1	M145 *ftsI*::Tn*5062*	SC4A10.1.C09 (2246734)	This study
DSCO2090-2	M145 *ftsI*::Tn*5062*	SC4A10.2.G05 (2245233)	This study
DSCO2083	M145 *ftsW*::Tn*5062*	SC4A10.2.B05 (2236542)	This study

* Details of each transposon insertion can be found at http://strepdb.streptomyces.org.uk; NA – Not applicable

2.2 Plasmids/Cosmids

Plasmids and cosmids used in this work are listed in Table 2.2. The map and details of construction of respective plasmid originating from this study can be found in the respective results chapters.

Table 2.2: Plasmids and Cosmids

Plasmid/Cosmid	Characteristics	Source
pBluescript II SK (+)	Cloning vector; Ampicillin resistance, lac promoter (*lacZ*), f1, ColE1	Stratagene, (Alting-Mees and Short, 1989)
pBSI1	pBluescript II SK (+) containing *ftsI, ftsL* and *SCO2092*	This study
pBSW1	pBluescript II SK (+) containing *ftsQ, murG, ftsW,* part of *murD* and part of Tn*5062* (excluding *egfp*)	This study
pBSW12	pBluescript II SK (+) containing *ftsW* and part of *murG*	This study
pIJ8600	*tipAp* expression vector, *aac(3)IV, tsr, ori* pUC18, *oriT* RK2, *int* ØC31, *attP* and *tipA* inducible promoter	(Sun *et al.*, 1999)
pIJSFR	pIJ8600 containing *sfr* fused to *tipAp*	This study
pKF41	pIJ8600 containing *ftsZ::egfp*	(Grantcharova *et al.*, 2005)
pQM5066	Ampicillin^R, Hygromycin^R, Tn*5066*	R. Del Sol
pSF152	*E. coli-S. coelicolor* shuttle vector, derivative of pSET152 with streptomycin and spectinomycin resistance marker	P. Herron
pSH152	*E. coli-S. coelicolor* shuttle vector, derivative of pSET152 with hygromycin resistance marker	R. Del Sol
pSFMB1	pSF152 containing *mreB*	This study

Table 2.2: Plasmids and Cosmids (Continued)

Plasmid/Cosmid	Characteristics	Source
pSFTI1	pSH152 containing *ftsI, ftsL* and *SCO2092*	This study
pSFTI2	pSH152 containing *ftsI, ftsL, SCO2092, SCO2093* and part of Tn*5062* (excluding *oriT* and T4t1)	This study
pSFTI3	pSH152 containing *ftsI, ftsL, SCO2092* and *SCO2093*	This study
pSHBW1	pSH152 containing *ftsW, murG* and *ftsQ*	This study
pSHBW12	pSHBW1 with in-frame deletion in *ftsW*	This study
pSHBW4	pSH152 containing *ftsW* and part of *murD*	This study
pSHBW7	pSH152 containing *ftsQ*	This study
pSHRC1	pSH152 containing *SCO3843* to *SCO3847*	This study
pRCLu2	pUWL219 containing *SCO3843* to *SCO3847* and Tn5062 transposon	R. Del Sol
SC4A10	Supercos-1 containing chromosomal DNA from *S. coelicolor, bla, kan*	(Redenbach *et al.*, 1996)
SC4A10.2.E07	SC4A10 cosmid containing Tn*5062* insertion in the non-coding region between *ftsQ* and *ftsZ* genes, *bla, kan, aac3(IV) oriT*(RK), *egfp*	P. Herron
SC4A10.2.H12	SC4A10 cosmid containing Tn*5062* insertion in the non-coding region between *murE* and *ftsI* genes, *bla, kan, aac3(IV) oriT*(RK), *egfp*	P. Herron
SCC88.1.E03	SCC88 cosmid containing Tn*5062* insertion in *SCO2612* gene	P. Herron

2.3 Chemical reagents

Chemicals used during this study were mostly purchased from SIGMA Chemical Company, Fisher Scientific Ltd., BDH Chemicals Ltd. and Molecular Probes. The chemical solutions and buffers were generally prepared using de-ionized water (dH_2O), provided by the MILLI-RO (reverse osmosis) water purification system. Solutions requiring ultra-pure de-ionized water (ddH_2O) were prepared using ddH_2O provided from MILLI-Q water purification system. pH of the solutions was measured at room temperature. Solutions were routinely autoclaved at 121° C, 15 psi for 15 minutes when required. When sterilization of solutions by autoclaving was not possible, solutions were filter sterilized using 0.2 µm Millipore filter units. The components of all the commonly used reagents and buffers are listed in Tables 2.3.

Table 2.3: Reagents and buffers

Reagent/Buffer Solution	**Composition (Final concentration)**	**Quantity in grams per litre of dH_2O (unless otherwise stated)**
10% Glycerol solution (v/v)	100% Glycerol dH_2O	100.00 ml Up to 1.00 l
20% Glycerol solution (v/v)	100% Glycerol dH_2O	100.00 ml Up to 500 ml
10X TBE	Tris Boric Acid EDTA Adjust pH to 8 with HCl	108.00 55.00 9.30
Bromophenol Blue DNA loading dye	Sucrose Bromophenol Blue 1 x TBE dH_2O	40.00 60.00 mg 10.00 ml 90.00 ml
TE buffer	Tris (10 mM) EDTA (1 mM) Adjust pH to 8.0	1.21 372.00 mg
10X concentrated dNTP mix	dATP 10 mM dCTP 10 mM dGTP 10 mM dTTP 10 mM Digoxigenin-11-dUTP dH_2O	7.10 µl 7.10 µl 7.10 µl 7.10 µl 25.00 µl 20.30 µl
10% SDS	Sodium dodecyl sulphate dH_2O	10.00 Up to 100.00 ml

Table 2.3: Reagents and buffers (continued)

Reagent/Buffer Solution	**Composition (Final concentration)**	**Quantity in grams per litre of dH_2O (unless otherwise stated)**
Denaturing Buffer	NaOH (0.5 M) NaCl (1.5 M)	20.00 87.75
Neutralizing Buffer	Tris (1 M) NaCl (1.5 M) Adjust pH to 7.5	121.00 87.75
20X SSC	NaCl (3.0 M) tri- Sodium citrate (0.3 M)	175.50 88.20
Buffer I	Tris (0.1 M) NaCl (0.15 M)	12.10 8.80
Buffer II / prehybridization solution	20 x SSC 10% N-Lauryl sarcosine (w/v) 10% SDS (w/v) Blocking reagent Formamide dH_2O	25.00 ml 1.00 ml 200.00 µl 5.00 50.00 ml 24.00 ml
Wash solution I	20× SSC 10% SDS dH_2O	24.00 ml 2.40 ml 213.60 ml
Wash solution II	20× SSC 10% SDS dH_2O	1.20 ml 2.40 ml 236.40 ml
Colour solution	NBT/ BCIP Tablets (Roche) ddH_2O	1.00 tablet 10.00 ml
Antibody solution	Anti-digoxigenin AP conjugate Buffer I	3.00 µl 15.00 ml
PBS (Phosphate buffer saline)	NaCl (137 mM) KCl (2.7 mM) Na_2HPO_4 (10 mM) KH_2PO_4 (2 mM) Adjust pH to 7.5	8.00 0.20 1.44 0.24
Cell Fixing solution	25% glutaraldehyde solution 40% Formaldehyde solution PBS	2.00 µl 700.00 µl 10.00 ml
Lysozyme solution	Lysozyme 1M Tris 0.5M EDTA 50% Glucose solution dH_2O	20.00 mg 200.00 µl 400.00 µl 180.00 µl 9.20 ml

Table 2.3: Reagents and buffers (continued)

Reagent/Buffer Solution	**Composition (Final concentration)**	**Quantity in grams per litre of dH_2O (unless otherwise stated)**
Fluo–WGA / PI solution	FITC-coupled Wheat Germ Agglutinin solution Propidium Iodide solution 2% BSA in PBS	20.00 µl 4.00 µl 10.00 ml
PI wash solution	PI solution PBS	4.00 µl 10.00 ml
PI solution	Propidium Iodide dH_2O	25.00 mg 1.00 ml
Minor elements solution	$ZnSO_4.7H_2O$ $FeSO_4.7H_2O$ $MnCl_2.4H_2O$ $CaCl_2$ (anhydrous)	1.00 1.00 1.00 1.00
Trace element solution	$ZnCl_2$ $FeCl_3.6H_2O$ $CuCl_2.2H_2O$ $MnCl_2.4H_2O$ $Na_2B_4O_7.10H_2O$ $(NH_4)_6Mo_7O_{24}.4H_2O$	40.00 mg 200.00 mg 10.00 mg 10.00 mg 10.00 mg 10.00 mg
20% Glucose (w/v)	Glucose dH_2O	20.00 Up to 100.00 ml
50% Glucose (w/v)	Glucose dH_2O	50.00 Up to 100.00 ml
1M glucose	Glucose dH_2O	18.00 Up to 100.00 ml
20% Mannitol (w/v)	Mannitol dH_2O	20.00 Up to 100.00 ml
20% Sucrose (w/v)	Sucrose dH_2O	20.00 Up to 100.00 ml
0.5% KH_2PO_4	KH_2PO_4 dH_2O	0.50 100.00 ml
5M $CaCl_2.2H_2O$	$CaCl_2.2H_2O$ dH_2O	73.51 Up to 100.00 ml
1N NaOH	NaOH dH_2O	40.00 Up to 1.00 l
20% L-proline (w/v)	L-proline dH_2O	20.00 Up to 100 ml
0.1M NaH_2PO_4	NaH_2PO_4	12.00
0.1M K_2HPO_4	K_2HPO_4	17.42
250 mM KCl	KCl dH_2O	1.86 100 ml
0.15M NaOH	NaOH dH_2O	0.60 100 ml

Table 2.3: Reagents and buffers (continued)

Reagent/Buffer Solution	Composition (Final concentration)	Quantity in grams per litre of dH_2O (unless otherwise stated)
2.5M $MgCl_2$	$MgCl_2$ dH_2O	23.80 Up to 100 ml
2M $MgCl_2$	$MgCl_2$ dH_2O	19.00 Up to 100 ml
2M $MgSO_4$	$MgSO_4$ dH_2O	24.07 Up to 100 ml

2.4 Culture media

The bacterial growth media used during this study are described in Table 2.4. Ingredients for Bacterial growth media were purchased from DIFCO, Oxoid Ltd., Gibco BRL., SIGMA Chemical Company and Fisher Scientific Ltd. De-ionized water (dH_2O) required to prepare the media was provided by the MILLI-RO water purification system. pH of the solutions and media was measured at room temperature. Media were routinely autoclaved at 121° C, 15 psi for 15 minutes. Solutions required for media preparation were either autoclaved or filter sterilized as applicable.

Table 2.4: Culture media

Medium	Composition	Quantity per litre (unless otherwise stated)
Luria Bertani (LB) Medium (Broth and Solid)	Tryptone Yeast Extract NaCl Glucose Adjust pH to 7.0 with NaOH For solid LB add agar	10.00 g 5.00 g 5.00 g 1.00 g (optional) 10.00 g
2X YT (Broth and Solid)	Tryptone Yeast Extract NaCl Adjust pH to 7.0 with NaOH For solid 2X YT add agar	16.00 g 10.00 g 5.00 g 10.00 g

Table 2.4: Culture media (continued)

Medium	Composition	Quantity per litre (unless otherwise stated)
Soya Flour Mannitol (SFM) agar	Soy Flour Mannitol Agar Use tap water in place of dH_2O	20.00 g 20.00 g 20.00 g
Solid NMMP	$(NH_4)_2SO_4$ Casaminoacids $MgSO_4.7H_2O$ Trace elements solution Dispense 80 ml aliquots into 250 ml flask containing 2.00 g Agar and autoclave. At time of use, add: NaH_2PO_4 / K_2HPO_4 buffer (0.1M, pH 6.8) Carbon Source (20%)	2.00 g 5.00 g 0.60 g 1.00 ml 15.00 ml 2.50 ml
Minimal Medium	L-asparagine / $(NH_4)_2SO_4$ K_2HPO_4 $MgSO_4.7H_2O$ $FeSO_4.7H_2O$ Agar Adjust pH to 7.2 with NaOH After autoclaving add filter sterilised glucose to 1% w/v	0.50 / 1.00 g 0.50 g 0.20 g 0.01 g 10.00 g
R5	Sucrose K_2SO_4 $MgCl_2.6H_2O$ Glucose Casaminoacids Trace element solution Yeast extract TES buffer Dispense 100 ml aliquots into 250 ml flask containing 2.20 g Agar and autoclave. At time of use, add the following solutions to each flask in the order listed: 0.5% KH_2PO_4 5M $CaCl_2.2H_2O$ 20% L-proline 1N NaOH Any required growth factors	103.00 g 0.25 g 10.12 g 10.00 g 0.10 g 2.00 ml 5.00 g 5.73 g 1.00 ml 0.40 ml 1.50 ml 0.70 ml 0.75 ml
Nutrient Agar	Oxoid Nutrient Broth Agar	13 g 12 g

Medium	Composition	Quantity per litre (unless otherwise stated)
SOC	Tryptone Yeast extract NaCl 250 mM KCl Adjust the pH to 7.0 Autoclave At time of use, add sterilized solutions of: 2M $MgCl_2$ 1M glucose	20.00 g 5.00 g 0.50 g 10.00 ml 5.00 ml 20.00 ml

2.5 Antibiotic and Blue-White selection

To use the antibiotics for selection of bacterial transformants, stock solutions of antibiotics were prepared in ddH_2O or other appropriate solvent, as applicable. Stock solutions prepared in ddH_2O were filter sterilized. All the stock solutions were stored at -20° C except Hygromycin solution which was stored at 4° C. Stock concentration and working concentration for respective antibiotic are listed in Table 2.5.

Table 2.5: Concentration of antibiotics, IPTG and X-gal

Antibiotic	Stock concentration (mg ml^{-1})	*E. coli* working concentration (µg ml^{-1})	*S. coelicolor* working concentration (µg ml^{-1})
Ampicillin	100	50	-
Apramycin	100	100	25
Chloramphenicol[1]	25	25	-
Hygromycin	100	100	50
Kanamycin	25	25	25
Nalidixic acid[2]	20	20	-
Thiostrepton[3]	25	-	25
IPTG	25	25	-
X-gal[4]	20	40	-

Solvent used to dissolve: [1]100% Ethanol; [2]0.15M NaOH; [3]DMSO (dimethyl sulfoxide); [4]Dimethylformamide or DMSO

In addition to antibiotic selection, plasmids containing multiple cloning sites within the *lacZ* gene may be analysed using blue-white selection. *E. coli* transformants containing the recombinant plasmid with a disrupted *lacZ* gene are easily distinguished from the *E. coli* transformants containing intact counterpart of the plasmid in the presence of chromogenic substrate X-gal (5-bromo-4-chloro-3-indolyl-β-D-galactopyranoside) and an inducer IPTG (isopropyl β-D-thiogalactopyranoside). Cells containing recombinant plasmid with a disrupted *lacZ* gene are unable to produce β–galactosidase, which is responsible for the conversion of the chromogenic substrate X-gal into a blue pigment, therefore the colonies with recombinant plasmid retain white colour, whereas the cells containing plasmid with intact *lacZ* gene are able to produce β–galactosidase that converts X-gal into a blue pigmented compound imparting blue colour to the colonies.

2.6 Culture conditions

2.6.1 Growth and storage of *E. coli* strains

E. coli cells were grown on LB media and incubated at 37° C either in a static temperature controlled incubator if being grown on plates or shaken at 220 rpm if liquid culture was used. Glycerol stocks of *E. coli* strains were prepared from 5 ml overnight grown cultures. Overnight grown cells were centrifuged and resuspended in 0.5 ml of sterile 20% (v/v) glycerol and stored at -20° C or -70° C. Short term storage of cultures was possible by storing culture broth or plates at 4° C.

2.6.2 Growth and storage of *S. coelicolor* strains

Streptomyces coelicolor cultures were grown on a variety of solid media and incubated at 30° C. For the preparation of spore or aerial mycelium suspensions (as applicable) lawn of the relevant strain was grown on SFM agar, containing appropriate antibiotic (if applicable) for 4-6 days. Spore or aerial mycelium suspensions of different *S. coelicolor* strains were stored at -20° C.

2.6.3 Preparation of spore or aerial hyphae suspensions of *S. coelicolor* strains

To prepare the spore suspensions, *S. coelicolor* cells were grown on SFM agar media as stated above. After appropriate incubation period, culture plates were flooded with 10 ml of sterile ddH_2O and gently scraped off the surface with a sterile inoculating loop to release the spores. The resulting suspension was poured into a sterile centrifuge tube, vortexed and filtered through a sterile 10 ml syringe containing non–absorbent cotton wool to remove mycelial fragments. The spores were then pelleted by centrifugation at 6000 rpm for 5 min and resuspended in 1 ml of sterile 20% glycerol solution. Stocks were stored in micorcentrifuge tubes at -20° C.

The procedure to prepare aerial mycelium suspensions of non-sporulating strains was similar to that of spore suspension preparation, except that the mycelial suspensions were not filtered through sterile syringe containing non–absorbent cotton wool.

2.7 Transformation

2.7.1 Preparation of electro-competent cells of *E. coli*

A 1/100 dilution of a fresh overnight *E. coli* JM109 or ET12567 culture was inoculated into 500 ml LB broth. At an OD_{600} 0.5 – 0.7 the cells were chilled on ice for 20 min then harvested by centrifugation at 4500 rpm for 15 min at 4° C. In all following procedures the cells were kept on ice as much as possible, and all glycerol solutions used were ice cold. The supernatant was decanted and the pelleted cells carefully resuspended in 500 ml ice-cold 10% glycerol. The cells were then pelleted and resuspended in 250 ml ice-cold 10% glycerol. The above step repeated using 20 ml ice-cold 10% glycerol. Finally, the cells were resuspended into 2 ml ice-cold 10% glycerol and 40 µl aliquots of the competent cells were dispensed into ice-cold microcentrifuge tubes to store at -70° C. The electro-competent cells can be kept frozen for many weeks without great loss in transformation efficiency.

2.7.2 Transformation of electro-competent *E. coli* cells

A 40 µl aliquot of electro-competent cells was thawed slowly on ice, 10 ng DNA was added and mixed by gentle pipetting. After 2 min incubation on ice the mixture was transferred into a chilled electroporation cuvette (0.1 cm). The cuvette was then placed in a MicroPulser^{TM} (BioRad) and electroporated using EC1 program. Immediately 1 ml LB medium or SOC was added and the mixture was incubated at 37° C for 90 min on shaker (225 rpm) after transferring to a Bijoux tube. The transformation mixture was then plated onto LB agar with appropriate antibiotic selection.

2.7.3 Preparation of calcium chloride competent *E. coli* cells

The competent cells of *E. coli* JM109 or ET12567 were prepared using calcium chloride ($CaCl_2$). To prepare $CaCl_2$ competent cells, the *E. coli* cultures were grown overnight at 37° C in 10 ml LB broth with appropriate selection antibiotic(s) if applicable. A 5 ml aliquot from overnight grown cultures were used to inoculate 250 ml LB broth supplemented with appropriate antibiotic if applicable. Cultures were grown at 37° C on shaker (225 rpm) to obtain an OD_{600} between 0.4-0.6. Then the cells were transferred to sterile, ice-cold 50 ml universal tubes and incubated on ice for 10 min. During the following steps the cells were kept on ice and all the glassware and equipments were chilled before use. The cells were pelleted by centrifugation at 4500 rpm for 5 min at 4° C. The pellet was gently resuspended in 20 ml ice-cold ice cold 50 mM $CaCl_2$, incubated for 30 min and then pelleted again. This $CaCl_2$ wash without further incubation was repeated three times in total. After the final wash the pelleted cells were resuspended in 2 ml $CaCl_2$. Finally, 80 µl aliquots of the competent cells were dispensed into ice-cold microcentrifuge tubes and quickly frozen in liquid nitrogen and stored at -70° C.

2.7.4 Transformation of calcium chloride competent *E. coli* cells

The aliquots of *E. coli* competent cells were thawed on ice for 10-15 min. Purified DNA (plasmid or ligation mixture) was added and mixed gently. The mixture was incubated on ice for 30 min. The cells were then heat-shocked at 42° C for 90 sec and immediately incubated on ice for 2 min. The mixture was then transferred to a universal tube after mixing with 900 µl of SOC medium and incubated at 37° C on an

orbital shaker (225 rpm) for 1 hr. Finally, the heat-shocked culture was plated on LB agar plate containing appropriate antibiotics and incubated overnight at 37° C.

2.7.5 Intergeneric conjugation

Electro-competent cells of *E. coli* ET12567 containing pUZ8002 were prepared as described in section 2.7.1. The vector of interest containing *oriT* (for mobilisation into *Streptomyces*) was introduced into *E. coli* ET12567 (pUZ8002) by electroporation and transforments were selected by growing the culture at 37° C, on LB agar plate containing 25 µg/ml chloramphenicol, 25 µg/ml kanamycin and other selective antibiotic required for the selection of vector of interest. A transformed colony was inoculated into 10 ml LB containing kanamycin, chloramphenicol and the antibiotic used to select for the *ori*T containing vector and grown overnight at 37° C, on shaker at 225 rpm. The overnight grown culture was diluted to 1:100 with fresh LB broth plus the antibiotic selection and grown under the same conditions until an OD_{600} of 0.4-0.6 was obtained. Cells were then pelleted and washed twice with an equal volume of LB to remove antibiotics that might inhibit *S. coelicolor* growth. After washing, the cells were resuspended in 1/10 volume of LB broth. While washing the *E. coli* cells, for each conjugation approximately 10^8 *S. coelicolor* spores or mycelial fragments (as applicable) were added to 500 µl 2 x YT broth, heat shocked at 50°C for 10 mins then cooled to room temperature. To the activated spores or mycelial fragments, 500 µl washed *E. coli* were added and mixed. The mixture was spin down briefly and the supernatant was decanted off. The pelleted cells were gently resuspended in the residual broth. This conjugation mixture was plated on SFM agar containing 10 mM $MgCl_2$ and incubated at 30° C for 16–20 h. After incubation the plates were overlaid with 1 ml sterile ddH_2O containing nalidixic acid (to inhibit *E. coli* growth) and the appropriate antibiotic selecting for the *ori*T containing vector. Plates were allowed to dry and further incubated at 30° C for 3–5 days until potential exconjugants could be picked and transferred to selective media containing nalidixic acid.

2.7.5.1 Selection of *S. coelicolor* double crossovers

After 3–5 days of incubation, single colonies of exconjugants on the overlayed SFM plates could then be screened for successful replacement of wild type gene with

the corresponding transposon disrupted gene in the *S. coelicolor* chromosome by double crossover recombination event. Two sets of plates were prepared, one containing the appropriate concentration of the antibiotic whose resistance gene is carried on the plasmid / cosmid (e.g. kanamycin) and the other containing the antibiotic whose resistance gene is carried on the transposon (e.g. apramycin or hygromycin). Replica plating was then carried out for a large sample of the individual colonies (100–200 colonies). Any colonies which grew on apramycin or hygromycin containing media plate but not on kanamycin containing media plates were selected as probable double crossover mutants, and these were confirmed using Southern hybridization.

2.8 DNA isolation and manipulation

2.8.1 Plasmid DNA isolation from *E. coli*

For small scale preparation of plasmid DNA the Wizard® *Plus* SV Minipreps DNA Purification System, from Promega Corp. or AccuPrep® Plasmid Mini Extraction Kit, from Bioneer Corp. was used. The overall principle of both the systems is based on the modified alkaline lysis method (Sambrook *et al.*, 1989) and the protocol in both the systems is same. *E. coli* cells containing appropriate plasmid DNA were grown overnight in 5 ml LB broth with suitable antibiotic selection. Cells from an overnight grown culture (1-5 ml) were pelleted at 13000 rpm for 5 min. The supernatant was discarded and the pellet was resuspended in 250 µl resuspension solution. Then 250 µl lysis solution was added to the suspension and mixed gently by inverting the tube 3-4 times. The mixture was incubated for 1-5 min at room temperature. After incubation, 350 µl Neutralisation solution was added, mixed by inversion and the resulting suspension was centrifuged at 13000 rpm for 5 min. The cell lysate was transferred to a spin column containing a DNA binding matrix and centrifuged at 13000 rpm for 1 min to allow binding of DNA to the matrix. The binding matrix was washed twice with 750 and 250 µl Wash buffer, respectively. Finally, the DNA was eluted in 100 µl sterile ddH_2O by centrifugation of the spin column, into a sterile microfuge tube, at 13000 rpm for 2min.

2.8.2 Genomic DNA isolation from *S. coelicolor*

The FastDNA® SPIN Kit for Soil (BIO 101 systems) from Q-BIOgene was used to rapidly isolate genomic DNA by lysing the cells using ceramic and silica particles. Lysing matrix tubes containing 978 µl Sodium Phosphate Buffer and 122 µl MT Buffer, were filled to 7/8 volume with mycelia from 24 h cultures grown on Nutrient agar plates. The tubes were securely fastened into the FastPrep® Instrument and processed for 30 sec at speed 5.5. After processing, the cell debris and lysis matrix were centrifuged to the bottom at 13000 rpm for 30 sec. The supernatant containing genomic DNA was transferred to a fresh tube and mixed by inversion with 250 µl PPS reagent. It was centrifuged again at 13000 rpm for 1 min and after centrifugation the supernatant was transferred to a 15 ml tube and incubated, gently shaking, for 2 min with 1 ml Binding Matrix Suspension. Once the DNA has bound to the matrix it is left to settle for 3 min then transferred into a spin filter, which captures the matrix and the bound DNA. The bound DNA was washed with 500 µl SEWS-M and eluted into a fresh catch tube with 50 µl DNase/ Pyrogen free water. Total DNA from *S. coelicolor* was used for Southern blots and as a PCR template for amplification of specific genes.

2.8.3 Enzymatic reactions

Restriction digestions were performed using restriction endonucleases purchased from New England Biolabs (NEB) or Promega Corp. All reactions were carried out according to the manufacturers' instructions. For blunt ending of 3′ and 5′ DNA overhangs, T4 DNA polymerase from NEB was used. T4 DNA ligase was purchased from Invitrogen or NEB and used in accordance with the manufacturers' instructions. To remove the 5′ phosphate groups from DNA, Calf intestinal alkaline phosphatase (CIP) purchased from NEB was used and reactions were performed as instructed.

2.8.3.1 Ligation reactions

Prior to ligation, DNA fragments were purified from their respective enzymatic reactions using QIAquick PCR Purification Kit from Qiagen. The DNA fragments, in their enzyme reaction mixtures, were mixed with five volumes of Buffer PB and applied

to QIAquick spin columns. The columns were then centrifuged at 13000 rpm for 1 min to allow DNA to bind on the matrix. Each column was then washed twice with 750 µl Buffer PE (wash buffer). After an additional centrifugation step at 13000 rpm for 1 min to dry the column, the DNA was eluted in the final step in 50 µl sterile ddH_2O by centrifugation of the spin column, into a sterile eppendorf, at 13000 rpm for 2min. To purify one particular fragment of DNA from agarose gel, the GFX kit from GE healthcare (formerly Amersham Biosciences) was used according to the manufacturers' instructions. The purified DNA (vector and insert) was analyzed by agarose gel electrophoresis and quantified. The ligation reactions were set by mixing the vector and insert DNA at a ratio of 1:3, and incubated at 14° C overnight.

2.8.4 Redirect technique to change the selective marker

To change the selective marker (from apramycin to hygromycin) in the Tn*5062* disrupted cosmid of a specific gene the Redirect technique was performed. The electro-competent cells of *E. coli* BW25113/pIJ790 were transformed with a *S. coelicolor* cosmid of interest and grown at 30° C in LB broth containing 25 µg/ml chloramphenicol, 100 µg/ml apramycin and 25 µg/ml kanamycin for the selection of a pIJ790 plasmid and a cosmid of interest. The plasmid pIJ790 contains the resistance marker *cat* (chloramphenicol resistance) and a temperature sensitive origin of replication (requires 30° C for replication). The cosmid contains the resistance marker for kanamycin and apramycin. Electro-competent cells of *E. coli* BW25113/pIJ790 containing a cosmid of interest were prepared as described earlier. These electro-competent cells were transformed with the extended hygromycin resistance cassette. The hygromycin resistance cassette was purified from pQM5066 plasmid as a 2669 bp *Hin*dIII fragment. The transformants of *E. coli* BW25113/pIJ790 containing a cosmid of interest with hygromycin resistance marker were selected by growing the culture on LB agar containing kanamycin (25 µg/ml) and hygromycin (100 µg/ml) at 37° C. Incubation of the culture at 37° C promotes the loss of pIJ790. The replacement of the apramycin cassette with the hygromycin cassette was promoted by the λ RED (*gam, bet, exo*) functions present in the λ RED recombinant plasmid pIJ790.

2.9 Polymerase chain reaction (PCR)

PCR reactions were cycled on a PTC-200 DNA Engine (M.J. Research Inc.) using DyNAzyme EXT™ polymerase (Finnzymes). Primers were designed with Beacon Designer 2 software from Premier Biosoft international, and purchased from MWG-Biotech. Primers used in this study are shown in Table 2.6.

Table 2.6: Primers used in PCR reaction to amplify *sfr*.

Primer name	**Sequence (Bold letters indicate restriction site for relevant restriction enzyme)**	**Restriction enzyme**
SfrF1 (Forward)	5′ - TCA**CATATG**ACCGGCAACAGCTTCC – 3′	*Nde*I
SfrR1 (Reverse)	5′ - C**TCTAGA**CCGCTGCCGCCCCGGGTGCC - 3′	*Xba*I

Reactions were carried out in thin-walled 0.5 ml microfuge tubes with a total reaction volume of 50µl. A typical reaction scheme is as follows:

Template DNA (approx. 100 µg/ml)	2.0 µl
10X DyNAzyme EXT™ buffer	5.0 µl
Sense primer (10 pmol/µl)	2.0 µl
Antisense primer (10 pmol/µl)	2.0 µl
2.5 mM dNTP mix	4.0 µl
dH_2O	34.0 µl
DyNAzyme EXT™ polymerase	1.0 µl
---	---
Total volume	50.0 µl

PCR cycle program used for the reaction mix was as follows:

	Temperature	Time	Cycle number
Initial denaturation	94° C	4 min	1
Denaturation	94° C	30 sec	
Annealing	55° C	30 sec	30
Extension	72° C	1 min	
Final extension	72° C	10 min	1
	4° C	Hold	

2.10 Qualitative and quantitative analysis of DNA

2.10.1 Agarose gel electrophoresis

DNA was separated out according to size by electrophoresis through agarose gels. The percentage of agarose is varied to reflect the size of the DNA of interest. 1% or 0.8% agarose (w/v) gels used to separate restriction digests of plasmid DNA (0.5 to 15 Kb), 0.5% gels were used to visualise large pieces of DNA, for example, *Streptomyces* chromosomal DNA. To separate smaller PCR products 1.5 to 2% agarose gels were used. Standard 100 ml of 1% (w/v) agarose gels containing a final concentration of 0.1 μg/ml ethidium bromide were routinely prepared in 1X TBE buffer. The gel was immersed in the BIORAD electrophoresis tank filled with 1X TBE buffer and the samples were loaded into wells after mixing with Bromophenol blue DNA loading dye at the ratio of 5:1 (DNA:dye). Gel was run by applying an electric field of 100 V through the gel using BIORAD power supply, for 45 – 60 min. To estimate the size of DNA samples an appropriate DNA marker (Phage λ DNA digested with *Hin*dIII was used in most cases) was run along side of the samples. Once the DNA was migrated upto desired distance, the gel was exposed to UV light using a BIORAD transilluminator at 254 nm and the DNA samples were visualized through BIORAD gel documentation (GelDoc) system.

2.10.2 DNA Quantification

The quality and quantity of DNA was also assayed using a NanoDrop® ND-1000 Spectrophotometer. The quantity of DNA was measured by applying 1 µl sample on the pedestal of the instrument after initializing the instrument and setting the blank. The ratio of A_{260} / A_{280} determines the purity of the DNA, where pure DNA in 10 mM Tris-Cl (pH 8.5) has an A_{260}/ A_{280} ratio of 1.8 – 2.0.

2.11 DNA sequencing

Recombinant plasmids constructed during this study were confirmed by sequencing. Wizard DNA preparations were quantified using the spectrophotometer and the appropriate amount of template DNA (relative to the size of the plasmid) was denatured at 96°C for 3 min. This partially uncoiled DNA was cooled on ice for 1 min and mixed with appropriate sequencing primers (1-2 µl from a 10 pmol/µl stock solution) and 8 µl DTCS quick start master mix (Beckman Coulter). The total volume of the reaction was 20 µl. Sequencing reactions were amplified by thirty cycles of 96° C for 20 sec/ 50° C for 20 sec/ 60° C for 4 min, using PTC-200 DNA Engine (M.J. Research Inc.). Sequencing reactions were separated using the Beckman CEQ 8000. Several sequencing primers were used routinely; these are listed in Table 2.7. In some cases, oligonucleotides used for PCR reaction were also used as sequencing primers.

Table 2.7: Commonly used sequencing primers

Primer name	Sequence
1224	5′ - CGCCAGGGTTTTCCCAGTCACGAC - 3′
1233	5′ - AGCGGATAACAATTTCACACAGGA - 3′
T7 universal primer	5′ - TAATACGACTCACTATAGGG - 3′

2.12 Southern Hybridization

The successful replacement of a wild type gene with transposon disrupted copy of the same gene in *S. coelicolor* mutant chromosomes was confirmed using Southern hybridization analysis. In brief, a restriction digest of chromosomal DNA from the mutant strain and a positive control (often the relevant cosmid) were run on an agarose gel. The DNA samples were then transferred to a nitrocellulose membrane and detected immunologically using an appropriate probe (usually Tn*5062*). These steps are described in more detail below:

2.12.1 Preparation of Digoxigenin labelled probes

Suitable DNA fragment(s) was selected and labelled randomly with alkali-labile Digoxigenin-11-2′-deoxy-uridine-5′-triphosphate (DIG-11-dUTP) using DIG DNA Labelling Kit form Roche Applied Sciences. For most Southern hybridization analysis, a 3442 bp *Pvu*II fragment of Tn*5062* DNA excised from pQM5062 was used as a labelled probe. For Southern hybridization analysis of few *ftsW* mutants, a 4896 bp *Hin*dIII fragment, containing *ftsW, murG* and *ftsW* genes, was excised from pBSW1 and the fragment was labelled with alkali-labile Digoxigenin-11-2′-deoxy-uridine-5′-triphosphate (DIG-11-dUTP) as follows. This gene specific probe was used for the hybridization of some *ftsW* mutants. Phage λ DNA digested using *Hin*dIII was labelled and used as a probe to hybridise with the λ *Hin*dIII marker. Random priming method, based on hybridization of random oligonucleotides to the denatured DNA template, was used to label respective purified DNA fragments. To label the DNA, the DNA fragments were denatured by heating at 95° C for 10 min and cooled quickly on ice. Then, hexanucleotide mix, DIG-11-dUTP/dNTP mixture and Klenow enzyme were added to the denatured DNA. The reaction was mixed properly and incubated at 37° C overnight. The reaction was stopped by adding 2 µl of 0.2 M EDTA, pH 8. A standard reaction scheme is as follows:

Denatured DNA	1-15 µl (10 ng – 3 µg DNA)
ddH_2O (sterile) (to make the final volume 15 µl)	x µl
Final volume	15 µl
Hexanucleotide mix	2 µl
DIG-11-dUTP/dNTP mixture	2 µl
Klenow polymerase	1 µl
Total volume of reaction mix	20 µl

Prior to hybridization, 10µl each of labelled probes (Tn*5062* or gene specific and λ *Hin*dIII) is denatured by boiling for 10 min in boiling water bath, cooled quickly by keeping it on ice for 1-2 min and added to 15-20 ml of prehybridization solution. The solution thus prepared is called as 'probe solution' from here after.

2.12.2 Blotting

Chromosomal DNA of interest and the corresponding cosmid DNA control were digested with suitable restriction enzyme and the DNA fragments of digested DNA (chromosomal and cosmid) along with marker (λ *Hin*dIII) were separated on a 0.8% agarose gel in 1X TBE until the loading dye had progressed close to the end of the gel. The gel was visualized under UV transilluminator to check the digestion. The gel was then immersed in denaturing buffer for 15min with gentle shaking. This step was repeated twice. The gel was then rinsed twice with dH_2O. After quick rinse, the gel was immersed in neutralisation buffer for 20min with gentle shaking. This step was repeated twice. During the neutralization step, an appropriate size (gel size) of neutral nylon membrane (Hybond-N, Amersham Pharmacia Biotech) was soaked in dH_2O for 20min and then soaked in 10X SSC solutions for 10 min. Two pieces of Whatman filter paper (1 cm bigger in width and height than the gel) were also soaked in 10X SSC solutions for 10 min.

A Stratagene Posiblot Pressure blotter was used to transfer the DNA from the gel onto the treated nitrocellulose membrane prior to hybridization and immunological detection. The pressure blotter was assembled with Whatman filter paper, soaked in

10X SSC at the bottom, then the nitrocellulose membrane and on top of this was a plastic mask, containing a hole (0.5 cm smaller than the gel in width and height) in the centre. Once assembled the gel was positioned on top of the mask, sealing the hole. Finally a sponge saturated with 10X SSC was placed over the gel and the apparatus was closed. The pressure of 75 mmHg was applied for 1 hour to transfer the DNA efficiently on to the membrane. Once transfer was complete, the membrane was baked at 80°C for 60 min to fix the DNA.

2.12.3 Hybridization

Once the DNA was fixed to the membrane, it was rinsed in dH_2O and rolled in a piece of nylon mesh soaked in 2X SSC with the DNA facing upwards. The rolled membrane with the mesh was placed into a hybridization tube (Appligene) and washed with 2X SSC. A 10 ml of prehybridization solution was added in the hybridization tube and incubated at 42° C for 1 h. After the prehybridization step the solution was decanted and a 20 ml denatured labelled probe solution was added to the tube and incubated at 42° C for overnight in the rotating oven. The following day, the probe was collected and stored at -20°C for future use. The membrane was washed twice in wash solution 1 at 42°C for 5 min each and then it was washed twice in wash solution 2 at 68°C for 15 min each.

2.12.4 Immunological detection

After wash with wash solution 2, the membrane was rinsed in Buffer I for 1 min at room temperature and incubated with freshly prepared Buffer II (Prehybridization solution) for 30 min. After this, another brief wash of 1 min with buffer I was given to the membrane. The membrane was then incubated with Anti-digoxigenin antibody solution (15 ml Buffer I with 3 µl Anti-digoxigenin AP) for 30 min in rotating incubator at room temperature. To remove unbound antibody, the membrane was washed twice in Buffer I for 15 min each. After these washes in the hybridization tube, the membrane was transferred to a plastic bag where 10 ml of colour solution was added and the bag was sealed. To facilitate the colour reaction the membrane was placed flat in the dark, at 37°C. After sufficient band intensity had been

reached (30 min to 2 h incubation), the reaction was stopped by washing the membrane in dH_2O.

2.13 Microscopy

2.13.1 Sample preparation

Coverslip impressions:

S. coelicolor strains were grown on the surface of SFM agar medium for 2 to 4 days, as appropriate. After incubation, a clean coverslip was pressed against the surface of the growing culture. The coverslip was placed in a clean Petri plate with the aerial mycelium fragments and/or spores attached to the glass facing up. The attached cells or spores were fixed by flooding the coverslip surface with fixing solution and incubating for 15 min. Alternatively, cells were fixed by gently washing the coverslip twice with methanol. The fixing solution or methanol was removed. Samples fixed with the fixing solution were washed twice with phosphate buffer saline (PBS) solution. The samples were then left to dry thoroughly and stained for fluorescence microscopic analysis as described in the section 2.13.2.

Inserted Coverslips:

S. coelicolor strains were inoculated with 2-5 µl of spore suspension for sporulating strains or 6-10 µl of aerial mycelium suspension for non-sporulating strains, at the acute angle formed by the inserted coverslip in agar plates of the desired medium. After an appropriate incubation time the coverslip was removed and placed in a clean Petri plate with cells facing up after removing any remaining agar piece attached on the surface opposite to the attached cells. The cells were then fixed as described above and stained as follows. For fluorescent labelled vancomycin (FL-vancomycin) staining the cells were stained directly without fixing.

2.13.2 Staining

Fluo-WGA/PI staining:

The lectin staining protocol described by Schwedock *et al.*, 1997, was used to stain the cell wall and DNA of *S. coelicolor*. For cell wall staining, fluorescein-conjugated wheat germ agglutinin (Fluo-WGA) from Molecular Probes was used at the concentration of 2 μg/ml and for DNA staining; propidium iodide (PI) was used at 10 μg/ml concentration. After fixing the cells as described above, the fixed cells were rehydrated by treating the cells with PBS for 5 min. The PBS was gently removed and the cells were treated 2% BSA in PBS (w/v) for 5 min. The BSA solution was removed and the cells were incubated with Fluo-WGA/PI solution for 30 min to 3 h in dark at room temperature. After appropriate incubation period, the cells were washed 4-8 times with PBS containing 10 μg/ml PI. Cells were then washed twice with Slow Fade equilibration buffer (SlowFade light antifade kit; Molecular Probe). The second wash was incubated at room temperature for 2-5 min. The buffer was aspirated off and Slow Fade antifade/glycerol or 40% glycerol in PBS solution was added. The coverslip was mounted on clean slide and excess solution was removed by aspiration. The borders of coverslip were sealed with nail varnish to avoid desiccation and the slide was observed under the microscope.

FL-Vancomycin staining:

To stain nascent peptidoglycan in *S. coelicolor*, commercially available fluorescein conjugated vancomycin, BODIPY® FL vancomycin from Invitrogen, was used. For optimal staining the FL-vancomycin was mixed with an equal amount of unlabelled vancomycin and the mixture was added into sterile 2X YT broth at the final concentration of 1 μg/ml. An inserted coverslip with attached cells was removed after appropriate incubation and placed in a clean Petri plate with the cells facing up after removing any remaining agar piece attached on the surface that is opposite to the attached cells. The cells were directly flooded with 2X YT broth containing FL-vanocmycin/vancomycin and incubated for 20 min in the dark at room temperature to allow absorption of the antibiotic. The cells were then gently washed twice with PBS and the coverslip was mounted on a clean slide by adding 40% glycerol in PBS

solution. Excess solution was removed by gentle aspiration and the borders of coverslip were sealed with nail varnish to avoid desiccation. Slides thus prepared were observed under microscope.

2.13.3 Visualization of samples under microscope

The samples prepared for microscopy were observed under a Nikon Eclipse E600 epifluorescent microscope. For phase contrast microscopy, samples were illuminated with visual light. The microscope is equipped with a FITC filter (Excitation 465-495, DM 505, BA 515-555) for visualization of Fluo-WGA attached to the cell wall and a G-2A filter (Excitation 510-560, DM 575, BA 590) for PI stained DNA. Phase contrast and fluorescence images were taken using the Coolsnap digital camera attached to the microscope. The images obtained were later processed using Adobe Photoshop 6.0.

2.13.4 Atomic force microscopy (AFM)

The instrument used for atomic force microscopy (AFM) was a Dimension 3100 (Nanoscope IV controller; Thermomicroscopes). Different strains of *S. coelicolor* under study were grown on SFM agar plates and impressions were taken after appropriate incubation period (48-72h for wild type and 4-5 days for mutants) at 30° C. Aerial hyphae or spores attached to glass coverslips were imaged in air (at 20°C and 40% rH) using tapping mode tips (Olympus, cantilever nominal spring constant, k = 0.064 N m^{-1}). A scan rate of 1 Hz was employed with resolution of 512 by 512 or 1,024 by 1,024 lines. Height and phase images were simultaneously recorded. Height images provide quantitative information on sample surface topography whereas phase images, although they do not represent the true topography of the sample, reveal a higher sensitivity to small surface features, resulting in images with greater detail. Phase images are derived from the phase angle between the actual vibration and the applied signal used to oscillate the AFM cantilever so that the tip intermittently taps the surface and reduces the lateral force that is applied during imaging.

2.14 Viable count

Quantification of viable spores or aerial hyphae fragments of *S. coelicolor* strains in their respective stock suspensions was carried out using a spread plate method. In this method, ten-fold serial dilutions from $1/10^3$ to $1/10^7$ for each spore or hyphal stock suspension (as applicable) were prepared in 20% v/v sterile glycerol solution. Then a 100 µl aliquot of each dilution was transferred to individual SFM agar plate and spreaded evenly with a sterile bent glass rod. Cultured plates were allowed to dry and incubated at 30° C for 3 days. After 3 days of incubation the number of isolated colonies obtained per plate was counted. Plates containing more than 400 colonies and less then 30 colonies were not taken in to account. The number of viable spores or hyphal fragments per ml of original stock was calculated using following general formula.

$$\text{Number of CFUs} = \frac{\text{Number of colonies obtained per plate}}{\text{Dilution aliquote plated (0.1 ml)} \times \text{Dilution factor}}$$

CFUs:- Colony forming units

The experiment for each strain was performed in duplicates and average CFUs per ml was taken.

2.15 Antibiotic susceptibility

For antibiotic susceptibility, a dilution method was used to determine the minimum inhibitory concentrations (MICs) of different cell wall specific antibiotics for different *S. coelicolor* strains. In this test, different strains of *S. coelicolor* were tested for their ability to produce visible growth on a series of agar plates each containing a different concentration of the respective antibiotic. The test was performed using 2X YT agar medium or soya flour mannitol (SFM) agar medium. The antibiotics used and their stock concentrations are showed in Table 2.8.

Table 2.8: Antibiotics used for minimum inhibitory concentration (MIC) test.

Antibiotic	Stock concentration (mg/ml)
Ampicillin	500 mg/ml
Bacitracin	50 mg/ml
Vancomycin	200 mg/ml

Sterile agar plates with the range of concentrations of each antibiotic along with drug-free control were prepared. The density of spore stock of each *S. coelicolor* strain tested was standardized using sterile 20% glycerol stock to give the final density of inoculum to 10^4 spores per spot on the agar plate. Inoculum of each strain was transferred to the series of agar plates, including a control plate without antibiotic. Plates were incubated at 30° C for 48 h. Finally, the plates were observed for visible growth of *S. coelicolor* colonies and the lowest concentration of the antibiotic that completely inhibits visible growth (as judged by the naked eye) of each strain was noted down.

2.16 Heat treatment

To test heat susceptibility of spores of different *S. coelicolor* mutant strains compare to that of wild type strain, spore suspensions of different strains (including wild type), each strain containing 10^7 spores per ml were incubated at 60° C for different time intervals. Spore suspension of each strain without heat treatment was used as a control. After heat treatment spore suspensions were diluted to 1:10, 1:100 or 1:1000 and 100 µl of each dilution was plated on SFM agar plate. Spore suspension of the *sfr, pbp2, rodA2/sfr* and *sfr*/pIJ8600 mutant strains incubated longer than 20 min at 60° C were plated without being diluted. Plates were incubated at 30° C for 3 days to cultivate the viable spores. The number of colonies obtained per plate for each heat treatment of respective strain was counted and viable spores per ml of suspension were calculated as described in section 2.14. Spore survival rate for each strain was

calculated as number of viable spores per ml after treatment at 60°C divided by the number of viable spores per ml without treatment at 60° C in percentage. The graph of percentage survival rate versus period of heat treatment at 60° C was prepared using Microsoft Excel.

2.17 Detergent treatment

To test the effect of detergent sodium dodecyl sulfate (SDS) on spores of wild type and different mutant strains of *S. coelicolor*, 50 µl of 10^8 ml^{-1} spore suspensions of wild type and mutant strains were incubated in 5% SDS, 1% SDS or dH_2O for 1 h at room temperature. After 1h incubation, serial dilutions of each sample were prepared and appropriate spore dilutions were plated on SFM agar plates. Plates were incubated at 30° C for 3 days. The number of colonies obtained per plate for each treatment was calculated and converted to the number of viable spores per ml of spore suspension. Spore survival rate of each strain with and without SDS treatment was calculated as the number of viable spores per ml after SDS treatment divided by the number of viable spores per ml without SDS treatment in percentage. The graph of percentage survival rate versus SDS concentration was prepared using Microsoft Excel.

2.18 Bioinformatics techniques

2.18.1 Databases

Gene annotations and protein sequences were obtained from publicly available databases: *Streptomyces coelicolor* genome database ScoDB (http://streptomyces.org.uk/); *S. avermitilis* genome database (http://avermitilis.ls.kitasato-u.ac.jp/); *S. griseus* genome database (http://streptomyces.nih.go.jp/griseus/); Sanger Institute bacterial genomes (http://www.sanger.ac.uk/Projects/Microbes/); NCBI Microbial Genome Project (http://www.ncbi.nlm.nih.gov/genomes/lproks.cgi); GenoList genome browser (http://genolist.pasteur.fr/); Joint Genome Institute Bacterial Genomics Database

(http://www.jgi.doe.gov/genome-projects/); *Nocardia farcinia* genome database (http://nocardia.nih.go.jp/). Sequences are referred to by the ordered locus name provided in these databases.

2.18.2 BLAST analyses

Sequence similarity searches were performed by BLASTP against complete microbial genome sequences deposited in the NCBI Microbial Genome Project and other bacterial genome databases mentioned above using the default parameters set by each database.

2.18.3 Multiple alignments and phylogenetic analyses

Multiple alignments of amino acid sequences were constructed by CLUSTAL-W2 from EMBL-EBI server (http://www.ebi.ac.uk/Tools/clustalw2/) using the default parameters. Phylogenetic analyses were conducted using the MEGA 4.0.1 version (Kumar *et al.*, 1994; Tamura *et al.*, 2007). All default parameters were used. Unrooted trees were computed by the Neighbor-Joining method (Saitou and Nei, 1987). The bootstrap value for the consensus tree was set to 1000 replicates. The evolutionary distances were computed using the Poisson correction method and are in the units of the number of amino acid substitutions per site. All positions containing gaps and missing data were eliminated from the dataset (Complete deletion option).

2.18.4 Topology predictions

For the topology prediction and hydropathy profile of different proteins, amino acid sequence of the relevant protein was submitted to TMHMM (Sonnhammer *et al.*, 1998), HMMTOP (Tusnady and Simon, 1998), TopPred II (Claros and von Heijne, 1994), TMpred (Hofmann and Stoffel, 1993) and TMAP (Persson and Argos, 1994). Default values of all the parameters set by each program were used for the analyses.

Chapter - 3

Analysis of Gene Loci Encoding SEDS Family Proteins in *Streptomyces coelicolor*

3.1 Introduction

With the wealth of complete genome sequences of a variety of bacteria, it is possible to compare whole genomes to understand genome structure, function and evolution. Conserved sequence similarity of gene sequences helps to predict function of a particular gene and establish orthologous relations to well characterized genes among bacteria. Analyses of conserved gene orders among different genomes helps to reveal general principles of how functionally coupled genes are physically encoded in the genome and possibly co-regulated at the level of gene expression (Fujibuchi *et al.*, 2000; Kihara and Kanehisa, 2000; Overbeek *et al.*, 1999).

The SEDS family of proteins that includes FtsW, RodA and SpoVE are highly conserved and have high similarity across the bacterial community (Gerard *et al.*, 2002; Ikeda *et al.*, 1989; Lara and Ayala, 2002). These proteins are well studied in model unicellular bacteria, *E. coli* and *B. subtilis*. Little is known about the SEDS family proteins in *Streptomyces*. In this chapter, the genetic organization of SEDS protein encoding genes of *Streptomyces* and other bacteria are analysed using bioinformatics tools. Genome comparison, sequence analysis and membrane topology prediction allowed to predict function(s) of *Streptomyces* SEDS proteins.

3.2 Genes encoding SEDS family proteins in Actinobacteria

In recent years complete genome sequences of many diverse actinobacteria have been made available (50 complete, out of which 20 are annotated at the time of writing) (http://www.ncbi.nlm.nih.gov/genomes/lproks.cgi). Expanding databases of complete actinobacterial genome sequences facilitate the study of SEDS proteins in actinobacteria using a comparative genomic approach in combination with functional classification of proteins and sequence comparison. To analyze SEDS proteins in actinobacteria, one representative species of each respective genus from each family in the phylum *Actinobacteria* was selected from available genome databases. Since the study is mainly focused on *Streptomyces*, four available genome sequences from *Streptomyces* are taken in to account for more understanding. Table 3.1 shows the list of actinobacteral genome databases, accession number and morphology of the organisms used for the analysis.

Table 3.1: Sequenced actinobacterial genome used for this study

Organism	Morphology	Accession number	Database
Streptomyces coelicolor	Mycelial, spore chains on aerial hyphae	AL645882	http://streptomyces.org.uk/
Streptomyces avermitilis	Mycelial, spore chains on aerial hyphae	BA000030	http://avermitilis.ls.kitasato-u.ac.jp/
Streptomyces griseus	Mycelial, spore chains on aerial hyphae		http://streptomyces.nih.go.jp/griseus/
Streptomyces scabies	Mycelial, spore chains on aerial hyphae		http://www.sanger.ac.uk/Projects/S_scabies/
Thermobifida fusca	Mycelial, spore clumped on aerial hyphae	CP000088	http://genome.jgi-psf.org/finished_microbes/thefu/thefu.home.html
Nocardioides sp. JS614	Rods	CP000509	http://genome.jgi-psf.org/finished_microbes/noc_j/noc_j.home.html
Frankia alni	Mycelial, spore forming	CT573213	http://img.jgi.doe.gov/cgi-bin/pub/main.cgi
Acidothermus cellulolyticus	Spore forming	CP000481	http://genome.jgi-psf.org/finished_microbes/acice/acice.home.html
Nocardia farcinica	Mycelial, spore forming	AP006618	http://nocardia.nih.go.jp/
Salinispora tropica	Mycelial, spore forming	CP000667	http://genome.jgi-psf.org/finished_microbes/saltr/saltr.home.html
Saccharopolyspora erythraea	Mycelial, spore forming	AM420293	http://jblseqdat.bioc.cam.ac.uk/gnmweb/
Rhodococcus sp.	Branched filamentous	CP000431	http://www.rhodococcus.ca/index.jsp
Bifidobacterium longum	Irregular or branched rods	AE014295	http://genome.jgi-psf.org/draft_microbes/biflo/biflo.home.html
Arthrobacter aurescens TC1	Rod-coccoid, motile	CP000474	http://img.jgi.doe.gov/cgi-bin/pub/main.cgi
Propionibacterium acnes	Rods	AE017283	http://img.jgi.doe.gov/cgi-bin/pub/main.cgi
Leifsonia xyli subsp. xyli str. CTCB07	Rods	AE016822	http://img.jgi.doe.gov/cgi-bin/pub/main.cgi
Tropheryma whipplei	Rods	BX072543	http://igs-server.cnrs-mrs.fr/mgdb/Tropheryma/
Corynebacterium glutamicum	Rods	BA000036	http://genome.ls.kitasato-u.ac.jp/esequenced.html
Mycobacterium tuberculosis	Rods	AL123456	http://genolist.pasteur.fr/TubercuList/

A BlastP search of the available actinobacterial genome databases using amino acid sequences of FtsW and RodA from *E. coli* and SpoVE from *B. subtilis,* revealed that there are 2 to 4 homologues of SEDS family proteins in actinobacteria. The FtsW, RodA and SpoVE sequences of *E. coli* and *B. subtilis* proteins were retrieved from http://genolist.pasteur.fr/Colibri/ and http://genolist.pasteur.fr/SubtiList/ databases respectively. Such a variation in the number of SEDS family proteins present in species belonging to the phylum *Actinobacteria* may be due to the fact that it includes a number of diverse species with different life cycles, from simple rods (*Mycobacteria)* to multicellular spore forming bacteria (*Streptomyces)*. The four genes found in the *Streptomyces coelicolor* genome are *SCO2085 (ftsW), SCO2607 (sfr), SCO3846* and *SCO5302.* These four genes are located in the central core region of the chromosome. Due to a high similarity and conservation of gene organization among the actinobacteria, from here onwards *SCO3846* is referred as *rodA* to be consistent with the annotation of the respective mycobacterial gene and *SCO5302* is referred as *rodA2*. Table 3.2 shows the list of genes encoding SEDS protein homologues found in different actinobacteria with respect to their counterparts in *E. coli* and *B. subtilis*. The genes are presented by their respective locus number and the gene name (if the name to that gene is assigned). All the *ftsW/rodA* family genes found in different actinobacteria are grouped on the basis of their position in the genome with respect to neighbouring genes, sequence similarity and proposed function(s) of respective SEDS proteins of *E.coli* and *B. subtilis*. In *E. coli,* with a simple unicellular life cycle, there are two SEDS protein paralogues (FtsW and RodA) specifically involved in division and elongation, respectively. However, the spore forming *B. subtilis* has three SEDS protein paralogues (FtsW, RodA and SpoVE), each functioning at the specific stage of division, elongation and sporulation, respectively. Thus, it is possible that there is a relation between the number of *ftsW/rodA* gene paralogues present per organism and the life cycle of the organism. That is, if an organism has a complex life cycle there may be more than two paralogues, and each gene may have a specific role at different stages of the life cycle. Genome comparison analysis revealed that there is no such correlation between the number of *ftsW/rodA* paralogues present per genome and complexity of bacterial life cycle, at least in the case of actinobacteria. Although they have complex multicellular life cycles, *Salinispora tropica, Saccharopolyspora erythraea* and *Nocardia farcinica* have only two *ftsW/rodA* paralogues while, simple rod shaped *Nocardioides sp.* have three paralogues in their genomes (Table 3.1 and 3.2).

Table 3.2: Genes encoding SEDS family proteins in different bacteria and percentage amino acid identity of SEDS proteins of different bacteria to their respective orthologue in *Streptomyces coelicolor*.

Organism	Locus number (Gene name) and % identity to *S. coelicolor* orthologues							
Sterptomyces coelicolor	*SCO2085 (ftsW)*		*SCO2607 (sfr)*		*SCO3846 (rodA)*		*SCO5302 (rodA2)*	
Streptomyces avermitilis	*SAV6121 (ftsW1)*	88%	*SAV5459 (ftsW2)*	84%	*SAV4340 (ftsW3)*	84%	*SAV2951 (ftsW4)*	84%
Streptomyces griseus	*SGR5420*	77%	*SGR4935*	81%	*SGR3727*	80%	*SGR2202*	80%
Thermobifida fusca	*TFU1109*	47%	*TFU2186*	50%	*TFU3063*	44%	*TFU0427*	43%
Nocardioides sp. JS614	*NOCA3064*	47%	*NOCA3461*	53%	*NOCA0025*	54%	NP	
Frankia alni ACN14a	*FRAAL2195 (ftsW)*	50%	*FRAAL1920 (mrdB)*	52%	*FRAAL6752*	50%	NP	
Acidothermus cellulolyticus	*ACEL1009*	49%	*ACEL0752*	44%	*ACEL0021*	56%	NP	
Nocardia farcinica	*NFA17650 (ftsW)*	42%	NP		*NFA830 (ftsW2)*	47%	NP	
Salinispora tropica	*STROP3214*	39%	NP		*STROP0045*	46%	NP	
Saccharopolyspora erythraea	*SACE5852 (ftsW)*	45%	NP		*SACE0047 (ftsW2)*	49%	NP	
Rhodococcus sp.	*RHA1RO01089*	43%	NP		*RHA1RO03699*	47%	NP	
Bifidobacterium longum	*BL1322*	35%	NP		*BL0586 (rodA)*	46%	NP	
Arthrobacter aurescens TC1	*AAUR1709*	41%	NP		*AAUR0031*	45%	NP	
Propionibacterium acnes	*PPA0757*	37%	NP		*PPA0186*	44%	NP	
Leifsonia xyli subsp. xyli str. CTCB07	*Lxx15270 & Lxx16950*	39% & 36%	NP		*Lxx00240*	44%	NP	
Tropheryma whipplei	*TW543 (ftsW)*	35%	NP		*TW786*	38%	NP	
Corynebacterium glutamicum	*NCGL2079*	36%	NP		*NCGL0043*	41%	NP	
Mycobacterium tuberculosis	*Rv2154c (ftsW)*	42%	NP		*Rv0017c*	47%	NP	
Escherichia coli	*B0089 (ftsW)*	31%	*B0634 (mrdB)*	34%	NP		NP	
Bacillus subtilis	*BSU15210 (spoVE)* and *BSU14850(ftsW)*	36% [SpoVE & FtsW]	*BSU38120 (rodA)*	38% (SpoVE) & 31% (RodA)	NP		NP	
Streptococcus pneumoniae	*SP1067 (ftsW)*	27%	*SP0803 (rodA)*	29%	NP		NP	

NP: - Not Present

Pair wise and multiple sequence alignments of amino acid sequences of FtsW/RodA homologues found in different actinobacteria revealed high identity and similarity between the proteins. The percentage identities of SEDS proteins from different bacteria were compared to those of the *S. coelicolor* SEDS proteins. Since SEDS proteins form a group of similar proteins, all SEDS proteins from different bacteria showed more or less similarity to all the four SEDS family proteins of *S. coelicolor*. Comparison of the percentage identities of different SEDS protein from different bacteria to that of *S. coelicolor* clearly separated FtsW homologues from RodA homologues (Table 3.2). For example, the *S. coelicolor* FtsW ($FtsW_{Sc}$) has 88%, 30%, 29% and 28% identity with *S. avermitilis* FtsW1, FtsW2, FtsW3 and FtsW4 respectively, whereas the Sfr sequence of *S. coelicolor* (Sfr_{Sc}) has 32%, 84%, 31% and 31% identity with *S. avermitilis* FtsW1, FtsW2, FtsW3 and FtsW4, respectively. Thus, the SEDS proteins from different organisms are grouped according to the highest percentage identity of a particular SEDS protein from different bacteria to the *S. coelicolor* SEDS proteins as well as the genomic organization of the locus encoding a particular SEDS protein (Table 3.2). Comparison of SEDS protein orthologues in three streptomycetes showed 54-88% identity, while identities between the orthologues of *S. coelicolor* and the other organisms ranged from 31-56% (Table 3.2). $FtsW_{Sc}$ shows 31% identity with *E. coli* FtsW ($FtsW_{Ec}$) and 36% identity with *B. subtilis* FtsW ($FtsW_{Bc}$) and SpoVE ($SpoVE_{Bc}$) proteins. Interestingly, the percentage identity of Sfr_{Sc} to $SpoVE_{Bc}$ is 38%, similar to that of $FtsW_{Sc}$.

Multiple alignments of FtsW protein orthologues from *E. coli, B. subtilis, S. pneumoniae, M. tuberculosis* and *S. coelicolor* showed highly conserved amino acids and most of them are located towards the C-terminal region of the protein (Fig. 3.1). Two proline residues P_{306} and P_{386} of *M. tuberculosis* FtsW ($FtsW_{Mt}$) and P_{368} and P_{375} residues of *E. coli* FtsW are required for interaction with their cognate penicillin-binding protein (PBP) (Datta *et al.*, 2006; Pastoret *et al.*, 2004). The counterparts of these proline residues are conserved in all the FtsW sequences analyzed, however only a few sequences are shown (Fig. 3.1). Corresponding conserved proline residues in $FtsW_{Sc}$ are P_{302}, P_{375} and P_{382}. Interestingly, multiple alignment analysis of all four SEDS protein sequences from all the available *Streptomyces* genome databases revealed that the proline residues equivalent to P_{375} and P_{382} of $FtsW_{Sc}$ are conserved in all four SEDS proteins, while the proline residue equivalent to P_{302} of $FtsW_{Sc}$ is found conserved


FtsW$_{Bs}$ ----------MLKKMLKSYDYSL 13
FtsW$_{Sp}$ ----------MKISKRHLLNYSI 13
SpoVE$_{Bs}$ ----------MTTKKTSPD-LLLVIITL 17
FtsW$_{Ec}$ ----------MRLSLPRLKMPRLPGFSILVWISTALKGWVMGSREKDTDSLIMYDRTL 48
FtsW$_{Sc}$ ------MPGSPQSRTGRPPVQRTVKRP-AAPGPPHDNGVLRLYHRLRRAWDRPLTAYYLI 53
FtsW$_{Mt}$ MLTRLLRRGTSDTDGSQTRGAEPVEGQRTGPEEASNPGSARPRTRFGAWLGRPMTSFHLI 60
IFAIVLLCGFGLVMVYSSSMITAVSRYGVSSNFFFMRQLFALIAGGALFILMALFPYKAL 73
LIPYLLLSILGLIVVYSTTSAILIE-EGKSALQLVRNQGIFWIVSLILIALIYKLRLDFL 72
LLLT-----IGLIMVYSASAVWADY-KFDDSFFFAKRQLLFAGIGVIAMFFIMNVDYWTW 71
LWLTFGLAAIGFIMVTSASMPIGQR-LTNDPFFFAKRDGVYLILAFILAIITLRLPMEFW 107
FGGSALITVLGLVMVYSASQITALQ-LSLPGSYFFRKQALAALIGAGLLVAAMKMPVKLH 112
IAVAALLTTLGLIMVLSASAVRSYD-DDGSAWVIFGKQVLWTLVGLIGGYVCLRMSVRFM 119
AHQKFQKGILLVSVLALISLFVFGHVAGNAQSWFKIGG-MSIQPGEFVKLVVILYLAAVY 132
RNERLIILVILIEMLLLFLARFIGISVNGAYGWISVAG-ITIQPAEYLKIIIIWYLAHRF 131
RTWSKLLMVICFFLLVLVLIPGVGMVRNGSRSWIGVGA-FSIQPSEFMKLAMIAFLAKFL 130
QRYSATMLLGSIILLMIVLVVGS-SVKGASR-WIDLGL-LRIQPAELTKLSLFCYIANYL 164
RALAYPILAGAVFLMILVQVPGIGVAVNGNQNWISLGGSFQIQPSEFGKLALVLWGADLL 172
RRIAFSGFAITIVMLVLVLVPGIGKEANGSRGWFVVAG-FSMQPSELAKMAFAIWGAHLL 178
AKK-QSYIDHLLTGVAPP----------VVMTLIICGLIAMQPDFGTAMIIGLIATCMI 180
SKQ-QEEIATYDFQVLTQNQWLPRAFNDWRFVLLVLIGSLGIFPDLGNATILVLVSLIMY 190
SEK-QKNITSFRRGFVPALG----------IVFSAFLIIMCQPDLGTGTVMVGTCIVMI 178
VRK-GDEVRNNLRGFLKPMG----------VILVLAVLLLAQPDLGTVVVLFVTTLAML 212
ARKHDKKLLTQWKHMLVPLVP----------AAFMLLGLIMIGGDMGTAIILTAILFGLL 222
AARRMER--ASLREMLIPLVP----------AAVVALALIVAQPDLGQTVSMGIILLGLL 226
LCSGFSGKTLVRLVILGGIVFILVSPIIYLN----QDKILTEGRLAR-FESLEDPFKYAN 235
TVSGIAYRWFSTILALVSAASVFVLTTISLIGVETFSKIPVFGYVAKRFSAFFNPFADRA 250
FVAGARIAHFVFLGLIGLSGFVGL----------VLSAPYRIKRITSYLNPWEDPL 224
FLAGAKLWQFIAIIGMGISAVVLL----------ILAEPYRIRRVTAFWNPWEDPF 258
WLAGAPTRLFAGVLSIALLLGFIL----------IKTSANRMARLNCLGATDPGPG 268
WYAGLPLRVFLSSLAAVVVSAAIL----------AVSAGYRSDRVRSWLNPENDPQ 272
SSGLQVINSYYAISSGGIFGLGLGESIQKYGYLPEESHTDFIMAVIAEELGIFGVLFVIFL 295
DAGHQLANSYFAMVNGGWFGLGLGNSIEKRGYLPEAHTDFVFSIVIEEFGFVGASLILAL 310
GSGFQIIQSLYAVGPGGLFGMGLGQSRQKFFYLPEPQTDFIFAILSEELGFIGGTLILLL 284
GSGYQLTQSLMAFGRGELWGQGLGNSVQKLEYLPEAHTDFIFAIIGEELGYVGVVLALLM 318
DSCWQAVHGIYALASGGLFGSGLGASVEKWGQLPEAHTDFIFAVTGEELGLAGTLSVLAL 328
DSGYQARQAKFALAQGGIFGDGLGQGVAKWNYLPNAHNDFIFAIIGEELGLVGALGLLGL 332
LGFVVIKGFYIA---RKCEDPFGSLLAIGISSMIAIQSFINLGGVSGLIPITGVTLPFIS 352
LFFMILRIILVG---IRAENPFNAMVALGVGGMMLVQVFVNIGGISGLIPSTGVTRPFLS 367
FSVLLWRGIRI---ALGAPDLYGSFVAVGIISMIAIQVMINIGVVTGLIPVTGITLPFLS 341
VFFVAFRAMSIGRKALEIDHRFSGFLACSIGIWFSFQALVNVGAAAGMLPTKGLTLPLIS 378
FAALGYAGIRVAG---RTEDPFVRYAAGGVTTWITAQAVINIGAVLGLLPIAGVPLPLFS 385
FGLFAYTGMRIAS---RSADPFLRLLTATTTLWVLGQAFINIGYVIGLLPVTGLQLPLIS 389
YGGSSLVLLLGSMGILANISMFVK---------- 376
QGGNSLLVLSVAVAFVLNIDASEK---------- 391
YGGSSLTLMLMAVGVLLNVSRYSR---------- 365
YGGSSLLIMSTAIMMLLRIDYETR---------- 402
YGGSALLPTMFAIGLLIAFARDEPGARAAL---------- 415
AGGTSTAATLSLIGIIANAARHEPEAVAALRAGRDDKVNRLLRLPLPEPYLPPRLEAFRD 449

```
FtsW_Bs     ----------YSENKKKKEPLAPKGMKKKQLKKTVYL---------------------- 403
FtsW_Sp     ----------RAKLYRELENQPMNLLLK------------------------------- 409
SpoVE_Bs    ----------Y------------------------------------------------ 366
FtsW_Ec     ----------LEKAQAFVRGSR------------------------------------- 414
FtsW_Sc     --------ALRQPRFGRKRGAGGPAAKRS-----PGSWNTMRR--RASAARSSGER---- 456
FtsW_Mt     RKRANPQPAQTQPARKTPRTAPGQPARQMGLPPRPGSPRTADPPVRRSVHHGAGQRYAGQ 509

FtsW_Bs     ---------------
FtsW_Sp     ---------------
SpoVE_Bs    ---------------
FtsW_Ec     ---------------
FtsW_Sc     ---------------
FtsW_Mt     RRTRRVRALEGQRYG 524
```

Figure 3.1: Multiple alignment of FtsW orthologue sequences from *B. subtilis* ($FtsW_{Bs}$), *B. subtilis* ($SpoVE_{Bs}$), *E. coli* ($FtsW_{Ec}$), *S. pneumoniae* ($FtsW_{Sp}$), *M. tuberculosis* ($FtsW_{Mt}$) and *S. coelicolor* ($FtsW_{Sc}$). Alignments were generated using ClustalW2 program from the European Bioinformatics Institute server (http://www.ebi.ac.uk/Tools/clustalw2/). Conserved proline residues that are required for interaction with cognate PBP in *E. coli* and *M. tuberculosis* are shown in rectangular box. Conserved lysine residue of FtsW is indicated by bold letter. Underneath the alignment, "*" means that residues are identical in the aligned sequences, ":" means that conserved substitution have been observed, and "." means that semi-conserved substitution are occurred. Characters in blue colour show identical residues in $FtsW_{Mt}$ and $FtsW_{Sc}$.

only in FtsW and Sfr orthologues (Fig. 3.2). Conservation of these proline residues in the SEDS proteins indicates that they may be important for the interaction with their cognate PBPs. No clear consensus sequence was found that can easily differentiate FtsW from RodA. A single position appears to always be occupied by a lysine in all FtsW proteins (Lys^{297} in *S. coelicolor*), whereas it is absent in RodA proteins. The clear separation of FtsW homologues from RodA homologues indicates the functional identity of the proteins of each group.

```
AV2951    -------MIQPGWPGTKAVADPLAPDLRLPRRRGIEFSLLVVAVLLSVYGYCAVGLAKRG 53
SSCRodA2  --------------------PSPPAVRPLRRRGVEFTLTVVAVLLSVSGYCAVGLAKNG 39
SCO5302   ----------------MAQADTPAPVARLPRRRGIELALILMAVLLSVFGYCNVGLAQHD 44
SGR2202   --------------MTATTADAPPPELRLPKRRGVELTLLVGGVLISVLGYAAVGLAHDG 46
SCO3846   ---------MSSTTNPSTHHTSTIGAIGAPSRRNTELALLVFAVLIPVFAYANVGLAIND 51
SAV4340   ---------MSSSTNTPTHHTSTIGSIGAPSRRNTELALLVFAVVIPVFAYANVGLAIDD 51
SSCRodA   ----------------------IGAIGTPSRRNTELALLAFAVVIPVFAYANVGLAING 37
SGR3727   ---------MSVVTN-----TTTIGAIDAPSRRNTELALVVFAVAISVFAYANVGLALNG 46
SCO2085   --------------------MPGSPQSR----TG----RPPVQRTVKRP---------- 21
SAV6121   ----------------------MPTSR----TG----RPPVQRATRRP---------- 18
SSCFtsW   --------------------VPPMPGSR----TS----RAPLQRVTRRP---------- 21
SGR5420   MPADERFAVRRDRARASVPRPLAAAPALSGLPLTGGLALRGRLATGARRPETPRGFGRGG 60
SAV5459   ------------------------------------------------------------
SSCSfr    ------------------------------------------------------------
SCO2607   ------------------------------------------------------------
SGR4935   ------------------------------------------------------------
```

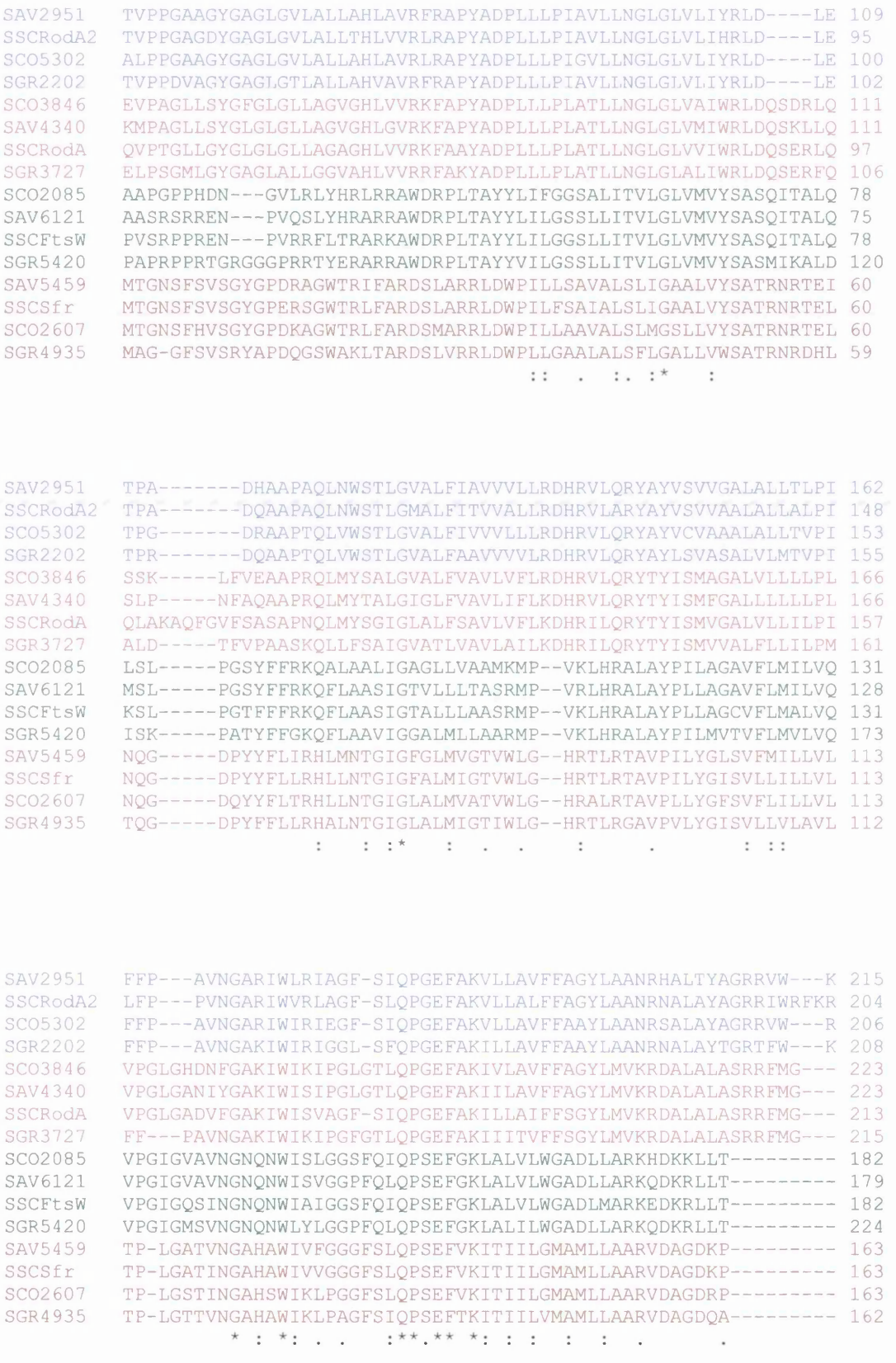

Figure 3.2: Continued on the next page……..

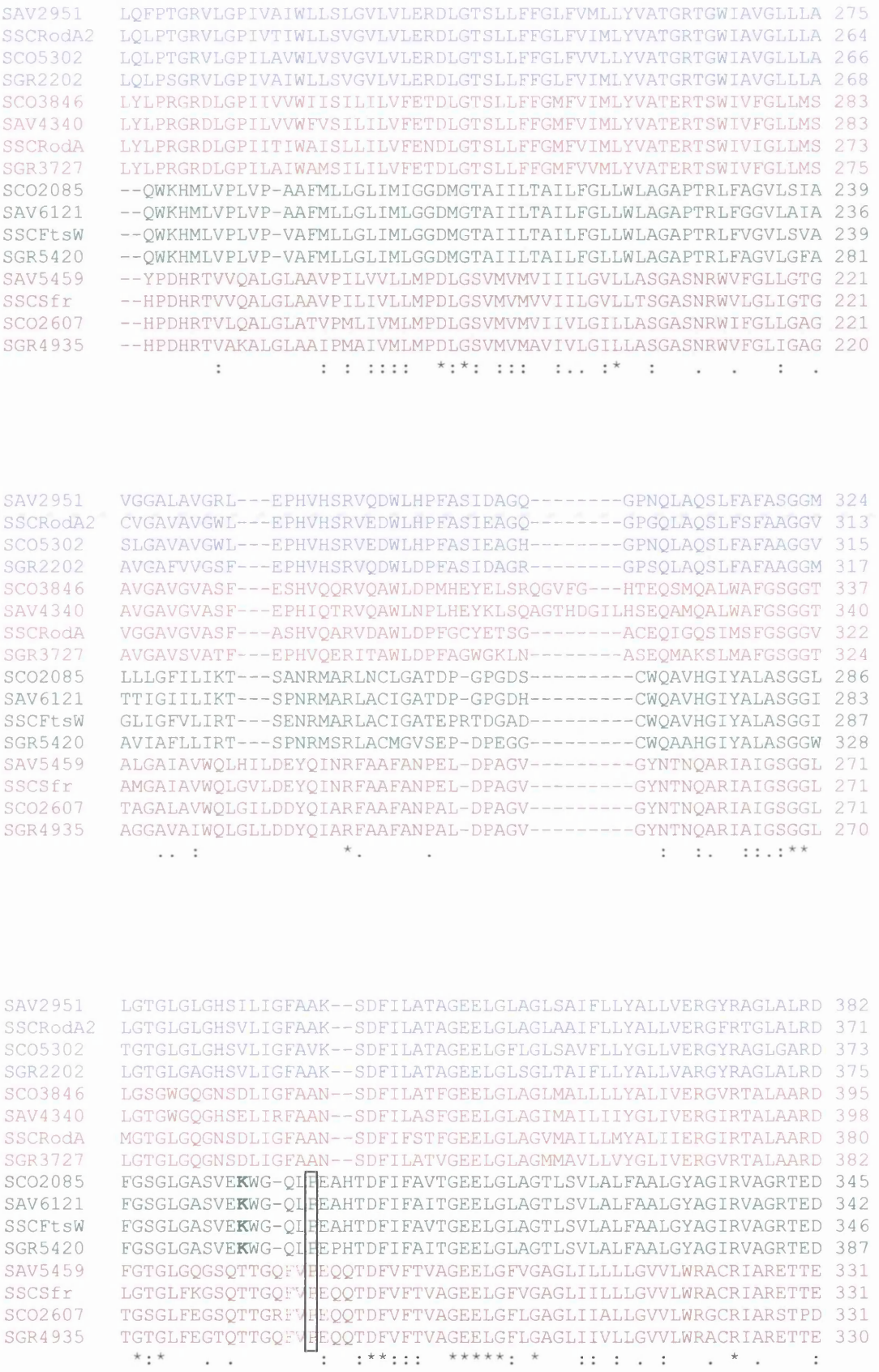

Figure 3.2: Continued on the next page……..

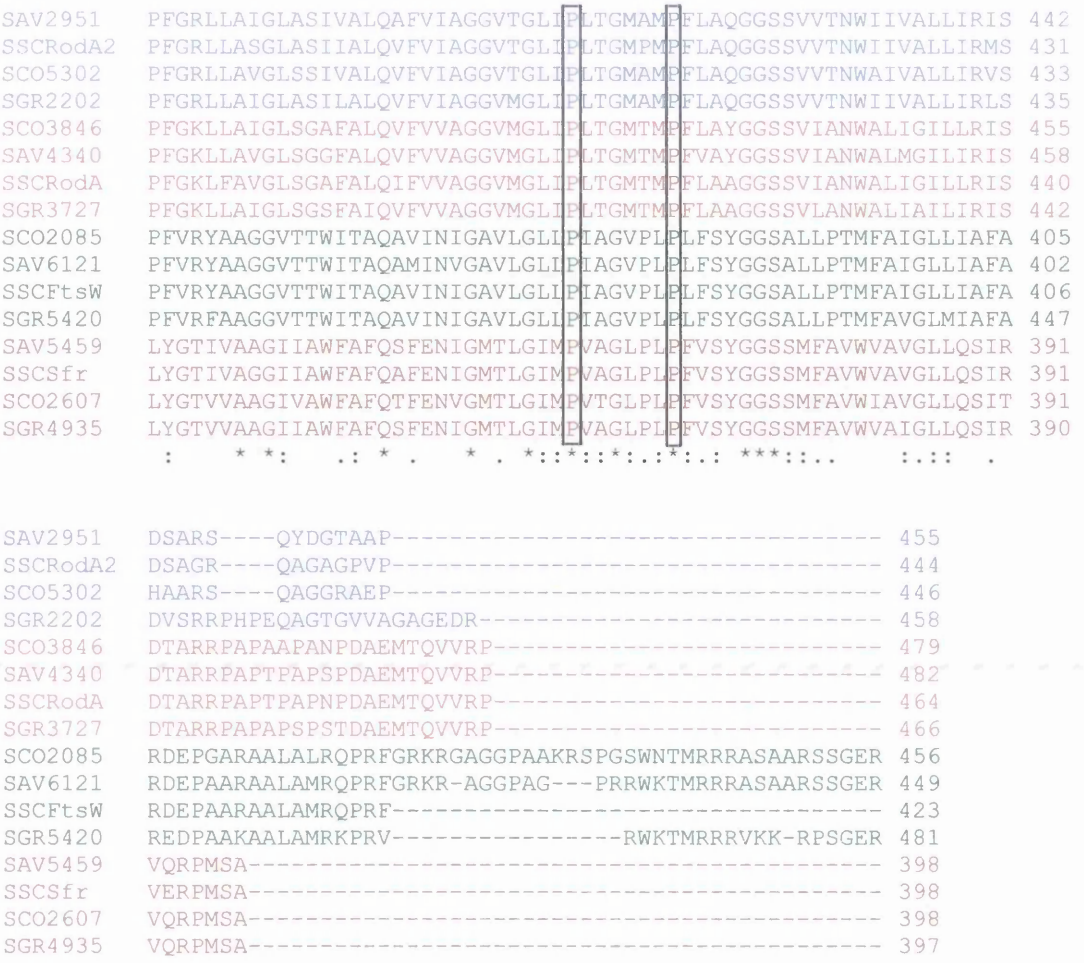

Figure 3.2: Multiple alignment of FtsW (green), Sfr (brown), RodA (red) and RodA2 (blue) orthologue sequences from different species of *Streptomyces*; SAV, *S. avermitilis*; SGR, *S. griseus*; SCO, *S. coelicolor*; SSC, *S. scabies*. Each SEDS protein is presented by abbreviation of the name or the organism followed by the number of gene, except in the case of *S. scabies*. Since the annotation of *S. scabies* genome is ongoing, the number of respective genes encoding respective SEDS protein is not assigned. Therefore for convenience the names given to *S. coelicolor* SEDS proteins are used to denote respective SEDS proteins of *S. scabies*. Alignments were generated using the ClustalW2 program from the European Bioinformatics Institute server (http://www.ebi.ac.uk/Tools/clustalw2/). Conserved proline residues that are required for interaction of FtsW with its cognate PBP in *E. coli* and *M. tuberculosis* are shown in the rectangular box. The Lysine residue found only in FtsW is indicated by bold letter. Underneath the alignment, "*" means that residues are identical in the aligned sequences, ":" means that conserved substitution have been observed, and "." means that semi-conserved substitution are occurred.

To further establish the relationship of *Streptomyces* SEDS proteins with that of other well studied SEDS proteins of actinomycetes and non-actinomycetes, the phylogenetic analysis of SEDS proteins was carried out based on the amino acid sequence alignment. An unrooted Neighbor-Joining tree was constructed by MEGA using amino acid sequences of SEDS proteins from different bacteria. The phylogenetic tree (Fig. 3.3) of SEDS homologues revealed four distinct groups of SEDS proteins, where one group includes FtsW orthologues of actinobacteria (red), second group is of FtsW orthologues from non-actinobacteria (purple), third group consists of Sfr from actinobacteria and RodA from non-actinobacteria (blue) and the fourth a group of RodA and RodA2 from actinobacteria (green). The four SEDS proteins of *S. coelicolor* are distributed into three of the four groups (Fig. 3.3). The tree shows that the Sfr protein of *S. coelicolor* is closely related to the RodA protein of non-actinobacteria such as *E. coli* and *B. subtilis* (Fig. 3.3). The tree also indicates that the genes encoding FtsW and RodA of actinobacteria are ancestral actinobacterial genes, while the gene encoding Sfr orthologue in actinobacteria may be acquired by some of the actinobacterial species, later during the course of evolution or it was also an ancestral gene that was subsequently lost in some actinobacterial species. The branching pattern of RodA paralogues of *S. coelicolor* [SCO3846 (RodA) and SCO5302 (RodA2)] and *T. fusca* paralogues (Tfu0427 and Tfu3063) indicates that the genes encoding these genes may have duplicated from an ancestral actinobacterial *rodA* gene during evolution (Fig. 3.3). There is also clear grouping according to the specific function, where the FtsW proteins known to be involved in septal cell wall synthesis group together, the RodA proteins of non-actinobacteria known to be involved in lateral cell wall synthesis groups with Sfr, while the actinobacterial RodA proteins make a separate cluster indicating some distinct function. Since actinobacteria grow by tip extension, it may be possible that the actinobacterial RodA proteins may function in cell wall synthesis at the tip.

Interestingly, the phylogenetic analysis of the respective cognate high molecular weight penicillin binding proteins (HMW PBPs) of SEDS proteins showed similar branching pattern to that of SEDS protein phylogenetic tree (Fig. 3.4). They also grouped in four clusters suggesting that the SEDS proteins and their cognate HMW PBP may have evolved together.

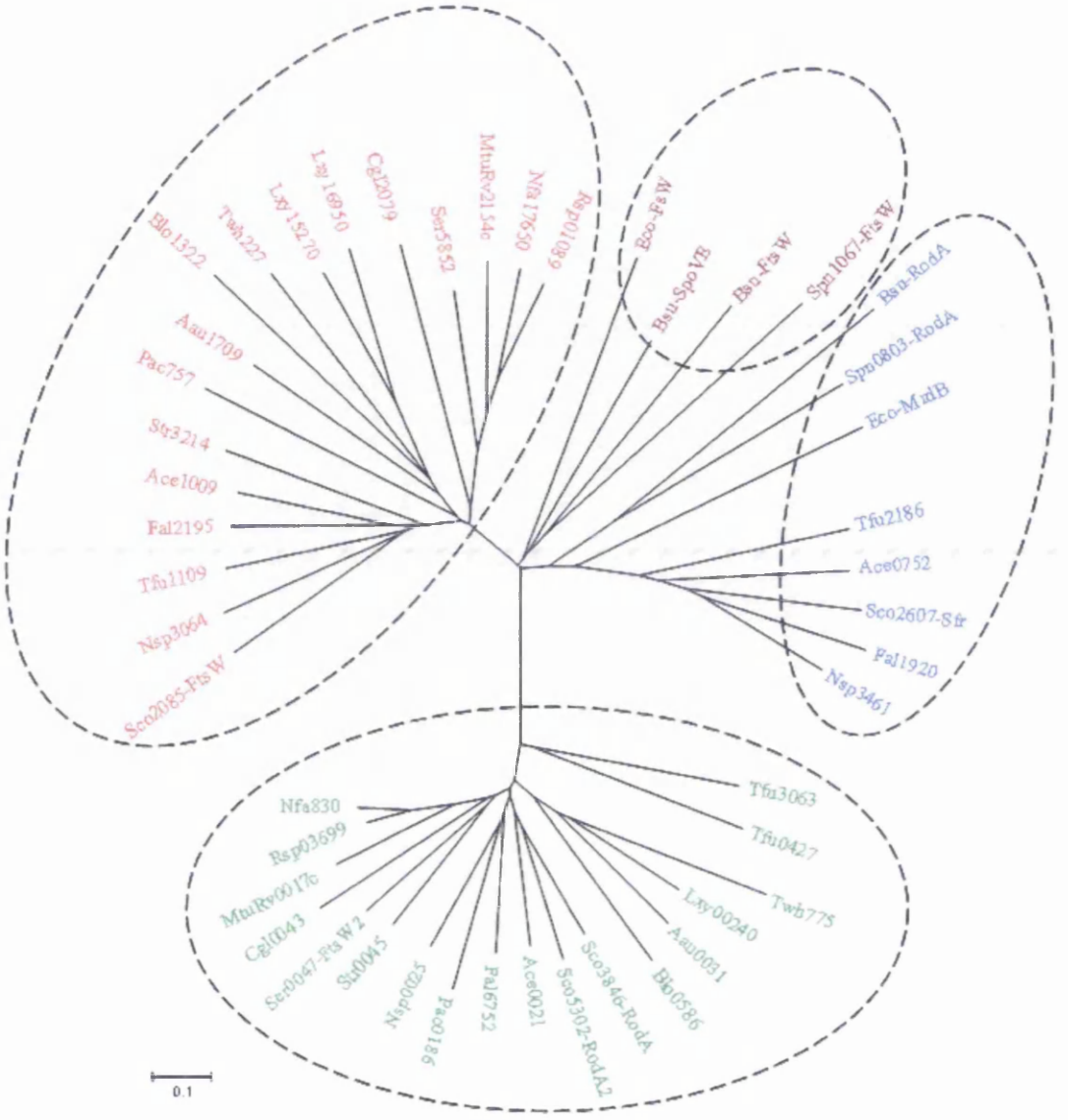

Figure 3.3: Phylogenetic tree showing relationship between SEDS protein orthologues of different bacteria. FtsW orthologues from actinobacteria are red in colour; those from non-actinobacteria are purple in colour. Sfr and non-actinobacterial RodA orthologues ($RodA_{Non\text{-}act}$) are indicated in blue and actionbacterial RodA ($RodA_{Act}$) orthologues are shown in green. Name of each species is indicated by three letter abbreviation followed by number and/or name of gene encoding particular protein. The species abbreviations are: *Aau, A. aurescens TC1; Ace, A. cellulolyticus; Blo, B. longum; Cgl, C. glutamicum; Fal, F. alni; Lyx, L. xyli subsp. xyli str.* CTCB07, *Mtu, M. tuberculosis; Nfa, Nocardia farcinica; Nsp, Nocardioides sp. JS614; Pac, P. acnes; Rsp, Rhodococcus sp.; Sco, S. coelicolor; Ser, S. erythraea; Str, Salinispora tropica; Tfu, T. fusca; Twh, T. whipplei; Bsu, B. subtilis; Eco, E. coli; Spu, S. pneumoniae.*

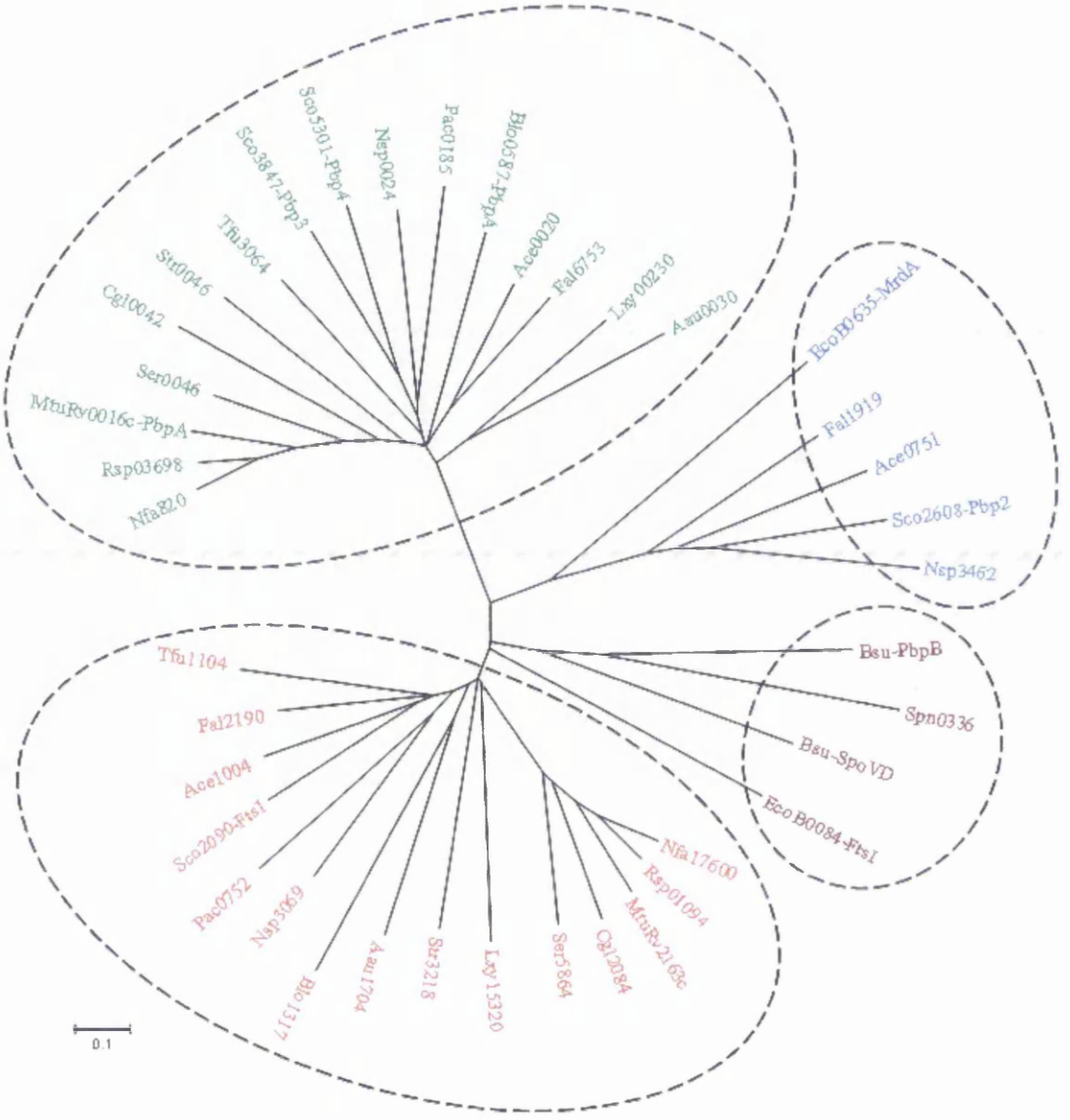

Figure 3.4: Phylogenetic tree showing relationship between cognate high molecular weight penicillin binding proteins (HMW PBPs) of SEDS proteins from different bacteria. The cognate HMW PBPs of FtsW orthologues from actinobacteria are red in colour; those from non-actinobacteria are purple in colour. The cognate HMW PBPs of Sfr and non-actinobacterial RodA orthologues ($RodA_{Non\text{-}act}$) indicated in blue colour. The cognate HMW PBPs of actionbacterial RodA ($RodA_{Act}$) orthologues showed in green colour. Name of each species is indicated by three letter abbreviation followed by number and/or name of gene encoding particular protein. The species abbreviations are: *Aau, A. aurescens TC1; Ace, A. cellulolyticus; Blo, B. longum; Cgl, C. glutamicum; Fal, F. alni; Lyx, L. xyli subsp. xyli str.* CTCB07, *Mtu, M. tuberculosis; Nfa, Nocardia farcinica; Nsp, Nocardioides sp. JS614; Pac, P. acnes; Rsp, Rhodococcus sp.; Sco, S. coelicolor; Ser, S. erythraea; Str, Salinispora tropica; Tfu, T. fusca; Twh, T. whipplei; Bsu, B. subtilis; Eco, E. coli; Spu, S. pneumoniae.*

3.3 Genomic organization of *ftsW/rodA* gene family loci in actinobacteria

Conserved gene clusters are known to be prominent features of bacterial chromosomes. Some of these are operons encoding sets of proteins that are co-ordinately expressed under special conditions, which make it easy to understand their continuing linkage. Demerec and Hartman in 1959 postulated that "regardless of how the gene clusters originated, natural selection must act to prevent their separation" and the "mere existence of such arrangements shows that they must be beneficial, conferring an evolutionary advantage on individuals and populations which exhibit them." The genomic organization studies of many conserved gene clusters by a comparative genomic approach have provided valuable insights into the role of uncharacterized proteins (Mingorance *et al.*, 2004; Tomii and Kanehisa, 1998). The division cell wall *(dcw)* cluster of different bacteria is the best example of a conserved gene cluster that has been studied using a comparative genomic approach (Mingorance *et al.*, 2004). The *dcw* cluster is highly conserved and it includes a group of genes that encode the proteins involved in the synthesis of peptidoglycan and cell division (Ayala *et al.*, 1994; Vicente and Errington, 1996). To shed some light on the functional and evolutionary role of *ftsW/rodA*-like genes found in actinobacteria, the genetic organizations of all the *ftsW/rodA*-like gene loci of sequenced actinobacterial genomes were compared with their respective *ftsW/rodA* gene loci of well characterized non-actinobacterial species such as *E. coli* and *B. subtilis.*

3.3.1 Division cell wall (*dcw*) cluster

Although the organization of the *dcw* cluster genes has already been analyzed in various bacteria, the organization of *dcw* cluster genes in actinobacterial genomes was re-analyzed to get some more understanding of relationship between *dcw* gene organization and the complexity of life cycle among actinobacteria. For genomic comparison analysis, nucleotide sequences of *dcw* clusters from different actionbacteria were selected from their respective genome database and a map of each cluster was prepared using the DNAMAN program. The well studied *dcw* clusters of *E. coli* and *B. subtilis* were also included in comparison analysis. Figure 3.5 shows comparison of *dcw* clusters from different actinobacterial and non-actinobacterial species. The comparison

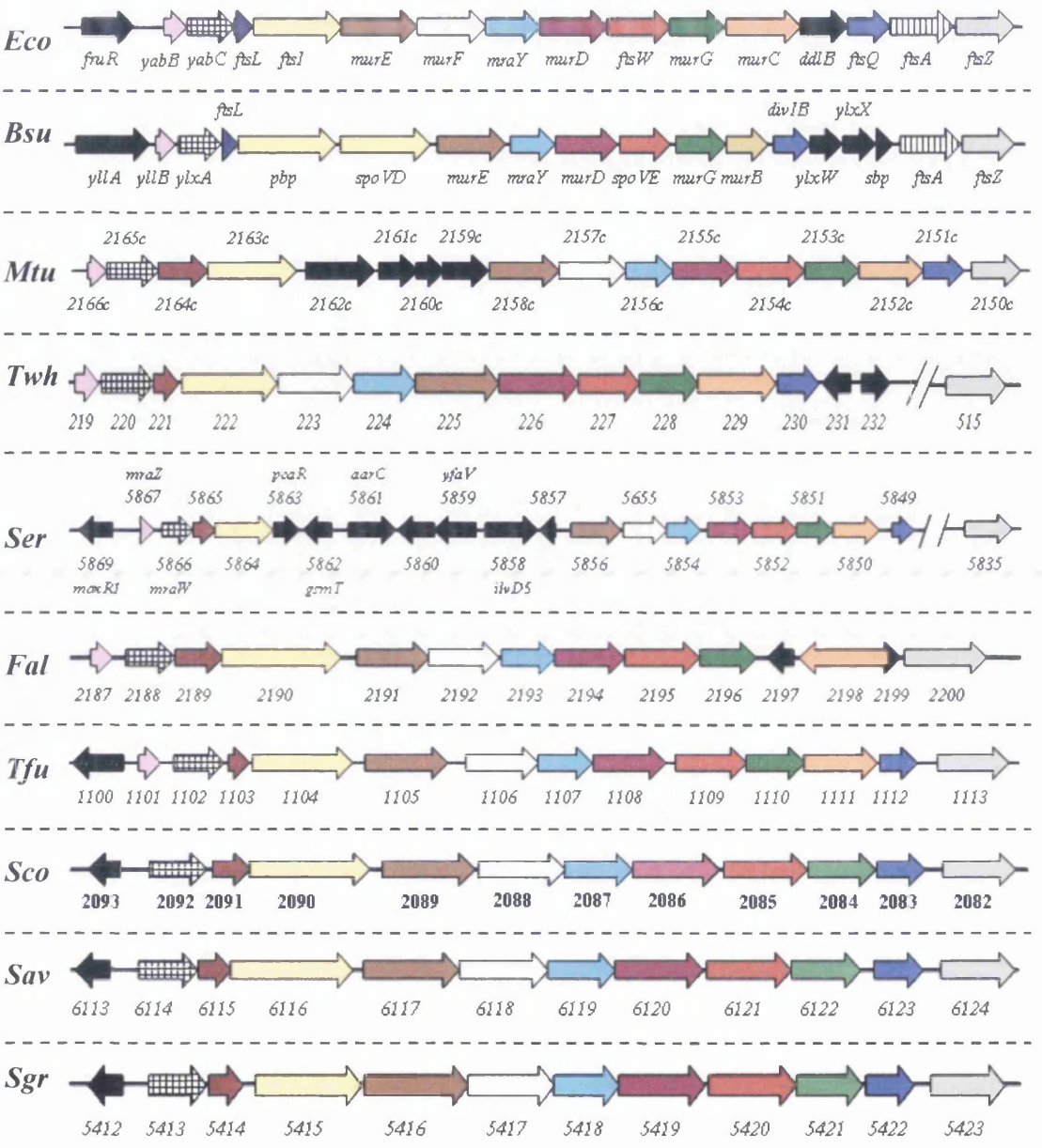

Figure 3.5: Comparison of *dcw* gene clusters from different bacteria. Conservation of the gene order in bacterial division cell wall *(dcw)* clusters. Arrows represent coding genes and their orientation. Gene names and/or numbers are given under each arrow. Homologues of each gene with respect to the gene in the *E. coli mra* cluster are shown either in the same colour or pattern. Solid black arrows indicate non-homologous genes in the clusters. Species name for the corresponding gene cluster is given at the left side of each cluster in the form of 3 letter abbreviation. *Eco,Escherichia coli; Bsu, Bacillus subtilis; Mtu, Mycobacterium tuberculosis; Thw, Tropheryma whipplei; Ser, Saccharopolyspora erythraea; Fal, Frankia alni ACN14a; Tfu, Thermobifida fusca; Sco, Strptomyces coelicolor; Sav, Streptomyces avermitilis;Sgr, Streptomyces griseus.*

of *dcw* cluster genes organization in different bacteria revealed high similarity across the bacterial genomes (Fig. 3.5). Although high similarity among the actinobacterial and non-actinobacterial *dcw* clusters was observed, some of the genes (*ftsA, murB, murC*) that are present in non-actinobacterial *dcw* cluster were missing from the respective actinobacterial *dcw* clusters. Interestingly, the BlastP analysis of different actinobacterial genomes used in this study revealed that the *ftsA* gene, encoding FtsZ interacting protein, is absent from all the actinobacterial genomes analyzed. The *ftsZ* gene in *Tropheryma whipplei* and *Saccharopolyspora erythraea* is around 300 kb and 14 kb downstream to the *dcw* cluster. Unlike all the *dcw* clusters where all the genes involved in cell division and cell wall synthesis are in same orientation, the *F. alni mreC* gene is in the opposite direction. The *ftsQ* gene is absent from the *dcw* cluster of both the *Frankia* species. In fact the BlastP performed using amino acid sequence of FtsQ homologoues from *E. coli, B. subtilis* or *S. coelicolor* revealed that *ftsQ* is absent from the genome of *Frankia* species. Failure to find *ftsQ* gene homologues in the genomes of *Frankia* species may be due to poor conservation of FtsQ sequences (Beall and Lutkenhaus, 1989; Harry and Wake, 1989). The *murC* gene is absent from the *dcw* clusters of all three *Streptomyces* species analyzed and it is located at different position in their respective genomes (Fig. 3.5). Characterization of *dcw* cluster from *Streptomyces collinus* genome also revealed a similar organization of genes in its *dcw* cluster (Mikulik *et al.*, 2000). This analysis suggests that the streptomycete chromosomes have undergone rearrangements during the course of evolution and there may be some differences in the mechanism of *dcw* genes regulation during cell division and cell wall synthesis in streptomycetes.

3.3.2 *sfr* gene region

The *S. coelicolor* genome contains another SEDS gene that is a part of the *mreBCD* genes cluster, which encodes proteins responsible for determining cell shape in *E. coli, B. subtilis* and *Caulobacter crescentus* (Figge *et al.*, 2004; Levin *et al.*, 1992; Varley and Stewart, 1992; Wachi *et al.*, 1987; Wachi *et al.*, 1989). The *mreB, mreC* and *mreD* genes are essential in *E. coli* and *B. subtilis* (Kruse *et al.*, 2005; Lee and Stewart, 2003). The *mreBCD* genes are located near *valS* and *folC* genes encoding

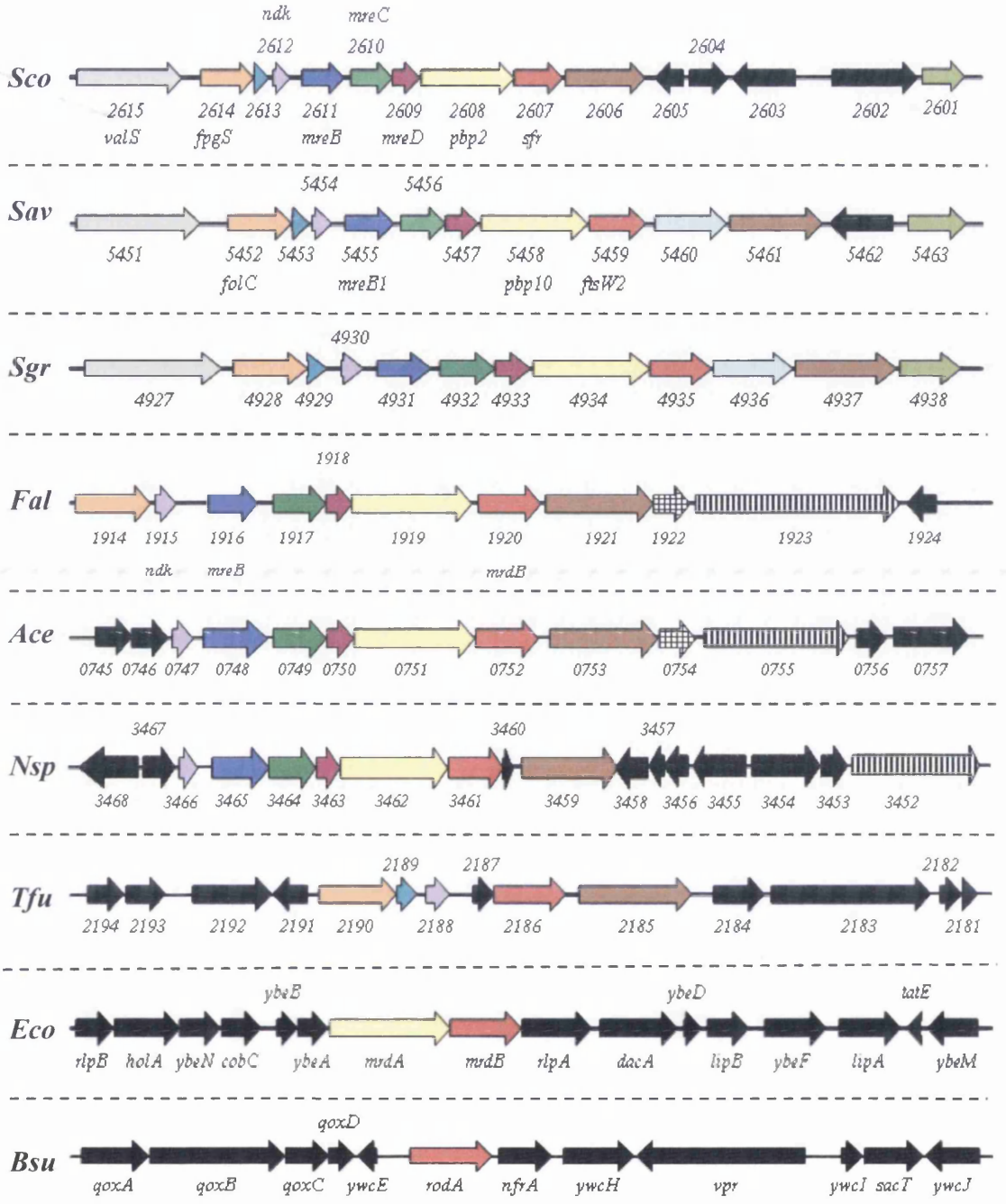

Figure 3.6: Comparison of *sfr* gene region of different Actinobacteria, *Bacillus subtilis* and *Escherichia coli.* Arrows represent coding genes and their orientation. Gene names and/or numbers are given under each arrow. Homologues of each gene with respect to the gene in the *S. coelicolor sfr* locus are shown either with same colour or pattern. Solid black arrows indicated non-homologous genes in the clusters. Species name for the corresponding gene cluster is given on the left side of each cluster in the form of 3 letter abbreviation. *; Sco, Strptomyces coelicolor; Sav, Streptomyces avermitilis; Sgr, Streptomyces griseus; Fal, Frankia alni ACN14a, Ace, Acidothermus cellulolyticus 11B, Nsp, Nocardioides sp. JS614, Tfu, Thermobifida fusca; Eco, Escherichia coli; Bsu, Bacillus subtilis.*

valyl-tRNA-synthetase and folylpolyglutamate synthetase, respectively in *S. coelicolor* and *B. subtilis* genomes (Burger *et al.*, 2000; Margolis *et al.*, 1993). The *mreB* gene encodes a bacterial actin homologue (van den Ent *et al.*, 2001). In the *S. coelicolor* genome one of the SEDS genes, *sfr,* and its cognate HMW PBP are located immediately downstream of *mreBCD* operon (Burger *et al.*, 2000) (Fig. 3.6). The product of the *sfr* gene showed 38%, 31% and 31% identity to the SpoVE, FtsW and RodA proteins of *B. subtilis* respectively. PBP2, a *pbp2* gene product of *S. coelicolor,* also has high similarity with *E. coli* PBP2, which is involved in elongation of lateral cell wall (Spratt, 1975).

A search for the homologous *sfr* gene locus across different actinobacterial genomes revealed that the *sfr* region is found in filamentous streptomycetes, *T. fusca*, *Frankia alni ACN14a,* and *Acidothermus cellulolyticus 11B* as well as in rod shaped actinomycetes *Nocardioides sp.* and *Rubrobacter xylanophilus.* The distribution of the *sfr* locus is unclear and is not confined to filamentous sporulating actinomycetes. Despite of having a mycelial spore forming life cycle, *Saccharopolyspora erythraea, Nocardia farcinica* and *Salinispora tropica* do not possess *mreBCD, pbp2* and *sfr* homologues in their genomes, while rod shaped *Nocardioides* and *R. xylanophilus* do possess these genes. As shown in the Figure 3.6, the gene organization is highly conserved among all the actinobacteria which have acquired the *sfr* gene locus during the course of evolution, except for *T. fusca* where the *mreBCD* and *pbp2* genes are missing. Although not shown in Figure 3.6, the *sfr* locus of *R. xylanophilus* shows a similar arrangement to that of other actinobacteria. In *E. coli* and *B. subtilis*, rodA and its cognate *pbp* (homologous to *sfr* and *pbp2* of *S. coelicolor,* respectively) are not a part of the *mreBCD* operon (Fig. 3.6). Recently, it has been shown that *mreBCD* genes of *S. coelicolor* are not essential and required for the integrity of spore wall during the late stage of development (Burger *et al.*, 2000; Mazza *et al.*, 2006). Figge and co-workers demonstrated that *C. crescentus* PBP2, which functions in lateral cell wall synthesis, was unable to form a helical structure similar to MreB when cells were depleted of MreB (Figge *et al.*, 2004). There were no helical filaments of MreB in *rodA* mutants of *E. coli* (Kruse *et al.*, 2005). All these observations suggest that the functions of Sfr and its cognate PBP in *Streptomyces* may be linked with each other and with MreBCD.

3.3.3 *rodA* gene region

The *S. coelicolor rodA* gene encoding putative SEDS family protein, RodA, is located in the cluster possibly involved in the regulation of peptidoglycan biosynthesis, close to the origin of replication. The organization of genes encompassing this region is highly conserved across actinobacterial genomes. (Dasgupta *et al.*, 2006; Del Sol, 2004; Jones and Dyson, 2006; Narayan *et al.*, 2007). A diagrammatic presentation of the region containing *rodA* in *S. coelicolor* and its homologous region found in other actinobacteria is shown in the Figure 3.7. Clusters shown in Figure 3.7 are from a few representative actinobacteria, but it is very similar in all other sequenced actinobacterial genomes. Immediately downstream to the *rodA* gene is a *pbp* gene, encoding another classB penicillin binding protein (PBP) believed to be involved in cell wall synthesis and cell division. Further downstream in the region there is a *crgA* gene implicated in control of sporulation septation in *Streptomyces* (Del Sol *et al.*, 2003; Del Sol *et al.*, 2006). The *crgA* gene encodes a small protein with two C-terminal membrane spanning domains. Disruption of *crgA* homologue in *S. avermitilis* abolished sporulation septation in aerial hyphae whereas in *S. coelicolor* disruption of *crgA* resulted in precocious growth of aerial hyphae and early antibiotic production on glucose-containing media (Del Sol *et al.*, 2003). In addition to morphogenetic genes, the region contains genes encoding proteins involved in signal transduction: serine/threonine kinases (STPKs), phosphatase and two proteins with Fork Head Associated (FHA) domains (Fig. 3.7). There are two serine/threonine kinases (PknA and PknB) in all clusters except *Streptomyces*, where there is only one (PknB). *In vitro* kinase assays showed that PknA and PknB of *M. tuberculosis* have the ability to autophosphorylate and the activity was dependent on Mn^{2+} and Mg^{2+} (Av-Gay *et al.*, 1999; Chaba *et al.*, 2002). Mutation in the counterpart of the *pbpA* gene of *M. smegmatis* resulted in a requirement for nutrient-rich medium for growth and the mutant grew more slowly than the wild-type, suggesting a role for PBPA during the active phase of growth (Dasgupta *et al.*, 2006). This was supported by the observation of Betts *et al.* (2002) that *pbpA* is downregulated during nutrient starvation. Immunofluorescence microscopy showed localization of PBPA to the septum along with newly synthesized peptidoglycan, indicating a role in cell division (Dasgupta *et al.*, 2006). The phosphatase protein PstP inactivated PknA, PknB and PBPA by dephosphorylation and inactivation of PBPA

leads to impaired growth kinetics and altered morphology of the cells (Boitel *et al.*, 2003; Chopra *et al.*, 2003; Dasgupta *et al.*, 2006).

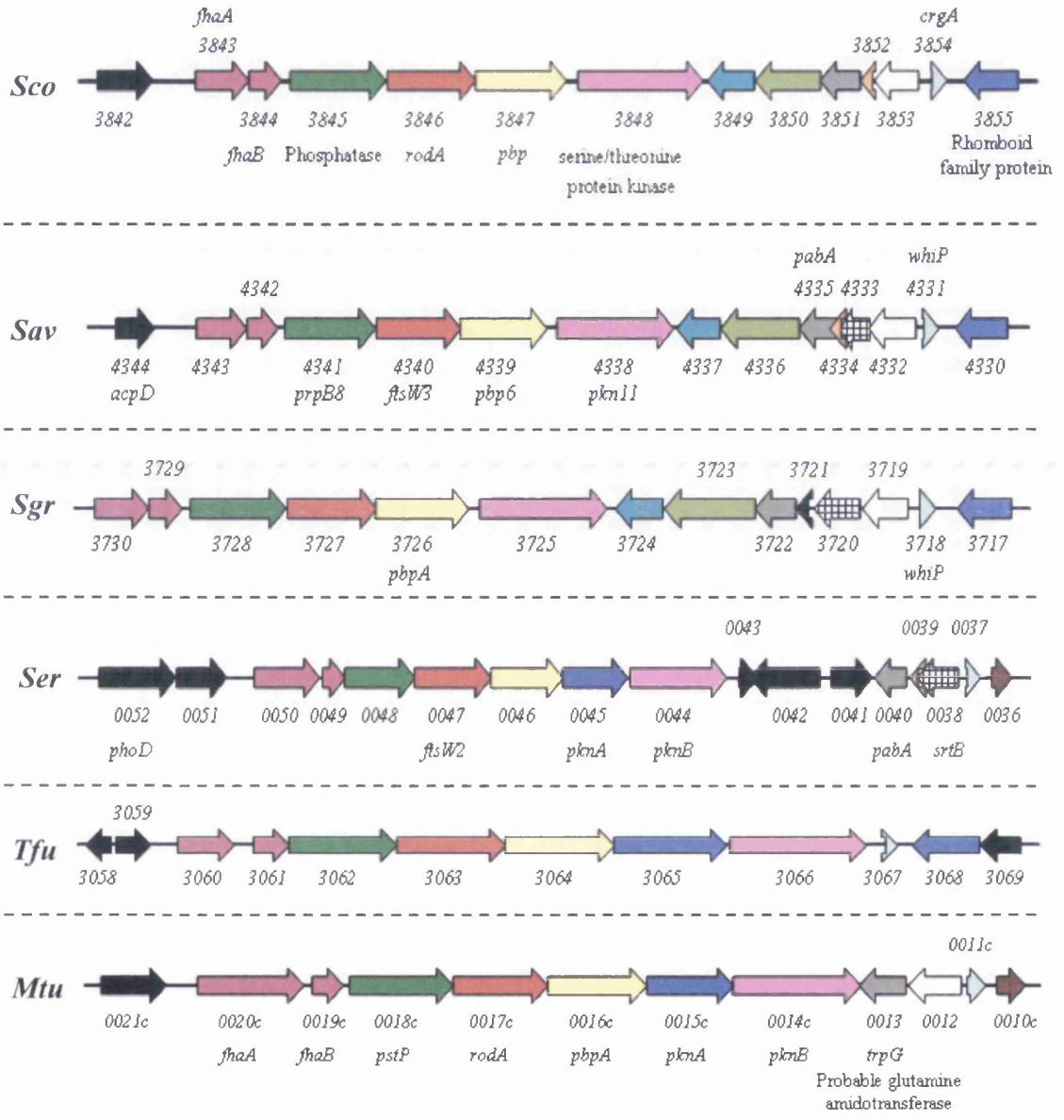

Figure 3.7: Comparison of *rodA* region of Actinobacteria. Arrows represents coding gene and the orientation. Gene name and/or number are given under each arrow. Homologues of each gene with respect to the gene in *S. coelicolor rodA* region are shown either with same colour or pattern. Solid black arrows indicated non-homologous genes in the clusters. Species name for the corresponding gene cluster is given on the left side of each cluster in the form of 3 letter abbreviation. *; Sco, Strptomyces coelicolor; Sav, Streptomyces avermitilis; Sgr, Streptomyces griseus; Ser, Saccharopolyspora erythraea; Tfu, Thermobifida fusca; Mtu, Mycobacterium tuberculosis.*

The two *fha* genes encode proteins that contain FHA domains (Fig. 3.7). The FHA domain is a phosphopeptide-binding domain present in a wide variety of proteins from both prokaryotes and eukaryotes (Li *et al.*, 2000). Studies suggest that FHA domains regulate many different regulatory pathways through their interaction with phosphorylated protein targets. Recently *M. tuberculosis* was shown to phosphorylate the FhaA protein encoded by *fhaA (Rv0020c)* present in this cluster and the phosphorylation depended on the FHA–phosphopeptide interaction (Grundner *et al.*, 2005).

There are also other conserved genes encoding putative peptidyl-prolyl cis-trans isomerase, probable glutamine amidotransferase and a rhomboid family protein. The role of these proteins is unclear.

The conservation of signalling protein genes in the cluster may indicate the presence of an unusual regulatory cascade controlling cell growth in actinobacteria. Thus, in a hypothetical signalling mechanism the STPK(s) senses some signal and induces autophosphorylation. The autophosphorylated STPK(s) binds and phosphorylates FHA-protein(s). This complex subsequently phosphorylates PBP. Then phosphorylated PBP may interact with RodA protein and other cell wall biosynthesis proteins to regulate cell wall synthesis. On the other hand during unfavourable conditions for growth the phosphatase protein could be activated which in turn inactivates STPK(s) and PBP proteins by dephosphorylation. The inactivation of STPK(s) and PBP proteins would lead to the termination of cell growth and division.

3.3.4 *rodA2* gene region

The *SCO5302 (rodA2)* is a fourth gene encoding a putative SEDS family protein in *S. coelicolor*. The region containing this gene is not well characterized. On the basis of annotation it contains genes encoding a putative penicillin binding protein, a putative sensor-like histidine kinase, a putative phosphatase, a DNA ligase, a probable transposase, and a TetR-family transcriptional regulator (Fig. 3.8). It is unclear what their roles may be and how they may be related to cell wall synthesis and division. The presence of the putative phosphatase and sensor-like histidine kinase suggest a signaling mechanism. This region is conserved only in *Streptomyces* which suggests that the genes in this cluster may have some specific role, unique to the *Streptomyces* life cycle (Fig. 3.8). *Thermobifida fusca* with a complex mycelial life cycle similar to

Streptomyces has a gene *TFU0427* whose product has high similarity with the *rodA2* gene product of *S. coelicolor* (Table 3.3, and Fig. 3.8). But there are no orthologues of neighboring genes in the *T. fusca* genome.

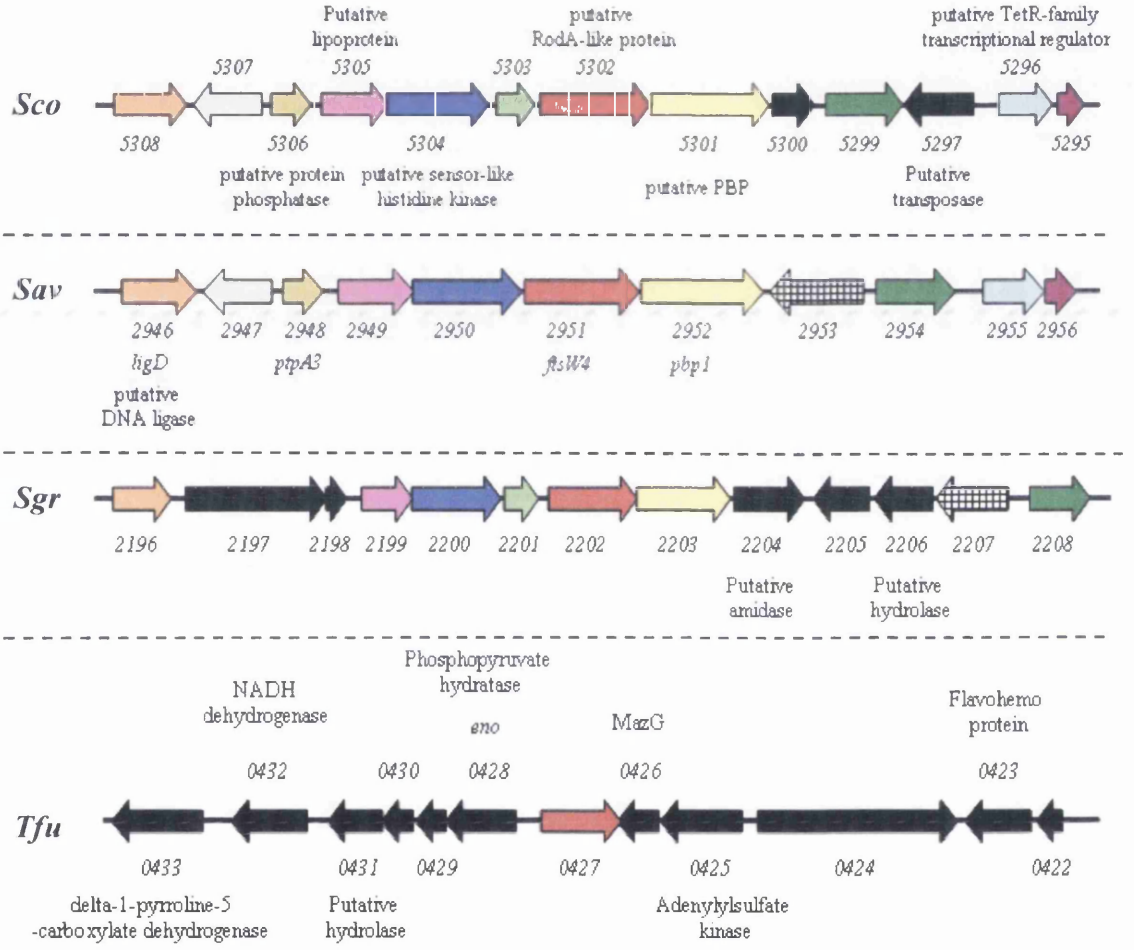

Figure 3.8: Comparison of *SCO5302 (rodA2)* gene region of *Streptomyces*. Arrows represents coding gene and the orientation. Gene name and/or number are given under each arrow. Homologues of each gene with respect to the gene in *S. coelicolor rodA2* region are shown either with same colour or pattern. Solid black arrows indicated non-homologous genes in the clusters. Species name for the corresponding gene cluster is given on the left side of each cluster in the form of 3 letter abbreviation. *; Sco, Strptomyces coelicolor; Sav, Streptomyces avermitilis; Sgr, Streptomyces griseus; Tfu, Thermobifida fusca.*

3.4 Membrane topology predictions of SEDS Proteins of *S. coelicolor*

A hydropathy profile of the amino acid sequences is a useful tool in membrane protein topology prediction and is widely used in membrane protein research (Dobrowolski *et al.*, 2007; Gerard *et al.*, 2002; Lara and Ayala, 2002). The alternating hydrophobic and hydrophilic regions in the profiles correspond to the transmembrane helices (TMHs) and connecting loop regions of the protein, respectively. The topology of *E. coli*, *S. pneumoniae* and *M. tuberculosis* FtsW proteins have been deduced previously using topology prediction programs and reporter protein fusion studies. Topological models of FtsW proteins of three organisms predict 10 transmembrane helices (TMHs), a large extracytoplasmic loop and both N and C termini located in the cytoplasm (Datta *et al.*, 2006; Gerard *et al.*, 2002; Lara and Ayala, 2002). Hydropathy profile of SEDS proteins of *S. coelicolor, M. tuberculosis* and *E. coli* calculated by the program of Kyte-Doolittle (Kyte and Doolittle, 1982) showed high hydrophobic regions with similar patterns of hydrophobicity (Fig. 3.9 and 3.10) among the proteins. For the prediction of the membrane topologies of the four SEDS proteins of *S. coelicolor*, five different topology prediction programs HMMTOP (Tusnady and Simon, 1998), TopPred II (Claros and von Heijne, 1994), TMpred (Hofmann and Stoffel, 1993), TMHMM (Sonnhammer *et al.*, 1998) and TMAP (Persson and Argos, 1994) were used. The results are obtained using default values of all the parameters set by each program. The diagrams of membrane topologies of respective SEDS protein shown in Figure 3.11 and 3.12 were prepared using Microsoft Powerpoint from the hydropathy profile data of each SEDS protein generated from each topology prediction program used. All the Programs predicted the presence of 8 to 12 TMHs for four SEDS proteins of *S. coelicolor* with some variation in positions of N and C termini of each protein.

Topologies predicted for $FtsW_{Sc}$ by all five programs showed 8 to 10 TMHs (Fig. 3.11). The number of amino acids per TMH ranged from 17 to 29 with an average value of 21 amino acids per TMH. A careful observation of each of the $FtsW_{Sc}$ predictions reveals that there is a reasonably good agreement among the various methods concerning the locations of 1, 2, 3, 5, 8, 9 and 10 putative TMHs, with minor variations. Agreement among the methods is, however, poorer over the 4, 6 and 7 TMHs. Although these recent methods for topology prediction are more sophisticated and computationally complex than classical hydropathy analysis, the Kyte-Doolittle

Figure 3.9: Hydropathy profiles of SEDS protein sequences of *E. coli* and *M. tuberculosis* calculated by the program of Kyte & Doolittle. (A) $FtsW_{Ec}$, (B) $FtsW_{Mt}$, (C) $RodA_{Ec}$ and (D) $RodA_{Mt}$.

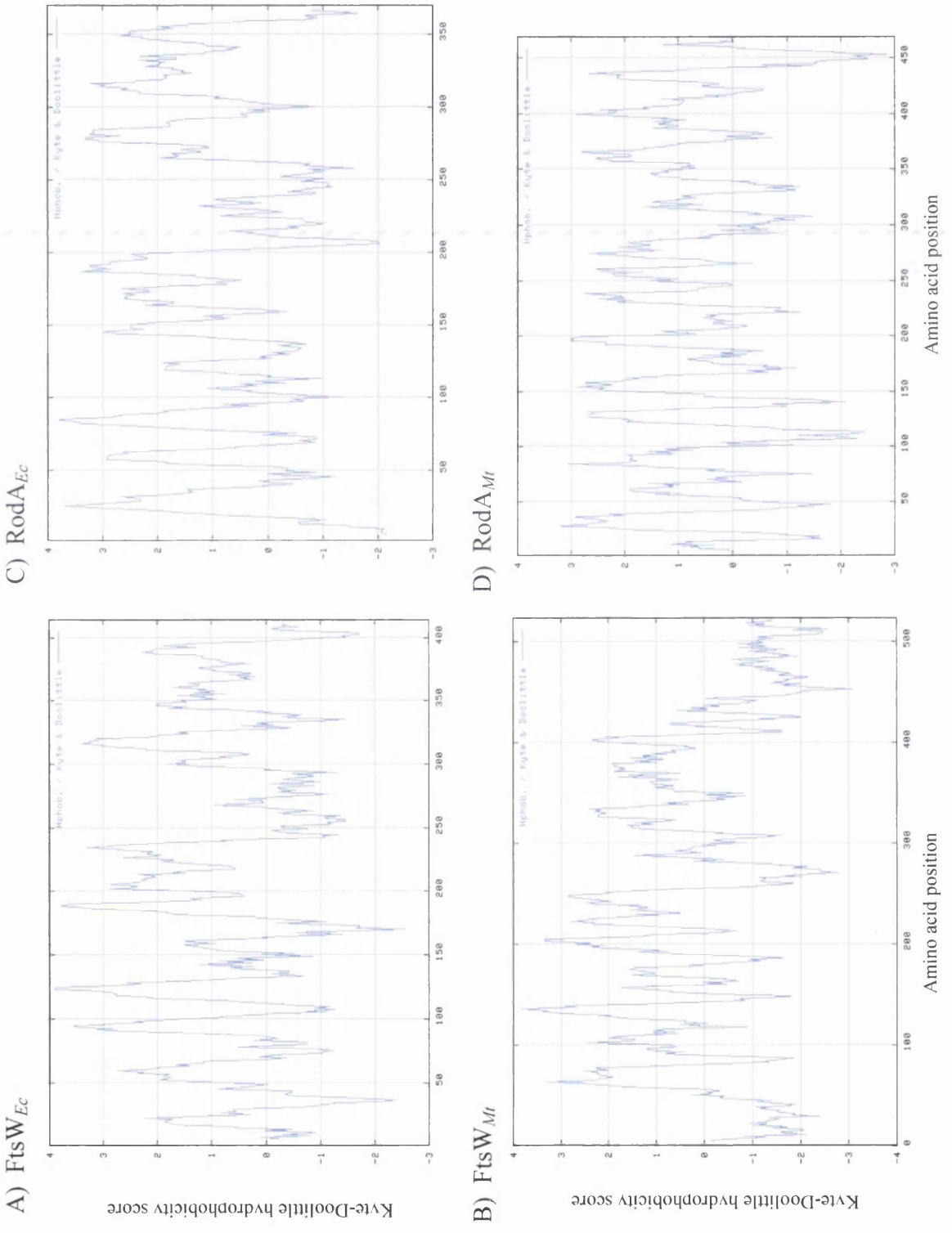

Figure 3.10: Hydropathy profiles of SEDS protein sequences of *S. coelicolor* calculated by the program of Kyte & Doolittle. (A) FtsW, (B) Sfr, (C) RodA and (D) RodA2.

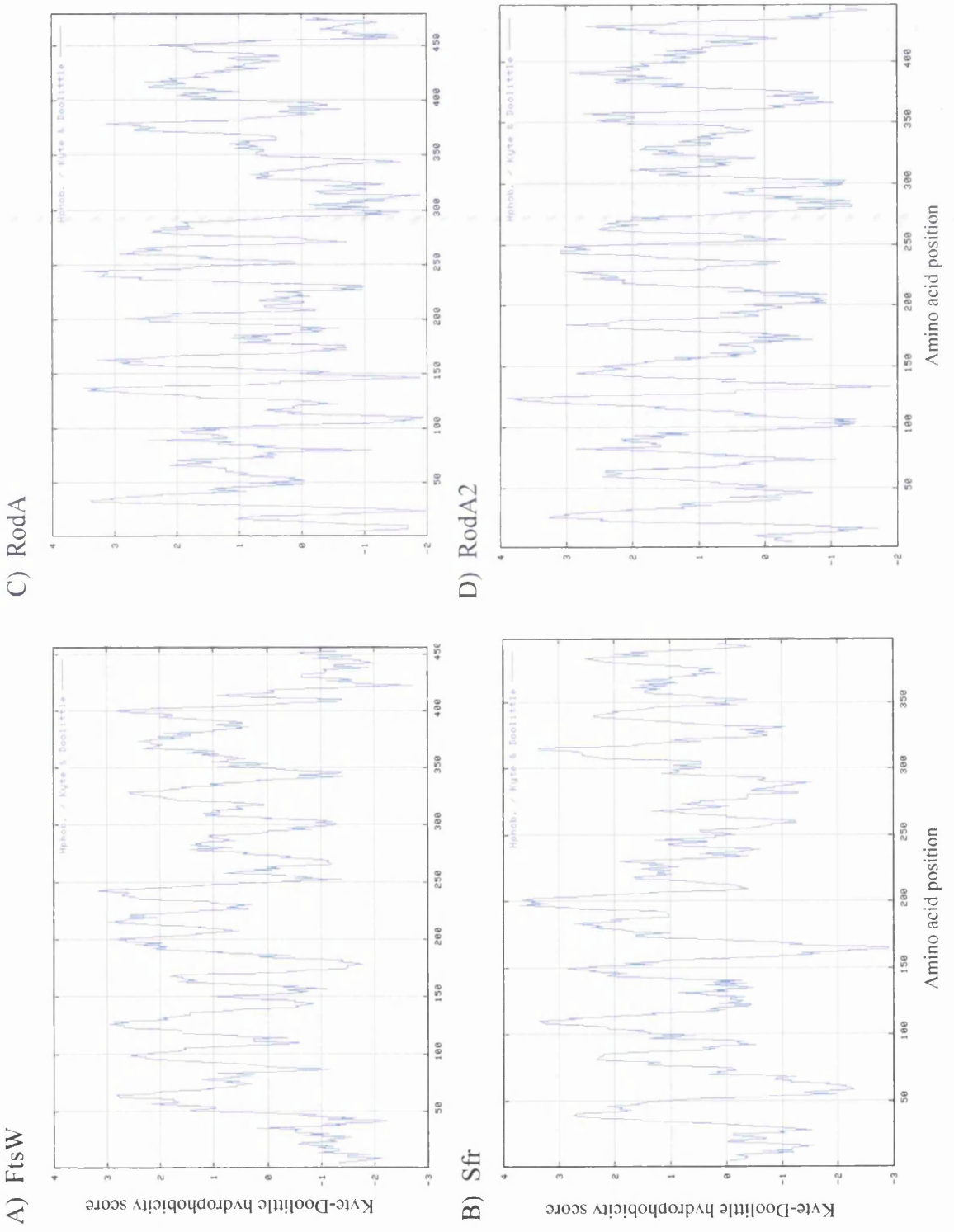

hydrophobicity plot shown in Figure 3.10A provides a simple explanation for these latter discrepancies, that the regions 4, 6 and 7 correspond to hydrophobic segments that are rather short for a TMH, making it difficult for some methods to predict possibilities of segments. The amino- (N) and carboxy- (C) termini consist of approximately 50 amino acid residues, containing more positively charged (10 and 14, respectively) residues than negatively charged (2 and 3, respectively) and they are unlikely to cross the membrane, according to positive-inside rule (von Heijne, 1989). Therefore, both N- and C- termini should be in the cytoplasm, similar to the topology of *E. coli, S. pneumonia* and *M. tuberculosis* FtsW. Unlike $FtsW_{Mt}$ topology, where it is predicted to have a long (~120 amino acids) C-terminus (Datta *et al.*, 2006), $FtsW_{Sc}$ is predicted to have shorter (~50 amino acids) C-terminal region (Fig. 3.11).

Unlike $FtsW_{Sc}$, the membrane topology predictions for Sfr_{Sc}, $RodA_{Sc}$, and $RodA2_{Sc}$ proteins using different programs were almost similar with minor variations. Sfr_{Sc} was predicted to have 10 TMHs, while $RodA_{Sc}$ and $RodA2_{Sc}$ were each predicted to have 12 TMHs, by most programs. Therefore the consensus predicted topology for each protein is presented in Fig. 3.12. The predicted topology of Sfr_{Sc} is almost similar to the *E. coli* and *S. pneumonia* FtsW proteins, having 10 TMHs, a large extracytoplasmic loop of about 69 amino acids between 7 and 8 TMHs, and both N and C terminal in the cytoplasm. Both $RodA_{Sc}$ and $RodA2_{Sc}$ are predicted to have 12 TMHs, a large extracytoplasmic loop of approximately 60 amino acids between 9 and 10 TMHs, and both the termini in the cytoplasm. These predictions are just based on the probability that a particular amino acid residue sits in a TMH or inside or outside the cell. To validate these predictions appropriate experiments such as detection by epitope-specific antibodies, gene fusions with reporter enzymes, protease protection assays and cysteine scanning need to be carried out.

Program	Topology prediction
TMHMM	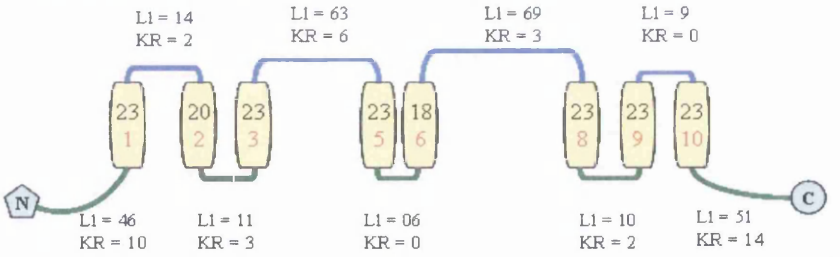
TMAP	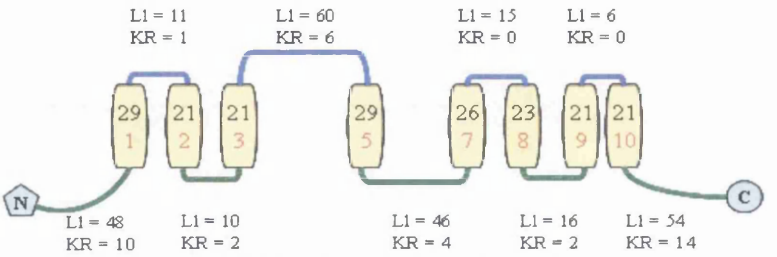
HMMTOP	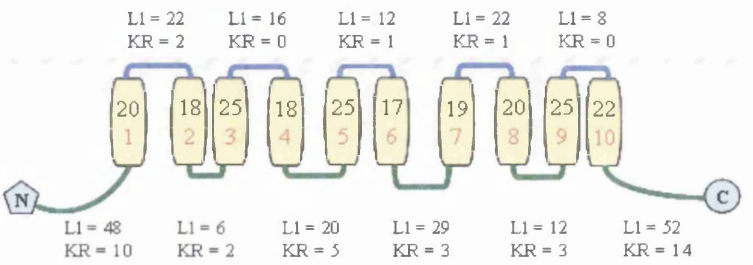
TOPpred	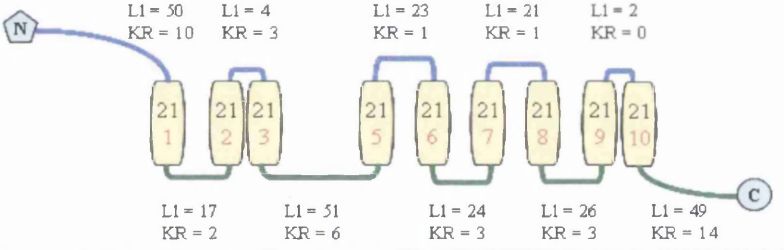
TMpred	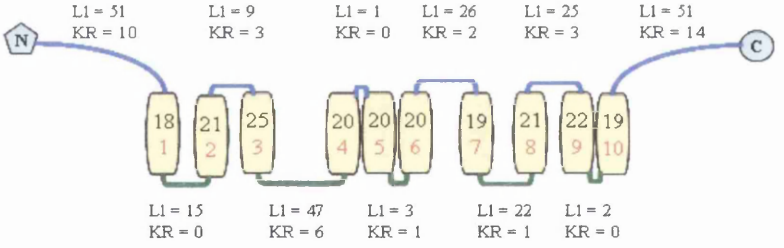

Figure 3.11: Diagrammatic presentation of membrane topologies of $FtsW_{Sc}$ by different programs. Yellow bars represent TMHs. Numbers in bars with black colour indicate number of amino acids per TMH and number with red colour represents number of TMH. Blue line indicates extracytoplasmic loops and green line indicates cytoplasmic loops. Ll: Number of amino acids per loop; KR: Number of positively charged residues Lysine and Arginine per loop.

Protein	Topology prediction
Sfr_{Sc}	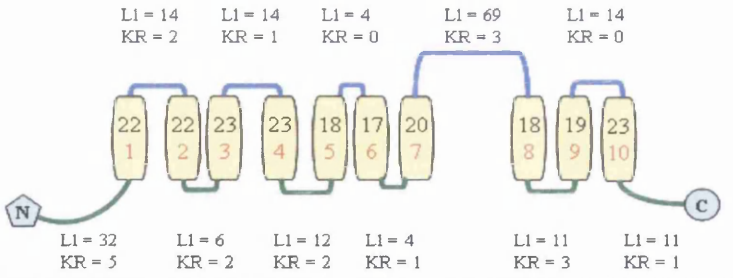
$RodA_{Sc}$	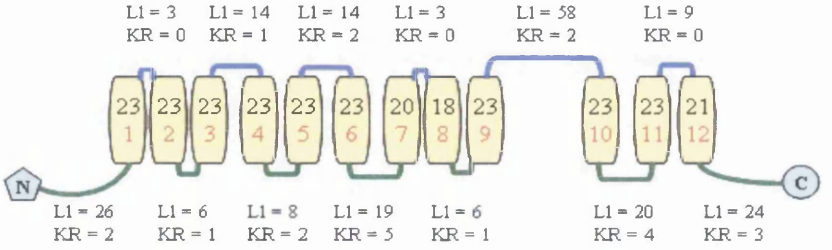
$RodA2_{Sc}$	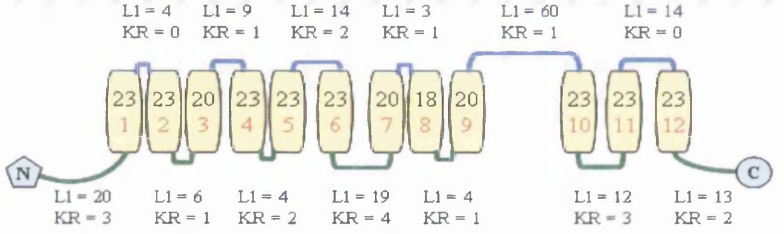

Figure 3.12: Diagrammatic presentation of membrane topologes of Sfr_{Sc}, $RodA_{Sc}$, and $RodA2_{Sc}$. Most of the topology prediction programs showed similar topology for each protein therefore just a consensus sequence for each protein is shown here. Yellow bars represent TMHs. Numbers in bars with black colour indicate number of amino acids per TMH and number with red colour represents number of TMH. Blue line indicates extracytoplasmic loops and green line indicates cytoplasmic loops. Ll: Number of amino acids per loop; KR: Number of positively charged residues Lysine and Arginine per loop.

3.5 Summary

Blast search and multiple alignments analysis of several actinobacterial genomes showed presence of 2 to 4 SEDS family proteins among actinobacteria. All the available *Streptomyces* genomes revealed the presence of four SEDS proteins and their cognate HMW PBPs. The genes encoding the four SEDS proteins in the *S. coelicolor* genome are *ftsW (SCO2085), sfr (SCO2607), rodA (SCO3846)* and *rodA2 (SCO5302).* All the four genes are located in the central core region of the chromosome and found

close to genes encoding HMW PBPs. This indicates some functional coupling between SEDS proteins and their cognate PBPs. At least two of the four SEDS proteins, FtsW and RodA, are found highly conserved with high similarity scores among the actinobacteria. Phylogenetic analysis of SEDS proteins displayed clear grouping of proteins with FtsW clustering with proteins involved in septal cell wall synthesis in *E. coli, B. subtilis* and *M. tuberculosis*. The proline residues in FtsW, which are shown to be essential for PBP interaction, are highly conserved in all the FtsW sequences. The *rodA* gene locus in actinobacterial genomes is unique and highly conserved among actionbacteria. This indicates some specific role of the RodA protein unique to actinobactera. Comparison of genetic loci of all SEDS proteins encoding genes in *S. coelicolor* with different bacteria showed a high conservation of gene arrangements among each locus. Topology predictions for *S. coelicolor* SEDS protein indicated that they are all polytopic membrane proteins containing 8 to 12 TMHs, a large extracytoplasmic loop and both N and C termini in the cytoplasm.

Chapter - 4

Analyses of *sfr*, *pbp2*, *rodA* and *rodA2* Mutants of *Streptomyces coelicolor*

4.1 Introduction

Sequence similarity and topological analysis of *S. coelicolor* SEDS proteins in the previous chapter have given some clues regarding structure and function of these proteins. The presence of four genes (*ftsW, sfr, rodA* and *rodA2*) encoding SEDS proteins in the genome of *S. coelicolor* led to the hypothesis that each gene, in conjunction with the gene encoding their cognate PBP, may function during different stages of the life cycle. The best way to reveal the function of a particular gene is the mutational analysis of that gene. To get some idea about the function of the four *ftsW/rodA*-like genes of *S. coelicolor*, independent mutants for each gene have been constructed using transposon disrupted insertions that are obtained by *in vitro* transposon mutagenesis of the ordered cosmid library of *S. coelicolor* genome using transposon Tn*5062* (Bishop *et al.*, 2004; Redenbach *et al.*, 1996). In this chapter *sfr, pbp2, rodA* and *rodA2* mutants are described. The *ftsW* mutant is described in the next chapter.

4.2 Mutagenesis of *sfr, pbp2, rodA* and *rodA2* genes

The *sfr* gene in *S. coelicolor* is located at the end of an operon like structure that includes *mreB, mreC, mreD, pbp2* and *sfr* (Burger *et al.*, 2000). For the mutagenesis of *sfr* (*SCO2607*) gene, C88.2.H10 transposon insertion at the chromosomal position 2830098 was used. The mutated cosmid containing C88.2.H10 insertion was purified from *E. coli* JM109 strain commonly used to enrich cosmid or plasmid DNA. The purified cosmid was transformed into *E. coli* ET12567 (pUZ8002) strain which was then used for intergeneric conjugal transfer (Flett *et al.*, 1997; Mazodier *et al.*, 1989) of the cosmid into *S. coelicolor* M145. The exconjugant colonies of *S. coelicolor* strain containing the *sfr* disrupted cosmid were obtained by intergeneric conjugal transformation and were replica plated on MS + Apramycin and MS + Kanamycin media plates to obtain the double crossover mutants that were Apramycin resistant (Apr^R) and Kanamycin sensitive (Kan^S). Several clones of an *sfr* disrupted mutant were obtained at 12% frequency of double crossovers. Six mutant clones were selected randomly for Southern hybridization and macroscopic analysis (Fig. 4.1).

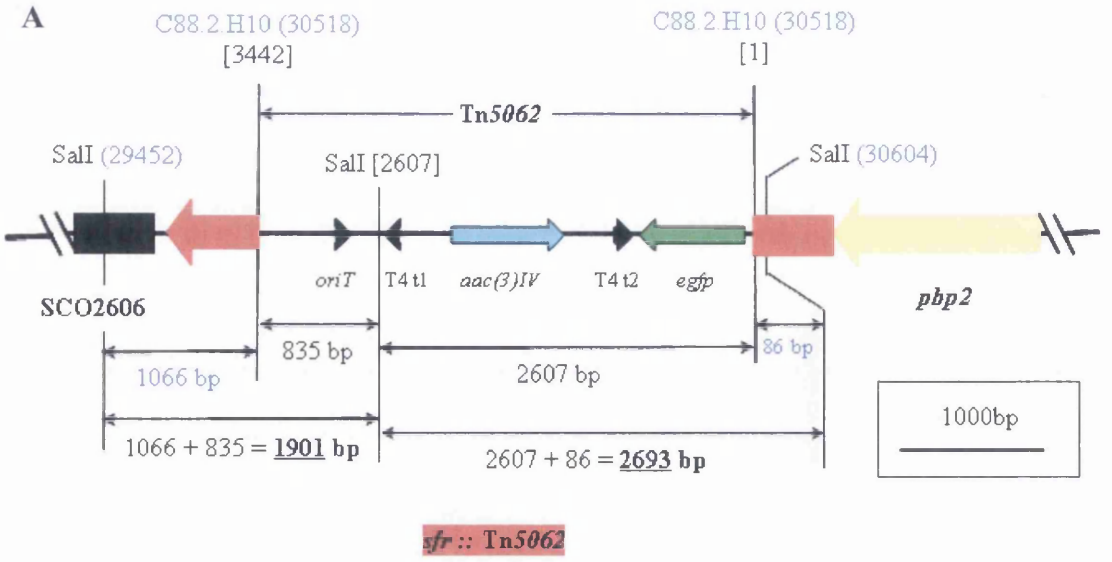

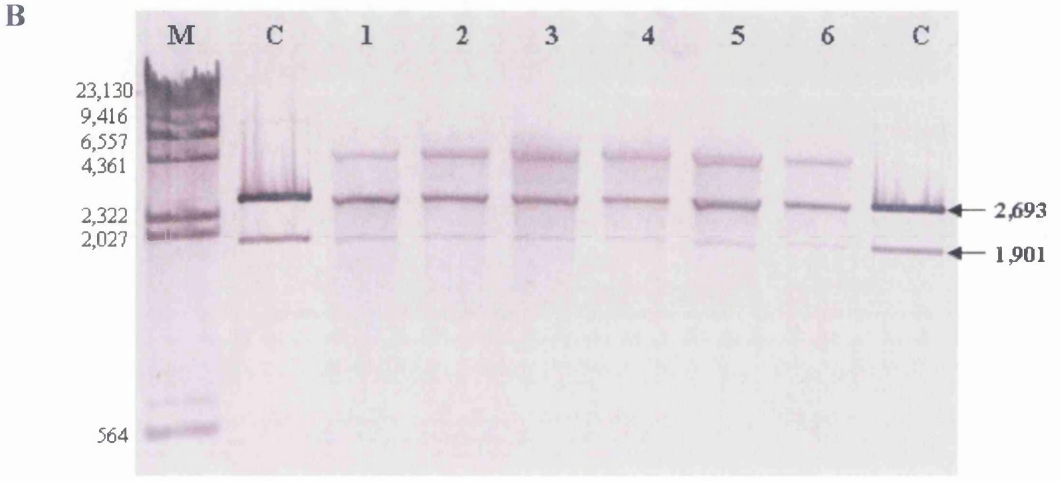

Figure 4.1: Southern Blot (SB) analysis of *sfr* mutant clones. **(A)** Diagrammatic representation of *sfr* gene region showing Tn*5062* insertion and *Sal*I restriction sites to calculate the size of bands that should be obtained after Southern hybridization analysis. The cosmid insertion used for *sfr* mutagenesis is shown in blue colour with the position of insertion in the cosmid presented in brackets. Just under the cosmid name and position, the start and end sites of Tn*5062* are written in square brackets. The position of important *Sal*I restriction sites in the *sfr* region of the cosmid are shown in the brackets and in Tn*5062* region is shown in square brackets. Arrows with different colours represent different genes and their directions. The name of each respective gene is shown just under each arrow. *aac(3)IV* – Apramycin resistance; T4 t1,2 – Transcription terminator t1 & 2; *egfp* – Enhanced green fluorescent protein gene; *oriT* – Origin of transfer. Expected size of bands that should be obtained in the SB is shown in bold letters with underlining. The rectangular box at the right bottom side shows the scale of the map. **(B)** SB of six *sfr* mutant clones. M –*Hin*dIII digested λ DNA marker with the size for each band presented on the left hand side; C – *Sal*I digested C88.2.H10 cosmid insertion; and 1 to 6 – *Sal*I digested chromosome of each *sfr* mutant clone. The size (in bp) of expected bands is shown on the right hand side in bold. Digoxigenin labelled Tn*5062* was used as a hybridization probe.

Southern blot (SB) analysis was carried out on six selected mutant clones using digoxigenin labelled Tn*5062* as a probe to confirm the replacement of the wild type *sfr* gene with the disrupted version. To obtain two distinct bands of the Tn*5062* disrupted *sfr* gene on SB, a *Sal*I restriction digest was selected using DNAMAN software program. The chromosomal DNA purified from the mutant clones and the purified cosmid DNA (C88.2.H10) were digested using *Sal*I restriction enzyme. The *Sal*I digested cosmid insertion C88.2.H10 was used as a positive control. Two clear bands of 1901 and 2693 base pairs (bp) that are identical to the positive control cosmid were obtained for all mutant clones analyzed, confirming true double crossover mutants (Fig. 4.1). The third band of ~4500 bp in Figure 4.1B is because of incomplete digestion of chromosomal DNA where *Sal*I enzyme did not cut in the Tn*5062* sequence (Fig. 4.1A). One (second clone) of the six *sfr* mutant clones, designated as DSCO2607, was selected for further characterization of the mutant.

Just upstream of *sfr* lies a *pbp2 (SCO2608)* that encodes a high molecular weight (HMW) penicillin binding protein (PBP) whose function is also unknown. The disruption mutants of *pbp2* gene were obtained using a similar approach as for isolation of the *sfr* mutant. Two independent cosmid insertions, C88.1.C05 (located near the start of the gene) and C88.2.B04 (located close to the end), were used. The position of each insertion in the chromosome is 2831062 and 2832285, respectively. For the C88.1.C05 insertion five independent mutants (Fig. 4.2B) and for the C88.2.B04 insertion four independent mutants (Fig. 4.3B) were selected for SB. The chromosomes of C88.1.C05 disrupted mutants were digested using *Kpn*I (Fig. 4.2) while that of C88.2.B04 insertion mutants were digested by *Not*I (Fig. 4.3) for SB to confirm the mutants. SB of both the insertion mutants showed the correct sized bands as calculated for each insertion (Fig. 4.2 & 4.3). The mutant with the C88.1.C05 insertion was designated as DSCO2608-1 and that with the C88.2.B04 insertion mutant was designated as DSCO2608-2. The appearance of more than two bands in the blot shown in Figure 4.3 B may be due to partial digestion of the DNA.

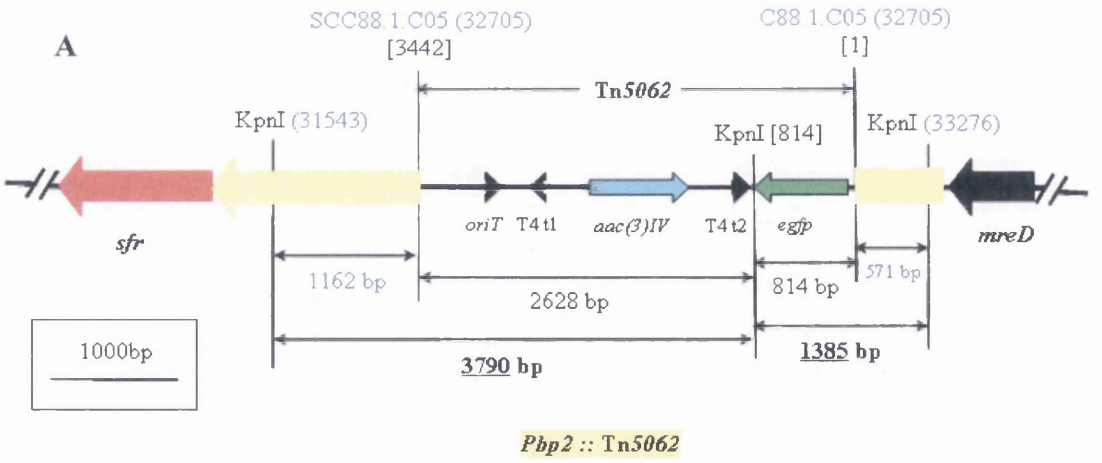

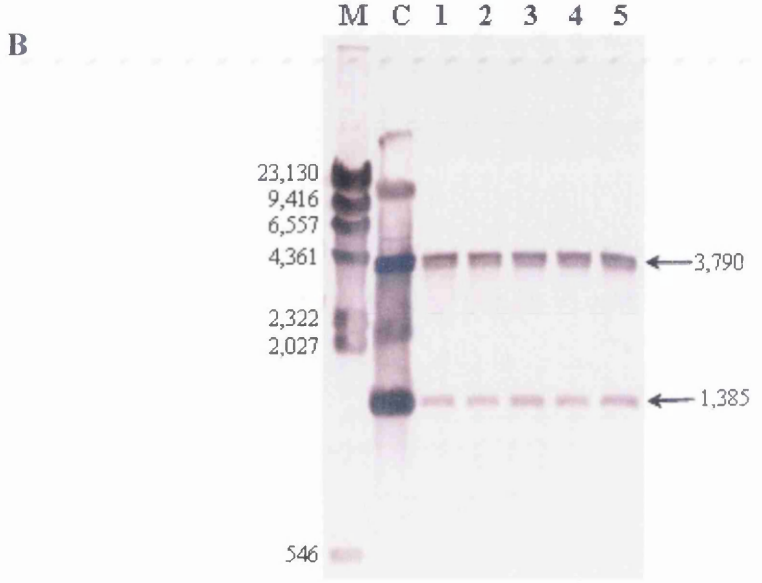

Figure 4.2: SB analysis of *pbp2 (SCO2608)* mutant clones. **(A)** Diagrammatic representation of the *pbp2* gene region showing Tn*5062* insertion and *Kpn*I restriction sites to calculate the size of bands that should be obtained after SB analysis. The cosmid insertion used for *pbp2* mutagenesis is shown in blue colour with the position of insertion in the cosmid presented in brackets. Just under the cosmid name and position, the start and end sites of Tn*5062* are written in square brackets. The position of important *Kpn*I restriction sites in the *pbp2* region of cosmid are shown in the brackets and in the Tn*5062* region, it is shown in square brackets. Arrows with different colours represent different genes and their directions. Name of each respective gene is shown just under each arrow. *aac(3)IV* – Apramycin resistance; T4 t1,2 – Transcription terminator t1 & 2; *egfp* – Enhanced green fluorescent protein gene; *oriT* – Origin of transfer. The size of expected bands obtained after SB is shown in bold letters with underlining. The rectangular box shows the scale of the map. **(B)** SB of five *pbp2* mutant clones. M –*Hin*dIII digested λ DNA marker with the size (in bp) of each band presented on the left hand side; C – *Kpn*I digested C88.1.C05 cosmid insertion; and 1 to 5 – *Kpn*I digested chromosome of each *pbp2* mutant clone. The size (in bp) of each expected band on SB is shown on the right hand side. Digoxigenin labelled Tn*5062* was used as a hybridization probe.

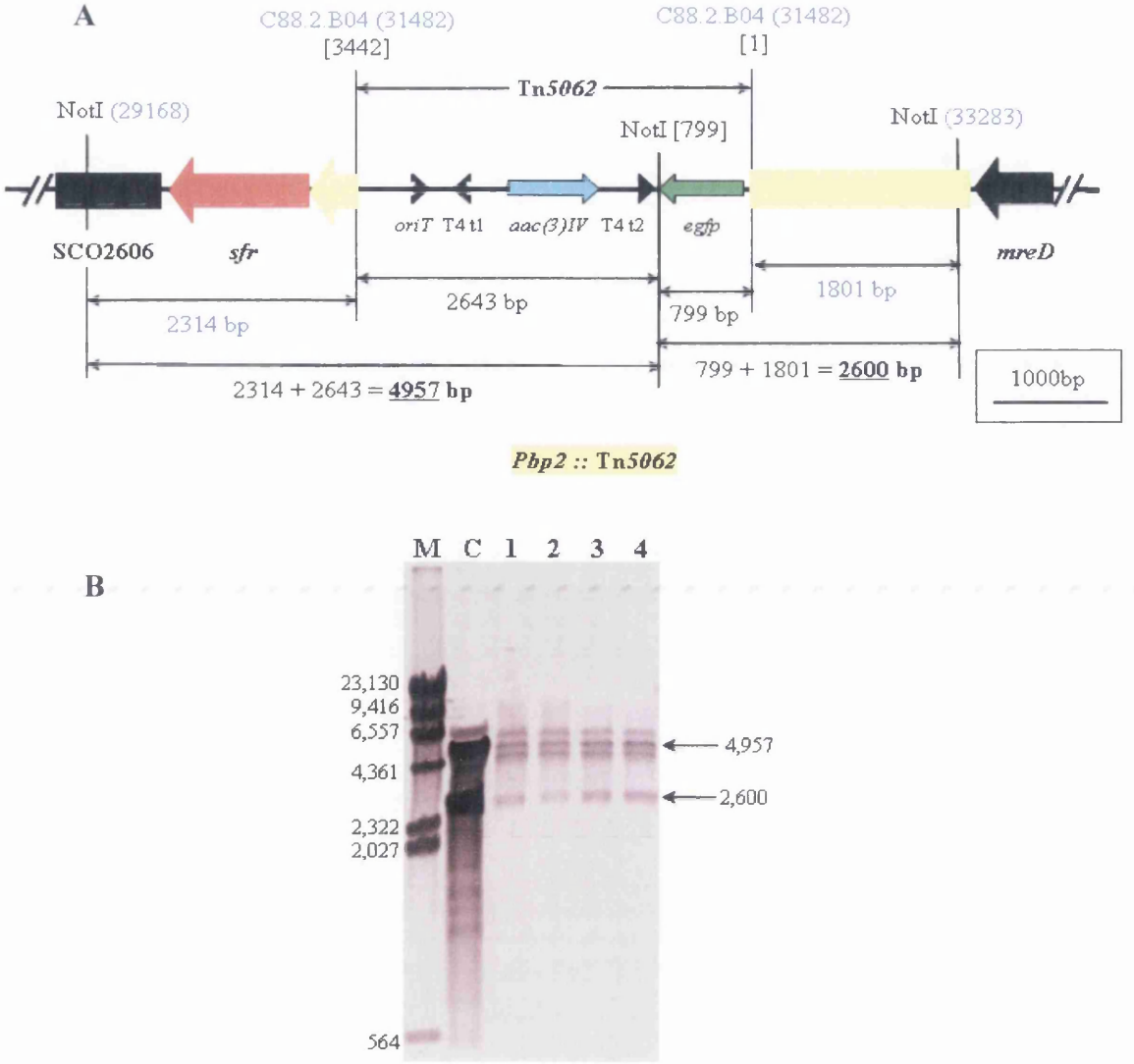

Figure 4.3: SB analysis of *pbp2 (SCO2608)* mutant clones. **(A)** Diagrammatic representation of the *pbp2* gene region showing Tn*5062* insertion and *Not*I restriction sites to calculate the size of bands that should be obtained after SB analysis. The cosmid insertion used for *pbp2* mutagenesis is shown in blue colour with the position of insertion in the cosmid presented in brackets. Just under the cosmid name and position, the start and end sites of Tn*5062* are written in square brackets. The position of important *Not*I restriction sites in the *pbp2* region of cosmid are shown in the brackets and in Tn*5062* region, it is shown in square brackets. Arrows with different colours represent different genes and their directions. Name of each respective gene is shown just under each arrow. *aac(3)IV* – Apramycin resistance; T4 t1,2 – Transcription terminator t1 & 2; *egfp* – Enhanced green fluorescent protein gene; *oriT* – Origin of transfer. The expected size of the bands obtained after SB is shown in bold letters with underline. The rectangular box shows the scale of the map. **(B)** SB of four *pbp2* mutant clones. M –*Hin*dIII digested λ DNA marker with the size (in bp) of each band presented on the left hand side; C – *Not*I digested C88.2.B04 cosmid insertion; and 1 to 4 – *Not*I digested chromosome of each *pbp2* mutant clone. The size (in bp) of each expected band is shown on right hand side. Digoxigenin labelled Tn*5062* was used as a hybridization probe.

Similarly, disruption mutants of *rodA2* (*SCO5302*) gene were obtained using two independent cosmid insertions, 6G9.1.D07 (close to the beginning of the gene) and 6G9.1.B07 (near the end of the gene). The double crossover mutants for each insertion occurred at a frequency of 11 to 12 double crossovers per 100 exconjugants. To confirm the replacement of the wild type *rodA2* gene by the transposon disrupted copy of the gene, SB was performed for both the insertions. Digestion of the 6G9.1.B07 disrupted chromosome using *Kpn*I should give 3915 bp and 2507 bp size bands whereas that of 6G9.1.D07 insertion mutant should show 3354 bp and 3068 bp size bands (Fig. 4.4). A mutant with the 6G9.1.D07 insertion is designated as DSCO5302-1 and that of 6G9.1.B07 insertion is designated as DSCO5302-2. Mutagenesis of *SCO5302* (encoding putative cognate PBP) could not be performed due to lack of an insertion in this gene.

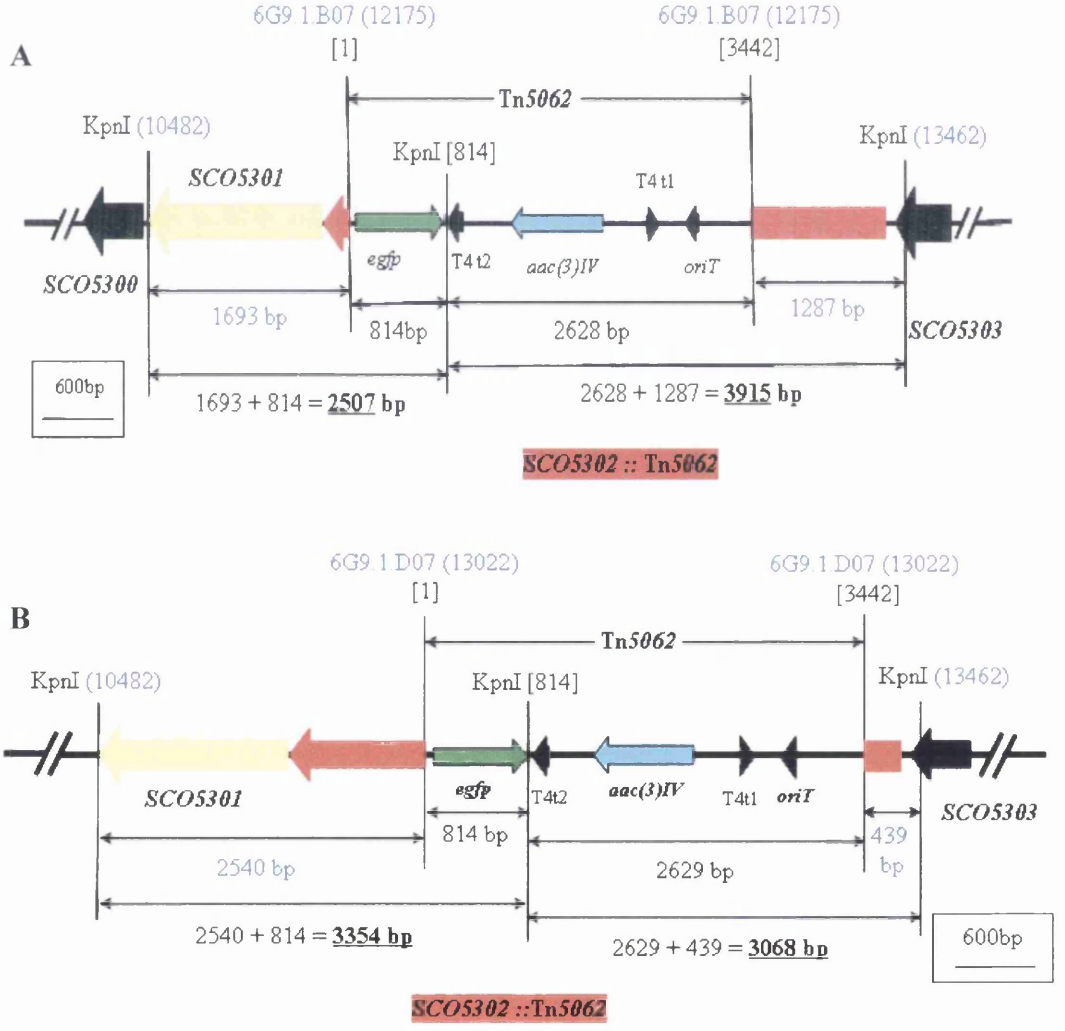

Figure 4.4: Continued on the next page....

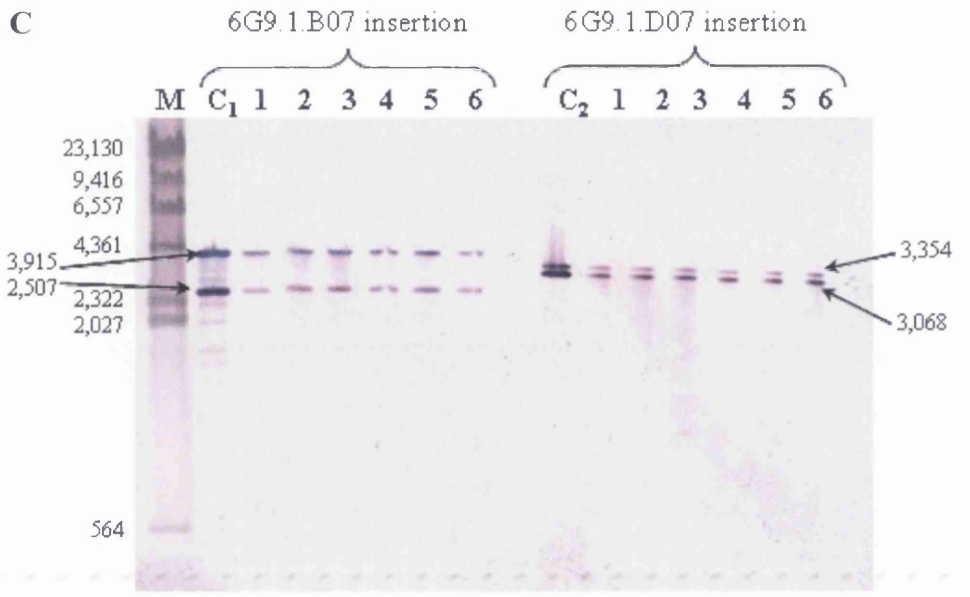

Figure 4.4: SB analysis of *rodA2* mutants. **(A) & (B) -** Maps of *rodA2* gene region with Tn*5062* insertions at different positions in the gene and the respective *Kpn*I restriction sites to calculate the size of bands that should be obtained by Southern hybridization. Each of the cosmid insertions used for *rodA2* mutagenesis are shown in blue colour with the position of insertion in the cosmid written in brackets. Just under the cosmid name and position, the number in square bracket indicates the beginning and end of Tn*5062*. The position of the important *Kpn*I restriction sites in *rodA2* region of cosmid are shown in brackets and that of Tn*5062* is shown in square brackets. Arrows with different colours represents different genes and their directions. A scale bar of each map is shown in a rectangle. The name of each respective gene is shown just under each arrow. *aac(3)IV* – Apramycin resistance; T4 t1,2 – Transcription terminator t1 & 2; *egfp* – Enhanced green fluorescent protein gene; *oriT* – Origin of transfer. The size of bands that should be obtained by SB is shown in bold letters with underlining. **(C)** SB of six *rodA2* mutant clones for each insertion. M – *Hin*dIII digested λ DNA marker with the size for each band presented on the left hand side; $C_{1\ \&\ 2}$ – *Kpn*I digested 6G9.1.B07 and 6G9.1.D07 cosmid insertions, respectively; and 1 to 6 – *Kpn*I digested chromosome of each *rodA2* mutant clone for each respective insertion. The size of expected bands is indicated by arrows. Digoxigenin labelled Tn*5062* was used as a hybridization probe.

For the mutagenesis of the *rodA (SCO3846)* two independent insertions H69.1.E11 and H69.1.H03 (Fig. 4.5) were introduced individually into *S. coelicolor* M145 by intergeneric conjugation. To isolate the mutants for each insertion approximately 250 exconjugants of each insertion were screened for the loss of Supercos-1 vector (Kan^S) and presence of apramycin resistance (Apr^R). Surprisingly, despite several attempts using two different insertions, not a single true double

crossover mutant of *rodA* gene was obtained where the hybridization patterns in isolated clones would have consistency with genuine allelic replacement. The inability to create *rodA* disruption mutants suggests that it is essential for growth and survival in *S. coelicolor*.

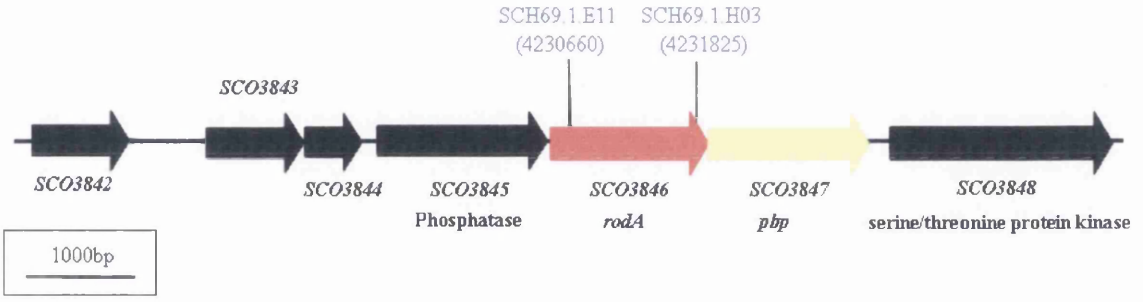

Figure 4.5: Map of *rodA (SCO3846)* gene locus showing the positions of Tn*5062* insertions in *S. coelicolor* chromosome.

An easy way to verify the essentiality of a particular gene is by introducing an extra copy of that gene into the organism and constructing the mutants with one intact copy of the gene. To introduce an additional copy of the *rodA* gene in *S. coelicolor*, a recombinant plasmid pSHRCI containing the *rodA* gene locus was constructed using an integrating plasmid vactor pSH152 that integrates at the ØC31 *att* site in the *S. coelicolor* chromosome (Fig. 4.6). To construct plasmid pSHRCI, a ~7 kilo base pairs (kbp) fragment was purified from a high copy number recombinant plasmid pRCLu2 (kindly provided by Dr. Ricardo Del Sol) after digesting with *Xba*I. The purified ~7 kbp fragment of the *rodA* locus was then cloned into *Xba*I digested pSH152 containing a hygromycin resistance marker (Fig. 4.6). The resulting recombinant plasmid pSHRCI was verified by restriction analysis and sequencing. This plasmid was then introduced into *S. coelicolor* by intergeneric conjugation and selecting for hygromycin resistant clones. The *S. coelicolor* strain containing pSHRCI was designated as M145::pSHRCI. Mutagenesis of *rodA* in the M145::pSHRC1 genetic background was carried out using the same approach of intergeneric conjugation as described previously for *sfr* mutagenesis. Two independent transposon insertions, H69.1.E11 and H69.1.H03, at the

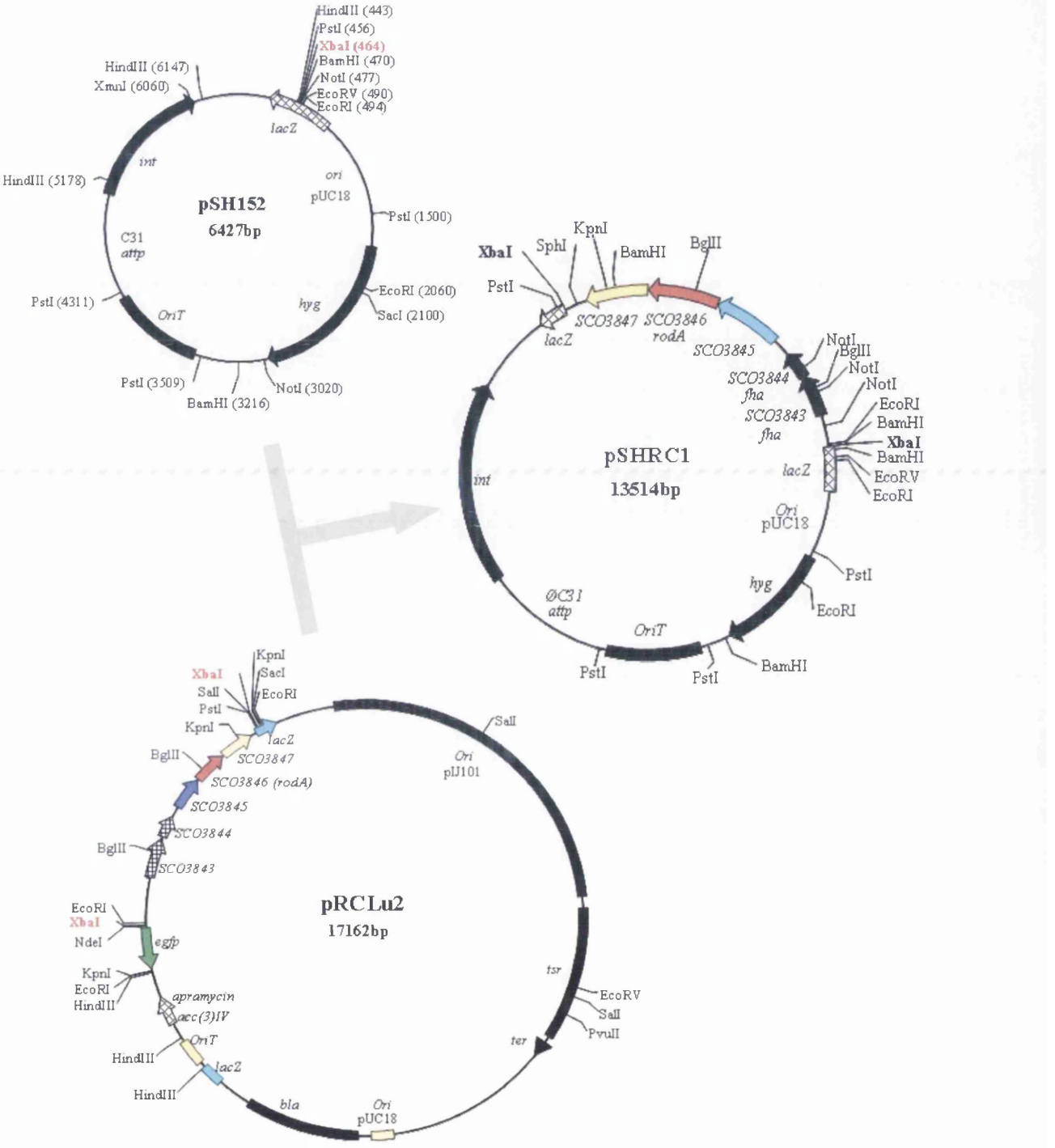

Figure 4.6: Map of plasmids used to construct pSHRCI plasmid. Restriction enzyme used for cloning the *rodA* locus is indicated in red colour. The maps are not drawn to the scale. (For description see the text)

position 4230660 and 4231825 in the chromosome, respectively, were used for the mutagenesis of *rodA* in M145::pSHRC1 genetic background (Fig. 4.5). The exconjugant colonies obtained after intergeneric conjugation were screened for hygromycin resistance (Hyg^R), Apr^R and Kan^S. Interestingly, double crossover mutants of *rodA* were obtained for both the insertions used at a frequency of 7% in the M145::pSHRC1 genetic background. To confirm the *rodA* mutants, three clones of each insertion mutant were randomly selected for Southern hybridization analysis. Purified chromosomal DNA of *rodA* mutants in the M145::pSHRC1 background and their respective cosmid insertion were digested with *Xho*I to obtain distinct bands for each insertion mutant after Southern hybridization (Fig. 4.7 A & B). A Southern blot of the mutants showed that two out of three selected clones of H69.1.H03 insertion and all the three clones of H69.1.E11 insertion were true mutants (Fig. 4.7 C). The mutant strains thus obtained were designated as DSCO3846::pSHRC1-1 and DSCO3846::pSHRC1-2 for H69.1.E11 and H69.1.H03 insertions, respectively. These results confirm that *rodA* is indeed essential for *S. coelicolor*. Surprisingly, a PBP encoding gene *SCO3847* located just downstream to *rodA* is despensible for growth and survival in *S. coelicolor*. The mutant of this gene constructed by Dr. Ricardo Del Sol using H69.1.B04 insertion did not show any discernible phenotype under the conditions used (Del Sol, 2004).

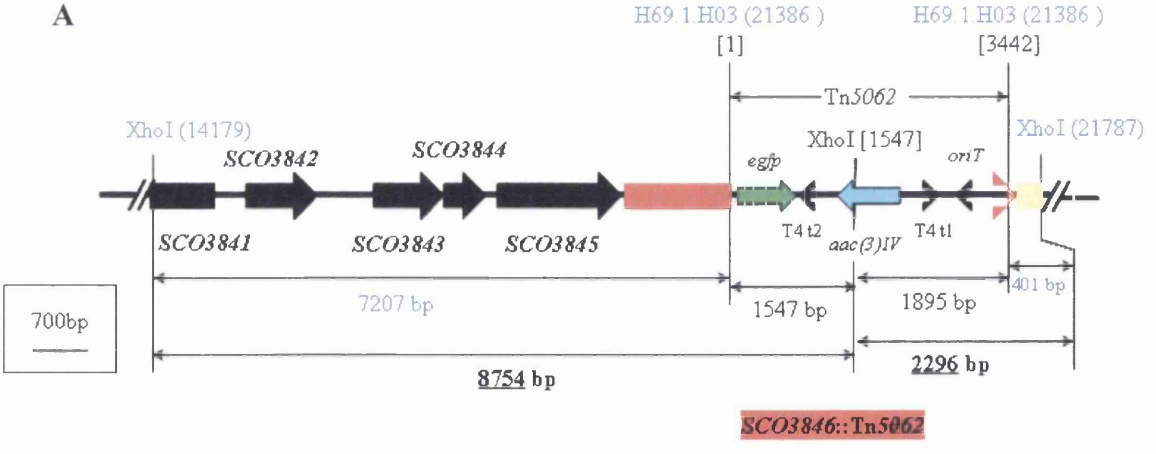

Figure 4.7: Continued on the next page....

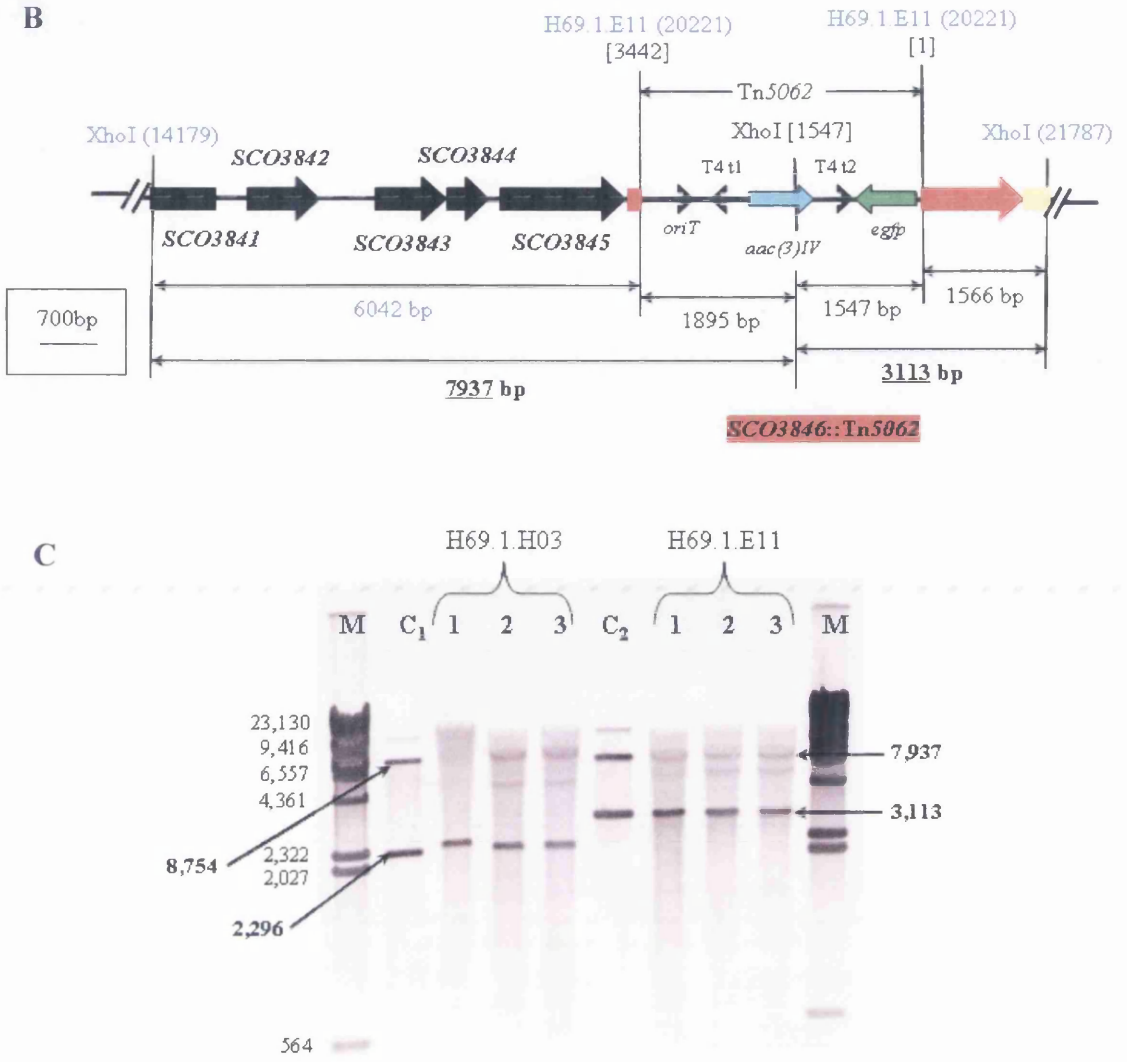

Figure 4.7: SB analysis of *rodA* mutants in M145::pSHRC1 background. **(A) & (B)** - Maps of *rodA* gene region with Tn*5062* insertions at different positions in the gene and the respective *Xho*I restriction sites to calculate the size of bands that should be obtained by Southern hybridization. Each of the cosmid insertions used for *rodA* mutagenesis are shown in blue colour with the position of insertion in the cosmid is written in brackets. Just under the cosmid name and position, the number in square bracket indicates the beginning and end of Tn*5062*. The position of the important *Xho*I restriction sites in *rodA* region of cosmid are shown in brackets and that of Tn*5062* is shown in square brackets. Arrows with different colours represents different genes and their directions. A scale bar of each map is shown in a rectangle. The name of each respective gene is shown just under each arrow. *aac(3)IV* – Apramycin resistance; T4 t1,2 – Transcription terminator t1 & 2; *egfp* – Enhanced green fluorescent protein gene; *oriT* – Origin of transfer. The size of bands that should be obtained by SB is shown in bold letters with underlining. **(C)** SB of three *rodA* mutant clones for each insertion. M – *Hin*dIII digested λ DNA marker with the size for each band presented on the left hand side; C_1 & C_2 – *Xho*I digested H69.1.H03 and H69.1.E11 cosmid insertions, respectively; and 1 to 3 – *Xho*I digested chromosome of each *rodA* mutant clone for each respective insertion. The size of expected bands for each mutant is indicated by arrows. Digoxigenin labelled Tn*5062* was used as a hybridization probe.

4.3 Phenotypic analysis of *sfr*, *pbp2* and *rodA2* Mutants

For phenotypic characterization, *S. coelicolor* M145 and its mutant derivatives of *sfr*, *pbp2* and *rodA2* genes were plated on some commonly used media. All the mutant strains were visually assessed for the production of grey pigmented spores and/or antibiotics by plating on soya flour mannitol (SFM), R5, NMMP containing either sucrose or mannitol and 2×YT agar media. All the strains were incubated at 30° C for three days. All the mutants produced normal grey pigmented spores and antibiotics similar to the wild type on all the media tested (Fig. 4.8). The growth of all the mutants was also normal compared to the wild type strain. In the case of *rodA2* and *pbp2* mutants, where two independent insertions at different positions in the gene are used, only the mutants with the insertion at the beginning of the gene are shown in the figure. Mutants with other insertions also showed similar phenotypes. Also, there was no apparent phenotypic difference between mutants and wild type stains when grown on minimal medium containing glucose or mannitol as a carbon source (not shown). The colony shape, size and texture of all the mutants were also normal.

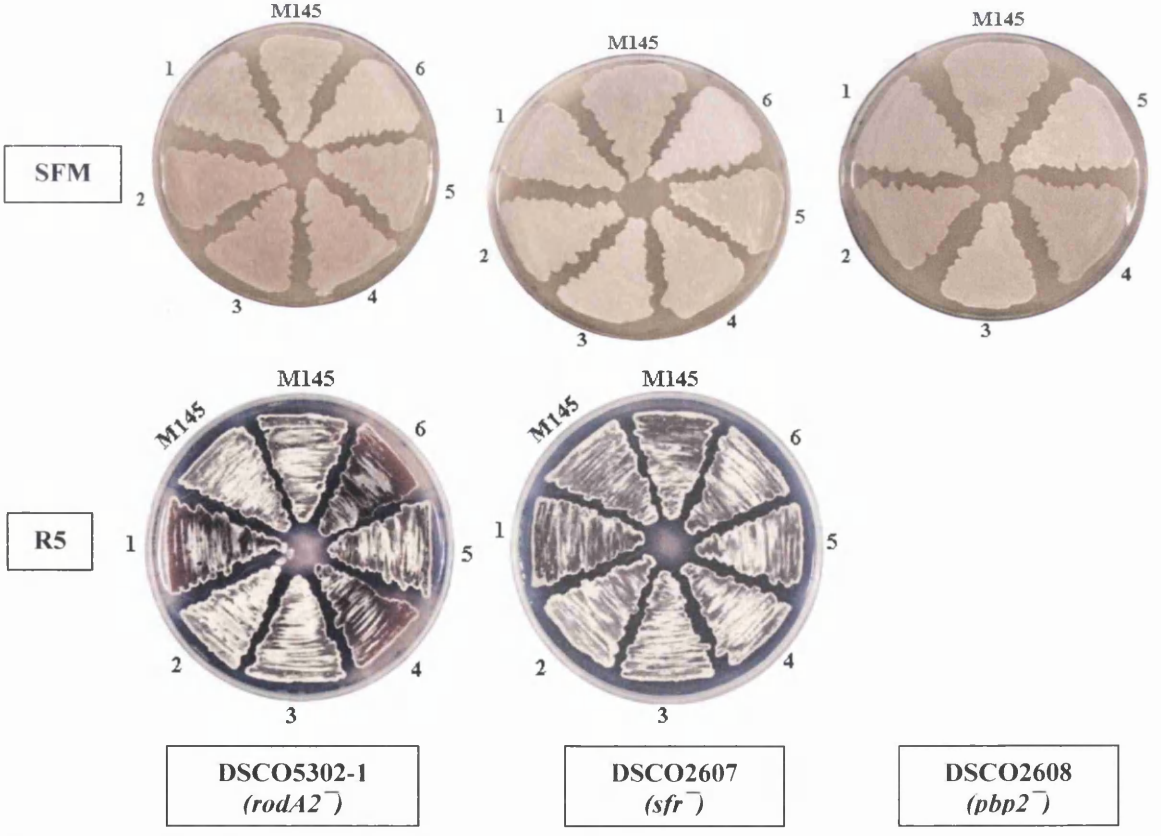

Figure 4.8: Continued on the next page....

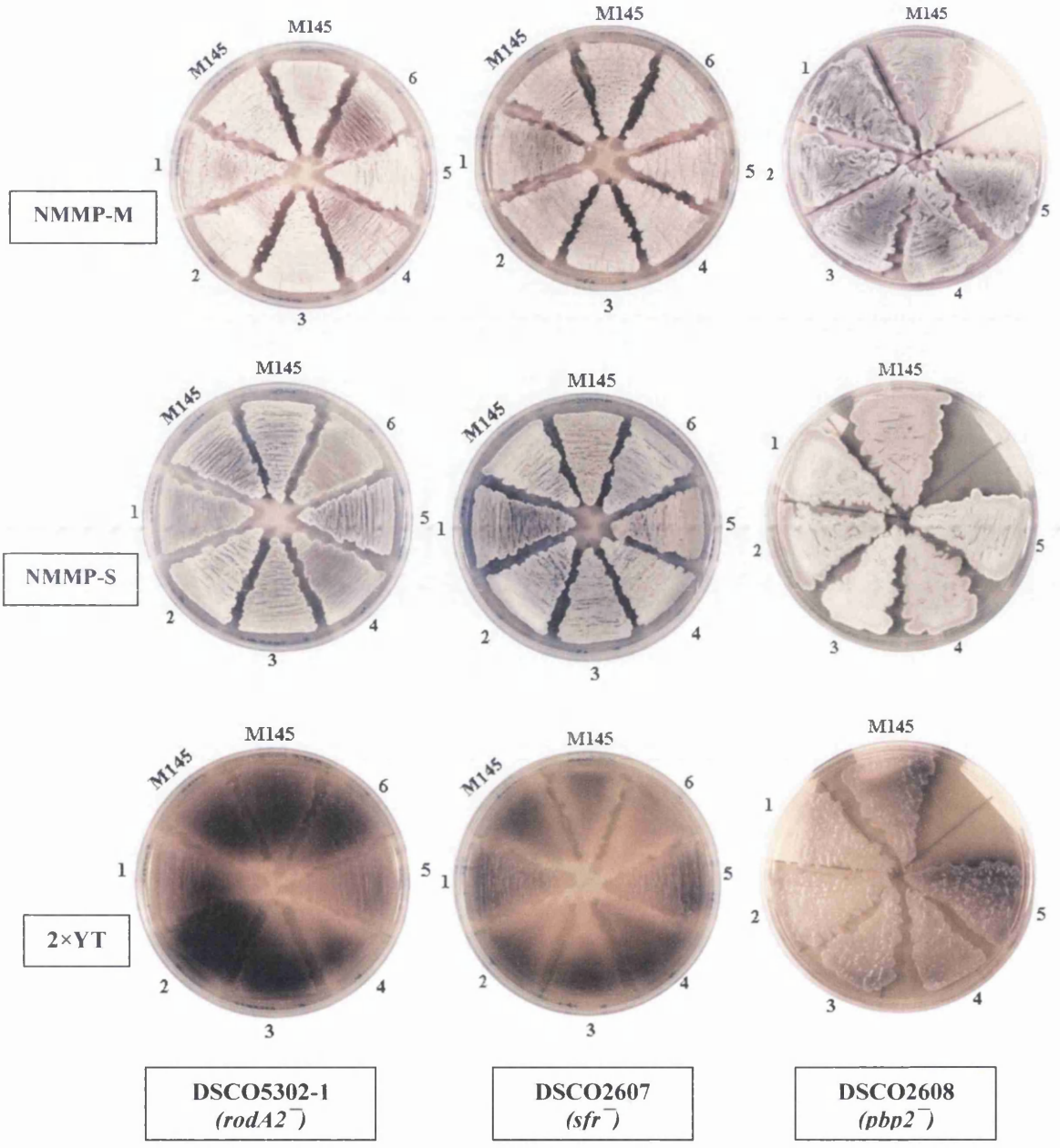

Figure 4.8: Phenotype of *rodA2, sfr* and *pbp2* mutants and their congenic parental strain *S. coelicolor* M145 on different media. Strains were grown for 3 days at 30° C on SFM, R5, NMMP-Mannitol (M), NMMP-Sucrose (S) and 2×YT agar media. Name of the mutants are indicated at the bottom of the figure in rectangle. Numbers surrounding each plate picture represent clones of each respective mutant. Name of the media is presented on the extreme left side of the figure in rectangle.

The lack of any discernible macroscopic phenotype in *SCO2607 (sfr)* or *SCO5302 (rodA2)* disrupted mutants may be due to the functional redundancy of the protein encoded by each gene. The best way to check this is by constructing a double mutant of both *sfr* and *rodA2* genes. To construct this double mutant and for easy screening of the mutants, the Apr^R cassette of the transposon insertion, C88.2.H10, in the *sfr* gene was replaced by a hygromycin resistance (Hyg^R) marker using the Redirect technique as described in Materials and Methods (Gust *et al.*, 2003). The replacement of the marker in the cosmid insertion was confirmed by restriction analysis and sequencing. The C88.2.H10 insertion cosmid with the Hyg^R cassette was then introduced into the DSCO5302-1 *(rodA2)* mutant by intergeneric conjugation. At the same time the C88.2.H10-Hyg^R insertion was also introduced into the wild type strain of *S. coelicolor* to obtain single gene mutants just to check that the marker replacement did not affect any other gene in the cosmid that may result in some false phenotype and also to use the Hyg^R *sfr* mutant to construct double mutant with *ftsW* that will be described in the next chapter. The exconjugants obtained by conjugation in both the cases were screened for hygromycin resistance and kanamycin susceptibility to isolate double crossover mutants of the *sfr* gene in the *rodA2* disrupted background and wild type background. Several double crossover recombinant mutants of the *sfr* gene were obtained in both wild type and *rodA2* disrupted background. Seven clones of the *sfr* (Hyg^R) single mutant and six clones of the *rodA2-sfr* double mutant were selected randomly for SB to confirm the mutants. For SB analysis of both single and double mutants, the chromosomes of respective mutant clones and the corresponding cosmids containing Tn*5062* insertion in respective genes were digested with *Not*I (Fig. 4.9 A & B). SB of both single and double mutants showed the expected sizes of fragments that corresponded with the sizes of the fragments obtained by *Not*I digestion of cosmids with the relevant insertion used for mutagenesis (Fig. 4.9 C & D). The *sfr-hyg*^{R} mutant thus obtained was designated as DSCO2607-hyg^R, where as the *rodA2-sfr* double mutant was designated as DSCO5302-1/2607.

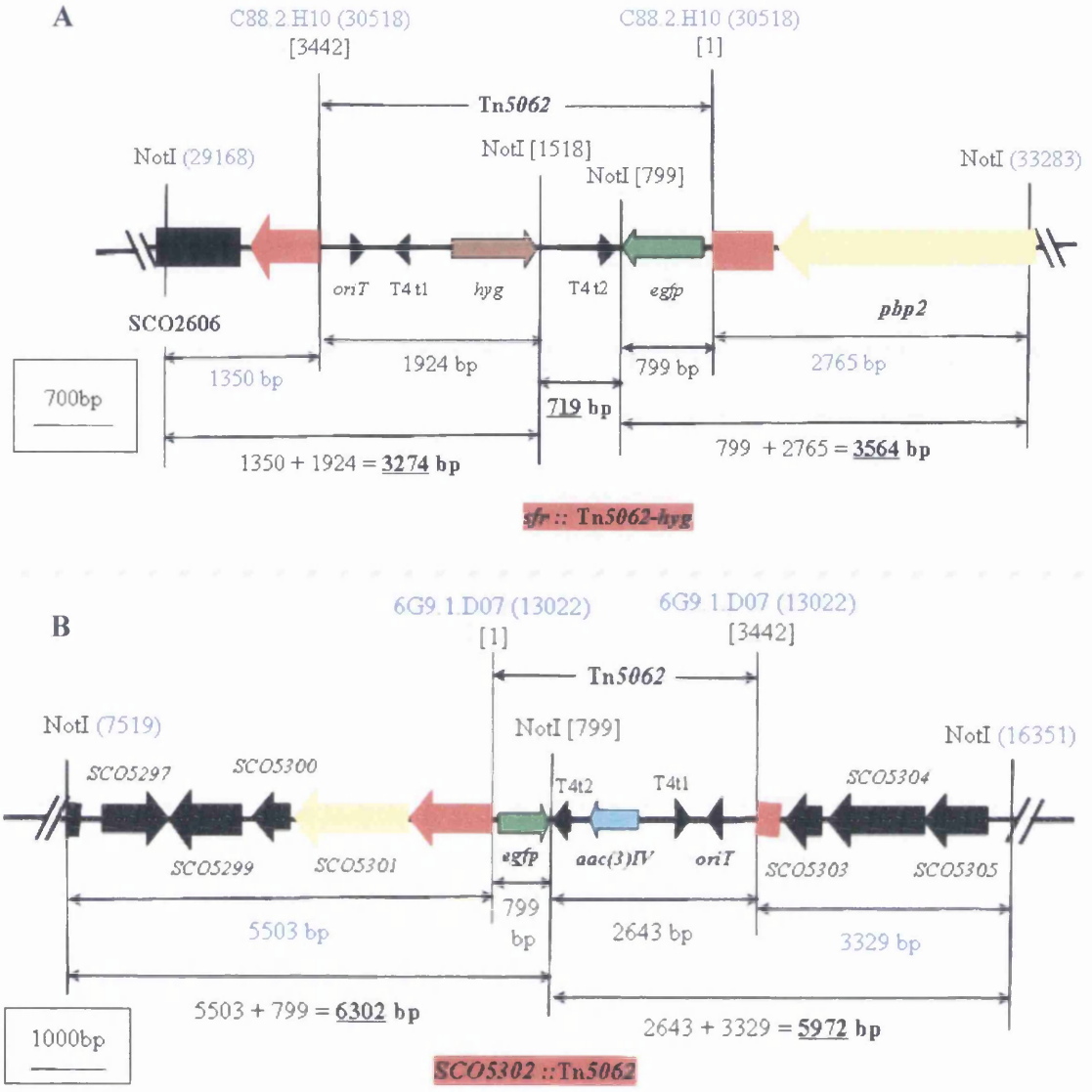

Figure 4.9: Continued on the next page….

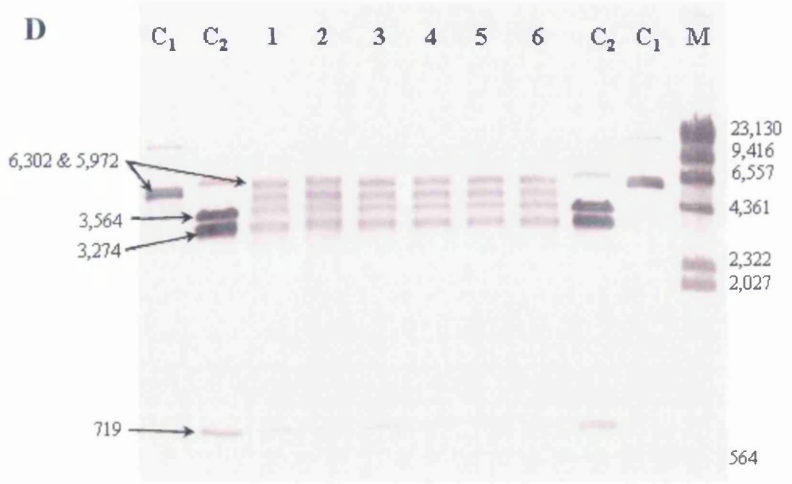

Figure 4.9: SB analyses of *sfr-hyg*^{R} and *rodA2/sfr-hyg*^{R} double mutants. **(A) & (B) -** Maps of the *sfr* insertion containing the Hyg^R cassette and *rodA2* insertion, respectively, showing the position of Tn*5062* in each respective gene and *Not*I restriction sites to calculate the size of bands that should be obtained by Southern hybridization. The cosmid insertions used for the mutagenesis are shown in blue colour with their respective position in the cosmid written in the brackets. Just under the cosmid name and position, the number in square bracket indicates the beginning and end of Tn*5062*. The position of the important *Not*I restriction sites in the cosmid region are shown in the brackets next to the name of the enzyme and that of Tn*5062* is shown in square brackets. Arrows with different colours represents different genes and their directions. The name of each respective gene is shown just under each arrow. *aac(3)IV* – Apramycin resistance; T4 t1,2 – Transcription terminator t1 & 2; *egfp* – Enhanced green fluorescent protein gene; *oriT* – Origin of transfer. The sizes of resulting bands after SB are shown in bold letters with underline. A scale bar for each map is shown in a rectangle. **(C)** SB of seven of *sfr-hyg*^{R} mutant clones. M –*Hin*dIII digested λ DNA marker with the size for each band presented on the left hand side; C – *Not*I digested 6G9.1.D07 cosmid insertion and 1 to 7 – *Not*I digested chromosome of each *sfr-hyg*^{R} mutant clones. The size of expected bands is indicated by arrows. **(D)** SB of six of *rodA2/sfr-hyg*^{R} double mutant clones. M –*Hin*dIII digested λ DNA marker with the size for each band presented on the left hand side; $C_{1\ \&\ 2}$ – *Not*I digested 6G9.1.D07 and C88.2.H10-Hyg^R cosmid insertions, respectively, and 1 to 6 – *Not*I digested chromosome of each *rodA2/sfr-hyg*^{R} mutant clones. The size of expected bands is indicated by arrows. Extra bands that are not of expected size are due to partial digestion of the DNA. Digoxigenin labelled Tn*5062* was used as a hybridization probe.

When grown on different solid media that are used to phenotype single gene mutants as mentioned above, both *sfr-hyg*^{R} single mutant (results not shown) and *rodA2/sfr-hyg*^{R} double mutant also did not show any discernible phenotype different from wild type (Fig. 4.10). This result suggests that functional redundancy between RodA2 and Sfr did not conceal a phenotype in single gene disruption strains.

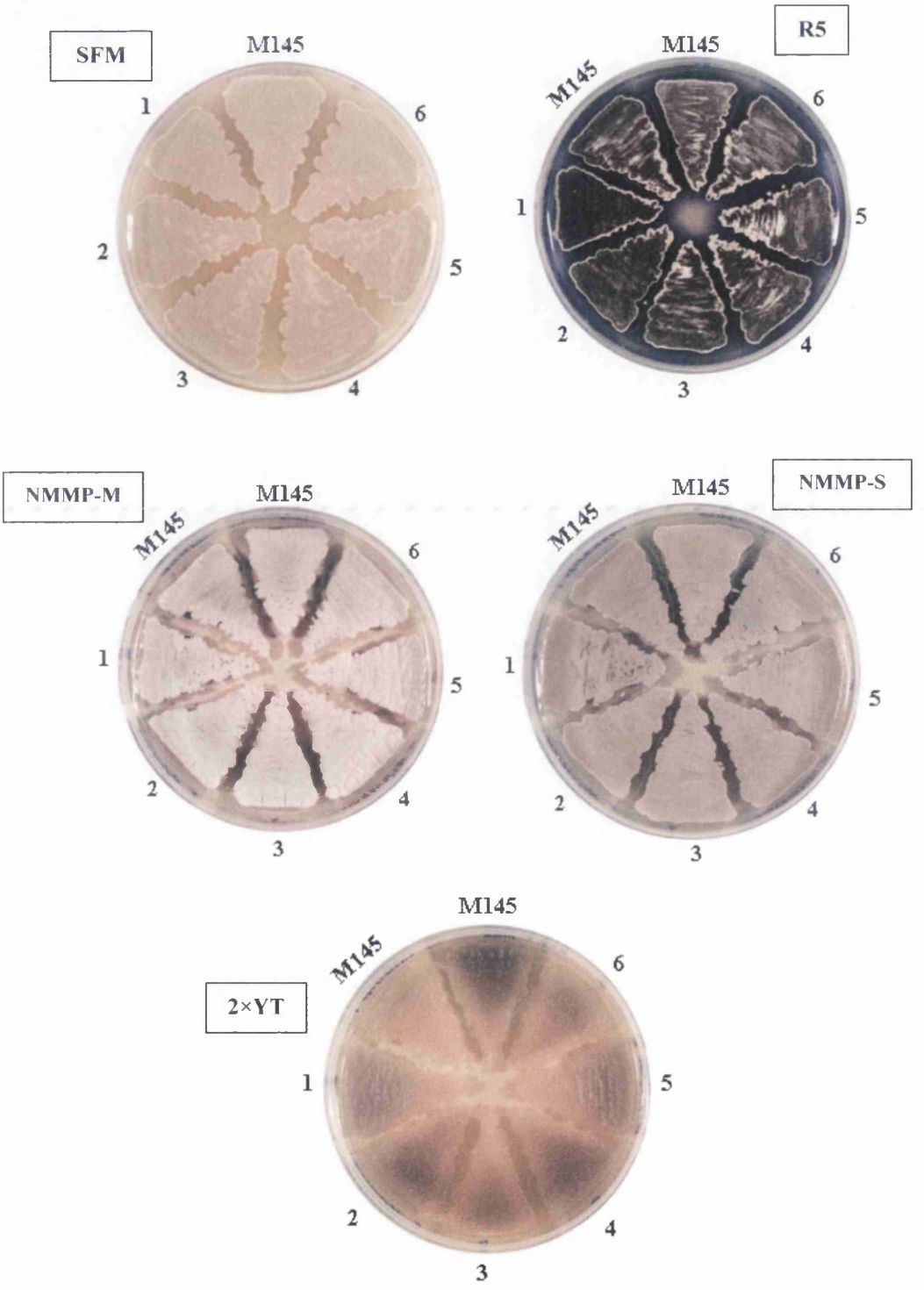

Figure 4.10: Phenotype of *rodA2/sfr-hyg*^{R} *(DSCO5302-1/DSCO2607)* double mutant and their congenic parental strain *S. coelicolor* M145 on different media. Strains were grown for 3 days at 30° C on SFM, R5, NMMP-Mannitol (M), NMMP-Sucrose (S) and 2×YT agar media. Name of the each medium is indicated in rectangle. Numbers surrounding each plate picture represent clones of the double mutant.

4.4 Microscopic Analysis of *sfr, pbp2, rodA2* and *rodA2/sfr* mutants

Fluorescence microscopy was used to visualize the cytological effects of *sfr, pbp2, rodA2* and *rodA2/sfr-hyg*^{R} mutations on peptidoglycan synthesis and chromosome distribution in these *S. coelicolor* mutants. Active peptidoglycan synthesis during vegetative septation was visualized by using BODIPY FL vancomycin, a fluorescent labelled vancomycin, as described in Materials and Methods. Cell wall synthesis during sporulation was examined by staining the aerial hyphae with fluorescein-labelled wheat germ agglutinin (Fluo-WGA). Both FL vancomycin and Fluo-WGA stain the cell wall by binding to peptidoglycan precursors that are produced as a result of active peptidoglycan synthesis and breakdown. Chromosomal DNA was stained with propidium iodide (PI), which requires fixing the cells and therefore it was only used with Fluo-WGA staining.

To visualize vegetative septa in wild type and the above mentioned mutants, the cultures were prepared by growing each strain on 2×YT medium with an inserted acute angled coverslip for 48 h and staining with FL vancomycin. The cultures were then observed under the fluorescence microscope to observe the pattern of fluorescence in vegetative mycelium. As shown in the Figure 4.11B the vegetative mycelium of *S. coelicolor* M145 showed infrequent brightly stained septa. Fluorescence microscopy of the vegetative mycelium of the *sfr, pbp2, rodA2* and *rodA2/sfr-hyg*^{R} mutant strains also showed similar staining pattern of vegetative septa to the wild type strain, suggesting that these genes are not required for vegetative septation in *S. coelicolor* (Fig. 4.11 C-J).

Due to the requirement of peptidoglycan oligomers for the binding of Fluo-WGA, it only stains actively synthesized peptidoglycan, whereas fully polymerized peptidoglycan is not stained by Fluo-WGA. The pattern of sporulation septation and chromosome distribution in the wild type was observed using Fluo-WGA. As expected the Fluo-WGA stained individual septa of actively dividing aerial hyphae (38 to 48 hours old culture) giving a ladder-like pattern that is similar to the FtsZ ladders formed during the early stage of sporulation septation (Grantcharova *et al.*, 2005; Schwedock *et al.*, 1997) (Fig. 4.12A). When the aerial hyphae in the early stage of sporulation were stained simultaneously with PI to stain the chromosome, the DNA appeared to be

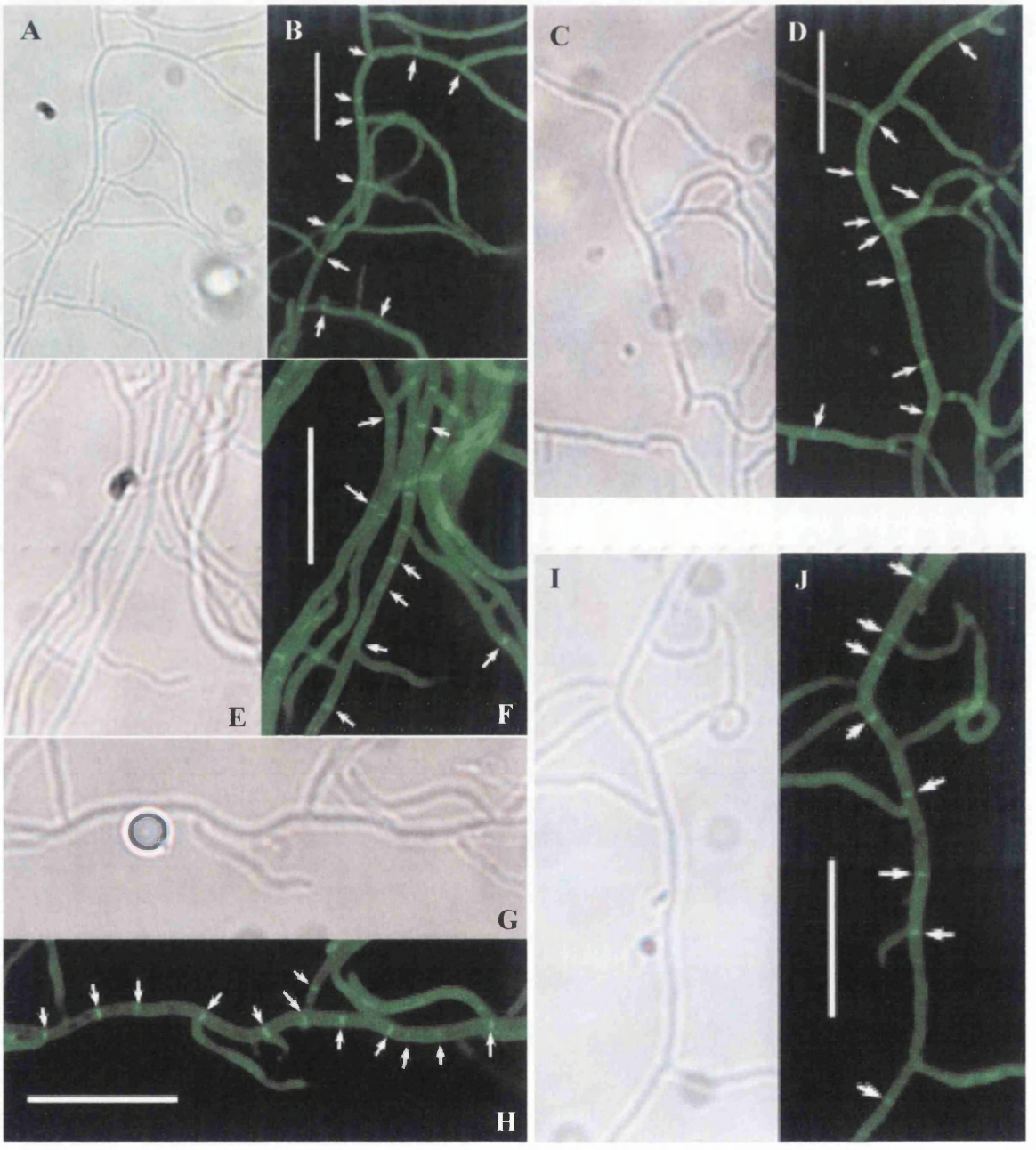

Figure 4.11: Fluorescence microscopy of vegetative mycelium of parental strain *S. coelicolor* M145, *rodA2, sfr, pbp2* and *rodA2/sfr-hyg*^{R} mutants using FL-vancomycin to visualize vegetative septa. Samples were prepared from cultures grown on 2×YT agar with inserted coverslips for 48 hours at 30° C. Phase contrast and fluorescence microscopy of wild type M145 (A and B); DSCO5302-1 (*rodA2*$^{-}$) (C and D); DSCO2607 (*sfr*$^{-}$) (E and F); DSCO2608 (*pbp2*$^{-}$) (G and H); and DSCO5302/2607 (*rodA2*$^{-}$/*sfr*$^{-}$) (I and J). Septa are indicated by white arrows. (Scale bar 10 μm)

distributed evenly in each hyphae with a single chromosome in each pre-spore compartment formed by two successive septa (Fig. 4.12 A and B). This suggests that DNA segregation is followed by septal peptidoglycan synthesis. In contrast, the Fluo-WGA staining of the mature spore chains (more than 2 days old culture) did not stain at the division septa suggesting that septum is completely formed and no more peptidoglycan synthesis is taking place at the division site. On the other hand the surface of mature spore chain was poorly stained by Fluo-WGA indicating some peptidoglycan synthesis and breakdown activity required for the final stage of spore maturation (Fig. 4.12 B). Completely mature spores did not show any Fluo-WGA staining as no peptidoglycan synthesis or breakdown takes place at this stage, as expected (Fig. 4.12 A). Analysis of sporulation septation and chromosome distribution in *sfr, pbp2, rodA2* and *rodA2/sfr-hyg*^{R} mutants, prepared in the same way as the wild type sample, showed similar morphologies as the wild type without affecting the growth (Fig. 4.12 C-F). To check further the effect of mutations in *sfr, pbp2* and *rodA2* genes on the dimensions of spores of each mutant, the length and width of pre-spore compartments of wild type and mutants were measured using the Scion Image program. To measure the dimensions of pre-spore compartments Fluo-WGA stained images of the strains were used. The dimensions of 200 pre-spore compartments from each strain were measured randomly. The length of pre-spore compartments of all the strains including the wild type strain ranges from 0.8 to 2.2 μm (Fig. 4.13), where the length of the majority of the pre-spore compartments lies between 1 to 1.3 μm (Fig. 4.13) with the average length of nearly 1.2 μm for each strain (Table 4.1). The width of pre-spore compartments in all the cases was ranging between 0.65 to 0.8 μm with the average width for each strain almost similar to each other (Table 4.1).

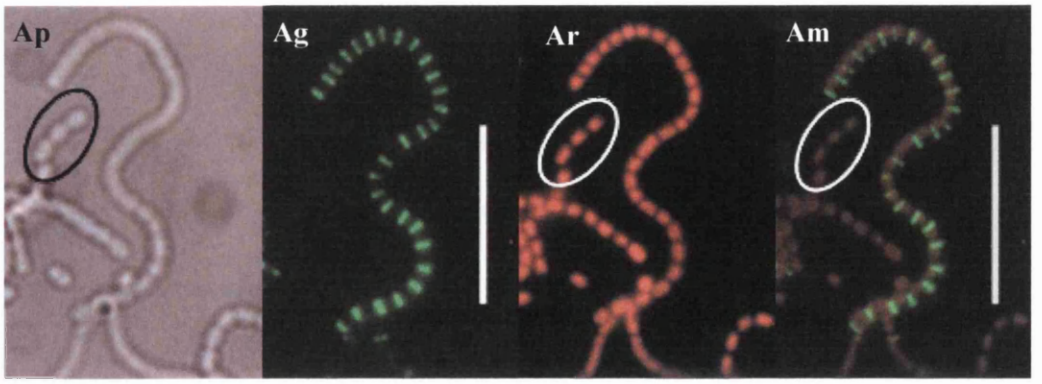

Figure 4.12: Continued on the next page....

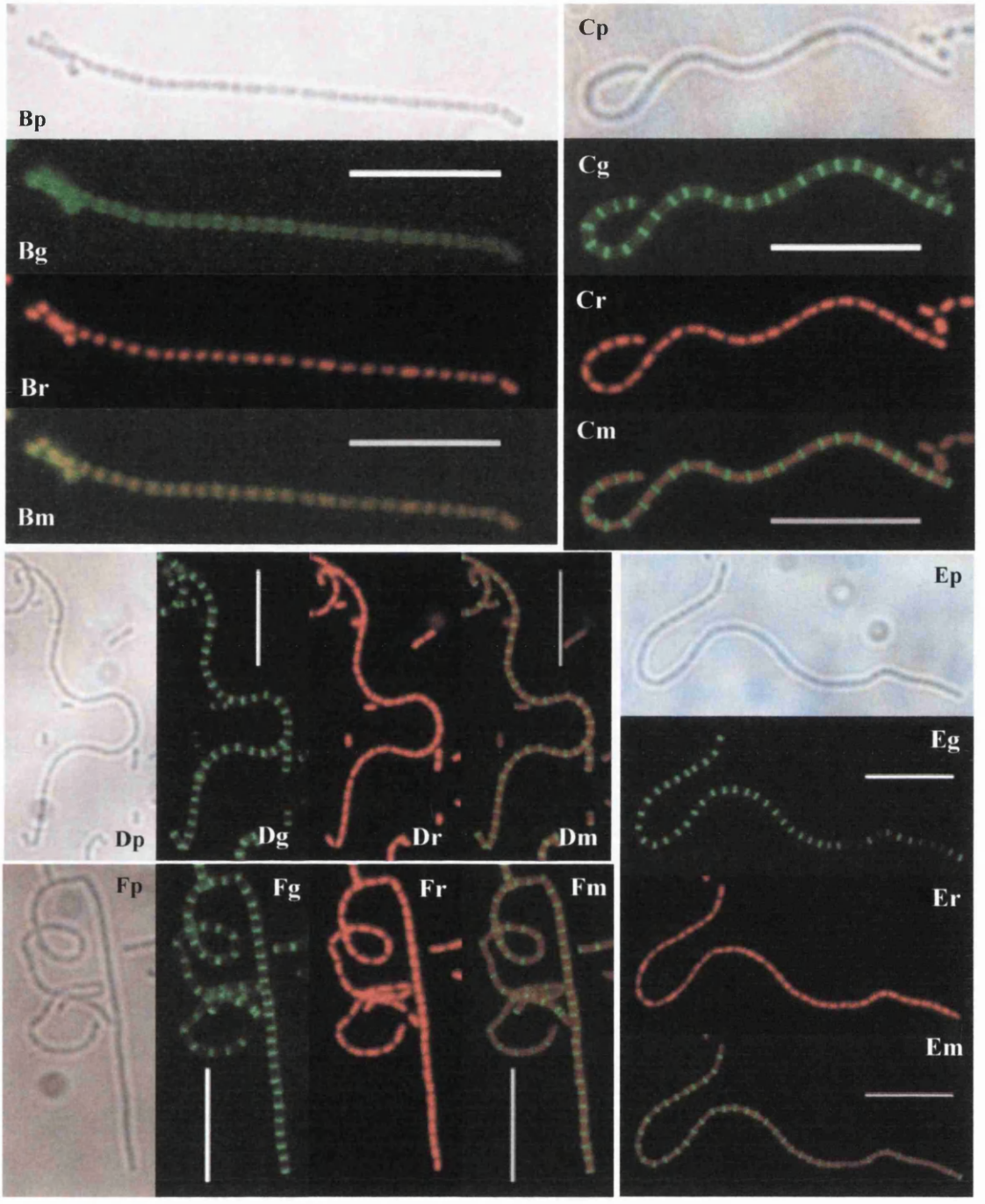

Figure 4.12: Fluorescence microscopy of aerial hyphae of parental strain *S. coelicolor* M145, *rodA2, sfr, pbp2* and *rodA2/sfr-hyg*^{R} mutants using Fluo-WAG (for cell wall) and PI (chromosomal DNA) staining to visualize sporulation septa and chromosome distribution. Samples were prepared by taking the impression of each culture grown on the surface of SFM agar medium for 38 to 40 hours at 30° C. Panel A and B- *S. coelicolor* M145 at early and late sporulation stage, respectively; Panel C- DSCO5302-1 (*rodA2*$^{-}$); Panel D- DSCO2607 (*sfr*$^{-}$); Panel E- DSCO5302/2607 (*rodA2*$^{-}$/*sfr*$^{-}$); and Panel F- DSCO2608-1 (*pbp2*$^{-}$). Each panel shows phase contrast (p), Fluo-WGA staining (g), PI staining (r) and merged (m) images of Fluo-WGA and PI staining of aerial hyphae of respective strains. In panel A portion indicated by oval shape shows completely mature spores that are not stained by Fluo-WGA staining. (Scale bar 10 μm)

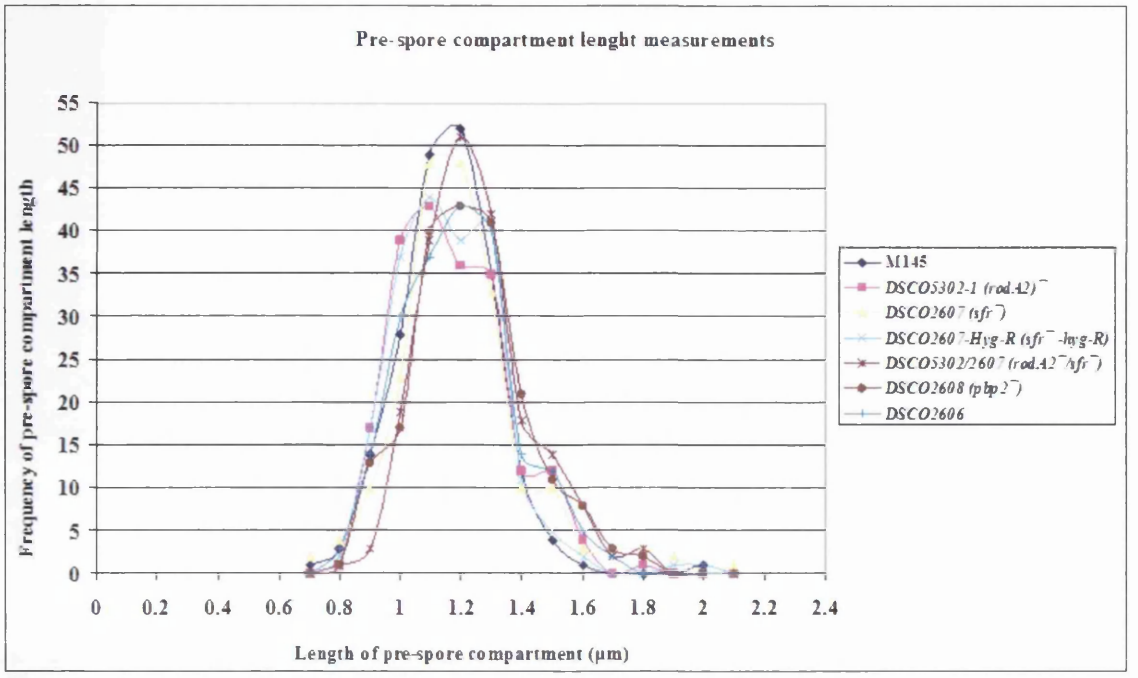

Figure 4.13: Graph of pre-spore compartment length versus frequency of the length of pre-spore compartment in wild type and different mutant strains. The length of randomly selected 200 pre-spore compartments of each strain was measured from the Fluo-WGA stained images using Scion Image software.

Table 4.1: Average length and width of pre-spore compartments in the sporulation aerial hyphae of M145, DSCO5302-1, DSCO2607, DSCO2607-hyg^R, DSCO5302/2607, DSCO2608-1 and DSCO2606 strains.

Strain	Average Length in µm	Average width in µm
S. coelicolor M145 (wild type)	1.17 ± 0.15	0.77 ± 0.11
DSCO5302-1 (*rodA2*$^-$)	1.18 ± 0.18	0.75 ± 0.08
DSCO2607 (*sfr*$^-$)	1.20 ± 0.21	0.70 ± 0.08
DSCO2607-hyg^R (*sfr*$^-$*-hyg*^{R})	1.17 ± 0.17	0.73 ± 0.09
DSCO5302/2607 (*rodA2*$^-$/*sfr*$^-$)	1.26 ± 0.17	0.75 ± 0.09
DSCO2608-1 (*pbp2*$^-$)	1.24 ± 0.19	0.71 ± 0.07
DSCO2606	1.19 ± 0.19	0.79 ± 0.09

4.5 *sfr, rodA2/sfr* and *pbp2* mutant spores are sensitive to heat and detergent

Streptomyces spores are dormant cells which are relatively resistant to desiccation, sonic vibration, enzymatic digestion and exposure to moderately high temperature (McBride and Ensign, 1987). To test whether the *rodA2, sfr, pbp2* and *rodA2/sfr-hyg*^{R} mutant spores were as heat resistant as those of the wild type strain, the spore suspension containing 10^7 spores per ml of each strain was incubated at 60° C for different time intervals. After heat treatment, appropriate dilutions of the spore suspensions were plated on SFM agar plates and further incubated at 30° C for 3 days to cultivate the viable spores for the calculation of survival rate of spores for each strain. The experiment was performed in triplicate and the average of survival rate at each time point was taken. After 5 min of heat treatment the survival rate of wild type M145 spores was 71% and that of DSCO5302 (*rodA2*$^-$) mutant was 73% (Fig. 4.14). On the

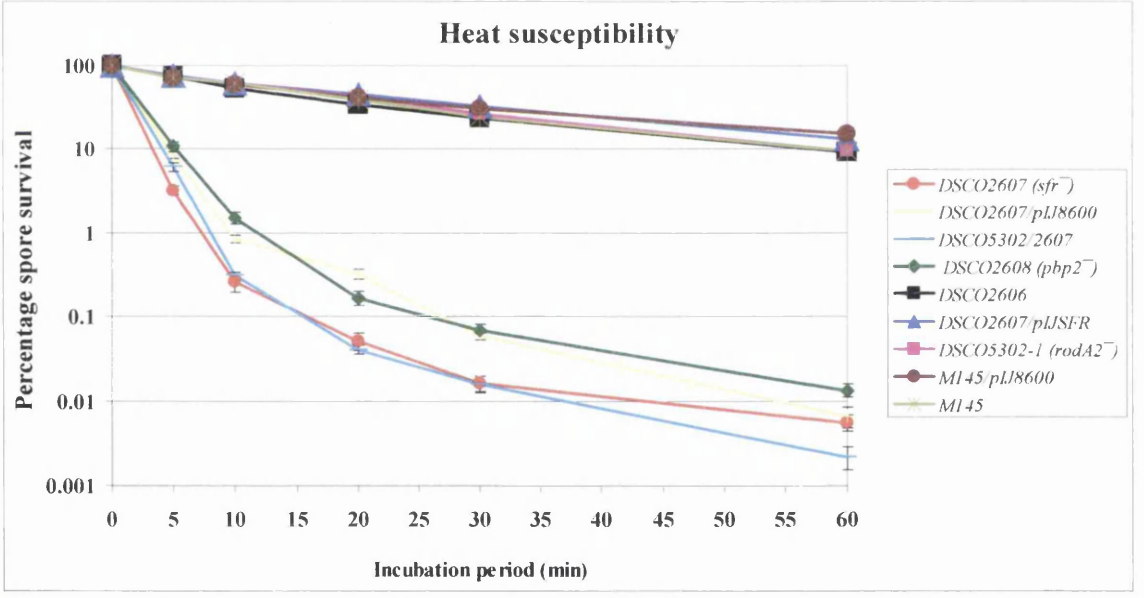

Figure 4.14: Heat susceptibility of the spores of *rodA2, sfr, pbp2, SCO2606* and *rodA2/sfr-hyg*^{R} mutants. Spore suspensions of *S. coelicolor* M145 (wild type), M145/pIJ8600, DSCO5302 (*rodA2*$^-$), DSCO2607 (*sfr*$^-$), DSCO5302/2607 (*rodA2*$^-$/*sfr*$^-$), DSCO2608-1 (*pbp2*$^-$), DSCO2606, DSCO2607/pIJ8600 and DSCO2607/pIJSFR strains were incubated at 60°C for different intervals and different dilutions of each spore suspension were plated on MS agar to perform viable count. Survival rate was calculated as described in Experimental procedures. After 60 min heat treatment the survival rates of *sfr, pbp2* and *rodA2/sfr-hyg*^{R} mutant spores were about 1000 fold lower than that of the parental strain *S. coelicolor* M145. Each value is the mean of four replicates.

other hand the survival rates of DSCO2607 (*sfr*¯), DSCO2608-1 (*pbp2*¯) and DSCO5302/2607 (*rodA2*¯/*sfr*¯) were reduced to 3%, 11% and 6%, respectively (Fig 4.14). With prolonged heat treatment, up to 60 min, the survival rates of wild type and DSCO5302 spores were reduced to nearly 10%, while for the same treatment period only 0.006%, 0.01% and 0.002% spores of DSCO2607 (*sfr*¯), DSCO2608-1 (*pbp2*¯) and DSCO5302/2607 (*rodA2*¯/*sfr*¯) mutants, respectively, survived (Fig 4.14). Considering the short distance between *sfr* and the downstream gene *SCO2606*, encoding a hypothetical protein, it may be possible that the heat susceptibility of *sfr* and *pbp2* mutants may be due to a polar effect. To check whether the phenotype of *sfr* and *pbp2* is due to a polar effect a disruption mutant of *SCO2606* was constructed using C88.2.H08 insertion cosmid. Out of several double crossover exconjugants of *SCO2606::*Tn*5062*, three clones were selected randomly for Southern blot analysis and characterization. SB analysis of the three selected clone was carried out on *Sal*I digested chromosomal DNA of each mutant clone and the respective cosmid used for mutagenesis. SB analysis of the *SCO2606* mutant clones confirmed that out of three clones two were true mutants of the *SCO2606* gene (Fig. 4.15). The *SCO2606* mutant strain was designated as DSCO2606. No apparent phenotype of DSCO2606 was observed when plated on SFM agar plate (not shown). Fluorescence microscopic observations of vegetative and aerial mycelia of the DSCO2606 mutant also showed no difference in pattern of septation and chromosome condensation from wild type (not shown). The spores of DSCO2606 were as heat resistant as the wild type strain suggesting that there was no polar effect on the *SCO2606* gene in the *sfr* mutant (Fig.4.14).

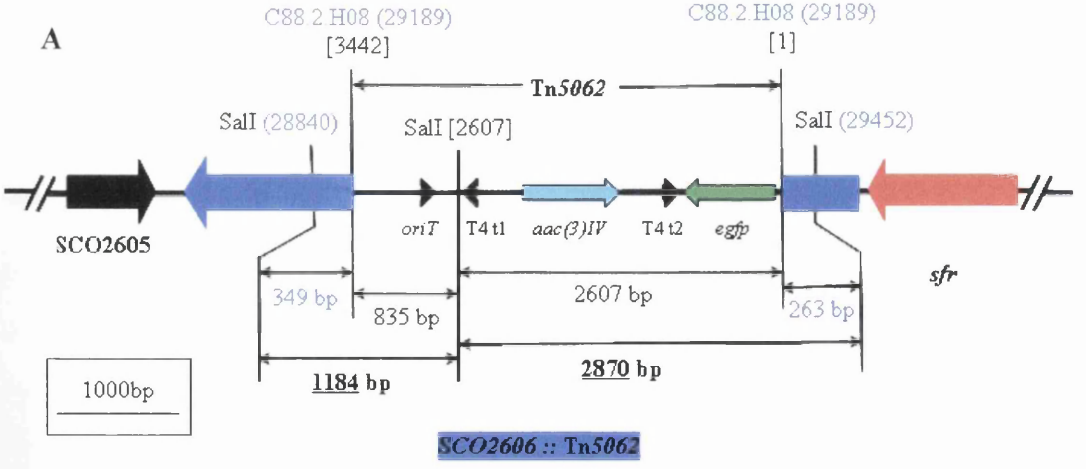

Figure 4.15: Continued on the next page....

B

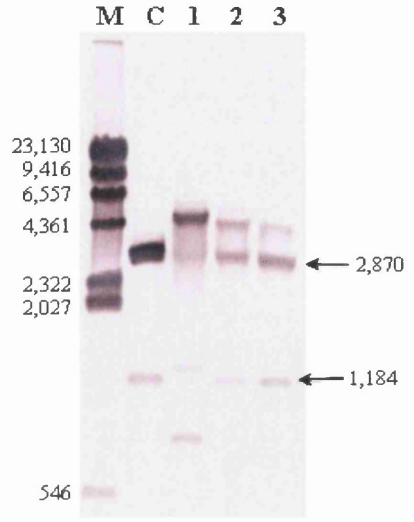

Figure 4.15: SB analysis of *SCO2606* mutant clones. **(A)** Diagrammatic representation of *SCO2606* gene region showing Tn*5062* insertion and *Sal*I restriction sites to calculate the size of bands that should be obtained after SB analysis. The cosmid insertion used for *SCO2606* mutagenesis is shown in blue colour with the position of insertion in the cosmid presented in brackets. Just under the cosmid name and position, the start and end sites of Tn*5062* are written in square brackets. The position of important *Sal*I restriction sites in the *SCO2606* region of the cosmid are shown in the brackets and in Tn*5062*, it is shown in square brackets. Arrows with different colours represent different genes and their directions. The name of each respective gene is shown just under each arrow. *aac(3)IV* – Apramycin resistance; T4 t1,2 – Transcription terminator t1 & 2; *egfp* – Enhanced green fluorescent protein gene; *oriT* – Origin of transfer. The size of expected bands obtained after SB is shown in bold letters with underline. The rectangular box shows the scale of the map. **(B)** SB of five *SCO2606* mutant clones. M –*Hin*dIII digested λ DNA marker with the size (in bp) of each band presented on the left hand side; C – *Sal*I digested C88.1.H08 cosmid insertion; and 1 to 3 – *Sal*I digested chromosome of each *SCO2606* mutant clone. The size (in bp) of each expected band is shown on right hand side. Digoxigenin labelled Tn*5062* was used as a hybridization probe.

A recombinant plasmid pIJSFR (construction described in section 4.8), containing the *sfr* gene regulated by the *tipA* promoter, was introduced into DSCO2607 *(sfr⁻)* strain to obtain the complementing strain DSCO2607/pIJSFR. As a result of complementation, the spores became as resistant to temperature as the wild type strain (Fig. 4.13). On the other hand the spores of the strain DSCO2607/pIJ8600, containing the empty vector pIJ8600, were as susceptible as *sfr* mutant spores (Fig. 4.13). This suggested that the heat susceptibility of *sfr* mutant spores was due to the disruption of the *sfr* gene. The complementation analysis was performed exactly in the same way as mutants using SFM medium without adding any thiostrepton to induce the *sfr* gene

expression suggesting that there is detectable basal level expression from *ptipA* promoter. Interestingly, Ali *et al.,* in 2002 showed the activity of *ptipA* without the inducer, thiostrepton. Thomas in 2001 also showed that the *tipA* promoter was up-regulated by some unknown compound present in soya extract. Although, the *sfr* mutant was complemented by the *sfr* gene under the control of *tipA* promoter, the complementation analysis of the *sfr* mutant using *sfr* gene regulated by its own promoter needs to be performed. Considering the operon-like structure of *sfr* and *pbp2* genes, the heat susceptibility of *pbp2* mutant spores may be due to the polar effect on the *sfr* gene. This needs to be checked by complementation analysis of the *pbp2* mutant using *sfr* and *pbp2* genes individually and with both the genes as an operon.

It is known that *Streptomyces* spores are resistant to treatment with SDS and this detergent has also been reported to activate spore germination (Grund and Ensign, 1982). The effect of SDS (Sodium Dodecyl Sulfate) on *rodA2, sfr, pbp2* and *rodA2/sfr-hyg*^{R} mutant spores was therefore tested. SDS at a final concentration of 1% or 5% was added to spore suspensions of M145 (wild type), DSCO5302-1 (*rodA2*$^-$), DSCO2607 (*sfr*$^-$), DSCO2608-1 (*pbp2*$^-$) and DSCO5302/2607 (*rodA2*$^-$/*sfr*$^-$) strains, each containing 10^8 spores per ml and incubated at room temperature for one hour. As a control, water instead of SDS was added to spore suspensions and incubated at room temperature for a similar time period. After one hour spores were diluted and plated on SFM agar plates. Plates were further incubated at 30° C for three days and a viable count was performed to calculate the survival rate of each strain. There was no major decrease in the viable count of wild type spores after SDS treatment compared to that of water (Fig. 4.16). Similarly, there was only a ~10% decrease in the viable count of DSCO5302-1 (*rodA2*$^-$) and DSCO2606 spores after treatment with 5% SDS (Fig. 4.16). However, the viable counts of the *sfr, pbp2* and *rodA2/sfr-hyg*^{R} mutants were reduced drastically to nearly 1% in case of *sfr* and *pbp2* mutants and ~0.5% for the *rodA2/sfr-hyg*^{R} double mutant (Fig. 4.16). The minor difference of 0.5% between the viable count of single and double mutants may be due to some experimental error. Complementation analysis of the *sfr* mutant by introducing chromosome integrating plasmid pIJSFR showed that the SDS susceptibility of *sfr* mutant was due to the *sfr* gene disruption (Fig. 4.16). Introduction of the empty vector pIJ8600 did not have any effect on the phenotype of the wild type as well as the *sfr* mutant. Complementation analysis of the

sfr, pbp2 and *rodA2/sfr-hyg*^{R} mutants using the respective genes expressed by their own promoter needs to be performed.

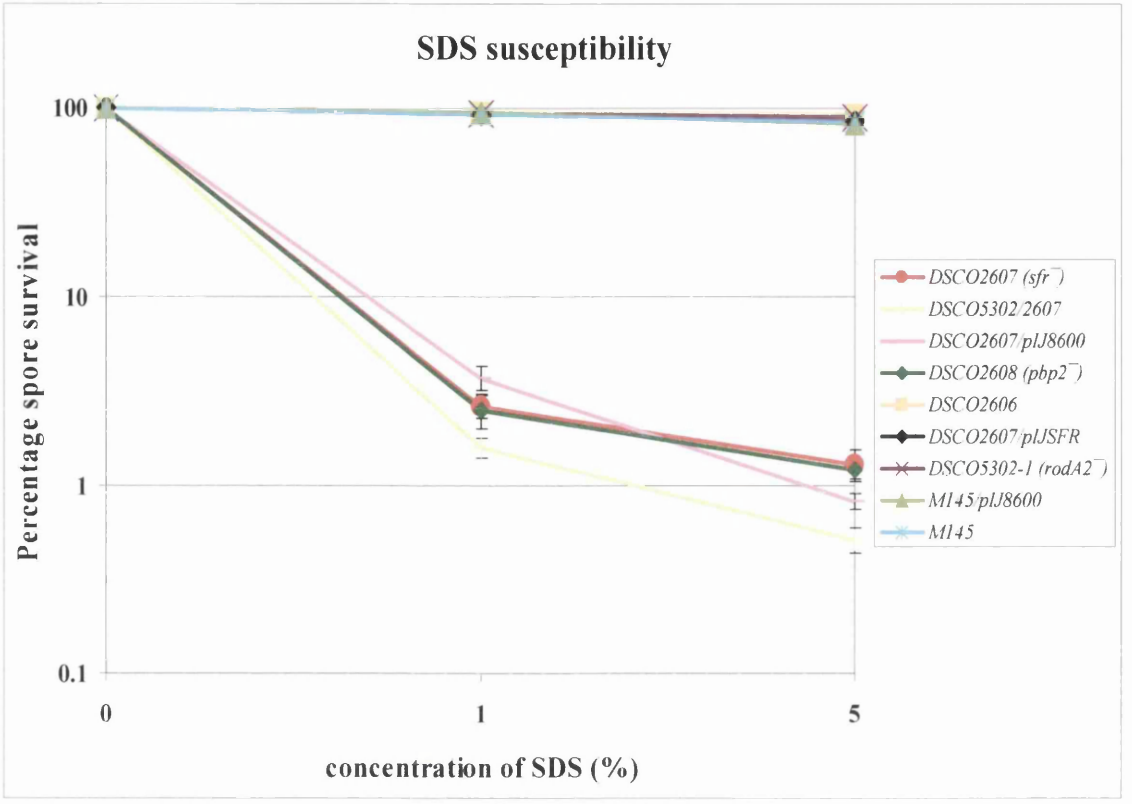

Figure 4.16: Effect of SDS on the spores of *rodA2, sfr, pbp2, SCO2606* and *rodA2/sfr-hyg*^{R} mutants. Spore suspensions of *S. coelicolor* M145 (wild type), M145/pIJ8600, DSCO5302, DSCO2607, DSCO2608-1, DSCO2606, DSCO5302/2607, DSCO2607/pIJ8600 and DSCO2607/pIJSFR strains were incubated with water (0% SDS), 1% SDS and 5% SDS for one hour and quantification of spores of each strain was carried out by plating serial dilution of each spore suspension on SFM agar plates. Survival rate was calculated as described in Experimental procedures. The survival rate of *sfr, pbp2* and *rodA2/sfr-hyg*^{R} mutant spores was reduced to ~3% and ~1% after treatment with 1% and 5% of SDS, respectively. Each value is the mean of four replicates.

4.6 *sfr, rodA2/sfr* and *pbp2* mutants are susceptible to antibiotics that inhibit a late stage of cell wall synthesis

S. coelicolor is known to be highly resistant to beta-lactam antibiotics and vancomycin, that inhibit cell wall synthesis (Hong *et al.*, 2004; Ogawara, 1981). SEDS family proteins and PBPs are required during the late stage of cell wall synthesis in

bacteria (Errington *et al.*, 2003; Harry *et al.*, 2006). Heat and detergent susceptibility of the spores of *sfr, pbp2* and *rodA2/sfr-hyg*^{R} mutants indicated that *sfr* and *pbp2* gene products play some role during cell wall synthesis. Therefore, minimum inhibitory concentrations (MICs) of some cell wall specific antibiotics were determined for wild type M145 and, *rodA2, sfr, pbp2, SCO2606* and *rodA2/sfr-hyg*^{R} mutants using a dilution method. Three different antibiotics bacitracin, vancomycin and ampicillin were selected for an MIC test. Bacitracin acts by inhibiting dephosphorylation of the lipid carrier required to transport cell wall precursors across the membrane (Fig. 4.17) (Greenwood and Whitley, 2003). Vancomycin and ampicillin both bind to the terminal D-alanyl-D-alanine unit of the muramylpentapeptide and prevent transpeptidation of peptidoglycan (Fig. 4.17) (Greenwood and Whitley, 2003; Reynolds, 1989). Vancomycin also inhibits transglycolysation, stopping the addition of new peptidoglycan precursors in the cell wall (Reynolds, 1989).

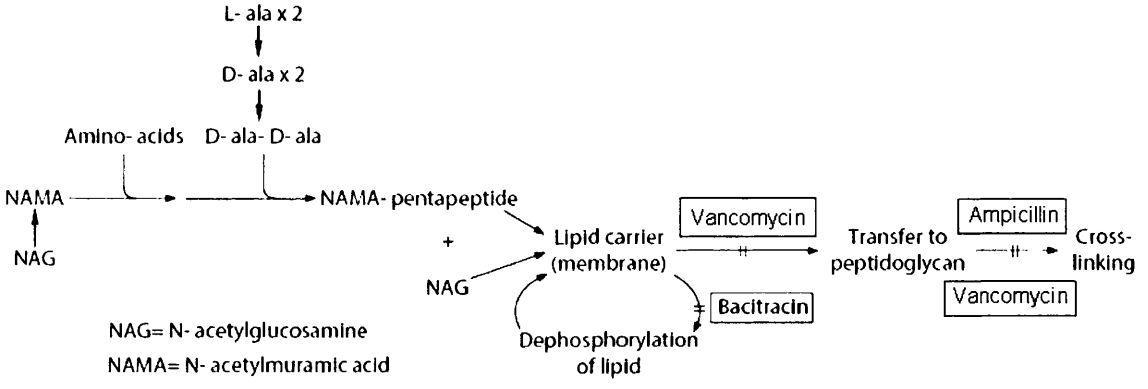

Figure 4.16: Schematic presentation of bacterial cell wall synthesis, showing the sites of action of ampicillin, bacitracin and vancomycin antibiotics. L/D-ala, L/D-alanine; D-ala-D-ala, D-alanyl-D-alanine. Adapted from Greenwood, D. and Whitley, R. (2003).

In the MIC experiment, the spore suspension of each strain containing 10^4 spores/ml (final concentration) was plated on a series of 2×YT agar plates containing appropriate dilutions of the respective antibiotic to produce visible growth. The lowest concentration of an antibiotic that inhibits growth was determined by observing the

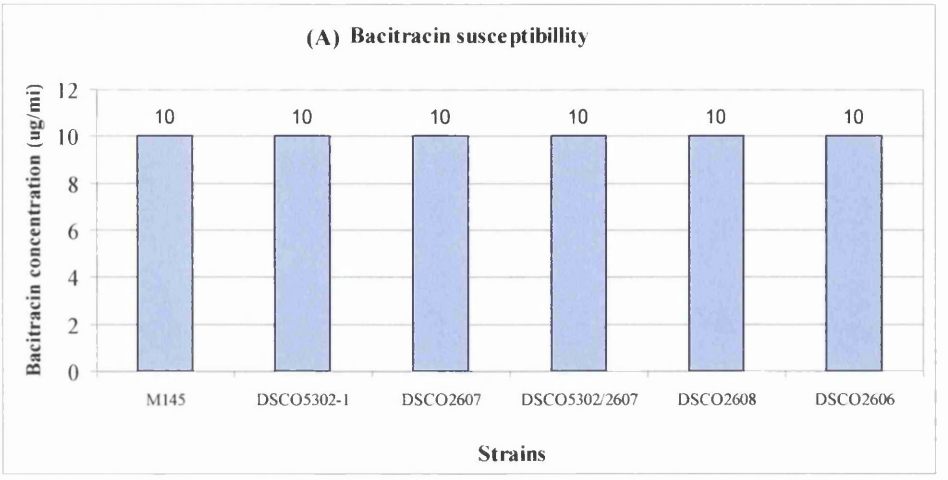

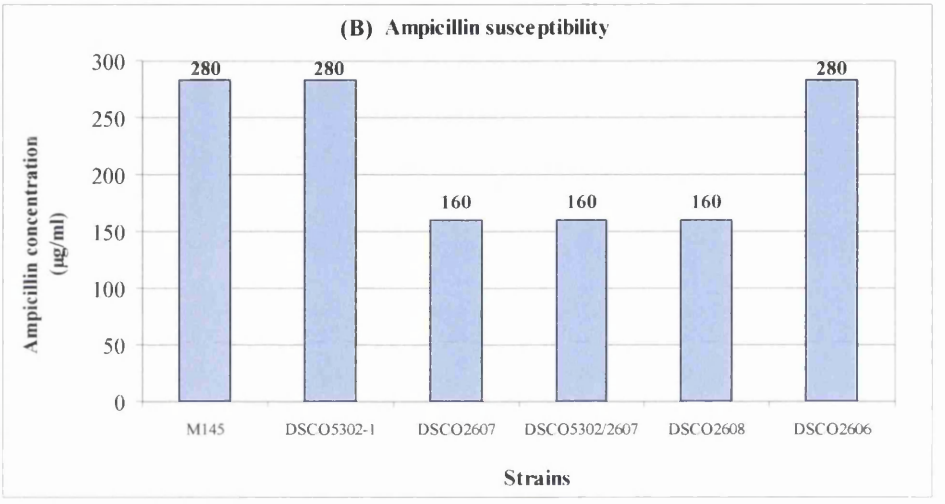

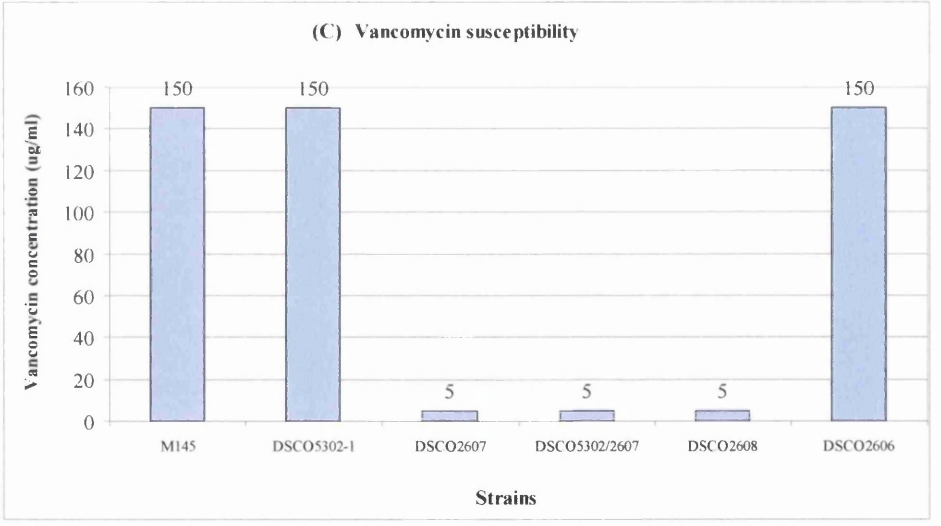

Figure 4.18: Minimum inhibitory concentration of bacitracin (A), ampicillin (B) and vancomycin (C) for M145 (wild type), DSCO5302 (*rodA2*$^{-}$), DSCO2607 (*sfr*$^{-}$), DSCO5302/2607 (*rodA2*$^{-}$/*sfr*$^{-}$), DSCO2608-1 (*pbp2*$^{-}$) and DSCO2606 strains. MICs of the antibiotics for all the strains were calculated using a dilution method as described in Materials and Methods. The experiment was performed in triplicate.

dilution plates for colony growth after 2 days of incubation at 30° C. The MICs of bacitracin, vancomycin and ampicillin for the wild type strain M145 were 10 μg/ml, 150 μg/ml and 280 μg/ml, respectively (Fig. 4.18). The MIC of bacitracin for *rodA2, sfr, pbp2, SCO2606* and *rodA2/sfr-hyg*^{R} was identical to that of the wild type MIC value (Fig. 4.18 A). Also, MICs of vancomycin and ampicillin for *rodA2* and *SCO2606* mutants were similar to that of the wild type (Fig. 4.18 B & C). Interestingly, the MICs of ampicillin and vancomycin for both *sfr* and *pbp2* mutants were reduced to 160 μg/ml and 5 μg/ml, respectively (Fig. 4.18 B & C). Such a high susceptibility of *sfr, pbp2* and *sfr/rodA2* mutants to the cell wall specific antibiotics that inhibits that last stage of cell wall synthesis further strengthens the probable role of *sfr* and *pbp2* in the last stage of cell wall synthesis, and possibly during spore germination. Further studies of Sfr and Pbp2 protein interaction and *in situ* localization are required to know the specific function of these proteins.

Surprisingly, when the MIC test was performed using SFM agar medium instead of 2×YT agar no toxic effect of the above used antibiotics was observed on wild type as well as the various mutants, even at much higher concentrations than the MIC obtained using 2×YT medium. The reason for such antibiotic resistance is unclear, however it was shown that inclusion of soya flour is the growth medium can produce a multiple antibiotic resistance phenotype in *S. griseus* and *S. lividans* (Thomas, 2001).

When pIJSFR containing the *sfr* gene under the control of the *tipA* promoter was introduced into the *sfr* mutant, it did not complement the mutant for antibiotic susceptibility. Surprisingly, introduction of pIJ8600 into the wild type strain made the strain highly susceptible to vancomycin. Similar results were also observed when another plasmid pSH152 (integrates at the same site as pIJ8600) was introduced in to the wild type strain. The reason for such susceptibility is not know.

4.7 Analysis of *sfr* mutant by atomic force microscopy

Changes in the cell surface occur during the complex developmental cycle of *S. coelicolor*. The surface of spore-bearing hydrophobic aerial hyphae of the organism is characterized by a relatively unstable dense heterogeneous fibrous layer of

various chaplin and rodlin proteins (Del Sol *et al.*, 2007; Wosten *et al.*, 1999) (Fig. 4.19). The susceptibility of *sfr* mutant spores to heat, detergent and cell wall specific antibiotics suggested some defect in spore cell wall synthesis. To check whether this defect has any effect on the *sfr* mutant spore surface, atomic force microscopy (AFM) of the wild type and *sfr* mutant was performed. Cultures of the wild type and the *sfr* mutant were grown on SFM agar plate for four days at 30° C. Samples for microscopy were prepared by taking impressions of each strain. Images obtained using tapping mode showed no discernible difference in the surface features of wild type and mutant spores (Fig. 4.19). However, the presence of a normal rodlet layer surrounding the spores of the *sfr* mutant does not exclude underlying differences to the cell wall.

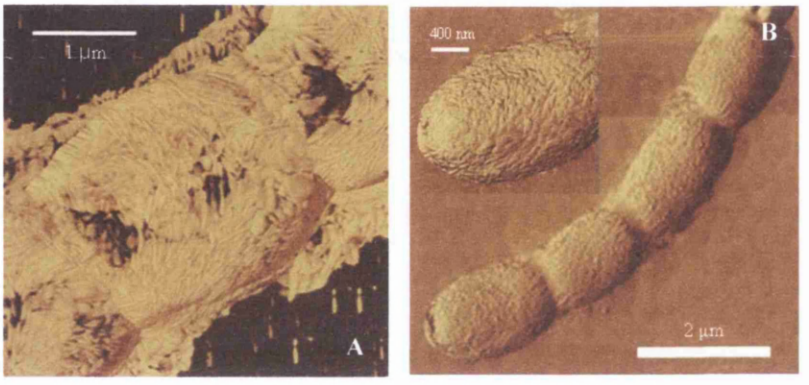

Figure 4.19: Atomic force microscopy image of wild type strain M145 (A) and *sfr* mutant strain DSCO2607 (B) obtained using tapping mode. Insert image in panel B is an enlarged portion of the *sfr* mutant image.

4.8 Overexpression of *sfr* in *S. coelicolor* does not affect growth and development

To analyse the effect of overexpression of *S. coelicolor* Sfr protein in *S. coelicolor*, the gene was amplified by PCR with the primers SfrF1 and SfrR1 that include *Nde*I and *Xba*I sites, respectively. The PCR amplified *sfr* gene was digested with *Nde*I and *Xba*I. The purified gene was cloned just downstream of the thiostrepton inducible *tipA* promoter in *Nde*I/*Xba*I digested pIJ8600 plasmid to obtain pIJSFR plasmid where the *sfr* gene is under the control of the *tipA* promoter (Fig. 4.20). The plasmid construct pIJSFR was confirmed by restriction digestion analysis and

sequencing. The pIJSFR construct was then transferred into *S. coelicolor* M145 by intergeneric conjugation to obtain an M145/pIJSFR strain. As a control an empty vector pIJ8600 was also introduced into *S. coelicolor* M145 to obtain M145/pIJ8600 strain.

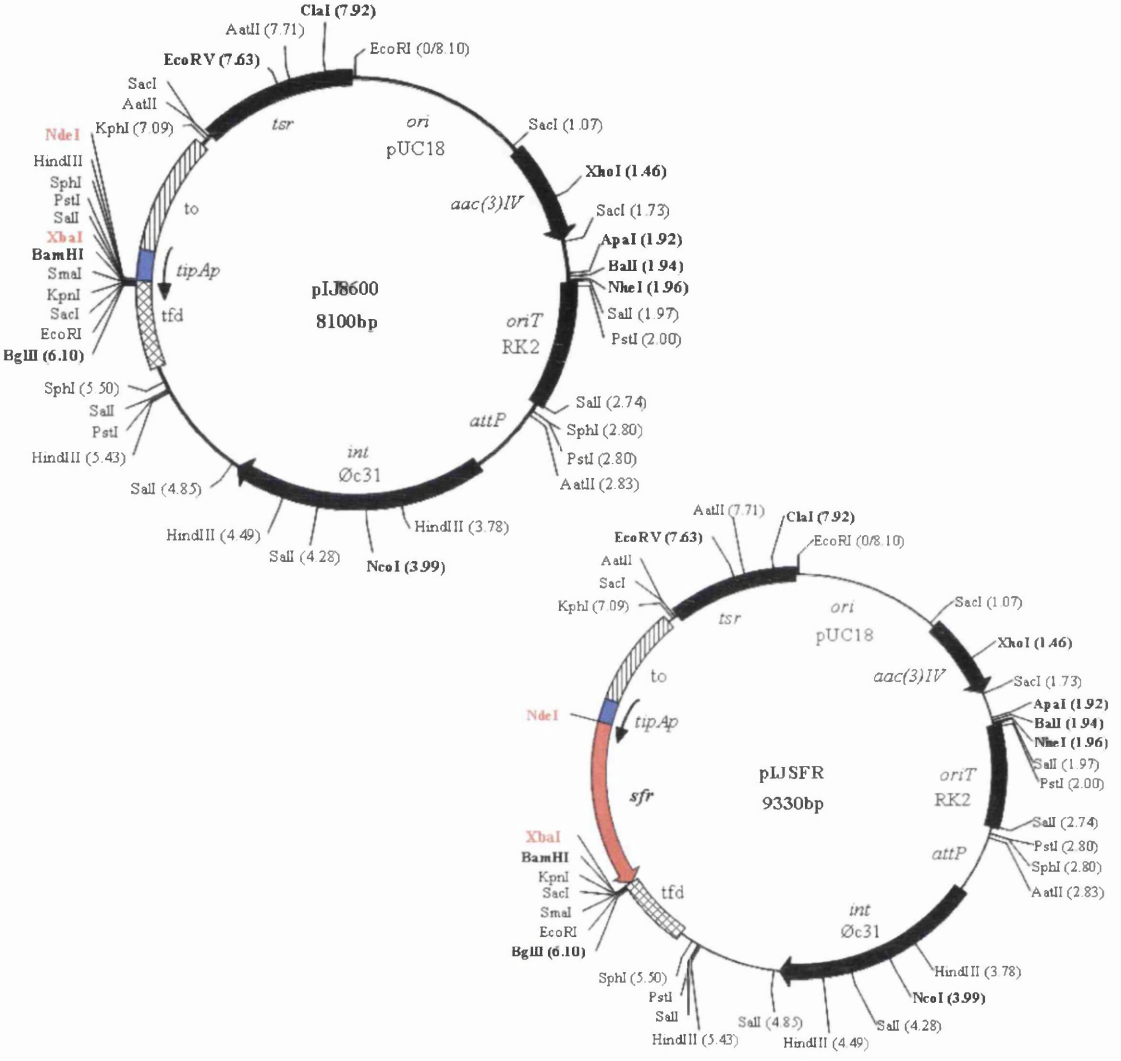

Figure 4.20: Map of plasmids pIJ8600 and pIJSFR showing the restriction site. Restriction enzymes used for cloning the *sfr* gene are indicated in red colour. The thiostrepton inducible *tipA* promoter is indicated in blue colour and its orientation is indicated by an arrow. The *sfr* gene is indicated by a red arrow. *aac(3)IV* – apramycin acetyltransferase; *attP* - attachment site of the temperate phage C31; *int* ØC31 - ØC31 integrase; *ori* pUC18 - origin of replication from pUC18; *oriT* RK2 – origin of transfer from plasmid RK2; *tipAp* – thiostrepton inducible promoter; *tsr* - thiostrepton-resistance gene; *tfd* - major transcription terminator of phage fd; *to* - transcription terminator from phage λ; The maps are not drawn to the scale. (For description see the text)

To study the effect of *sfr* overexpression on the growth and development of *S. coelicolor*, the strains containing either pIJSFR or pIJ8600 were plated on SFM agar plates containing 10 µg/ml or 25 µg/ml (final concentrations) of thiostrepton and grown for 3 to 4 days at 30° C. No apparent phenotype was observed in the *sfr* overexpressed *S. coelicolor* strain (Fig. 4.21). There was some delay in the development of both M145/pIJ8600 and M145/pIJSFR strain on the thiostrepton containing medium.

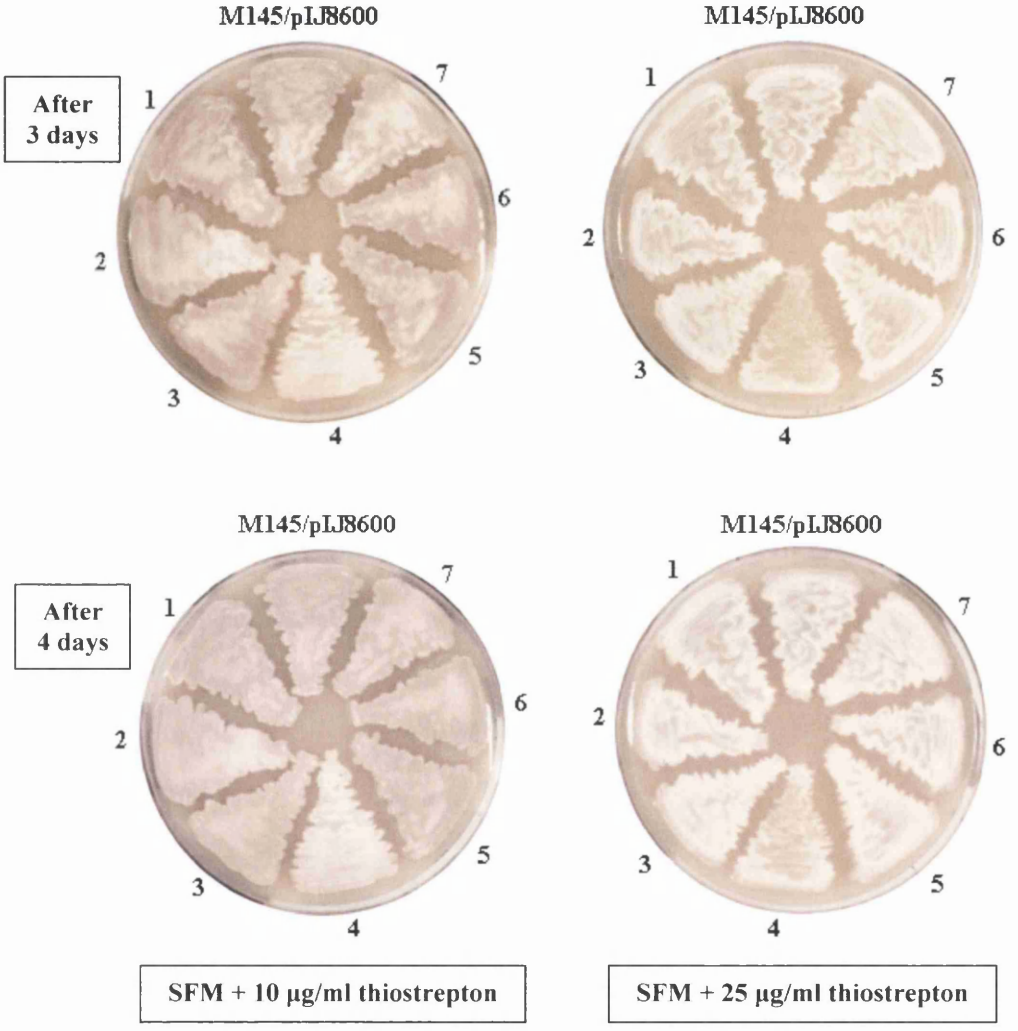

Figure 4.21: Overexpression of Sfr in *S. coelicolor* grown on SFM containing thiostrepton as an inducer of the *tipA* promoter. Plates were incubated at 30° C for three to four days. *S. coelicolor* strain containing pIJ8600 is indicated as M145/pIJ8600. Different clones of *S. coelicolor* strain containing *sfr* overexpressing plasmid pIJSFR are indicated by number.

For fluorescence microscopy, the M145/pIJ8600 and M145/pIJSFR strains were grown on the SFM agar containing 10 μg/ml thiostreption at 30° C for 3 days. After 3 days of cultivation impressions of each strain were taken and stained with Fluo-WGA and PI as described previously. Microscopic observations showed not difference in septation pattern and spore size of M145/pIJ8600 and M145/pIJSFR strains (Fig. 4.22).

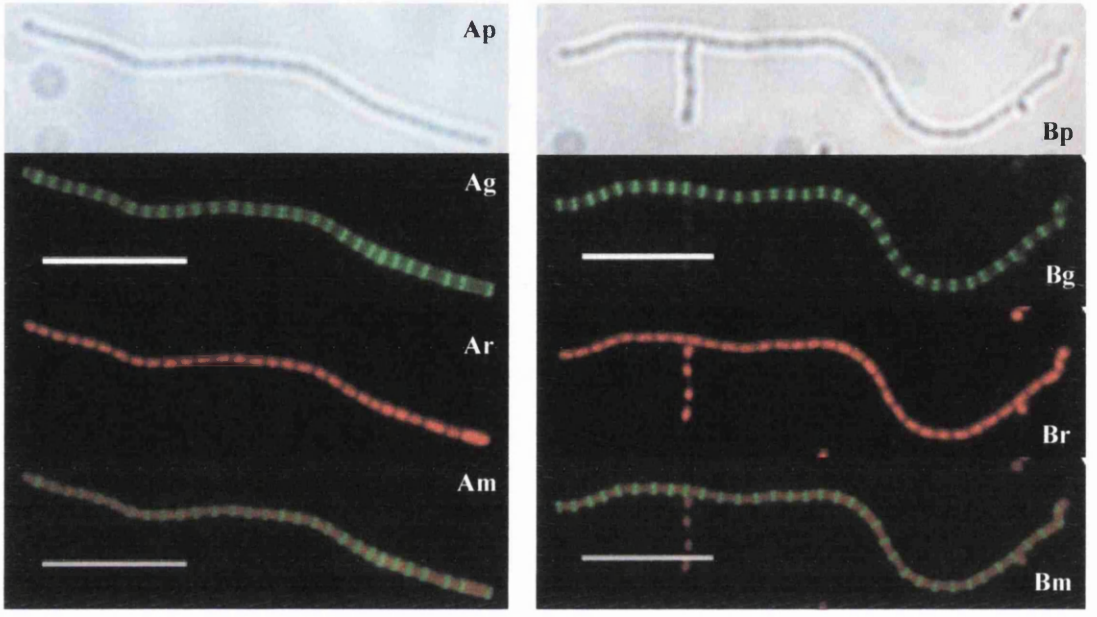

Figure 4.22: Fluorescence microscopy of aerial hyphae of *S. coelicolor* M145/pIJ8600 (A) and M145/pIJSFR (B) strain using Fluo-WGA (for cell wall) and PI (chromosomal DNA) staining to visualize sporulation septa and chromosome distribution. Samples were prepared by taking the impression of culture grown on the surface of SFM agar medium containing 10 μg/ml thiostreption for 3 days at 30° C. Each panel shows phase contrast (p), Fluo-WGA staining (g), PI staining (r) and merged (m) images of Fluo-WGA and PI staining of aerial hyphae of respective strains. (Scale bar 10 μm)

4.9 Construction and characterization of an *mreB* mutant

It has been shown that the *sfr* is a part of *mre* operon (Burger *et al.*, 2000) and there is a possible genetic link among the genes of *mre* operon. To understand the possible link between *sfr*, *pbp2* and *mreB* genes, *mreB* disruption mutants were constructed using C88.1.B06 (position in chromosome 2835672) cosmid insertion. The *mreB* mutants were constructed by intergeneric conjugation and selected for apparent

allelic replacement of the wild type copy of the *mreB* gene with that of disrupted copy of the same gene as described previously. The double crossover exconjugants of *mreB* mutant were obtained at the frequency of 7%. Six clones of the *mreB* disruption mutant were randomly selected and Southern hybridization was performed on *Kpn*I digested chromosomal DNA of these mutant clones (Fig. 4.23 A). A *Kpn*I digested C88.1.B06 cosmid insertion was used as a positive control. The digoxigenin labelled Tn*5062* was used as a probe to hybridize the blot. The Southern blot of the mutant clones confirmed that all the selected clones are true mutants (Fig. 4.23 B). The *mreB* mutant strain thus obtained was designated as DSCO20611.

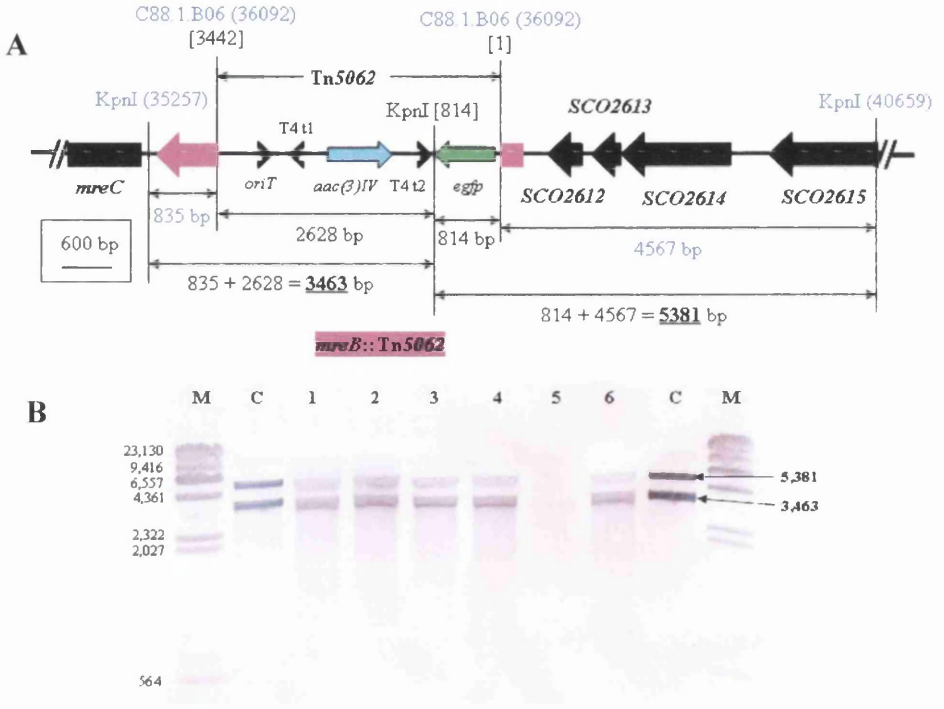

Figure 4.23: Southern Blot (SB) analysis of *mreB* mutant clones constructed using C88.1.B06 insertion. **(A)** Diagrammatic representation of *mreB* locus showing Tn*5062* insertion and *Kpn*I restriction sites to calculate the size of bands that should be obtained after Southern hybridization. The cosmid insertion used for *mreB* mutagenesis is shown in blue colour with the position of insertion in the cosmid presented in brackets. Just under the cosmid name and position, the start and end sites of Tn*5062* are shown in square brackets. The position of important *Kpn*I restriction sites in the *mreB* region of the cosmid are shown in brackets and in Tn*5062* in square brackets. Arrows with different colours represent different genes and their direction. The name of each respective gene is shown just under each arrow. *aac(3)IV* – Apramycin resistance; T4 t1,2 – Transcription terminator t1 & 2; *egfp* – Enhanced green fluorescent protein gene; *oriT* – Origin of transfer. Expected size of bands that should be obtained in SB is shown in bold letters with underlining. The rectangular box shows the scale of the map. **(B)** SB of six *mreB* mutant clones. M –*Hin*dIII digested λ DNA marker with the size for each band presented on the left hand side; C – *Kpn*I digested C88.1.B06 cosmid insertion; and 1 to 6 – *Kpn*I digested chromosome of each *mreB* mutant clone. The size (in bp) of each expected bands for *mreB* mutant is shown by arrows. Digoxigenin labelled Tn*5062* was used as a hybridization probe.

Phenotypic characterization of *mreB* mutant clones on different culture media did not show any difference in the phenotype compare to that of wild type strain (Fig. 4.24). The sporulation and antibiotic production were normal.

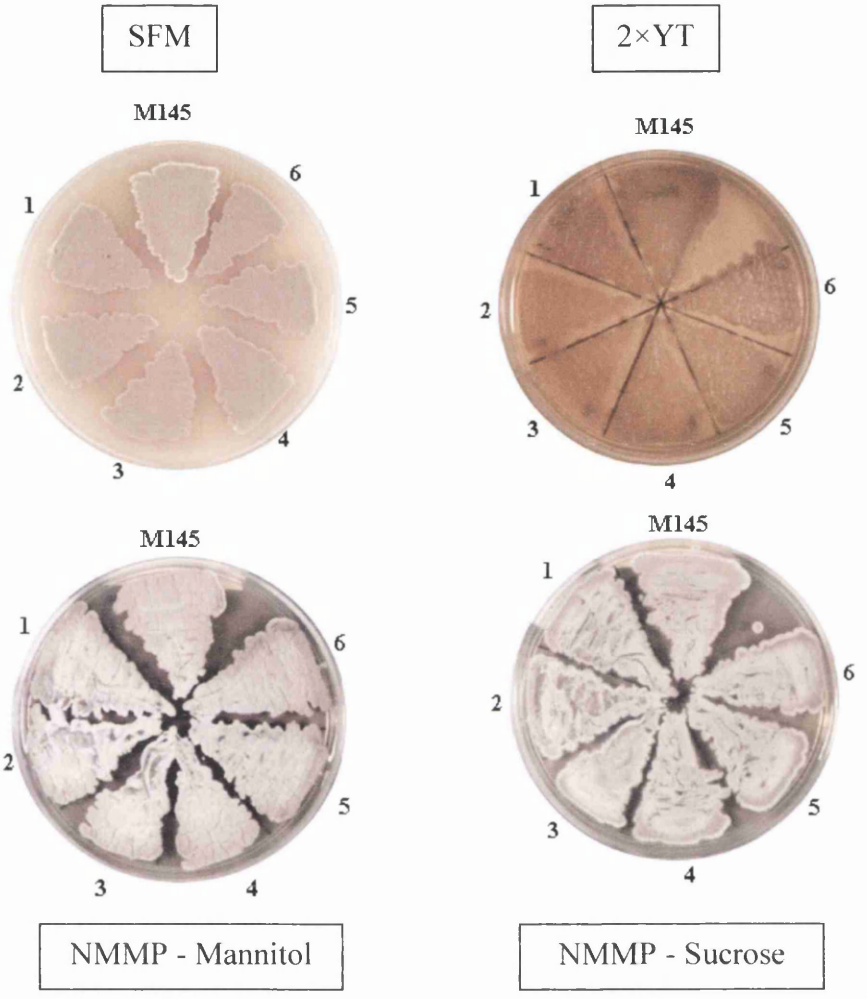

Figure 4.24: Phenotype of the *mreB* mutant and its congenic parental strain *S. coelicolor* M145 on different media. Strains were grown for 3 days at 30° C on SFM, NMMP-Mannitol, NMMP-Sucrose and 2×YT agar media. The *mreB* mutant clones are indicated by numbers 1-6 in each plate picture. The name of the respective medium is presented in rectangular boxes.

Fluorescence microscopy of sporogenic aerial hyphae of the *mreB* mutant was performed using Fluo-WGA/PI staining technique as described previously. No difference in either the pattern of sporulation septation or chromosomal condensation was observed (Fig. 4.25), suggesting that *mreB* is not required for sporulation septation. Measurements of pre-spore compartment dimensions showed that the pre-spore compartment lengths of the *mreB* disruption mutant were ranging from 0.9 to 2 μm, with the average length of 1.3 ± 0.2 μm, which is almost similar to the average length (1.17 ± 0.15) of wild type strain (Fig. 4.26). Thus, the apparent difference in average pre-spore compartment size between *mreB* disruption mutant and wild type was not statistically significant. However, the frequency of larger pre-spore compartments was higher in *mreB* disruption mutant compare to wild type (Fig. 4.26). On the other hand to the spores of *mreB* deletion mutant described by Mazza *et al.* in 2006 were significantly larger than the wild type. The difference in the phenotype of *mreB* mutants may be due to the strain differences and the way the respective mutants were constructed.

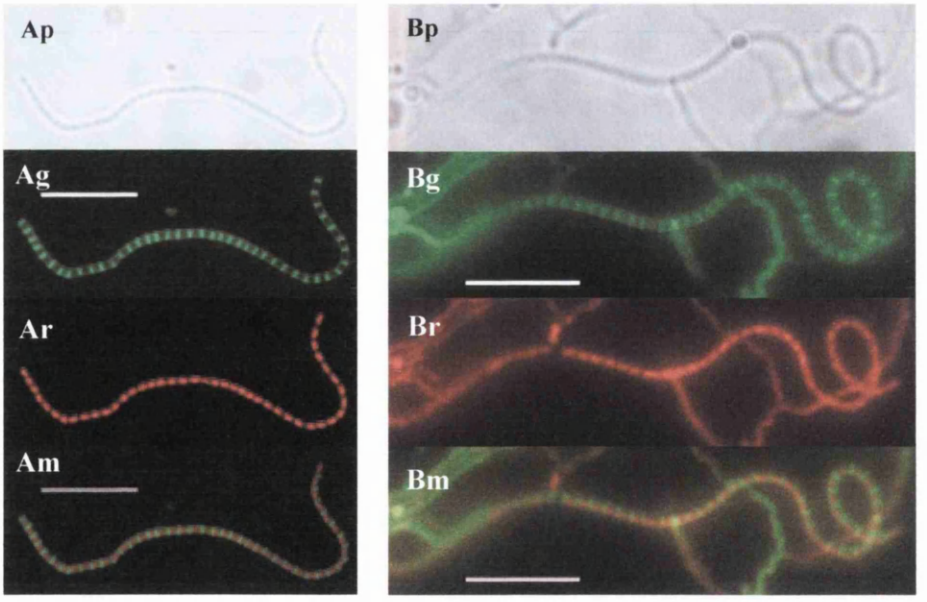

Figure 4.25: Fluorescence microscopy of aerial hyphae of parental strain *S. coelicolor* M145, DSCO2611 using Fluo-WAG (for cell wall) and PI (chromosomal DNA) staining to visualize sporulation septa and chromosome condensation. Samples were prepared by taking the impression of each culture grown on the surface of SFM agar medium for 38 to 40h. Panel A - *S. coelicolor* M145 and B- DSCO2611; Each panel shows phase contrast (p), Fluo-WGA staining (g), PI staining (r) and merged (m) images of Fluo-WGA and PI staining of aerial hyphae of respective strains. (Scale bar 10 μm)

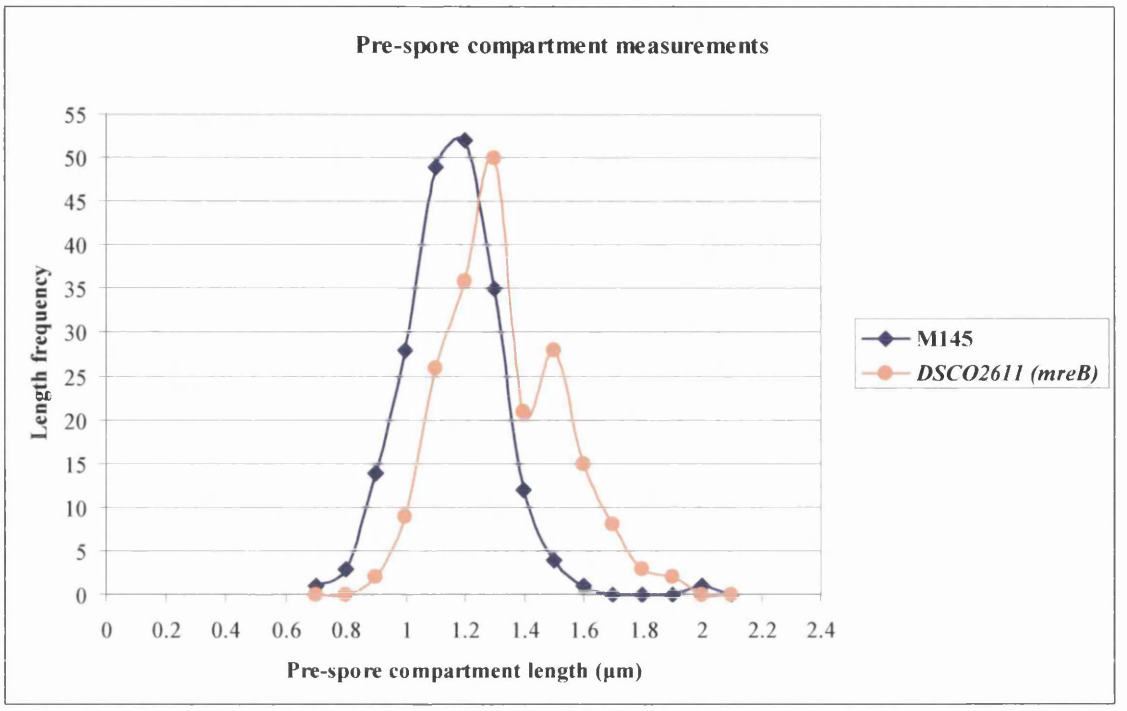

Figure 4.26: Graph of pre-spore compartment length versus frequency of the length of pre-spore compartment in wild type, CDSCO2085-11 and CDSCO2085-14 strains. The length of randomly selected 200 pre-spore compartments of each strain was measured from the Fluo-WGA stained images using Scion Image software.

To test the susceptibility of the *mreB* mutant spores to cell wall specific antibiotics, a MIC test was carried out using the same antibiotics (bacitracin, ampicillin and vancomycin) that were used for the *sfr* and *pbp2* mutant spores as described previously. The experimental procedure and conditions were the same as that of *sfr* spore susceptibility test described earlier in this chapter. Interestingly, the spores of *mreB* mutant were also found susceptible to the cell wall specific antibiotics (ampicillin and vancomycin) that function during last stages of cell wall synthesis (Fig. 4.27). Heat and SDS susceptibility tests of *mreB* mutant spores were further carried out. For heat susceptibility test the spore suspensions (10^7 spores per ml) of *mreB* mutant as well as wild type were incubated at 60° C for different time intervals. After heat treatment, the wild type and the mutant spores (with and without heat treatment) were quantified by performing viable count in exactly a similar way as described for *sfr* mutant spores

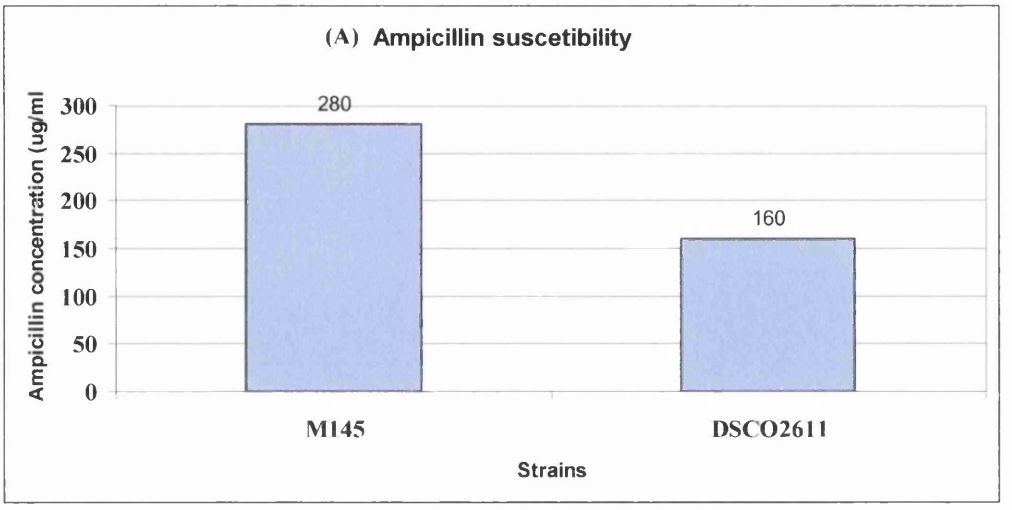

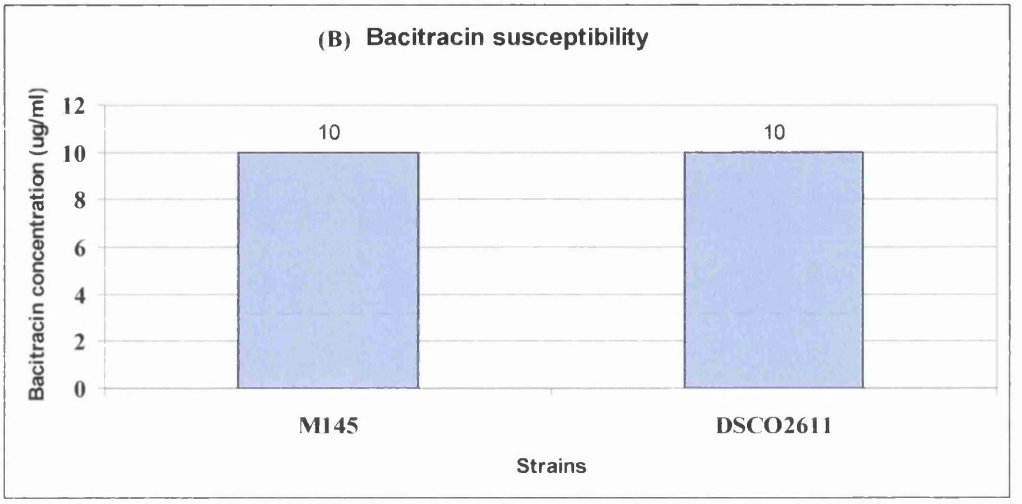

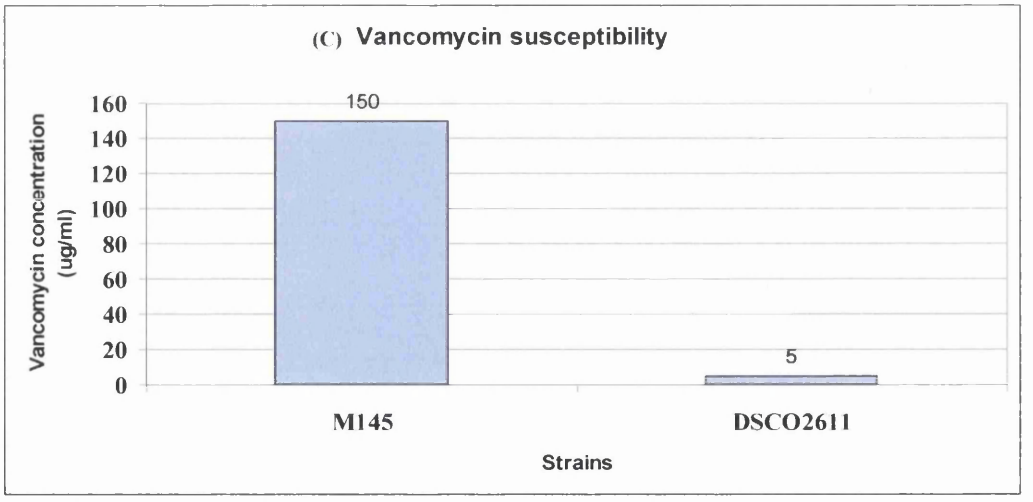

Figure 4.27: Minimum inhibitory concentration of bacitracin (A), ampicillin (B) and vancomycin (C) for M145 (wild type) and DSCO2611 *(mreB⁻)*. MICs of the antibiotics for all the strains were calculated using a dilution method as described in Materials and Methods. The experiment was performed in triplicate.

earlier to calculate the percentage survival rate of *mreB* mutant spores. The percentage survival rate of *mreB* mutant spores was reduced up to 0.003% compare to 8% for wild type spores after 60 min of 60° C heat treatment (Fig. 4.28). In the SDS susceptibility test, the wild type and *mreB* mutant spores (10^8 spores per ml) were treated with 0%, 1% and 5% (final concentration) SDS solution for an hour. The percentage survival rates of spores of wild type and *mreB* mutant were calculate in a similar way as described previously for *sfr* mutant spores. Up to 82% of wild type spores were survived after treatment with 5% SDS (Fig. 4.29), whereas only 0.4% spores of *mreB* mutant were survived a similar SDS treatment (Fig. 4.29). Thus, the *mreB* mutant spores are as susceptible to heat and detergent treatments as *sfr* and *pbp2* mutant spores. The heat and susceptibility data of *mreB* disruption mutant are also consistent with that of the *mreB* deletion mutants (Mazza *et al.*, 2006). This suggests that MreB also plays an important role in spore wall synthesis. All these results together imply that Sfr, MreB and PBP2 may be interdependent in terms of function during spore wall synthesis.

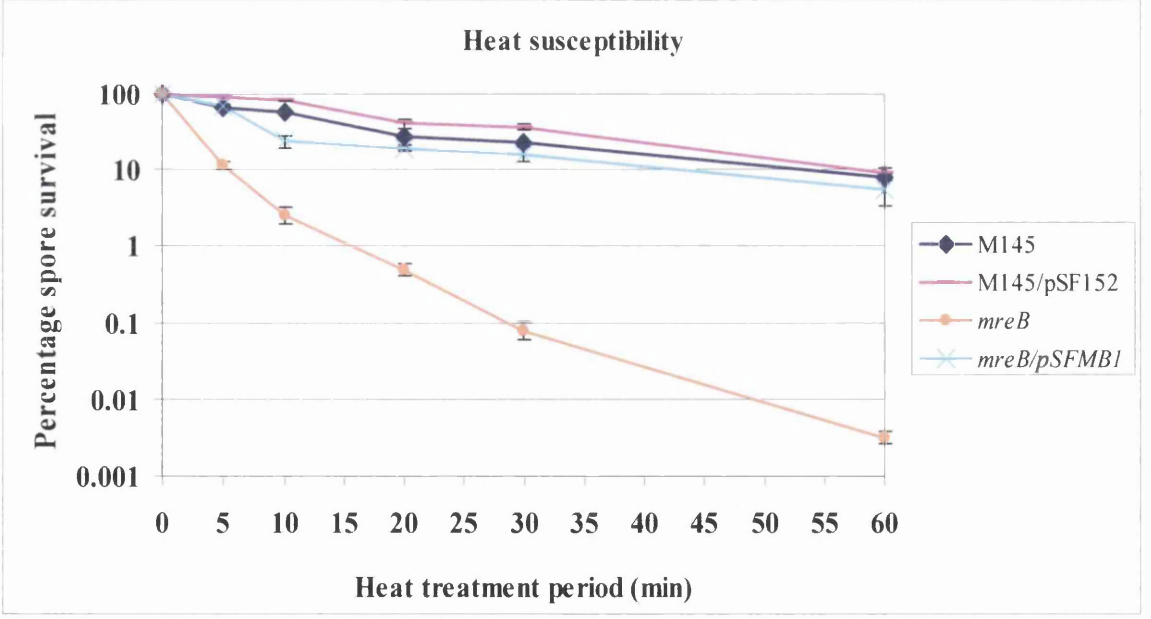

Figure 4.28: Heat susceptibility test of wild type and *mreB* mutant spores. Spore suspensions of *S. coelicolor* M145 (wild type), M145/pSF152, DSCO2611 *(mreB⁻)*, and *mreB*/pSFMB1 strains were incubated at 60°C for different intervals. Spores of each strain were quantified by serial dilution method. Survival rate was calculated as described in Material and Methods procedures. After 60 min heat treatment the survival rate of *mreB* mutant spore was about 1000 fold lower than that of the parental strain *S. coelicolor* M145. The experiment was performed in duplicates.

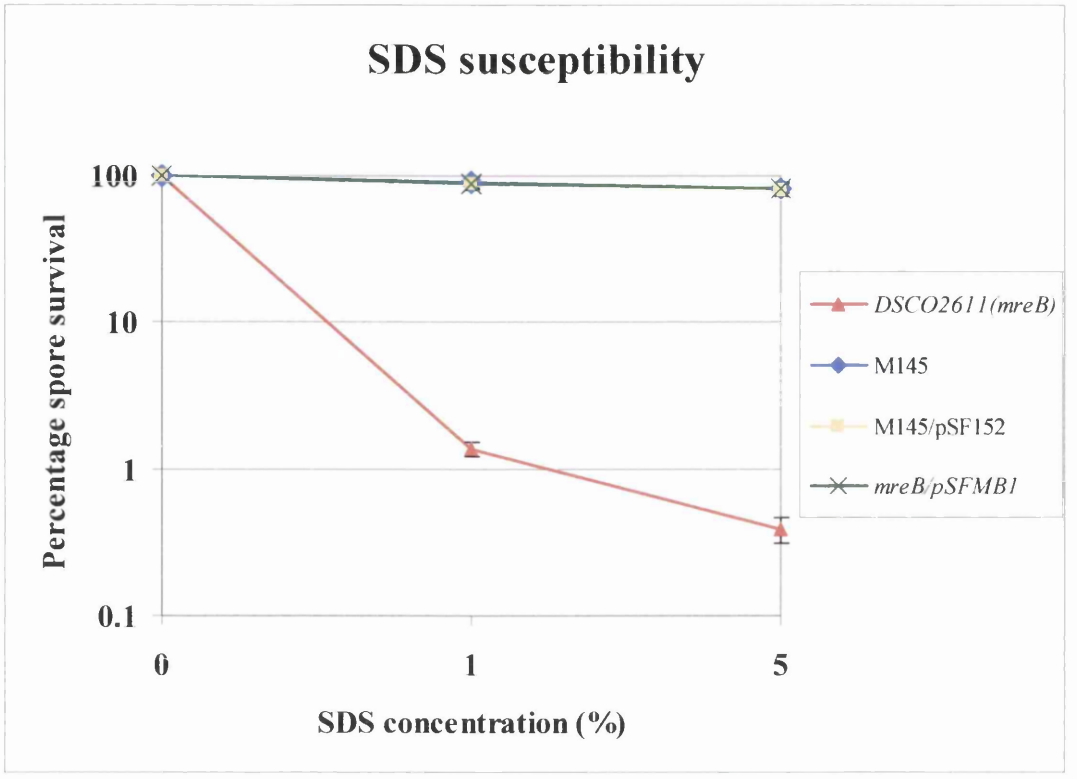

Figure 4.29: Effect of SDS on the spores of *S. coelicolor* M145 (wild type), M145/pSF152, DSCO2611 (*mreB*) mutant and *mreB*/pSFMB1. Spore suspension of each strain was incubated with water (0% SDS), 1% SDS and 5% SDS for one hour and quantification of spores of each strain was carried out by plating serial dilution of each spore suspension on SFM agar plates. Survival rate was calculated as described in Experimental procedures. The survival rate of *mreB* mutant spores was reduced to 1.4% and 0.3% after treatment with 1% and 5% of SDS, respectively. The experiment was performed in duplicates.

4.10 Complementation of *mreB* mutant

For complementation analysis of *mreB* mutant a plasmid pSFMB1 containing *mreB* gene and its promoter region was constructed. To construct pSFMB1, a 1667 bp *Eco*RI fragment from SCC88.1.E03 with a Tn*5062* insertion at position 36806 was cloned into pSF152 digested with the same enzyme (Fig. 4.30). The pSFMB1 was then introduced into *mreB* mutant by intergeneric conjugation. The *mreB* mutant with pSFMB1 was designated as DSCO2611/pSFMB1. Heat, SDS and antibiotic

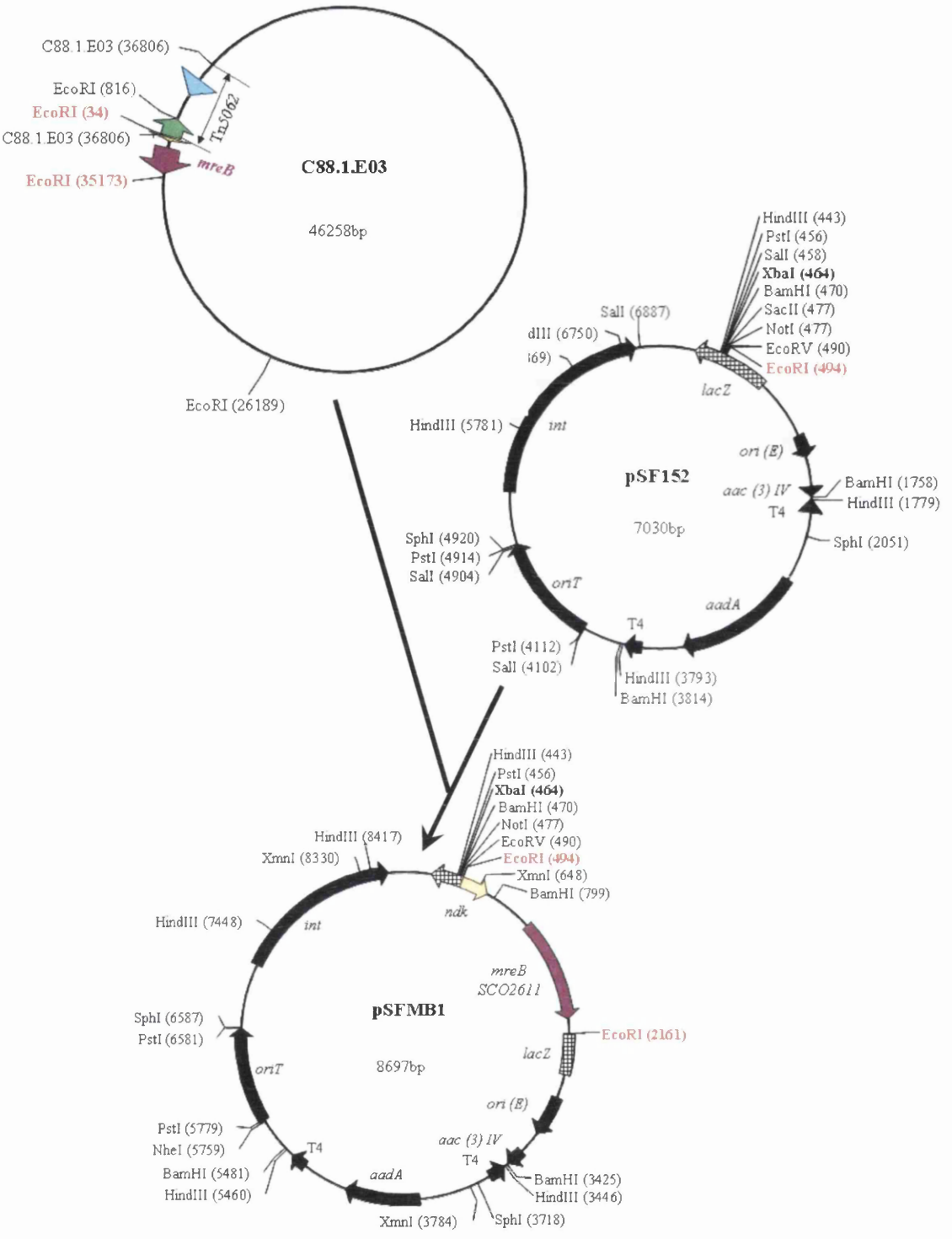

Figure 4.30: Plasmid and cosmid maps used to construct pSFMB1. A 1667 bp EcoRI (red) fragment from SCC88.1.E03 cosmid insertion was cloned into pSF152 vector at its unique *Eco*RI (red) site to construct pSHBW1. Maps are not drawn to the scale.

susceptibility tests were performed on the spores of DSCO2611/pSFMB1 strain, to check whether the introduction of *mreB* gene restores the phenotype of *mreB* mutants. Interestingly, the *mreB* mutant phenotype was restored to that of wild type for all the cases except vancomycin susceptibility. As mentioned previously, introduction of empty vector, pSF152, in to wild type made the strain susceptible to vancomycin. Therefore it was not possible to complement the *mreB* mutant with pSFMB1. The reason for this is not known. The complementation analysis of *mreB* mutant further confirms that the susceptibility of the mutant spores to heat, SDS and cell wall specific antibiotics is due to the loss of MreB function.

4.11 Summary

Insertion mutagenesis studies of *S. coelicolor rodA, rodA2, sfr, pbp2* and *SCO2606* genes revealed that except for the *rodA* gene all the other genes are dispensable for growth and survival. No apparent macroscopic phenotype of *rodA2, sfr, pbp2*, *SCO2606* and *rodA2/sfr* double mutants were observed on the culture media used for the characterization of the mutants. Fluorescence microscopy of all the mutants also showed no difference in septation, chromosomal condensation or spore dimensions. The spores of *sfr*, *pbp2* and *rodA2/sfr* were susceptible to heat and detergent treatments. The susceptibility of spores of an *sfr* single mutant and *rodA2/sfr* double mutant to heat and detergent are similar suggesting that *rodA2* does not have a detectable role in spore wall assembly. An MIC test for different cell wall specific antibiotics revealed that *sfr*, *pbp2* and *rodA2/sfr* mutants are susceptible to antibiotics that inhibit the late stage of cell wall synthesis. No effect of Sfr overexpression was observed under the conditions applied. Disruption of *mreB* resulted in susceptibility of spores to heat, SDS and cell wall specific antibiotics similar to *sfr* and *pbp2* disruption mutants.

Chapter - 5

Analysis of *ftsW* Mutants of *Streptomyces coelicolor*

5.1 Introduction

The division cell wall *(dcw)* gene cluster is a highly conserved gene cluster among bacteria and as the name of the cluster suggests, the genes within it play a vital role in cell division. The majority of the genes in the cluster are essential for viability in many bacteria. Mutagenesis studies of several important genes of the *S. coelicolor dcw* cluster that include *ftsZ, ftsQ* and *ftsL* have shown that cell division is not essential for viability in *Streptomyces* (Bennett *et al.*, 2007; McCormick *et al.*, 1994; McCormick and Losick, 1996). Out of four SEDS family protein encoding genes in *S. coelicolor* one of the genes, *ftsW,* is a part of the highly conserved *dcw* gene cluster. This chapter describes mutagenesis of the *ftsW* gene and the effects of *ftsW* disruption on *S. coelicolor*. To shed some light on the function of FtsW protein, morphological and cytological studies were performed. Further, to establish the role of FtsW in Z-ring formation in *S. coelicolor*, *in situ* localization studies of FtsZ in an *ftsW* mutant background were carried out.

5.2 Disruption of *ftsW* in *S. coelicolor*

To disrupt the *ftsW* gene in the *S. coelicolor* chromosome, the 4A10.2.H05 cosmid insertion was chosen from the mutated cosmid library generated by *in vitro* transposition. The position of the transposon insertion in the chromosome is at 2239002, which is close to the start of the *ftsW* gene. The same approach as described for the *sfr* disruption mutagenesis was applied to isolate double crossover mutants consistent with *ftsW* gene disruption. The frequency of double crossover ex-conjugants with kanamycin sensitivity and apramycin resistance was 46%. From several double crossover ex-conjugants of *ftsW* mutant six clones were selected randomly for Southern hybridization analysis to confirm the mutation. To perform Southern hybridization, the chromosomes of the six selected clones were purified as described previously. The purified mutant chromosomes and the respective cosmid insertion (control) were digested using *Not*I enzyme to obtain two distinct fragments of 6186 bp and 3396 bp size. Southern blot (SB) of the *ftsW* mutants confirmed that all the six clones were true double crossover mutants (Fig. 5.1). Thus, the *ftsW* mutant strain obtained using 4A10.2.H05 cosmid insertion was designated as DSCO2085-1, where number 1 represents the 4A10.2.H05 insertion for convenience in labelling different *ftsW* mutant strains.

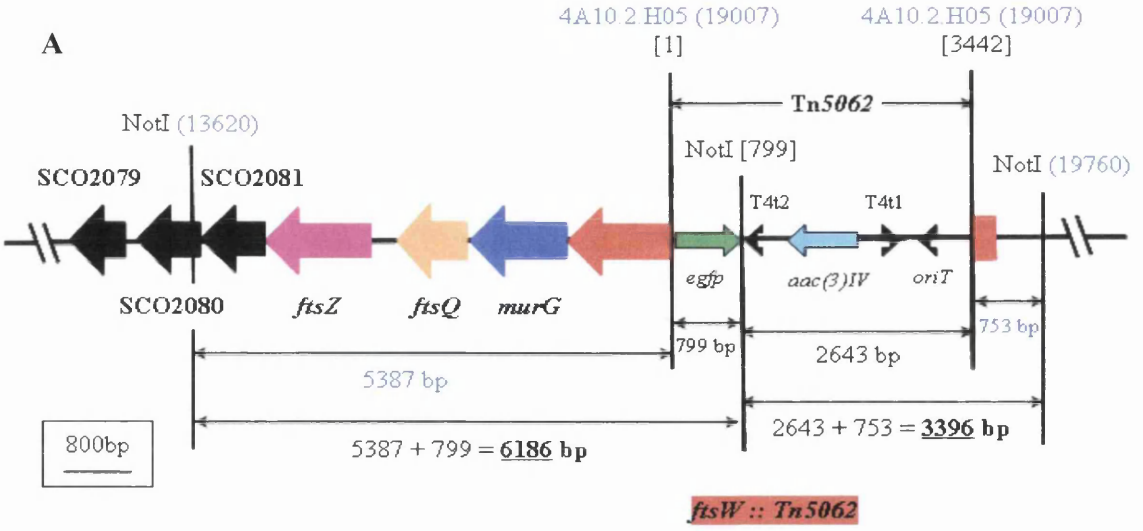

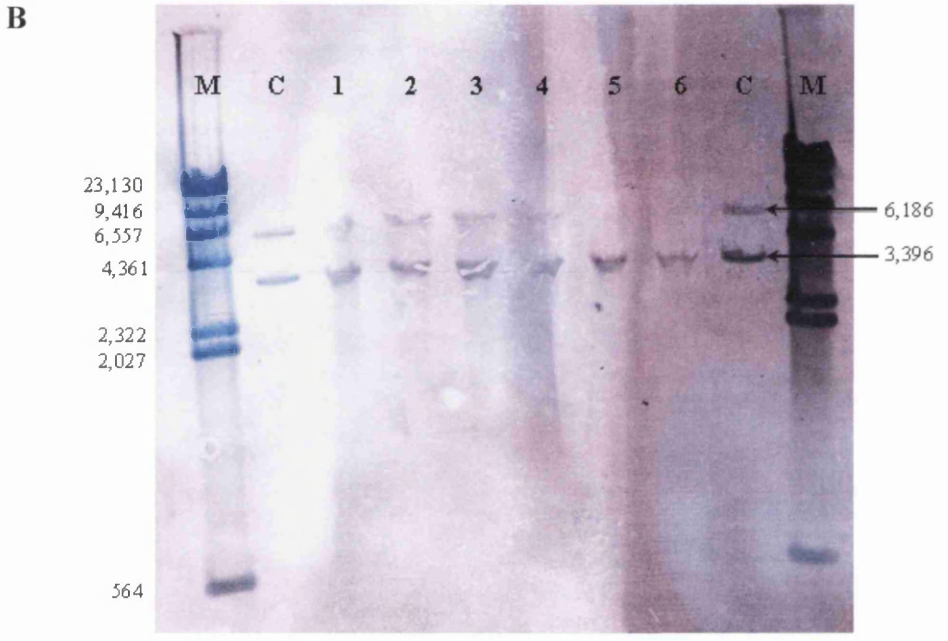

Figure 5.1: Southern Blot (SB) analysis of *ftsW* mutant clones with 4A10.2.H05 insertion. **(A)** Diagrammatic representation of *ftsW* locus showing Tn*5062* insertion and *Not*I restriction sites to calculate the size of bands that should be obtained after Southern hybridization. The cosmid insertion used for *ftsW* mutagenesis is shown in blue colour with the position of insertion in the cosmid presented in brackets. Just under the cosmid name and position, the start and end sites of Tn*5062* are written in square brackets. The position of important *Not*I restriction sites in the *ftsW* region of the cosmid are shown in brackets and in Tn*5062* in square brackets. Arrows with different colours represent different genes and their directions. Name of each respective gene is shown just under each arrow. *aac(3)IV* – Apramycin resistance; T4 t1,2 – Transcription terminator t1 & 2; *egfp* – Enhanced green fluorescent protein gene; *oriT* – Origin of transfer. Expected size of bands that should be obtained in SB is shown in bold letters with underlining. The rectangular box shows the scale of the map. **(B)** SB of six *ftsW* mutant clones. M –*Hin*dIII digested λ DNA marker with the size for each band presented on the left hand side; C – *Not*I digested 4A10.2.H05 cosmid insertion; and 1 to 6 – *Not*I digested chromosome of each *ftsW* mutant clone. The size (in bp) of each expected bands for *ftsW* mutant is shown by arrows. Digoxigenin labelled Tn*5062* was used as a hybridization probe.

Further, to analyze the effect of truncated FtsW protein on cell division and development in *S. coelicolor*, disruption mutants of *S. coelicolor* with truncated FtsW were constructed by using Tn*5062* insertions at different positions within the gene. Figure 5.2A shows the position of different insertions in the chromosome and Figure 5.2B shows the topological prediction of FtsW with the position of insertions where the protein is truncated at different positions due to the respective insertion in the *ftsW* gene.

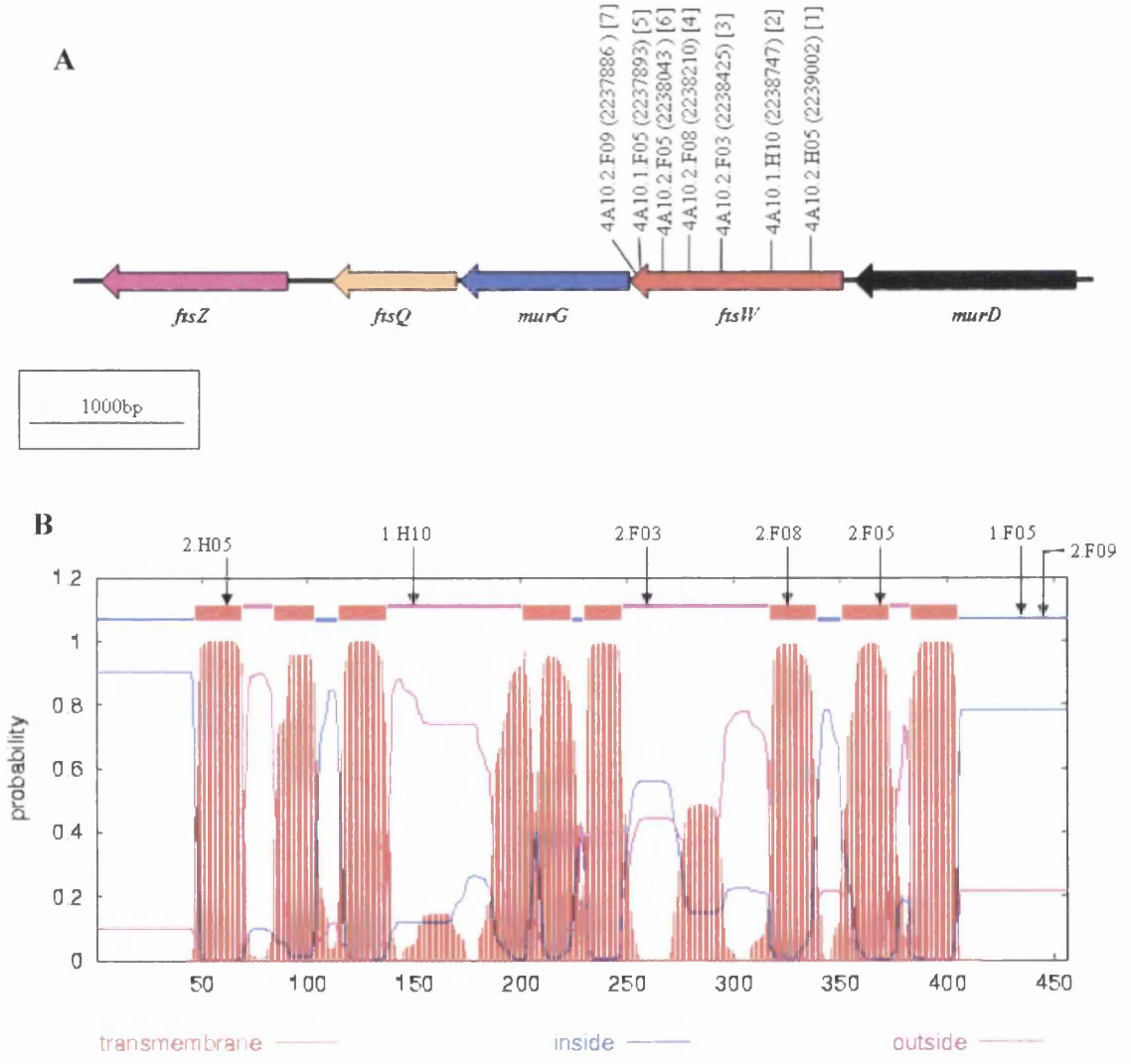

Figure 5.2: (A) Map of *ftsW* gene locus showing the position of different Tn*5062* insertions within the chromosome of *S. coelicolor*. Each insertion has given a number presented in square brackets for convenience. Arrows indicate different genes and their orientation. The scale of the map is shown in the rectangle box. **(B)** Topological prediction of FtsW with hydropathy plot constructed using TMHMM server. Red thick lines are predicted transmembrane domains; pink lines represent extra-cytoplasmic loops; blue lines indicate cytoplasmic loops; Arrows show positions of Tn*5062* insertions that result in different truncated FtsW proteins.

The insertions used to obtain *ftsW* mutants with truncated versions of FtsW were 4A10.1.H10, 4A10.2.F03, 4A10.2.F08, 4A10.1.F05, 4A10.2.F05 and 4A10.2.F09. Each insertion is designated as number 2, 3, 4, 5, 6 and 7, respectively, to distinguish the mutant strains with different insertions. A similar approach of intergeneric conjugal transfer, used for *sfr* mutagenesis, was applied to construct *ftsW* mutants using different Tn*5062* insertions mentioned above. Several double crossover ex-conjugants were obtained for each of the cosmid insertions with the frequency of double crossover recombination ranging from 42% to 75%, except for the 4A10.2.F09 insertion that is located at the very end of *ftsW*. Despite several attempts, no true double crossover mutants were obtained for the 4A10.2.F09 insertion, suggesting that this insertion could affect expression of the downstream gene that may be essential for *S. coelicolor* viability. Immediately downstream to *ftsW* is the *murG* gene which encodes a probable glycosyltransferase enzyme involved in the synthesis and assembly of peptidoglycan. In *E. coli* MurG is essential for viability and catalyzes the transfer of N-acetyl glucosamine (NAG) from UDP to lipid-linked N-acetylmuramoyl pentapeptide (NAM) to form NAG-NAM disaccharide that is transported across the membrane where it is polymerized with growing peptidoglycan (Mengin-Lecreulx *et al.*, 1991; Mohammadi *et al.*, 2007). To check the essentiality of the *murG* gene in *S. coelicolor*, mutagenesis of this gene was carried out using three different insertions 4A10.1.H11 (chromosomal position 2237349), 4A10.2.F10 (2237221) and 4A10.2.D10 (2236951), within the gene. No true double crossover mutants were obtained for any of the insertions after many attempts, suggesting that *murG* could be essential for viability in *S. coelicolor.* The essentiality of *murG* gene needs to be verified by constructing the mutants after introducing an extra copy to the gene.

For Southern hybridization of *ftsW* mutants obtained using 4A10.1.H10, 4A10.2.F03, 4A10.2.F08, 4A10.2.F05 and 4A10.1.F05 insertions, six clones of each insertion mutant were selected. The chromosomes of all the six clones of each insertion were purified and digested using *Sal*I. As a control, insertion cosmids of the respective mutants were also digested with *Sal*I. Digoxigenin labelled Tn*5062* was used as a probe for hybridization for all the mutants except 4A10.2.F05 insertion mutants (Fig. 5.3Ec) where a digoxigenin labelled DNA fragment spanning the *ftsW, murG* and *ftsQ* genes was used. Southern hybridization analysis (Fig. 5.3) confirmed that all the

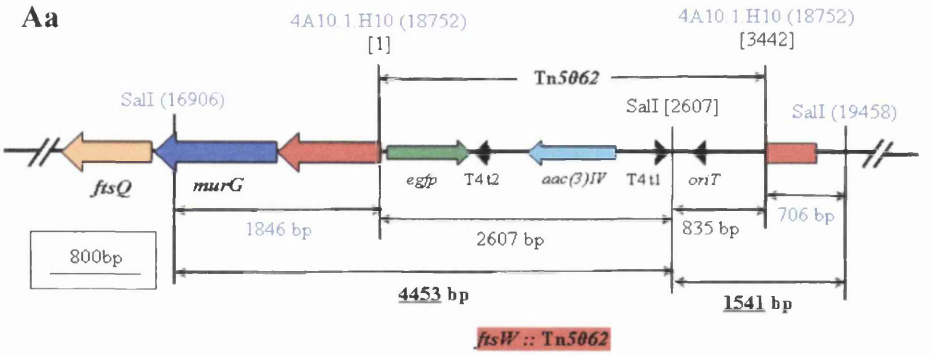

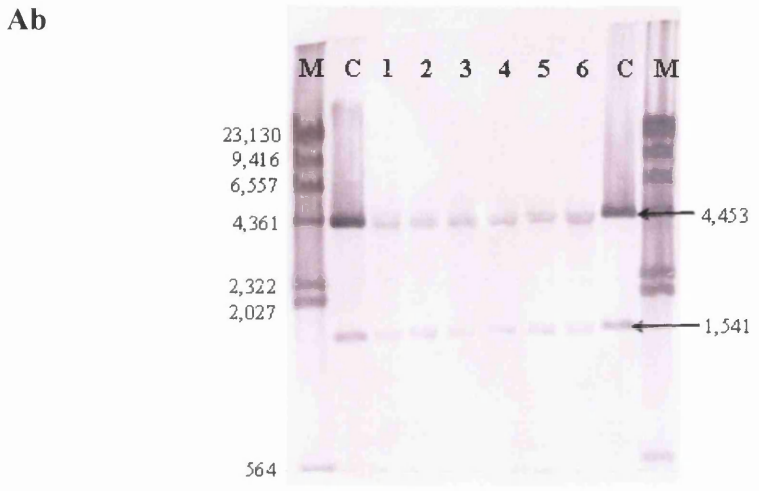

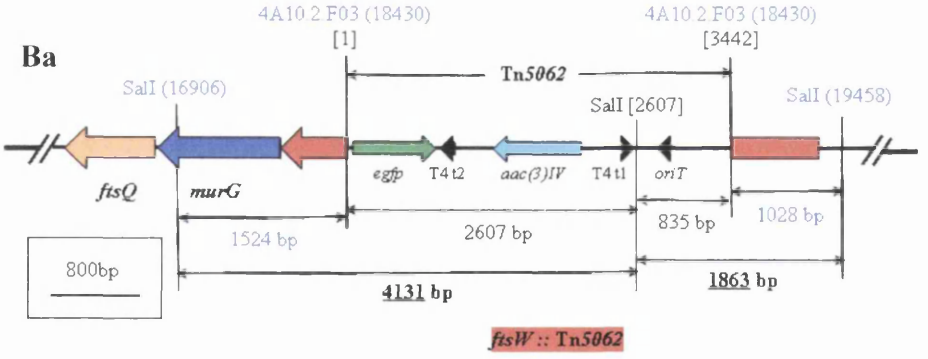

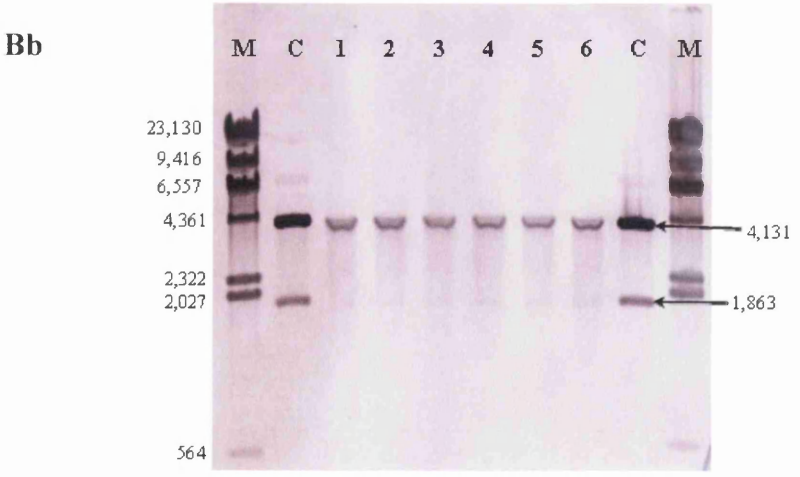

Figure 5.3: Continued on the next page….

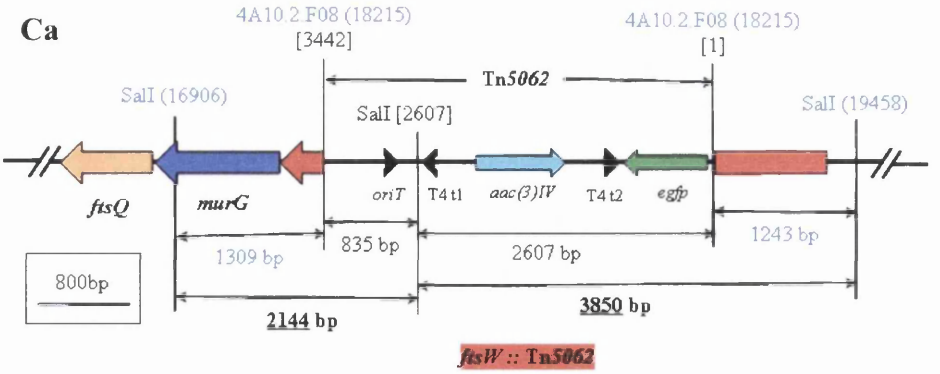

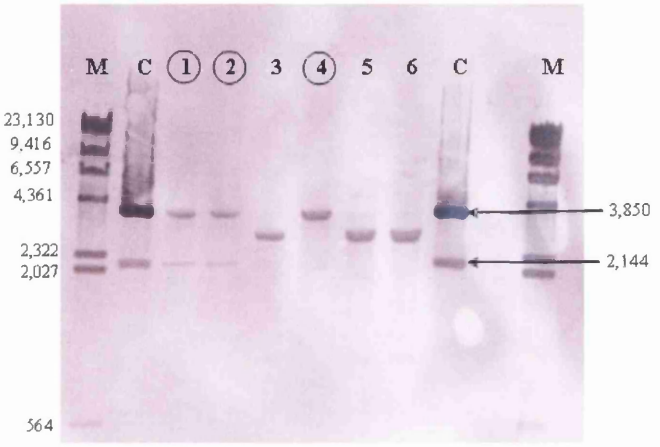

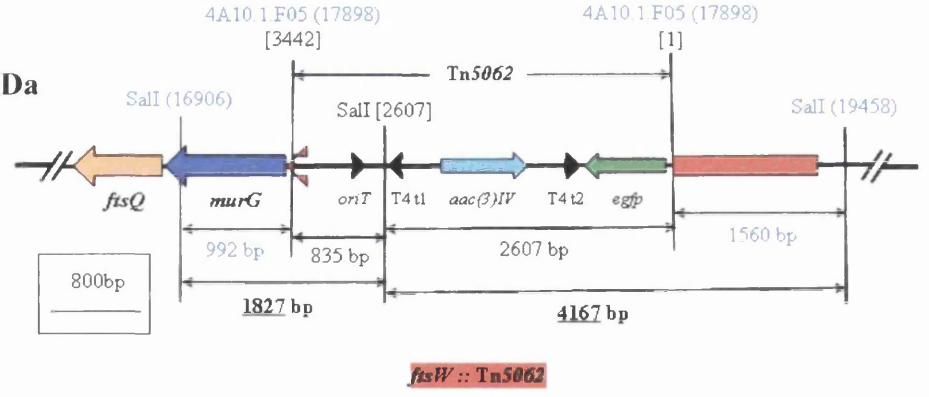

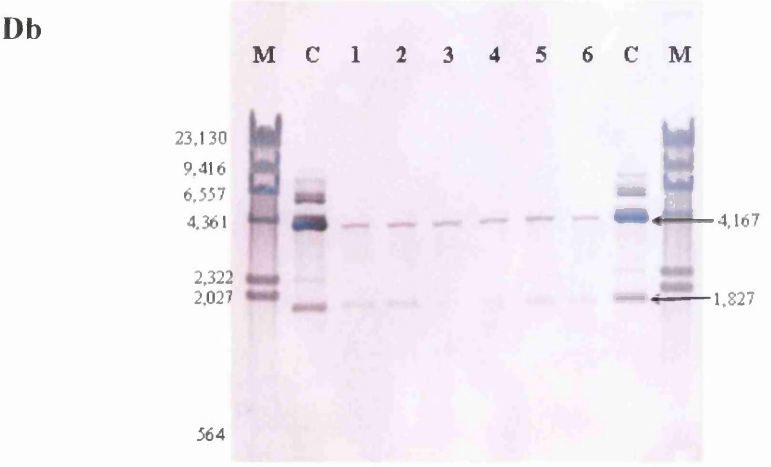

Figure 5.3: Continued on the next page….

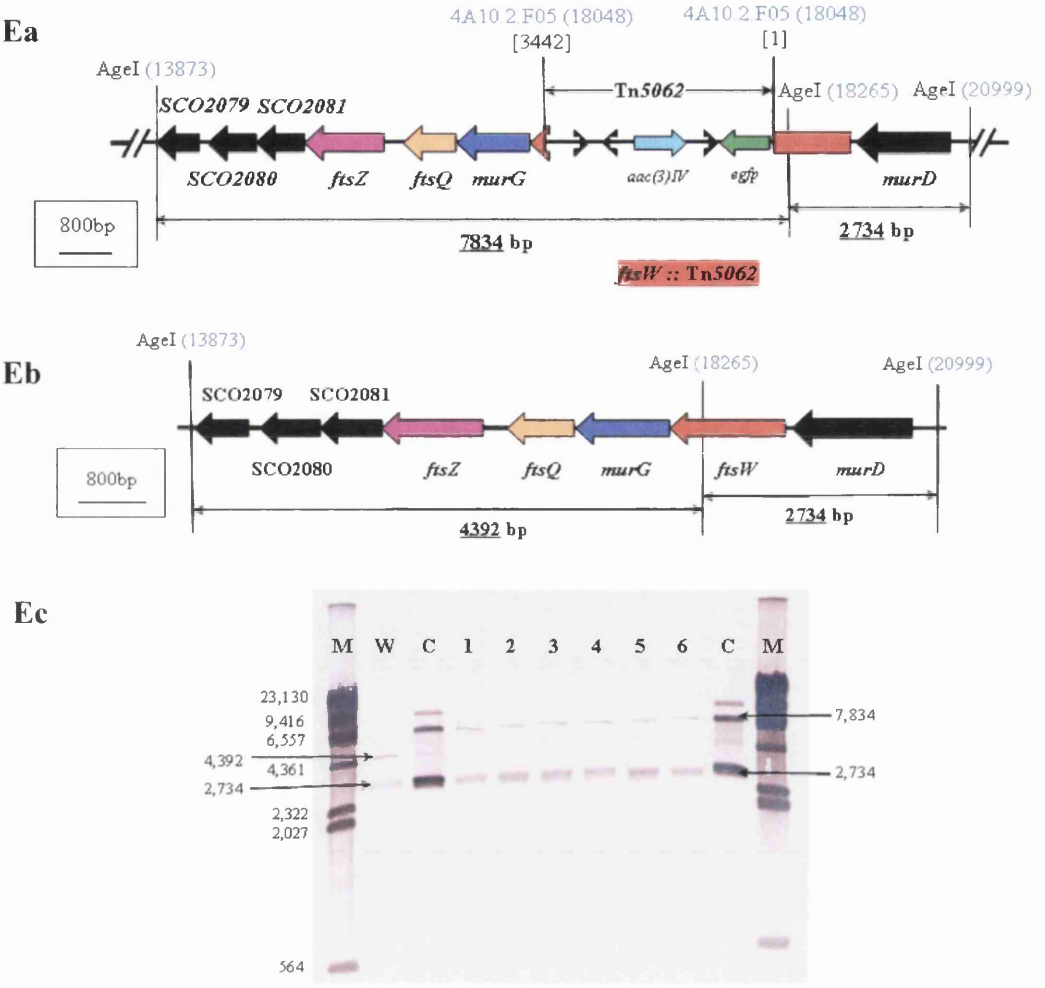

Figure 5.3: Southern Blot (SB) analysis of *ftsW* mutants constructed using 4A10.1.H10 (A), 4A10.2.F03 (B), 4A10.2.F08 (C), 4A10.1.F05 (D) and 4A10.2.F05 (E) insertions. **(Aa-Ea)** Diagrammatic representation of *ftsW* locus showing the position of Tn*5062* insertion and *Sal*I (in the case of Ea, *Age*I) restriction sites on respective cosmids mentioned above to calculate the size of the bands that should be obtained after Southern hybridization. The cosmid insertion used for *ftsW* mutagenesis and the position of Tn*5062* in respective cosmid insertion is shown in blue colour in each map. Just under the cosmid name and position, the start and end sites of Tn*5062* are written in square brackets. The position of the important *Sal*I or *Age*I restriction sites in the *ftsW* region of each cosmid are shown in the brackets and that in Tn*5062* is shown in square brackets. Arrows with different colours represent different genes and their directions. The name of each respective gene is shown just under each arrow. *aac(3)IV* – Apramycin resistance; T4 t1,2 – Transcription terminator t1 & 2; *egfp* – Enhanced green fluorescent protein gene; *oriT* – Origin of transfer. Expected size of bands that should be obtained in SB is shown in bold letters with underlining. The rectangular box shows the scale of the map. **(Eb)** Map of *ftsW, murG* and *ftsQ* gene region of wild type strain without any insertion. **(Ab-Db & Ec)** SB of six *ftsW* mutant clones of each insertion mentioned above. M – *Hin*dIII digested λ DNA marker with the size for each band presented on the left hand side; C – *Sal*I digested cosmid of respective insertion; and 1 to 6 – *Sal*I digested chromosomes of each *ftsW* mutants in each blot. In figure Ec, W is *Age*I digested wild type chromosome, C is *Age*I digested 4A10.2.F05 insertion cosmid and 1 to 6 are *Age*I digested chromosome of *ftsW* mutant with 4A10.2.F05 insertion. In the blot Ec gene specific probe was used. The size in bp of each expected bands for each *ftsW* mutant is shown by arrow. Digoxigenin labelled Tn*5062* was used as a hybridization probe for all the blots except E_C.

six clones of each insertion mention above are true mutants except 4A10.2.F08 (Fig. 5.3Cb) insertion mutants where only three clones out of six were true mutants. Thus, the mutants obtained using 4A10.1.H10, 4A10.2.F03, 4A10.2.F08, 4A10.1.F05 and 4A10.2.F05 insertions were designated as DSCO2085-2, DSCO2085-3, DSCO2085-4, DSCO2085-5 and DSCO2085-6, respectively.

5.3 Phenotypic characterization of *ftsW* mutants

To visually assess the sporulation of the *ftsW* mutant, the DSCO2085-1 strain containing disrupted *ftsW* was plated on the most commonly used sporulation specific soya flour mannitol (SFM) agar medium along with the parental strain M145. The plate was incubated at 30°C for 3 days. Sporulation of the wild type strain growing on SFM medium is easily distinguished, as it produces grey pigmented spores during development. Interestingly, the *ftsW* mutant DSCO2085-1 showed a typical white phenotype (Fig. 5.4) on the SFM medium, indicating a defect in differentiation of aerial hyphae into spores. The colony size of *ftsW* mutants growing on SFM medium was very similar to that of wild type. When the *ftsW* mutant was plated on R5 medium specifically to assess the production of the blue antibiotic actinorhodin, both wild type and mutant showed a substantial amount of actinorhodin production (Fig. 5.3). It was shown that the colonies of *ftsZ* and *ftsQ* mutants grown on minimal medium were smaller and produced copious amounts of actinorhodin (McCormick *et al.*, 1994; McCormick and Losick, 1996). Although *ftsW* is located very close to both *ftsZ* and *ftsQ* genes in the *dcw* gene cluster no such phenotype was observed for *ftsW* mutants grown on minimal medium after four days of incubation (Fig. 5.3). The *ftsW* mutant grown on NMMP medium containing either mannitol or sucrose showed no significant difference in the macroscopic phenotype (Fig. 5.3). However the *ftsW* mutants on these media were lighter grey than wild type. The antibiotic production phenotype of the DSCO2085-1 strain was media-dependent and the mutant was delayed in antibiotic production when grown on 2×YT medium (Fig. 5.3).

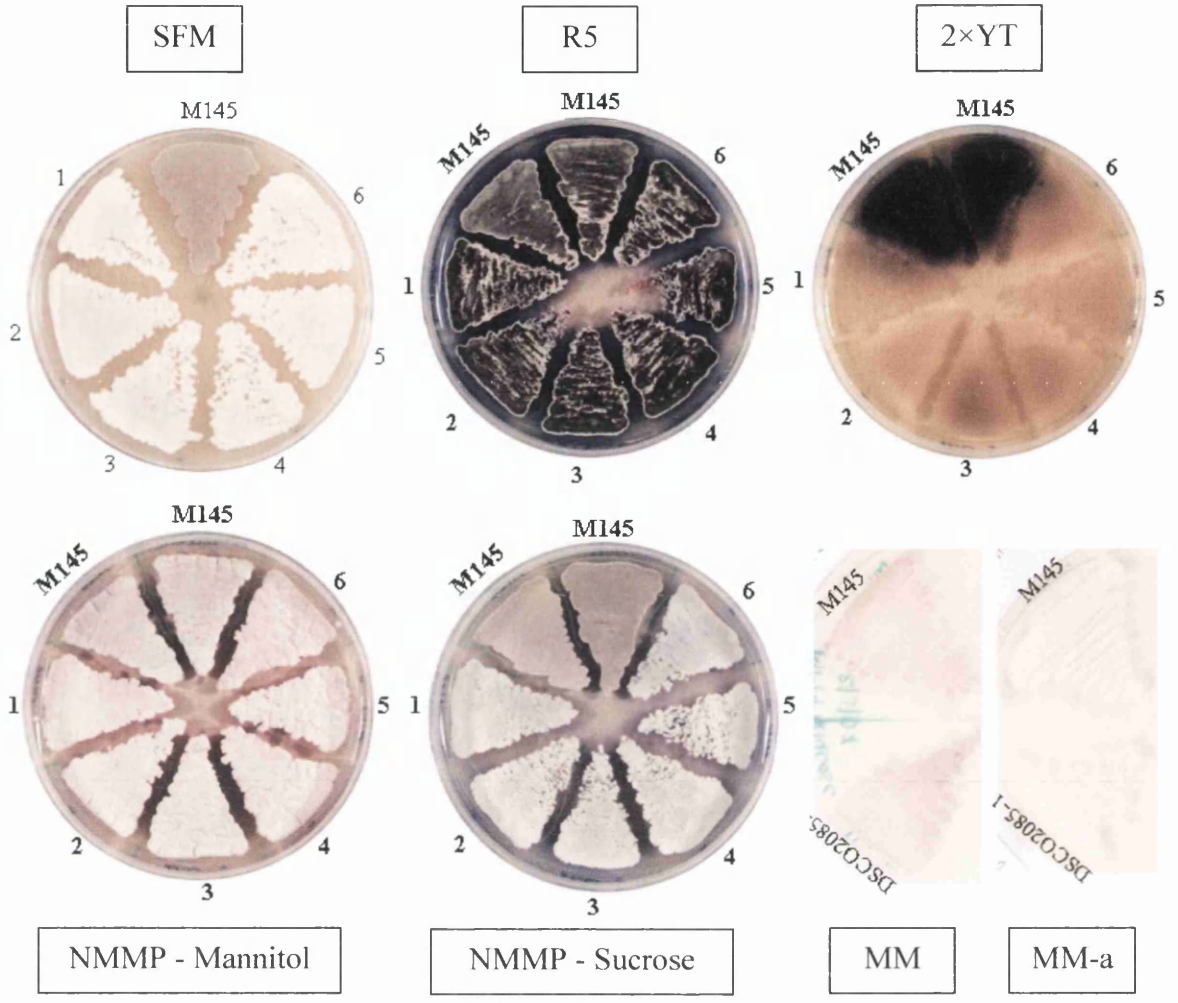

Figure 5.3: Phenotype of the *ftsW* mutant (DSCO2085-1 strain) and its congenic parental strain *S. coelicolor* M145 on different media. Strains were grown for 3 days (4 days for cultures grown on minimal medium) at 30° C on SFM, R5, NMMP-Mannitol, NMMP-Sucrose, 2×YT, Minimal Medium containing ammonium sulphate (MM) and Minimal medium containing L-asparagine (MM-a) agar media. In minimal medium, glucose was used as a carbon source. The *ftsW* mutant clones are indicated by numbers 1-6 in each plate picture. The name of the respective medium is presented in rectangular boxes.

Since the non-sporulating phenotype of DSCO2805-1 was more apparent and clear on SFM medium, all the other *ftsW* mutants constructed using different insertions (4A10.1.H10, 4A10.2.F03, 4A10.2.F08, 4A10.2.F05 and 4A10.1.F05), to study the effect of truncated FtsW in *S. coelicolor,* were characterized on SFM medium. All the

ftsW mutants grown on SFM medium showed a similar non-sporulating white phenotype (Fig. 5.4), except the mutant with 4A10.1.F05 insertion (DSCO2085-5) where most of the FtsW is intact with all the transmembrane domains. The 4A10.1.F05 insertion mutant was sporulating normally, producing grey pigmented spores similar to wild type (Fig. 5.4). The truncated FtsW of the DSCO2085-5 mutant lacks the last 18 amino acids of the predicted C-terminal cytoplasmic tail and ends with an 11 amino acid sequence encoded by one end of Tn*5062*, TVSYTHLNHHR that does not align with the

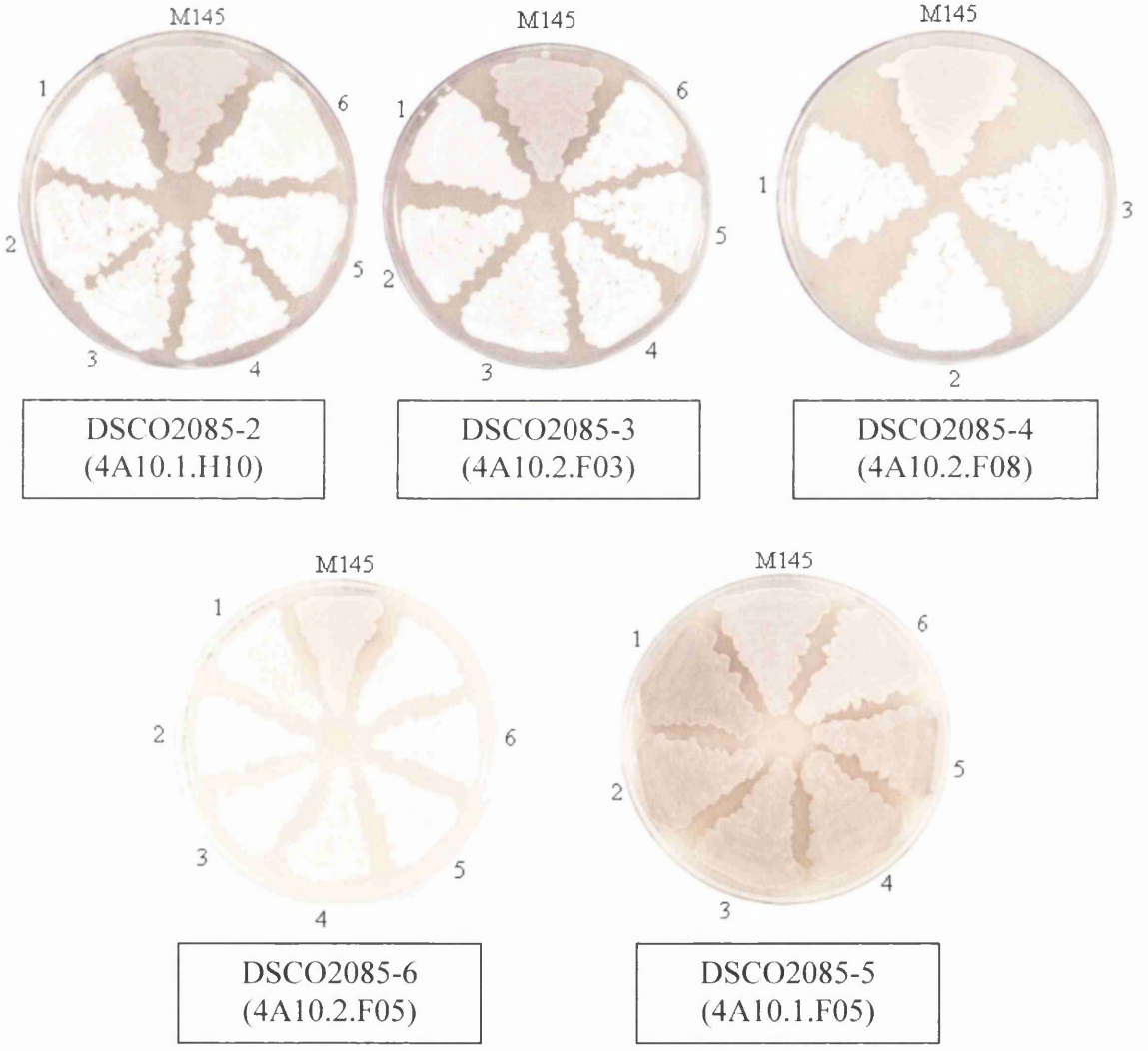

Figure 5.4: Phenotype of SFM grown *ftsW* mutants constructed using different insertions and their congenic parental strain *S. coelicolor* M145. Strains were grown for 3 days at 30° C. The *ftsW* mutant clones of each insertion are indicated by numbers in each plate picture. The name of the *ftsW* mutant strain and the insertion used to construct respective mutant is shown the respective in rectangular box.

native C-terminal sequence (Fig. 5.5). The wild type phenotype of DSCO2085-5 suggests that FtsW truncated at the C-terminal end is functional without having a major effect on phenotype. It also suggests that the white phenotype of the upstream insertion mutants is due to *ftsW* disruption and all the transmembrane domains are necessary for the function of FtsW.

```
FtsW_Sc    1 ------MPGSPQSRTGRPPVQRTVKRP-AAPGPPHDNGVLRLYHRLRRAW
FtsW_Mt    1 MLTRLLRRGTSDTDGSQTRGAEPVEGQRTGPEEASNPGSARPRTRFGAWL
                    *:.::  .:.   ..*    :.*  . : *  *   *:

FtsW_Sc   44 DRPLTAYYLIFGGSALITVLGLVMVYSASQITALQLSLPGSYFFRKQALA
FtsW_Mt   51 GRPMTSFHLIIAVAALLTTLGLIMVLSASAVRSYDDDGSAWVIFGKQVLW
             .**:*:::**:. :**:*.***:** *** : : : . ..  :* **.*

FtsW_Sc   94 ALIGAGLLVAAMKMPVKLHRALAYPILAGAVFLMILVQVPGIGVAVNGNQ
FtsW_Mt  101 TLVGLIGGYVCLRMSVRFMRRIAFSGFAITIVMLVLVLVPGIGKEANGSR
             :*:*     ..::*.*:: * :*:. :* ::.:::** *****  .**.:

FtsW_Sc  144 NWISLGGSFQIQPSEFGKLALVLWGADLLARKHDKKLLTQWKHMLVPLVP
FtsW_Mt  151 GWFVVAG-FSMQPSELAKMAFAIWGAHLLAARRMER--ASLREMLIPLVP
             .*: :.* *.:****:.*:*:.:***.*** :: ::  :. :.**:****

FtsW_Sc  194 AAFMLLGLIMIGGDMGTAIILTAILFGLLWLAGAPTRLFAGVLSIALLLG
FtsW_Mt  198 AAVVALALIVAQPDLGQTVSMGIILLGLLWYAGLPLRVFLSSLAAVVVSA
             **.: *.**:   *:* :: :  **:**** ** * *:* . *: .:: .

FtsW_Sc  244 FILIKTSANRMARLNCLGATDPGPGDSCWQAVHGIYALASGGLFGSGLGA
FtsW_Mt  248 AILAVSAGYRSDRVRSWLNPENDPQDSGYQARQAKFALAQGGIFGDGLGQ
              **  ::. *  *:..   .: .* ** :** :. :***.**:**.***

FtsW_Sc  294 SVEKWGQLPEAHTDFIFAVTGEELGLAGTLSVLALFAALGYAGIRVAGRT
FtsW_Mt  298 GVAKWNYLPNAHNDFIFAIIGEELGLVGALGLLGLFGLFAYTGMRIASRS
             .* **. **:**.*****: ******.*:*.:*.**. :.*:*:*:*.*:

FtsW_Sc  344 EDPFVRYAAGGVTTWITAQAVINIGAVLGLLPIAGVPLPLFSYGGSALLP
FtsW_Mt  348 ADPFLRLLTATTTLWVLGQAFINIGYVIGLLPVTGLQLPLISAGGTSTAA
              ***:*  :. .* *: .**.**** *:****::*: ***:* **::  .

FtsW_Sc  394 TMFAIGLLIAFARDEPGARAAL----------------------------
FtsW_Mt  398 TLSLIGIIANAARHEPEAVAALRAGRDDKVNRLLRLPLPEPYLPPRLEAF
             *:  **::   **.** * ***
                                                  [TVSYTHL--NHH
FtsW_Sc  416 ----------ALRQPRFGRKRGAGGPAAKRS-----PGSWNTMRR--RAS
FtsW_Mt  448 RDRKRANPQPAQTQPARKTPRTAPGQPARQMGLPPRPGSPRTADPPVRRS
                    *  **     * * * .*::      *** .*     * *
             R]
FtsW_Sc  449 AARSSGER-------------------
FtsW_Mt  498 VHHGAGQRYAGQRRTRRVRALEGQRYG
             . :.:*:*
```

Figure 5.5: Amino acid alignment between FtsW$_{Sc}$ and FtsW$_{Mt}$. An asterisk below the alignment indicates an identical amino acid at that position, a colon indicates a position of a conserved substitution, and a dot indicates a semiconserved substitution. The positions of the two conserved proline residues implicated as being important for interactions between FtsW*Mt* and FtsI*Mt* are boxed. The C-terminal amino acid sequence of the truncated FtsW of DSCO2085-5 is indicated in square brackets above the polypeptide sequence replaced in this mutant.

5.4 Microscopic analysis of *ftsW* mutants

To examine the cytological effects of the mutations of *ftsW*, fluorescence microscopy was carried out. For visualization of septa in the substrate mycelium fluorescent-labelled vancomycin (FL vancomycin) was used. The formation of septa and segregation of chromosomes in aerial hyphae of the *ftsW* mutants was examined after staining cell walls with Fluo-WGA and DNA with propidium iodide (PI). To prepare the substrate mycelium samples, cultures of *ftsW* mutants were inoculated on 2×YT medium at the acute angle formed between an inserted coverslip and the surface of the medium. After cultivating the cultures for 48 hours at 30° C, the samples were stained with FL vancomycin as described previously in Chapter 2. For controls, samples of the wild type strain were also prepared in a similar way. Microscopic observation of the wild type and mutant strains showed that the pattern of *de novo* cell wall synthesis at the vegetative septa was similar in the *ftsW* mutants and wild-type (Fig. 5.6). Phase contrast and fluorescence images of vegetative mycelium of the *ftsW* mutant shown in Figure 5.6 are from the DSCO2085-1 strain. Although not shown, other insertion mutants also showed a similar pattern of cross wall formation. To check that complete crosswalls were formed in the *ftsW* mutant, samples of *ftsW* mutants and wild type strains were sent to Kim Findlay, John Innes Centre, Norwich, for transmission electron microscopy (TEM). Scrutiny of TEM images revealed that complete crosswalls similar to wild type were formed in *ftsW* mutants.

Samples for fluorescence microscopy of aerial hyphae were prepared by taking impressions of wild type and *ftsW* mutants grown on the surface of SFM agar medium for 38 h and 96h, at 30° C. As described in the previous chapter, regularly spaced sporulation septa were observed in aerial hyphae of the wild type as a ladder-like pattern of green Fluo-WGA fluorescence that define pre-spore compartments each containing a single condensed nucleoid stained with red fluorescence dye (Fig. 5.7A). In contrast, the aerial hyphae of all the different *ftsW* insertion mutants that showed a typical non-sporulating white phenotype remained unseptated like an elongated continuous tube with no apparent chromosome condensation, even after prolonged incubation (Fig. 5.7B). Some of these hyphae exhibited coiling.

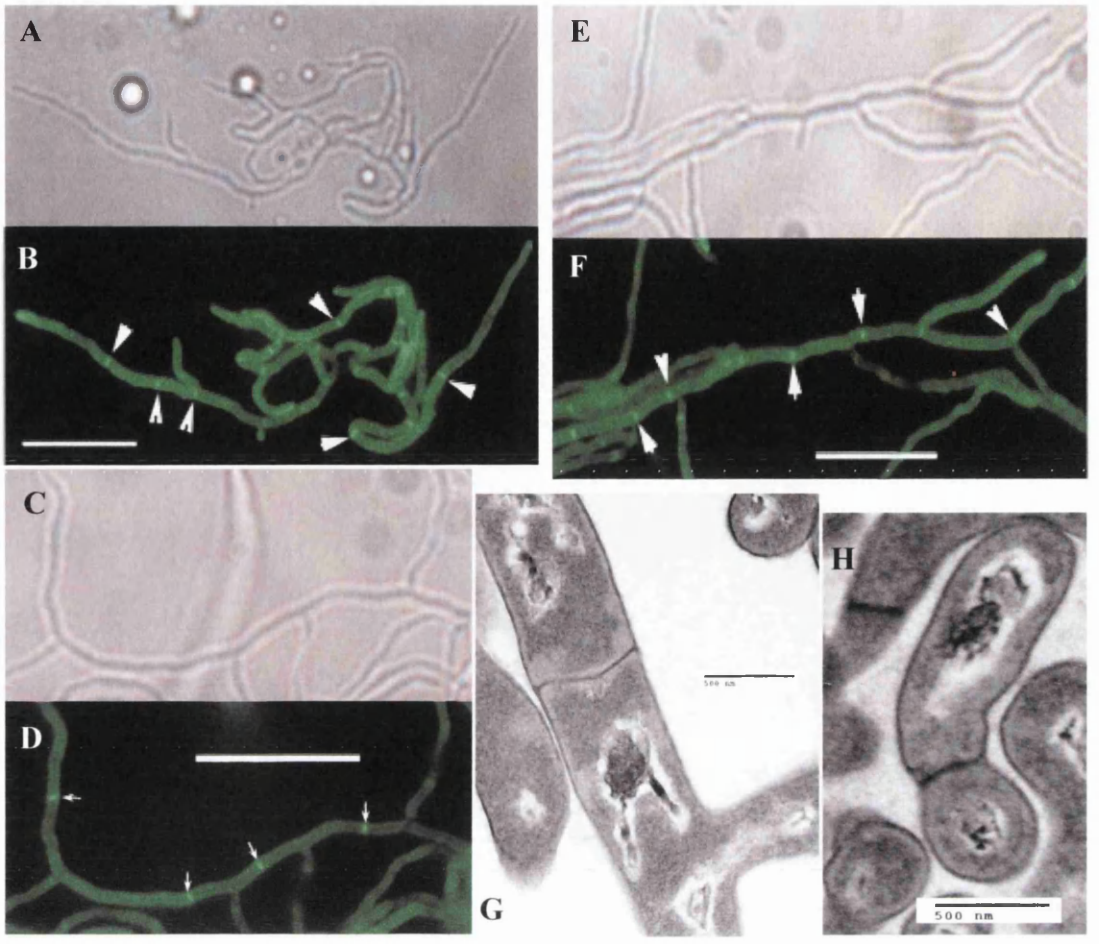

Figure 5.6: Complete vegetative cross-wall formation in wild type and *ftsW* mutants. Substrate mycelium from 48h grown culture of wild type and mutant strains stained with FL-vancomycin to reveal septa. Phase contrast and fluorescence microscopy (A and B) of wild type M145; (C and D) of DSCO2085-5; (E and F) of DSCO2085-1. Transmission electron microscopy of substrate hyphae of wild type (G) and DSCO2085-1 (H) to reveal complete cross walls. Scale bar = 10 μm for panels A-F. Scale bar = 500 nm for panels G and H

On the other hand, fluorescence microscopy of the DSCO2085-5 strain with the 4A10.1.F05 insertion revealed a phenotype similar to that of the wild type, with regularly spaced septa that form pre-spore compartments each containing a single condensed nucleoid (Fig. 5.7 C). The dimensions of pre-spore compartments of DSCO2085-5 were measured as mentioned earlier. The lengths of 200 pre-spore compartments measured were ranging from 0.6 to 1.6 μm, with the majority of compartments between 0.9 to 1 μm long in size (Fig. 5.8). The average length of the pre-spore compartments of DSCO2085-5 was 1 ± 0.16 μm which is not significantly lower than the average length of wild type pre-spore compartment that is 1.2 ± 0.15 μm.

The width of the pre-spore compartments was almost similar to that of wild type with the average width of around 0.8 ± 0.09 μm.

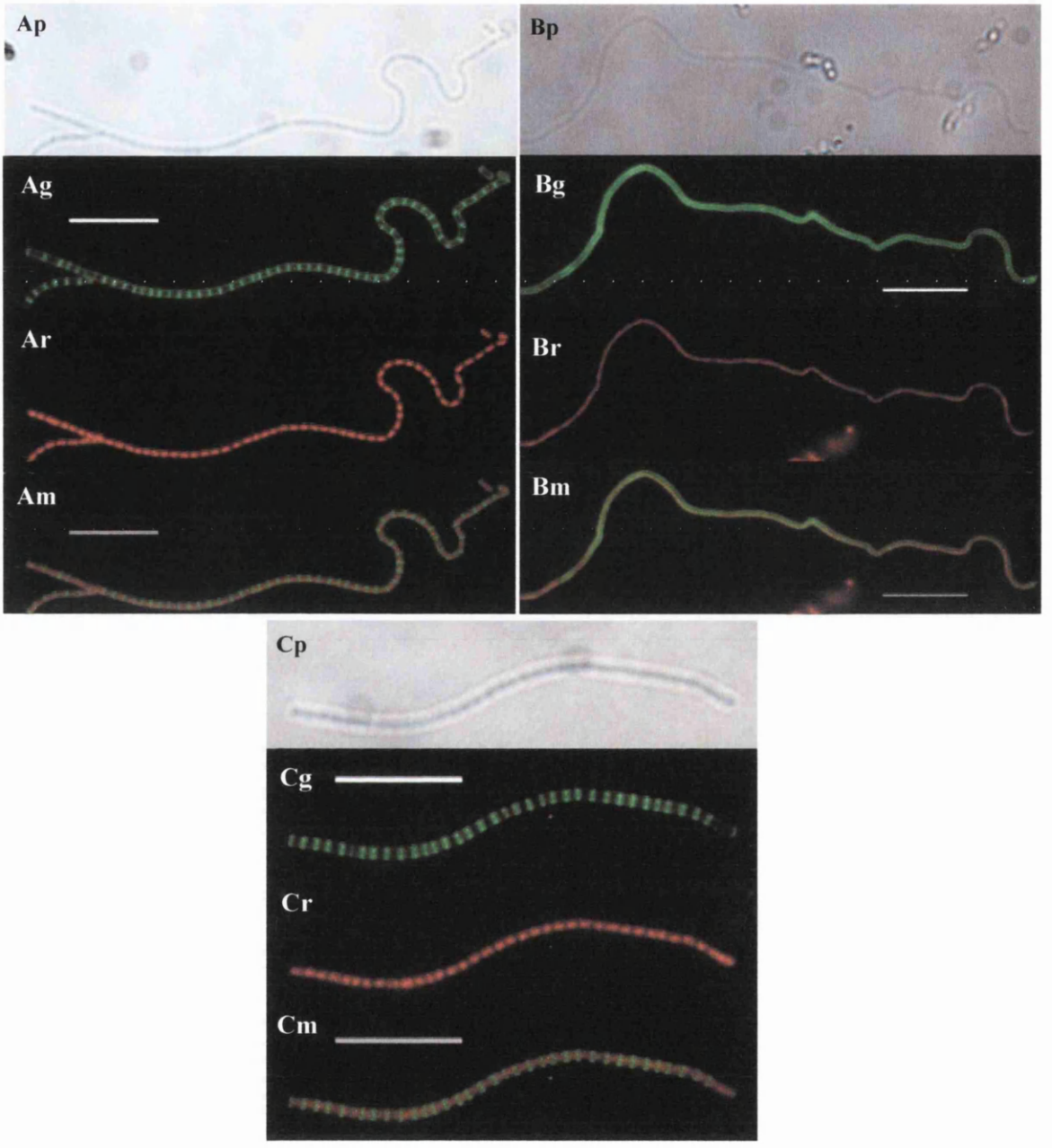

Figure 5.7: Fluorescence microscopy of aerial hyphae of parental strain *S. coelicolor* M145, DSCO2085-1 and DSCO2085-5 mutants using Fluo-WAG (for cell wall) and PI (chromosomal DNA) staining to visualize sporulation septa and chromosome condensation. Samples were prepared by taking the impression of each culture grown on the surface of SFM agar medium for 38 to 40h for M145 and DSCO2085-5 strains, whereas for DSCO2085-1 96h at 30° C. Panel A - *S. coelicolor* M145 sporulation stage, Panel B- DSCO2085-1; Panel C- DSCO2085-5; Each panel shows phase contrast (p), Fluo-WGA staining (g), PI staining (r) and merged (m) images of Fluo-WGA and PI staining of aerial hyphae of respective strains. (Scale bar 10 μm)

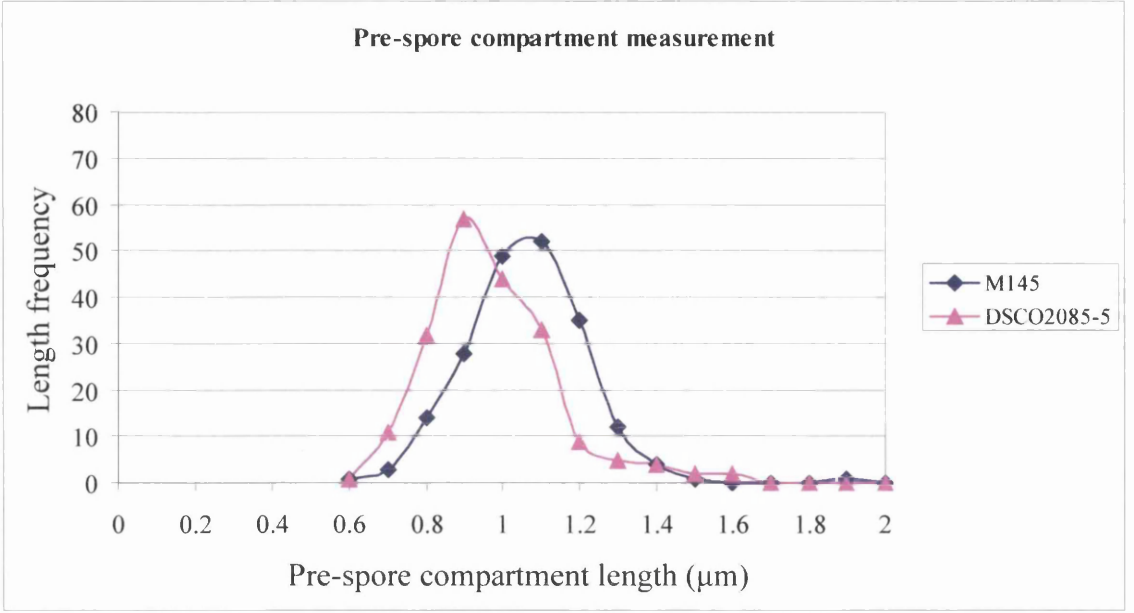

Figure 5.8: Graph of pre-spore compartment length versus frequency of the length of pre-spore compartment in wild type and DSCO2085-5 mutant. The length of randomly selected 200 pre-spore compartments of each strain was measured from the Fluo-WGA stained images using Scion Image software.

As mentioned earlier, the surface of spore bearing aerial hyphae of wild type *S. coelicolor* is covered with a fibrous layer of hydrophobic proteins, chaplins and rodlins, which modifies constantly as the aerial hyphae metamorphose into spore chains. The formation of sporulation septa results in the localized temporary disruption of the fibrous layer at the sites of cell division (Del Sol *et al.*, 2007) (Fig. 5.9 A). As the disruption of *ftsW* resulted in the block of sporulation septation, the effect of this block on the surface layer of *ftsW* mutants was analyzed by atomic force microscopy (AFM). The wild type and mutants were grown on SFM medium at 30° C for four days. Impressions of the samples were taken and the AFM images were obtained using tapping mode. A normal layer of chaplins and rodlins, similar to wild type was observed on the surface of *ftsW* mutant aerial hyphae. However, unlike wild type where the layer was disrupted at the site of sporulation septation, in the *ftsW* mutant the surface layer of aerial hyphae was continuous (Fig. 5.9 B).

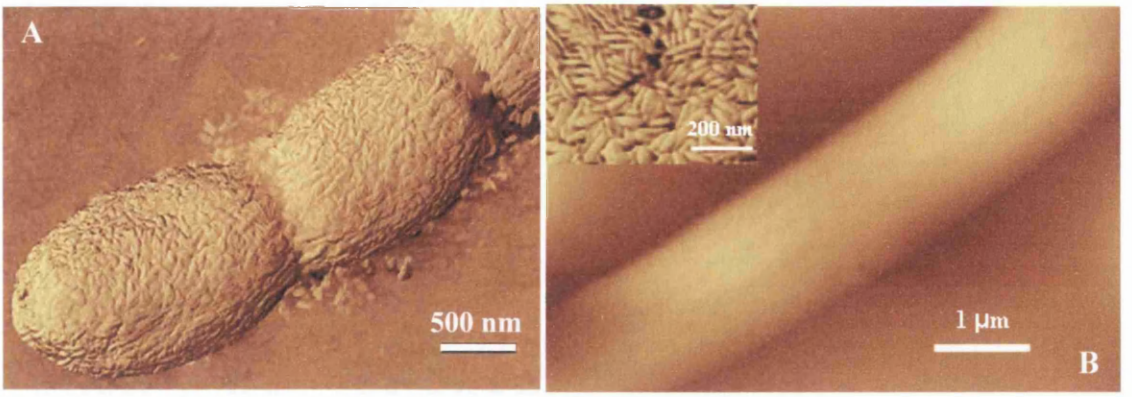

Figure 5.9: Atomic force microscopy of wild type strain M145 (A) and *ftsW* mutant strain DSCO2085-1 (B) revealing external features of the hyphae. The 'height' images obtained using tapping mode revealed indented hyphae of septating wild-type hyphae (A) and smooth hyphae of non-septating *ftsW* mutant (B). Inset image in panel B is a phase image revealing fibrous layer of chaplins and rodlins in *ftsW* mutant. Cultures were grown on SFM medium at 30° C for four days.

5.5 Analysis of FtsZ-EGFP distribution in *ftsW* mutants

So far phenotypic and microscopic analysis showed that a typical *ftsW* mutant lacks sporulation septa. Therefore to attempt to define the earliest stage in septation where the *ftsW* mutant is blocked, an EGFP (enhanced green fluorescence protein)-tagged FtsZ (FtsZ-EGFP) was expressed in different *ftsW* mutants and its distribution was compared to that in wild type. For the expression of FtsZ-EGFP, the recombinant plasmid, pKF41 (Grantcharova *et al.*, 2005) containing *ftsZ* translationally fused with *egfp* was introduced into wild type and *ftsW* mutant strain by intergeneric conjugation. Thus, the ex-conjugants obtained by conjugation were screened for thiostrepton resistance to obtain strains of wild type and mutants that contained pKF41. The wild type strain containing pKF41 plasmid was designated as M145/pKF41 and those of mutants were designated as DSCO2085-1/pKF41 and DSCO2085-5/pKF41. To analyze the distribution of FtsZ-EGFP in wild type and mutants, fluorescence microscopy was performed. For the analysis of vegetative mycelium, cultures of wild type and mutants were grown for 36-48h at 30° C on either SFM or 2×YT agar medium with coverslips inserted at an acute angle. The samples were then directly visualized under the

microscope. The fluorescence microscopy showed irregularly distributed FtsZ ring-like structures similar to the pattern of vegetative cross wall formation in both wild type and mutants (Fig. 5.10). This suggests that the early stage of Z-ring formation necessary for the cell division to occur is not affected in substrate mycelium.

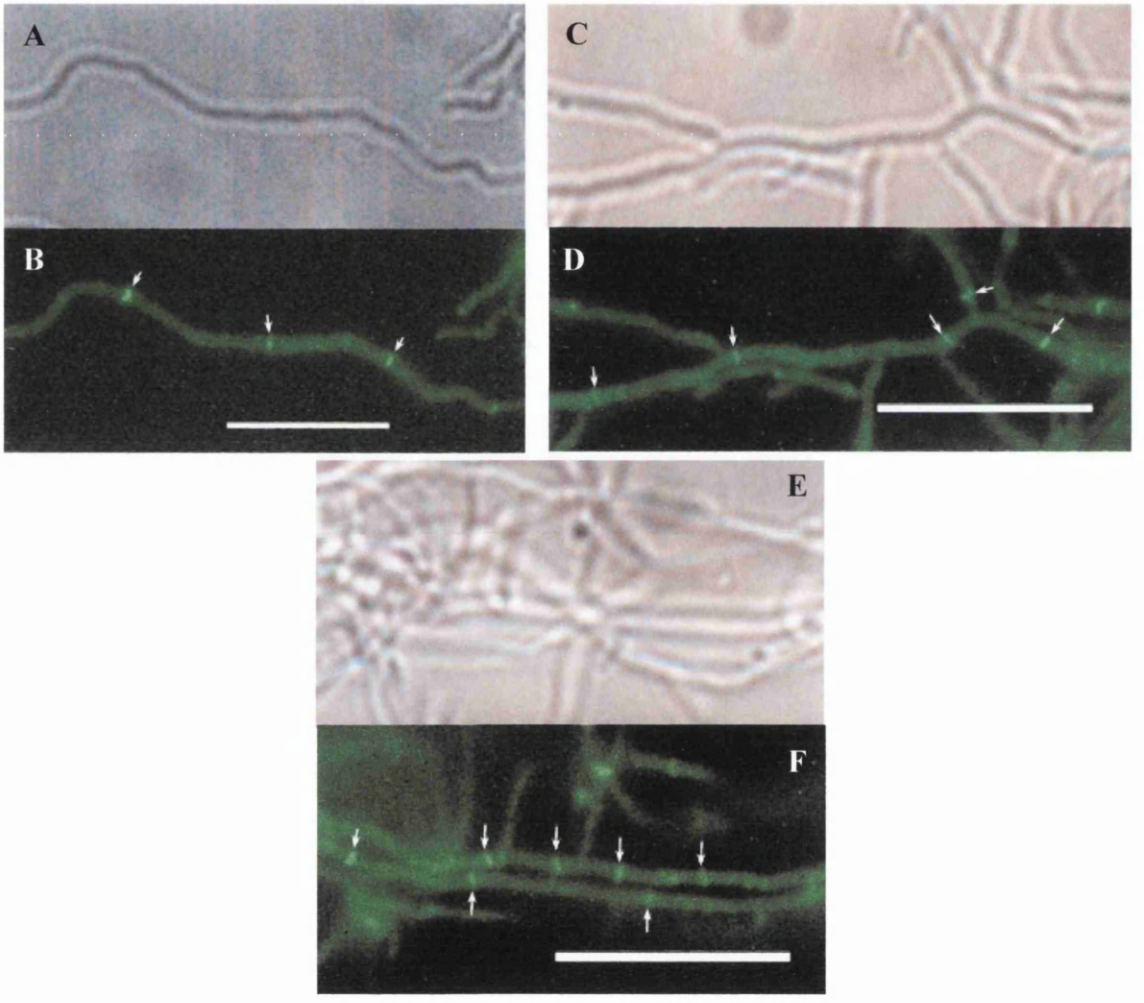

Figure 5.10: Expression of FtsZ-EGFP to observe distribution of FtsZ protein in vegetative mycelium of wild type and *ftsW* mutants. Substrate mycelium from 48h grown culture of wild type and mutants grown on SFM or 2×YT agar medium were observed by fluorescence microscopy. Phase contrast and fluorescence microscopy (A and B) of wild type M145; (C and D) of DSCO2085-1; (E and F) of DSCO2085-5 showing FtsZ rings. Some of the FtsZ rings are indicated by white arrows. Scale bar = 10 μm.

To observe the distribution of FtsZ-EGFP in the aerial hyphae of wild type and *ftsW* mutants, the cultures were grown on SFM medium at 30° C for 38 to 40 hours (M145 and DSCO2085-5 strains) and for 72h and up to 96h (DSCO2085-1). Impressions of each culture were taken and observed directly under the microscope. In the wild type aerial hyphae, a typical progression was observed with aerial hyphae sampled from earlier time points containing diffuse fluorescence typical of non-assembled FtsZ-EGFP (Fig. 5.11 A-B). As the hyphae mature occasional spiral like structures of FtsZ-EGFP were observed (Fig. 5.11 C-D). The older samples at around 38 to 40h of growth showed either spirals or multiple regularly spaced Z-rings (Fig. 5.11 E-F), or having progressed through cell division. Similar Z-ring dynamics were observed in the aerial hyphae of the DSCO2085-5 strain (Fig. 5.11 J-K). In contrast, the aerial hyphae of the DSCO2085-1 mutant examined over an extended period up to 96h showed only diffuse fluorescence or FtsZ-EGFP spirals, but no Z-rings were observed (Fig. 5.11 G-I). This data suggests that FtsW may directly or indirectly functions as a membrane anchor to stabilise FtsZ rings in aerial hyphae. Although not shown, the distribution of FtsZ-EGFP in other non-sporulating *ftsW* mutants was similar to that of the DSCO2085-1 strain.

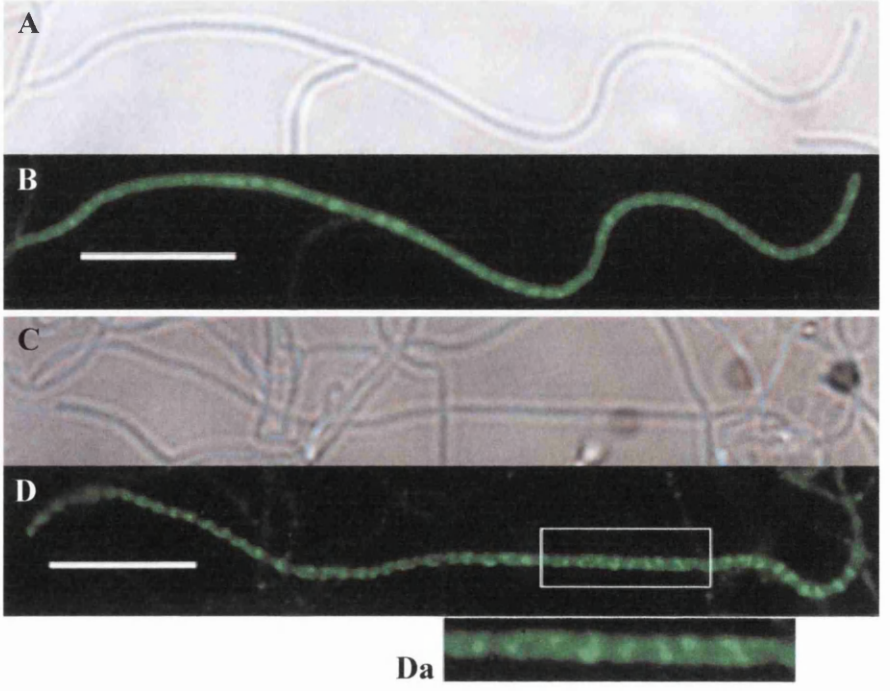

Figure 5.11: Continued on the next page....

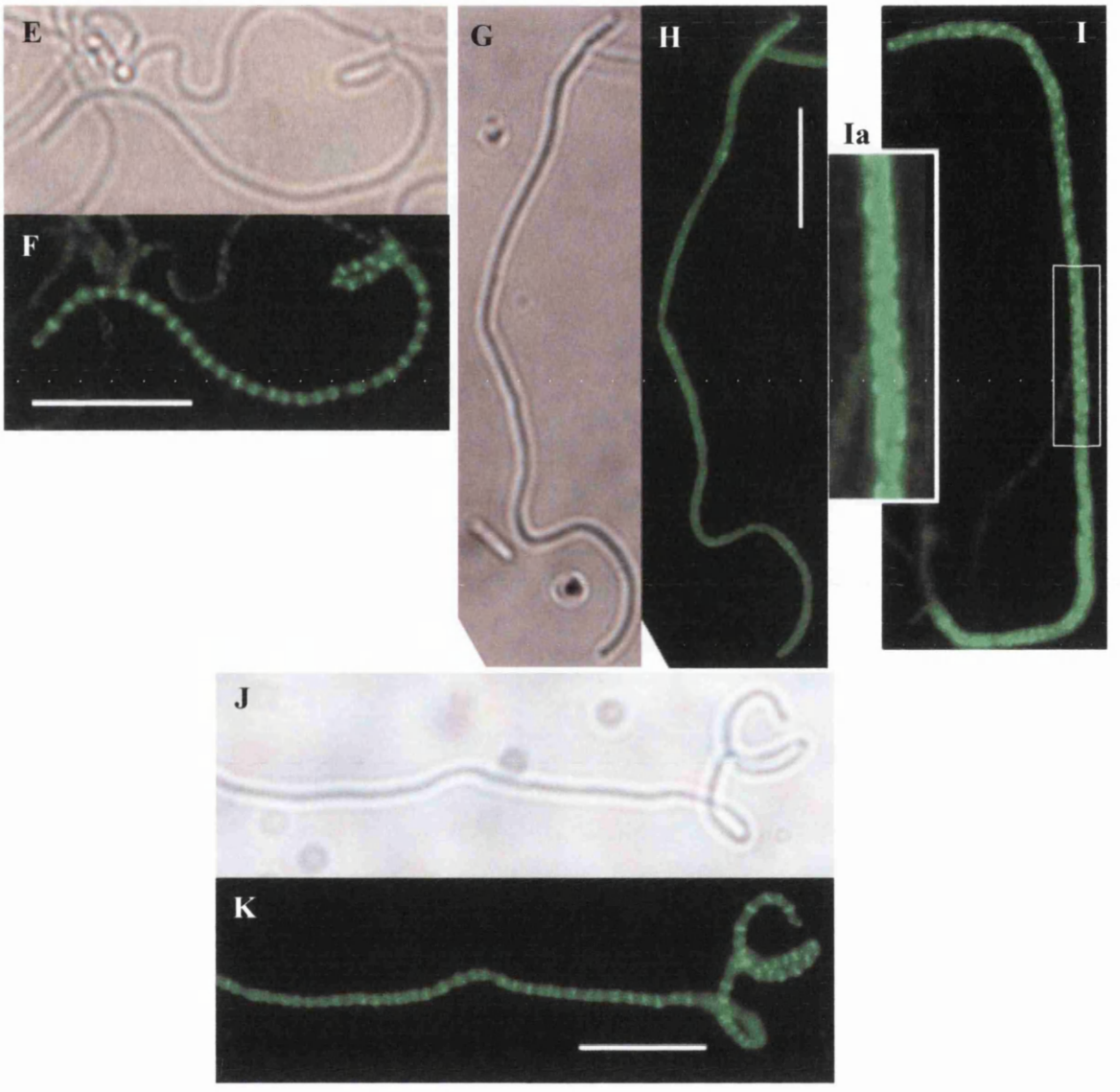

Figure 5.11: Phase contrast and fluorescence microscopy showing the assembly of FtsZ-EGFP in aerial hyphae of wild type and *ftsW* mutants. During early stage of aerial hyphae development (33h) in wild type diffuse fluorescence of non-assembled FtsZ-EGFP was observed (A and B). As the aerial hyphae develop spirals of FtsZ-EGFP were formed (C and D). Da is the enlarged portion of image D. Regular Z rings could be observed in older aerial hyphae (38h) of M145 (E and F). Diffuse fluorescence (G and H) or spiral structures (I) were observed, but not Z-ring in the aerial hyphae of DSCO2085-1/pKF41 mutant even after prolonged incubation. Ia is the enlarged potrion of image I. Images of the DSCO2085-1/pKF41 presented were taken after 84h (G and H) and 88h (I). Normal FtsZ-EGFP rings, similar to wild type, could be observed in the aerial hyphae of the DSCO2085-5/pKF41 (38h) mutant (J and K). (Scale bar = 10 μm)

5.6 Complementation of *ftsW* mutants

For complementation analysis of non-sporulating *ftsW* mutants, a 7478 bp *Eco*RI fragment from cosmid SC4A10 with a Tn*5062* insertion (4A10.2.E07) at position 15834, containing putative *ftsW* promoter region, *ftsW*, *murG*, and *ftsQ* genes and part of Tn*5062* (excluding *egfp*) was cloned into pBluescriptIISK(+) (Stratagene) digested with the same enzyme to obtain plasmid pBSW1 (Fig. 5.12). From pBSW1, a 3963 bp *NotI*/*Hin*dIII fragment containing *ftsW*, *murG* and *ftsQ* genes was excised and blunt-ended. The blunt-ended fragment of 3963 bp was then sub-cloned into the integrating plasmid vector pSH152 at its unique *Eco*RV site, to construct pSHBW1 (Fig. 5.13).

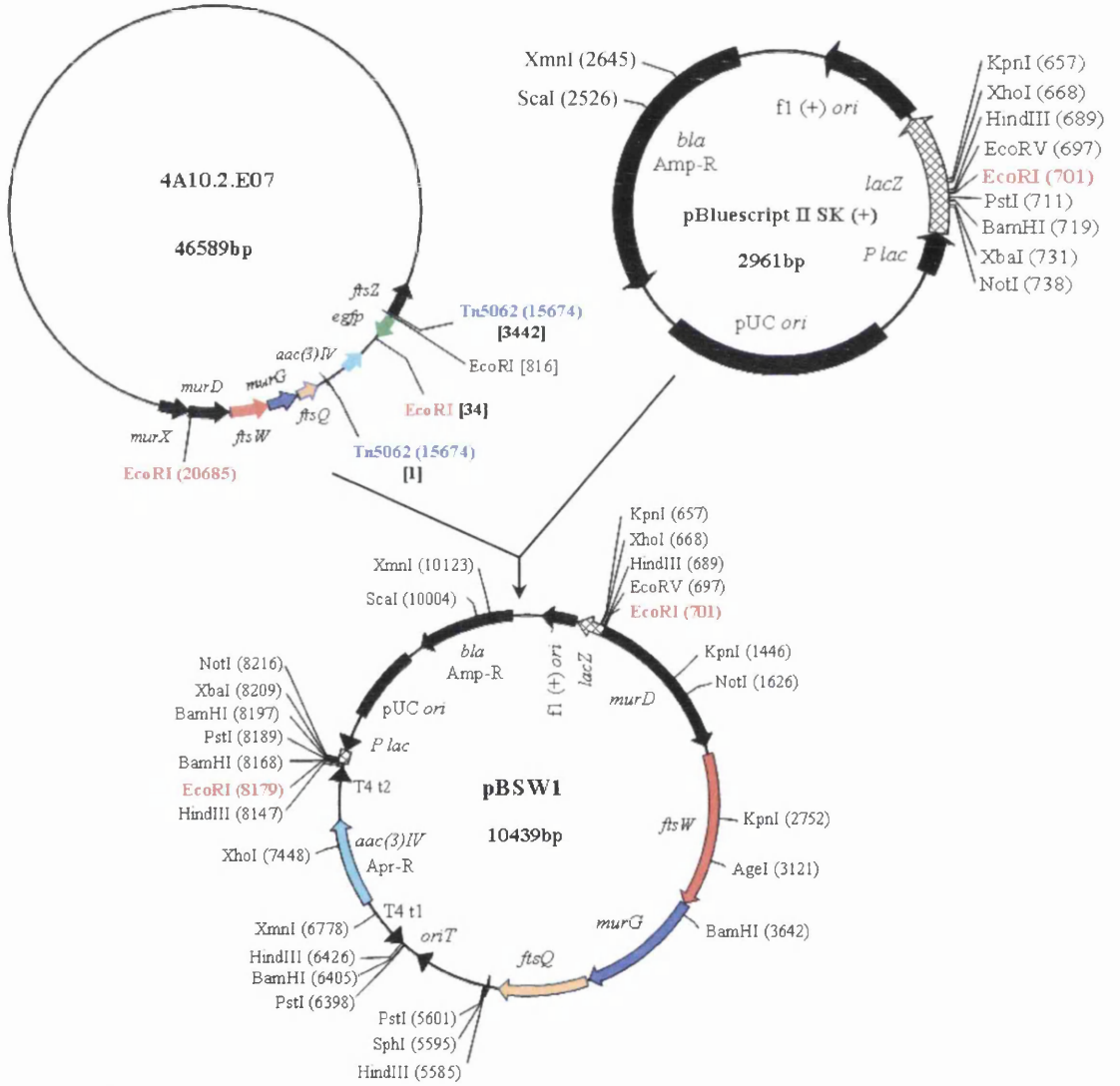

Figure 5.12: Plasmid and cosmid maps used to construct pBSW1 plasmid. An *Eco*RI (red) fragment from 4A10.2.E07 cosmid was cloned into pBluescript II SK (+) at its unique *Eco*RI (red) site to construct pBSW1. Maps are not drawn to the scale.

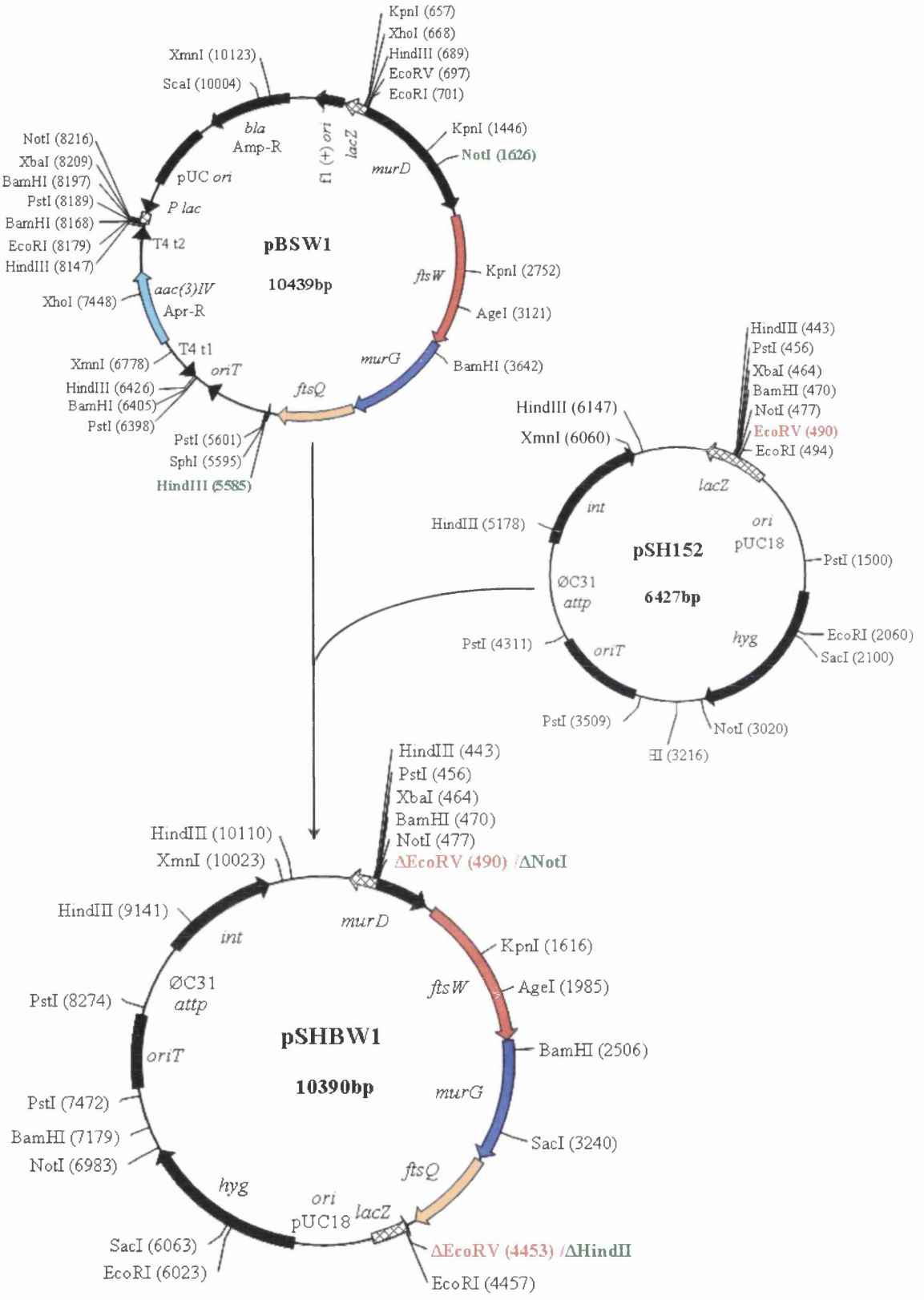

Figure 5.13: Plasmid maps used to construct pSHBW1 plasmid. A *Not*I/*Hin*dIII (green) fragment from pBSW1 plasmid was sub-cloned into pSH152 vector at its unique *Eco*RV (red) site after blunt ending the fragment to construct pSHBW1. Maps are not drawn to the scale.

Due to the arrangement of *ftsW, murG* and *ftsQ* in an operon-like structure there is a possibility that the non-sporulating phenotype of *ftsW* mutants may be due to the polar effect on down stream genes *murG* and *ftsQ*. To exclude this possibility and to confirm that the white phenotype of *ftsW* mutants is due to *ftsW* disruption, two other complementation plasmids pSHBW12 and pSHBW4 were constructed. To construct pSHBW12, pSHBW1 was digested with *Kpn*I and *Age*I restriction enzymes and self-ligated after blunt ending to generate pSHBW12 plasmid (Fig. 5.14) that contains all three genes (*ftsW, murG* and *ftsQ*) with an in-frame deletion in the *ftsW* gene. To generate the plasmid pSHBW4 containing only *ftsW*, pBSW1 was digested with *Bam*HI

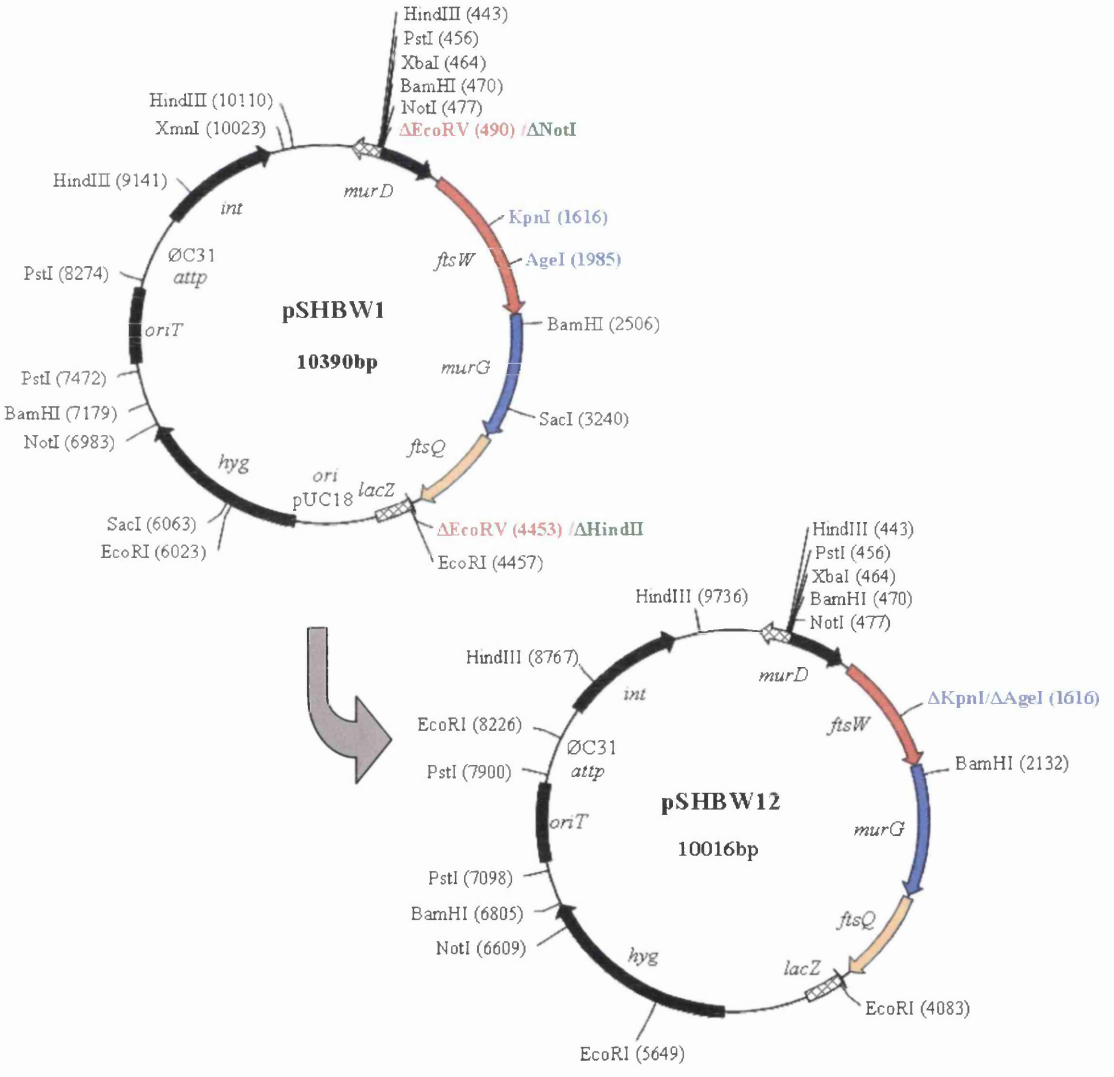

Figure 5.14: Plasmid maps showing the construct pSHBW12 plasmid. The pSHBW1 plasmid was digested with *KpnI/AgeI* (blue) and religated after blunt ending to obtain pSHBW12 plasmid containing an in-frame deletion in the *ftsW* gene. Maps are not drawn to the scale.

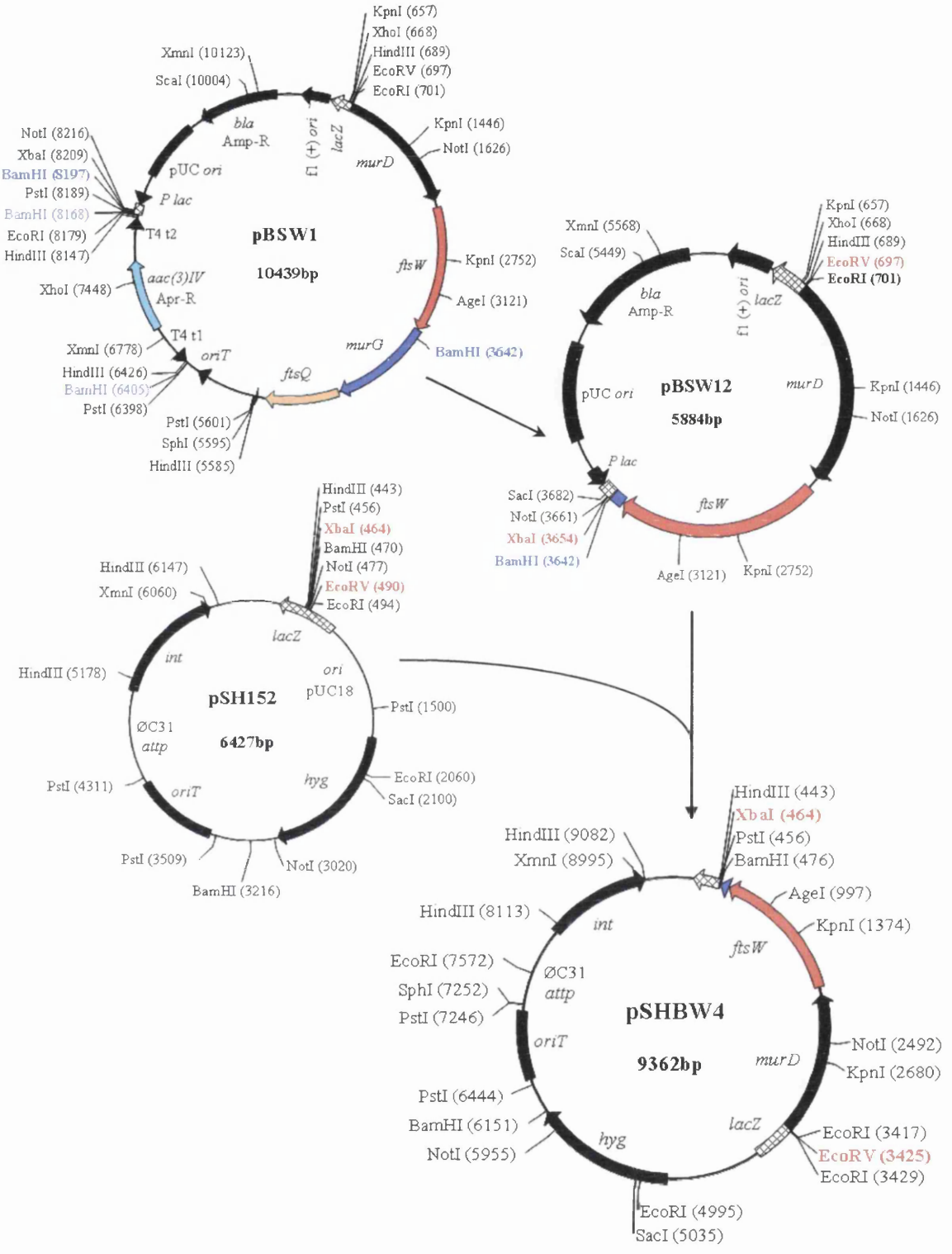

Figure 5.15: Map of the plasmids showing the construction of pBSW12 and pSHBW4. Plasmid pBSW1 was digested with *Bam*HI (blue) and self ligated to remove the *murG* and *ftsQ* genes, leaving the *ftsW* gene with its putative promoter region, generating pBSW12. An *Eco*RV/*Xba*I (red) fragment from pBSW12 was isolated and sub-cloned into pSH152 vector digested with the same enzymes to obtain pSHBW4. Maps are not drawn to the scale.

enzyme and a 5884 bp fragment containing the origin of replication (pUC *ori*), ampicillin resistance marker (*bla*), part of *murD* gene and *ftsW* was purified. The purified 5884 bp *Bam*HI band was then re-ligated to obtain pBSW12 (Fig. 5.15). From pBSW12, an *Eco*RV/*Xba*I fragment of 2957 bp was isolated and ligated with pSH152 cut with *Eco*RV and *Xba*I enzymes to generate pSHBW4 (Fig. 5.15). All the plasmids constructions were confirmed by restriction digestion and sequencing analysis.

To complement all the *ftsW* mutants (DSCO2085-1, DSCO2085-2, DSCO2085-3, DSCO2085-4 and DSCO2085-6) that shared a non-sporulating white phenotype, each of the complementing plasmids (pSHBW1, pSHBW12 and pSHBW4) was introduced individually in each *ftsW* mutant by intergeneric conjugal transfer. The ex-conjugants obtained for each complementing plasmid were screened for hygromycin resistance. The DSCO2085-1 strain with each complementing plasmid thus obtained was designated as CDSCO2085-11 (DSCO2085-1/pSHBW1), CDSCO2085-12 (DSCO2085-1/pSHBW12) and CDSCO2085-14 (DSCO2085-1/pSHBW4). Similarly, other *ftsW* mutant strains with a different complementing plasmid were designated as CDSCO2085-21, CDSCO2085-22, CDSCO2085-24, CDSCO2085-31, CDSCO2085-32, CDSCO2085-34, CDSCO2085-41, CDSCO2085-42, CDSCO2085-44, CDSCO2085-61, CDSCO2085-62 and CDSCO2085-64. To check that an empty vector does not have any effect on the phenotype of mutants, the pSH152 plasmid was introduced into each *ftsW* mutant strain as a control and designated as DSCO2085-1v (DSCO2085-1/pSH152), DSCO2085-2v (DSCO2085-2/pSH152), DSCO2085-3v (DSCO2085-3/pSH152), DSCO2085-4v (DSCO2085-4/pSH152) and DSCO2085-6v (DSCO2085-6/pSH152). For complementation analysis all the strains with a complementing plasmid were plated on SFM agar plates along with wild type, the respective mutant strain and the mutant strain with empty vector. Plates were incubated at 30° C for three days. The complementation analysis showed that the non-sporulating phenotype of all the *ftsW* mutants was restored by pSHBW1 as well as by the pSHBW4 complementing plasmid (Fig. 5.16). However, pSHBW12 plasmid, containing an in-frame deletion in *ftsW*, was not able to restore sporulation in any of the mutants (Fig. 5.16). This showes that the white phenotype is due to *ftsW* gene disruption and there are not polar effects of the *ftsW* transposon insertions on the downstream *murG* and *ftsQ* genes. No effect of plasmid vector pSH152 on the mutant phenotype was observed.

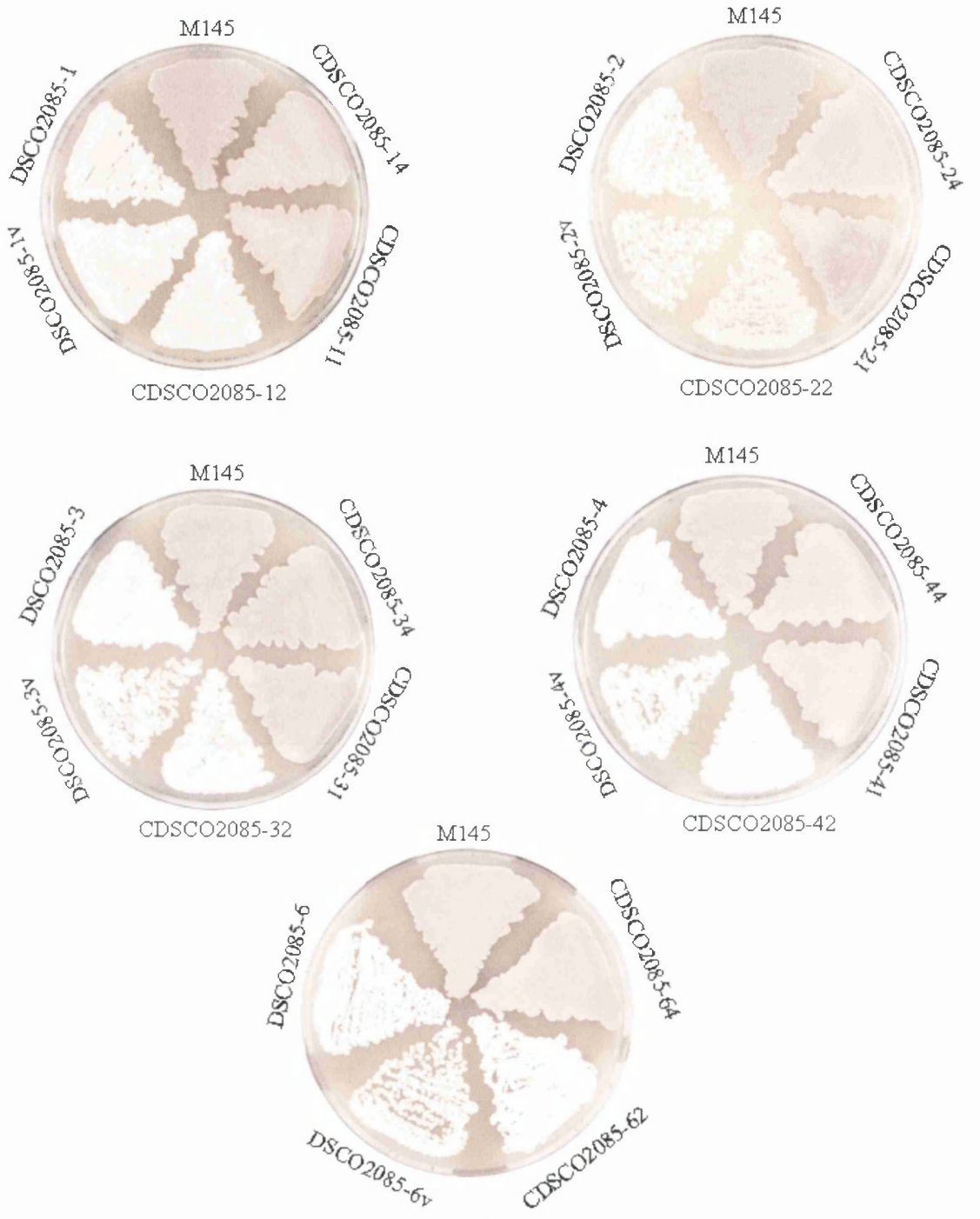

Figure 5.16: Complementation analysis of all the *ftsW* insertion mutants that shared white phenotype. Strains were grown on SFM sporulationn media for 3 days at 30° C. Wild type strain is labelled as M145; different *ftsW* mutant strains are labelled as DSCO2085-X, where X represents number (1-4 and 6) to indicate the respective insertion used to construct the mutants; DSCO2085-Xv, respective mutant strain with empty vector pSH152 (v); CDSCO2085-X1, respective DSCO2085-X mutant strain with pSHBW1 plasmid; CDSCO2085-X2, respective DSCO2085-X mutant strain with pSHBW12 plasmid; CDSCO2085-X4, respective DSCO2085-X mutant strain with pSHBW4 plasmid. All the *ftsW* mutant strains containing either pSHBW1 or pSHBW4 plasmid showed complementation where as pSHBW12 failed to complement any of the *ftsW* mutants.

Fluorescence microscopy of the all the complementing strains was carried out using Fluo-WGA and PI staining as described earlier. The microscopic analysis of aerial hyphae of different complementing strains also showed normal sporulation septa similar to the wild type in the mutant strains complemented with either pSHBW1 or pSHBW4 plasmid but not with pSHBW12 plasmid (Fig. 5.17). Only the microscopies of DSCO2085-1 complementation strains are shown in the Figure 5.17. Other strains also showed similar results.

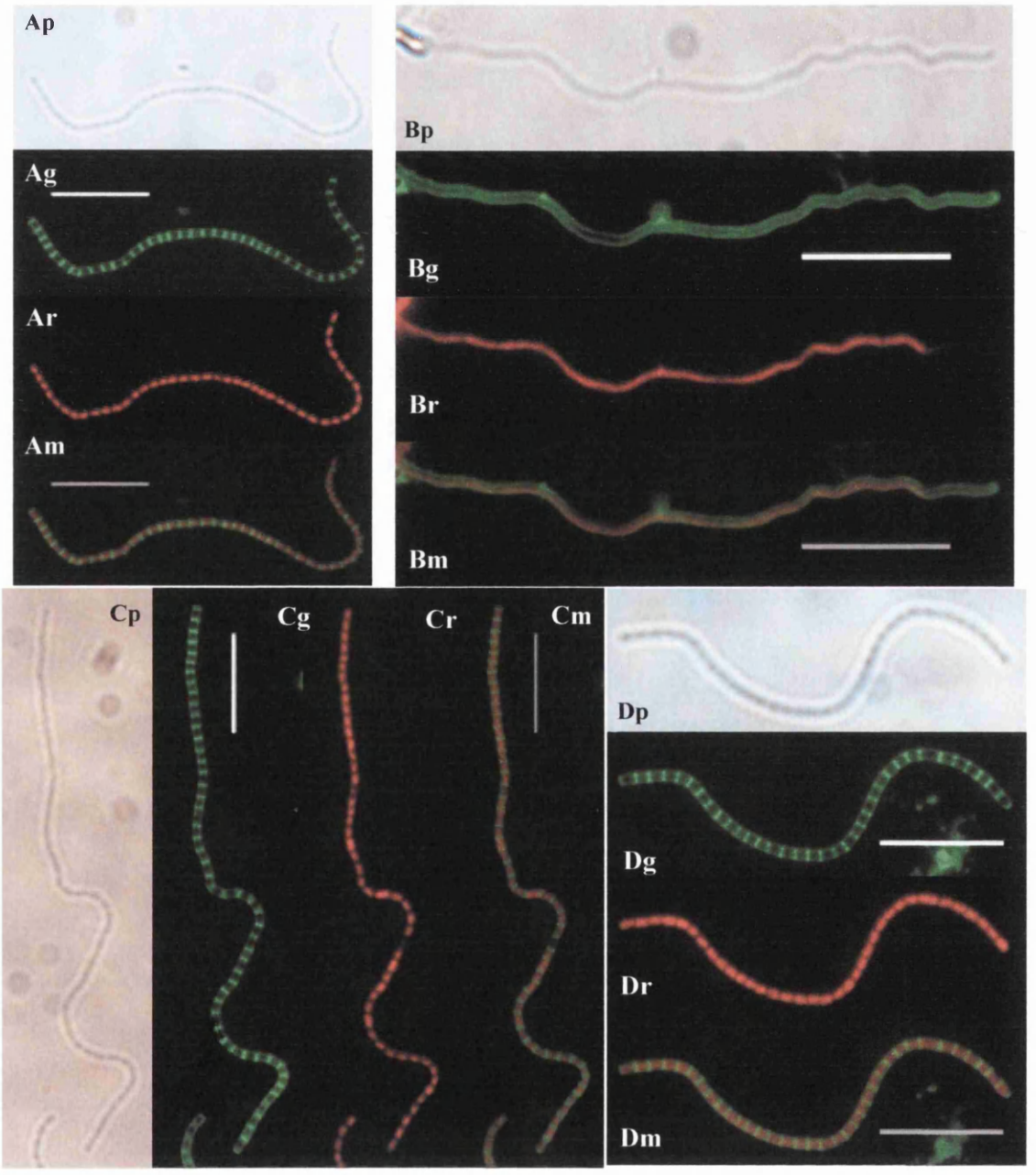

Figure 5.17: Continued on the next page....

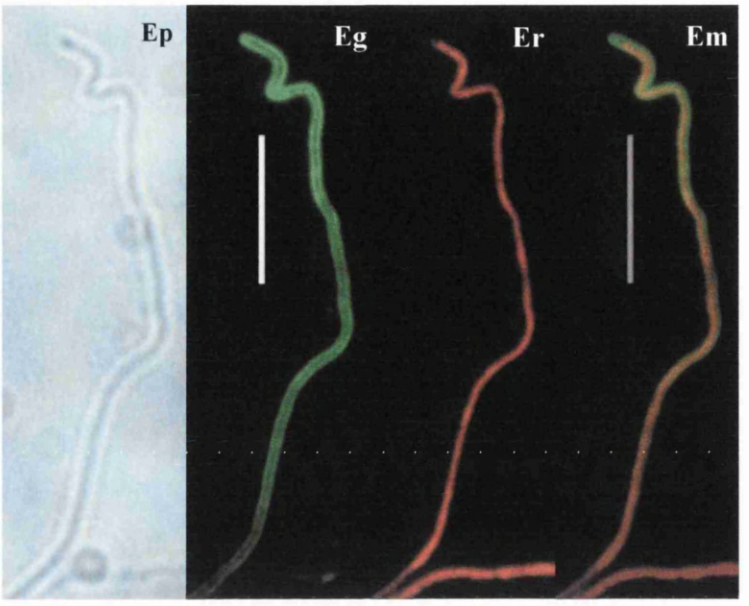

Figure 5.17: Fluorescence microscopy of aerial hyphae of parental strain *S. coelicolor* M145 (A), DSCO2085-1v (DSCO2085-1 with pSH152) (B), CDSCO2085-11 (DSCO2085-1 with pSHBW1) (C), CDSCO2085-14 (DSCO2085-1 with pSHBW4) (D) and CDSCO2085-12 (DSCO2085-1 with pSHBW12) (E) strains. Impressions of each sample grown on SFM agar were prepared by staining the samples with Fluo-WGA (for cell wall) and PI (chromosomal DNA) staining to visualize sporulation septa and chromosome condensation. Wild type, CDSCO2085-11 and CDSCO2085-14 strains were grown for 38h whereas CDSCO2085-12 was grown for 80h at 30° C. Each panel shows phase contrast (p), Fluo-WGA staining (g), PI staining (r) and merged (m) images of Fluo-WGA and PI staining of aerial hyphae of respective strains. (Scale bar 10 μm)

The length of pre-spore compartments (200 of each) of complementing strains CDSCO2085-11 and CDSCO2085-14 was similar to wild type pre-spore compartments. It ranged from 0.8 to 1.8 μm, with the majority of pre-spore compartments between 1 to 1.3 μm in length (Fig. 5.18). The average length of pre-spore compartments of CDSCO2085-11 and CDSCO2085-14 were 1.13 ± 0.13 μm and 1.14 ± 0.14 μm, respectively, which is similar to the average length (1.17 ± 0.13 μm) of wild type pre-spore compartments. The average width of the pre-spore compartments of the CDSCO2085-11 and CDSCO2085-14 strains were 0.8 ± 0.09 μm and 0.78 ± 0.08 μm, respectively, that is also similar to the wild type average width 0.77 ± 0.11 μm. Thus, the data further confirms that the disruption of *ftsW* gene is responsible for the non-sporulating white phenotype of *ftsW* mutants.

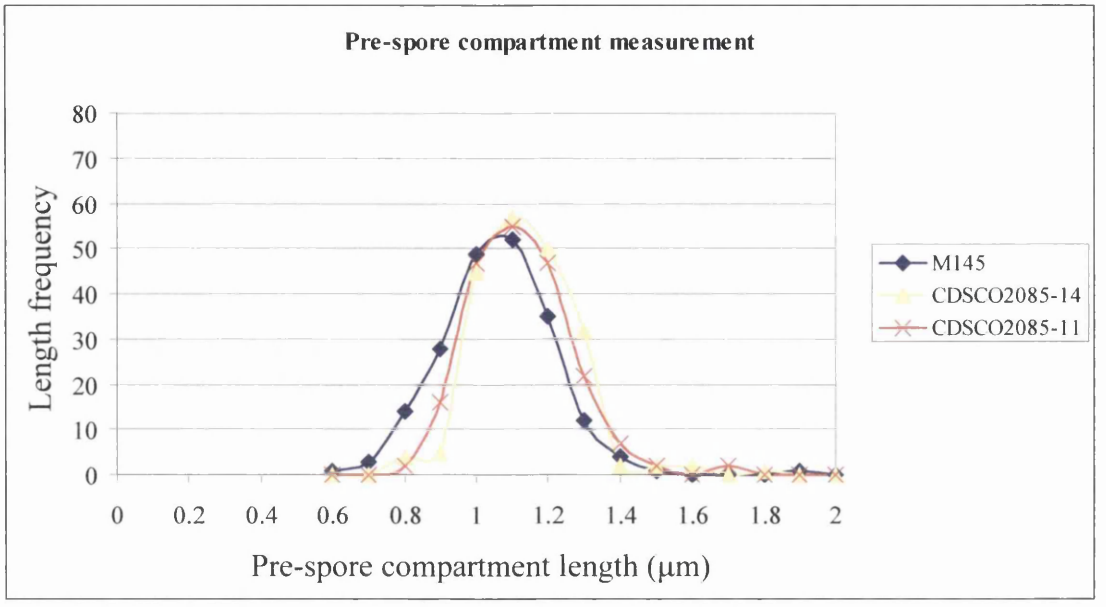

Figure 5.18: Graph of pre-spore compartment length versus frequency of the length of pre-spore compartment in wild type M145, CDSCO2085-11 and CDSCO2085-14 strains. The length of randomly selected 200 pre-spore compartments of each strain was measured from the Fluo-WGA stained images using Scion Image software.

5.7 Construction and characterization of *sfr/ftsW* and *rodA2/ftsW* double mutants

Normal Z-ring formation and vegetative septation in the *ftsW* mutants suggested that either the FtsW is not required for vegetative septation or the vegetative function of FtsW is substituted by one of the three other SEDS proteins (RodA, RodA2 or Sfr). Normal vegetative septation in *sfr*, *rodA2* and *rodA2/sfr* double mutants has already been discussed in the previous chapter. To exclude the possible functional redundancy among FtsW, Sfr and RodA proteins, another two double mutants, one with insertions in both *ftsW* and *sfr,* and the second with mutations in *ftsW* and *rodA2,* were constructed. To construct the *sfr/ftsW* double mutant, a *sfr-Hyg*^{R} single mutant was used. Construction and confirmation of a *sfr* single mutant with hygromycin resistance has already described in the previous chapter. The 4A10.2.H05 cosmid insertion of *ftsW* gene was introduced into the *sfr-Hyg*^{R} single mutant background by intergeneric conjugal transfer as described previously. The ex-conjugants thus obtained were screened for apramycin resistance and kanamycin sensitivity for the replacement of

parental *ftsW* gene with a disrupted copy of the gene. Several double crossover mutants of the *ftsW* gene were obtained in the *sfr-Hyg*^{R} mutant background with a frequency of 35%. For the construction of a *rodA2/ftsW* mutant, the Apr^{R} cassette of the transposon insertion 4A10.2.H05 in *ftsW* was replaced by the Hygromycin resistance (Hyg^{R}) marker using the Redirect technique as described earlier. The replacement of the marker in the cosmid insertion was confirmed by restriction analysis and sequencing. The *ftsW* disrupted cosmid insertion 4A10.2.H05 with the Hyg^{R} cassette was then introduced into the DSCO5302-1 *(rodA2)* mutant by intergeneric conjugation and screened for the replacement of the wild type *ftsW* gene with the mutated version of the gene. The frequency of the double crossover mutants of *ftsW* in *rodA2* background was 42%. To confirm both (*sfr/ftsW* and *rodA2/ftsW*) double mutants, Southern blot (SB) analysis was carried out. For Southern hybridization of *sfr/ftsW* double mutants, purified chromosomes of four randomly selected clones and the respective cosmid insertions (C88.2.H10-Hyg^{R} for *sfr* and 4A10.2.H05-Apr^{R} for *ftsW*) were digested with *Sal*I (Fig. 5.19). SB of *sfr/ftsW* mutants showed the expected sizes of fragments similar to the respective cosmid controls for *sfr* and *ftsW* disruption, thus confirming that all the clones of *sfr/ftsW* were true double mutants. The *sfr/ftsW* double mutant was designated as DSCO2607/2085.

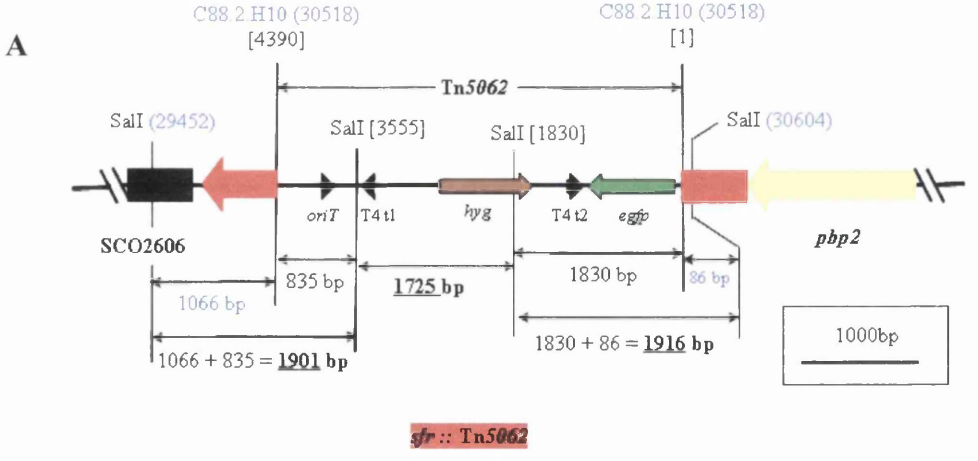

Figure 5.19: Continued on the next page....

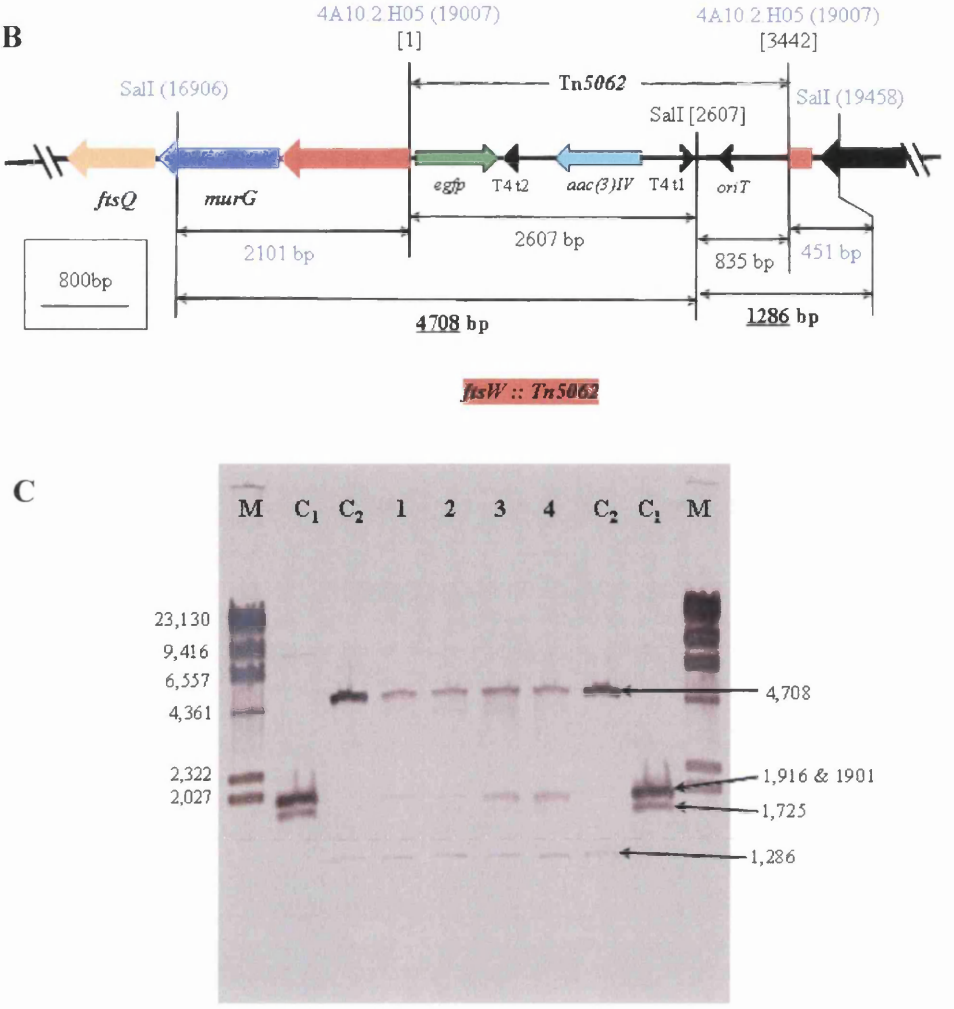

Figure 5.19: SB analysis of *sfr/ftsW* double mutants. **(A) & (B)** - Maps of *sfr* insertion with Hyg^R cassette and *ftsW* insertion, respectively, showing the positions of Tn*5062* insertions in the respective genes and the restriction sites of *Sal*I to calculate the size of bands that should be obtained by Southern hybridization. The cosmid insertions used for the mutagenesis are written in blue colour with their respective position in the cosmid written in the brackets. Just under the cosmid name and position, the number in square bracket indicates beginning and end of Tn*5062*. The position of the important *Sal*I restriction sites in the respective gene locus are shown in the brackets next to the name of the enzyme and that of Tn*5062* region is shown in square brackets. Arrows with different colours represents different genes and their directions. A scale bar for each map is shown in a rectangle. Name of each respective gene is shown just under each arrow. *aac(3)IV* – Apramycin resistance; T4 t1,2 – Transcription terminator t1 & 2; *egfp* – Enhanced green fluorescent protein gene; *oriT* – Origin of transfer. The sizes of resulting bands after SB are shown in bold letters with underline. **(C)** SB of four *sfr/ftsW* double mutant clones. M –*Hin*dIII digested λ DNA marker with the size (in bp) for each band presented on the left hand side; $C_{1\ \&\ 2}$ – *Sal*I digested C88.2.H10-Hyg^R and 4A10.2.H05 cosmid insertions, respectively, and 1 to 4 – *Sal*I digested chromosome of each *sfr/ftsW* mutant clones. The size (in bp) of expected bands is indicated by arrows. Digoxigenin labelled Tn*5062* was used as a hybridization probe.

To perform SB analysis on *rodA2/ftsW* double mutant clones, the purified chromosome of each clone and their respective cosmids (control) were digested using *Kpn*I enzyme. SB of *rodA2/ftsW* double mutant clones also showed the expected size of fragments confirming that the mutants were true mutants (Fig. 5.20). Thus, the *rodA2/ftsW* double mutant obtained was designated as DSCO5302/2085.

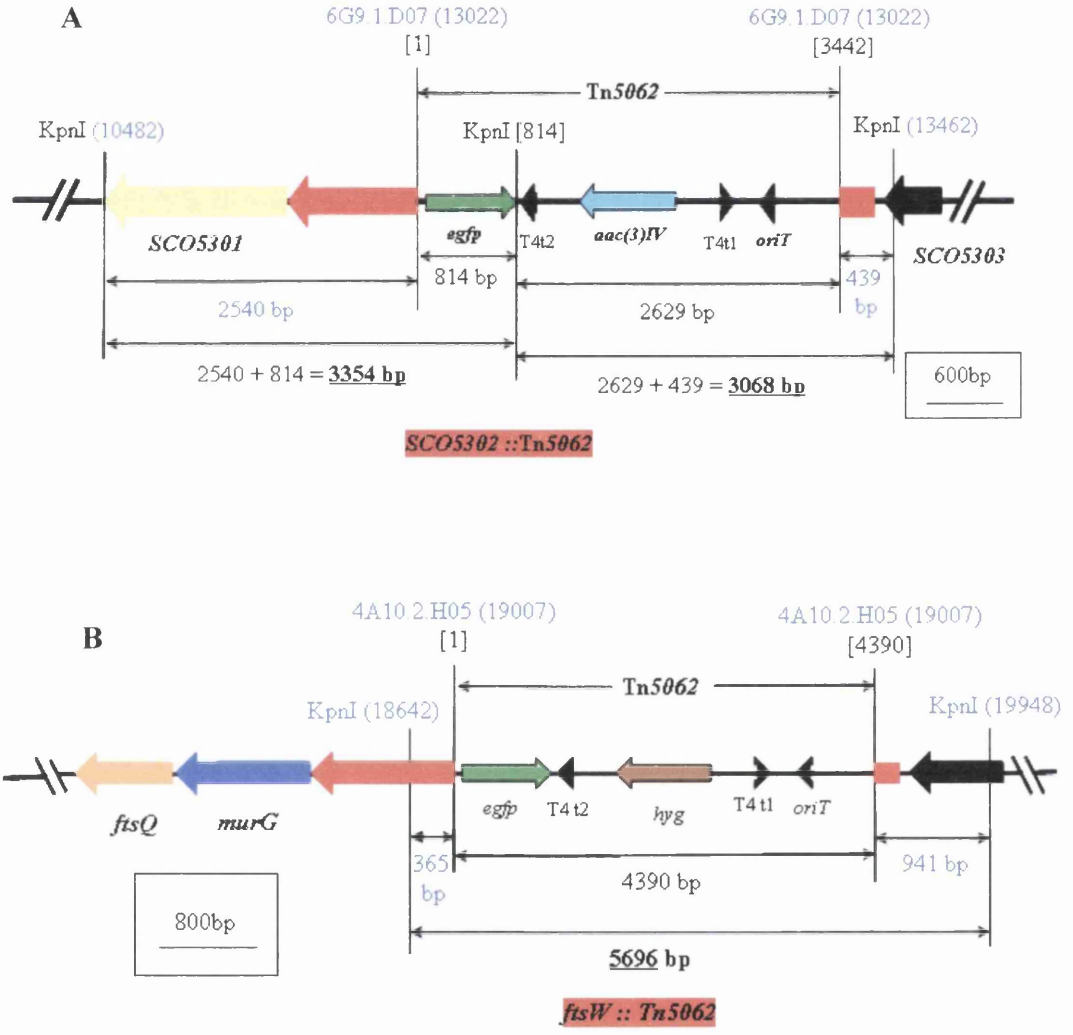

Figure 5.20: Continued on the next page….

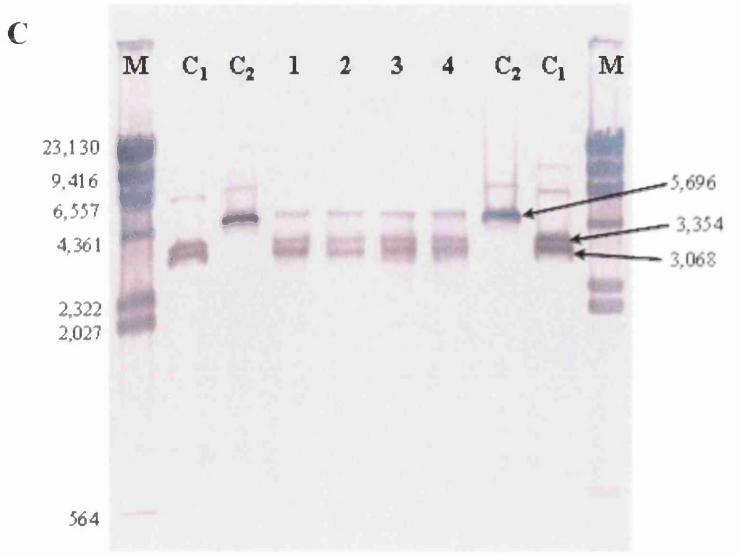

Figure 5.20: SB analysis of *rodA2/ftsW* double mutants. **(A) & (B)** - Maps of *rodA2* insertion and *ftsW* insertion with Hyg^R cassette, respectively, showing the positions of Tn*5062* insertions in the respective genes and the restriction sites for *Kpn*I enzyme to calculate the size of bands that should be obtained by Southern hybridization. The cosmid insertions used for the mutagenesis are written in blue colour with their respective position in the cosmid written in the brackets. Just under the cosmid name and position, the number in square bracket indicates beginning and end of Tn*5062*. The position of the important *Kpn*I restriction sites in the respective gene locus are shown in the brackets next to the name of the enzyme and that of Tn*5062* region is shown in square brackets. Arrows with different colours represents different genes and their direction. Scale bar of each map is shown in a rectangle. Name of each respective gene is shown just under each arrow. *aac(3)IV* – Apramycin resistance; T4 t1,2 – Transcription terminator t1 & 2; *egfp* – Enhanced green fluorescent protein gene; *oriT* – Origin of transfer. The sizes of resulting bands after SB are shown in bold letters with underline. **(C)** SB of four *rodA2/ftsW* double mutant clones. M –*Hin*dIII digested λ DNA marker with the size (in bp) for each band presented on the left hand side; $C_{1\ \&\ 2}$ – *Kpn*I digested 6G9.1.D07 and 4A10.2.H05-Hyg^R cosmid insertions, respectively, and 1 to 4 – *Kpn*I digested chromosomes of each *rodA2/ftsW* mutant clones. The size (in bp) of expected bands is indicated by arrows. Digoxigenin labelled Tn*5062* was used as a hybridization probe.

To phenotype both the double mutants (DSCO2607/2085 and DSCO5302/2085), all the clones were plated on SFM agar medium along with wild type M145 strain. Plates were incubated at 30° C and the cultures were grown for three days. As expected, all the mutants exhibited a white non-sporulating phenotype similar to that of *ftsW* single mutant (Fig. 5.21).

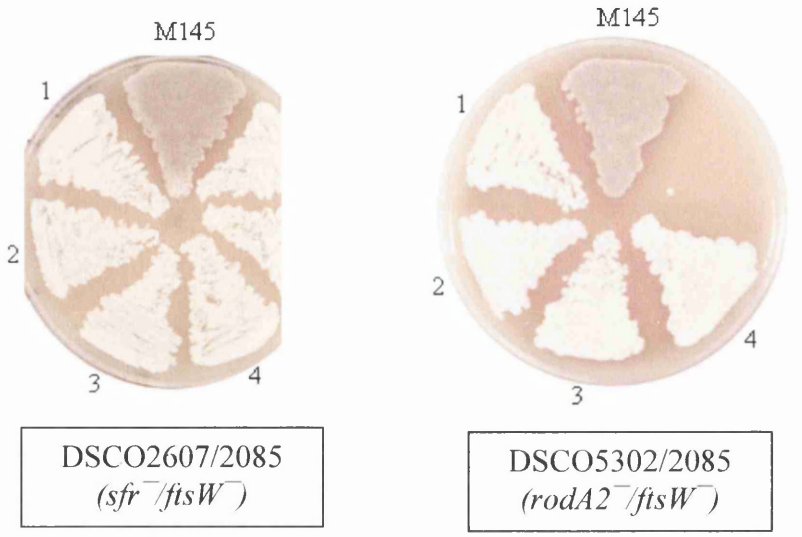

Figure 5.21: Phenotype of *sfr*⁻/*ftsW*⁻ and *rodA2*⁻/*ftsW*⁻ double mutants grown on SFM agar. Wild type strain is labelled as M145 and the clones of each mutant are labelled as numbers (1-4). Name for the respective mutant is written under each plate in a box. Strains were grown for 3 days at 30° C.

To analyze further whether vegetative septation is affected in these double mutants, fluorescence microscopy of vegetative mycelium of both the mutants were carried out using FL-vancomycin as described previously. A normal pattern of septation, similar to that of the wild type, was observed in both the mutant strains (Fig. 5.22), suggesting that there is no functional redundancy among the FtsW, Sfr and RodA2 proteins. It also suggests that these three proteins are not required for vegetative septation in *S. coelicolor*. Fluorescence microscopy of aerial hypha of both the mutants using WGA-PI staining revealed similar morphologies to that of *ftsW* single mutant, where the aerial hyphae were non-septated with uncondensed chromosomes.

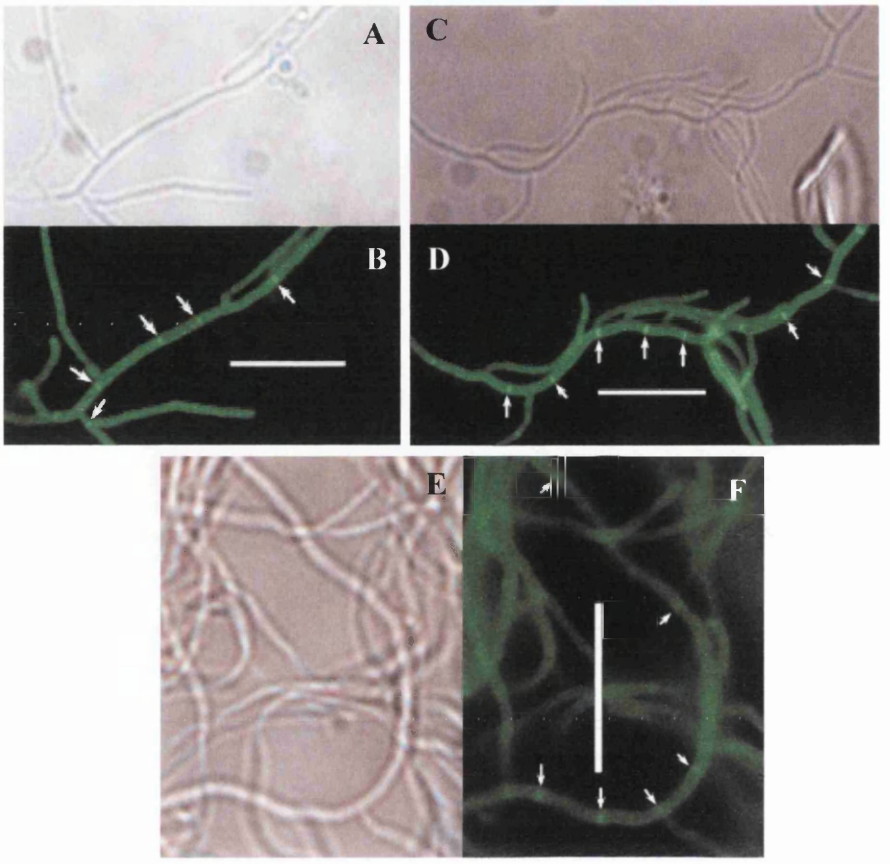

Figure 5.22: Complete vegetative cross-wall formation in wild type, *sfr/ftsW* and *rodA2/ftsW* double mutants. Substrate mycelium from 48h grown culture of wild type and mutant strains stained with FL-vancomycin to reveal septa. Phase contrast and fluorescence microscopy (A and B) of wild type M145; (D and E) of DSCO2607/2085 *(sfr⁻/ftsW⁻)*; (E and F) of DSCO5302/2085 *(rodA2r⁻/ftsW⁻)*.

5.8 Summary

Disruption of *ftsW* in *S. coelicolor* resulted in a non-sporulating white phenotype suggesting that the *ftsW* mutant was unable to sporulate. Microscopic analysis of the mutants revealed that sporulation septation is affected in *ftsW* mutants while there was no effect in vegetative septation. In addition to sporulation septation, chromosomal condensation was also affected in the mutants. Further localization studies for FtsZ-EGFP in the *ftsW* mutants revealed that the mutants were unable to form Z-

rings, necessary for septation to take place, in the aerial hyphae. This suggests some direct or indirect role of FtsW protein in Z-ring stabilization. Z-ring formation in the vegetative mycelium of the mutant was not affected suggesting some other protein is required for the Z-ring stabilization during vegetative septation. Disruption of the *ftsW* gene at the far C-terminal end did not affect the sporulation septation inferring that the C-terminal tail does not play a vital role in the functioning of FtsW. Normal vegetative cross-wall formation in the double mutants quite likely rules out the possibility of functional redundancy among the three non-essential SEDS proteins in *S. coelicolor.* However, functional redundancy among these proteins can only be completely ruled out by constructing a triple mutant with simultaneous inactivation of *ftsW*, *sfr* and *rodA2.*

Chapter - 6

Construction and Characterization of *ftsI* Mutants of *Streptomyces coelicolor*

6.1 Introduction

Each SEDS protein appears to work in conjunction with a specific class B penicillin-binding protein (PBP) during peptidoglycan synthesis (Datta *et al.*, 2006; Mercer and Weiss, 2002). Examples are RodA-PBP2 and FtsW-FtsI. These proteins are usually encoded in the same operon and inactivation of either affects the peptidoglycan synthesis (Matsuzawa *et al.*, 1989; Tamaki *et al.*, 1980). Among these pairs, FtsW and FtsI are the best characterized proteins with respect to their structure and function. FtsW and FtsI are specifically recruited at the cell division site and are the only pair of division proteins that showed perfect correlation (Harry *et al.*, 2006; Margolin, 2000).

In *S. coelicolor* the presence of four pairs of SEDS proteins and their cognate PBPs has been already discussed in previous chapters. However, the functional relation of these proteins in *S. coelicolor* is not clear. Results from the previous chapter have confirmed the role of FtsW in sporulation septation. Further, to address a role of the cognate class B PBP (FtsI) during sporulation and to establish a functional relationship between FtsW and FtsI, mutational analysis of the *ftsI* gene in *S. coelicolor* was carried out. Mutagenesis of the *ftsI* gene and the phenotypic characterization of *ftsI* mutants are discussed in this chapter.

6.2 Mutagenesis of *ftsI* in *S. coelicolor*

The Tn*5062* insertion mutants of *S. coelicolor ftsI* gene were constructed using the same approach as described earlier. To construct the disruption mutants of *ftsI,* two independent cosmid insertions, 4A10.1.C09 (close to the beginning of the gene) and 4A10.2.G05 (close to the end of the gene), at the position 2246734 and 2245233, respectively, in the chromosome were used. Upon screening of the exconjugants for the replacement of wild type *ftsI* with the disrupted copy of *ftsI* and loss of the Supercos-1 vector, the double crossover recombination events occurred at the rate of 73% with 4A10.1.C09 insertion and 92% with 4A10.2.G05 insertion. Four double crossover mutants for each insertion were selected for Southern hybridization analysis. For Southern hybridization of *ftsI* mutants, the purified chromosome of each mutant clone and the respective cosmid were digested with *Kpn*I enzyme to obtain distinct sizes of

fragments to confirm the mutants. The Southern blot (SB) was hybridized using digoxigenin labelled Tn*5062* probe to detect the expected sizes of fragments for each mutant. SB of 4A10.1.C09 insertion mutants showed expected fragments of 3617 bp and 3171 bp (Fig. 6.1A and C) while that of 4A10.2.G05 insertion mutants showed 5161 bp and 1326 bp frgaments (Fig. 6.1 B and C) as expected. Thus, it confirmed that all the *ftsI* mutant clones selected for each insertion were true mutants. The *ftsI* mutant strain with 4A10.1.C09 insertion is designated as DSCO2090-1 and the mutant with 4A10.2.G05 insertion is designated as DSCO2090-2.

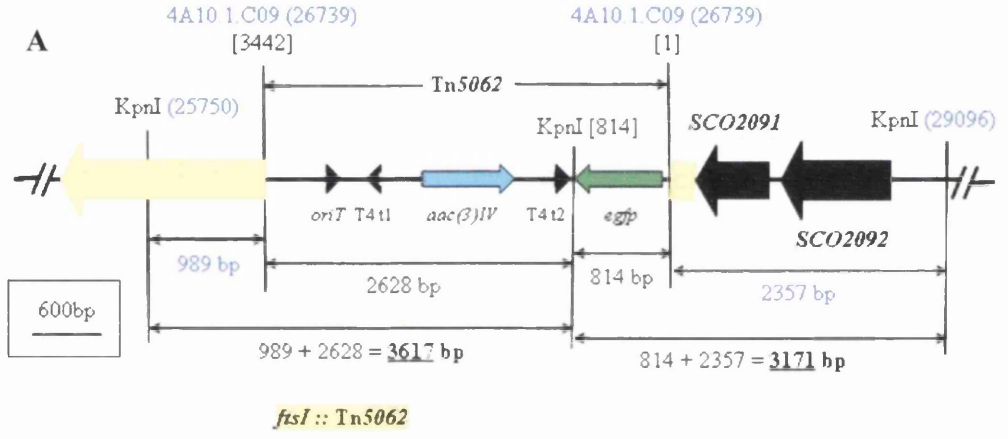

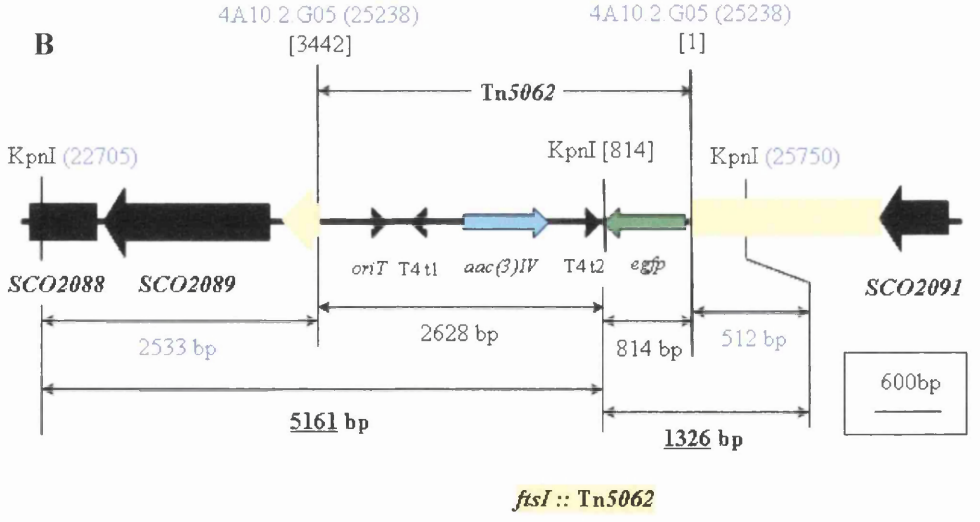

Figure 6.1: Continued on the next page....

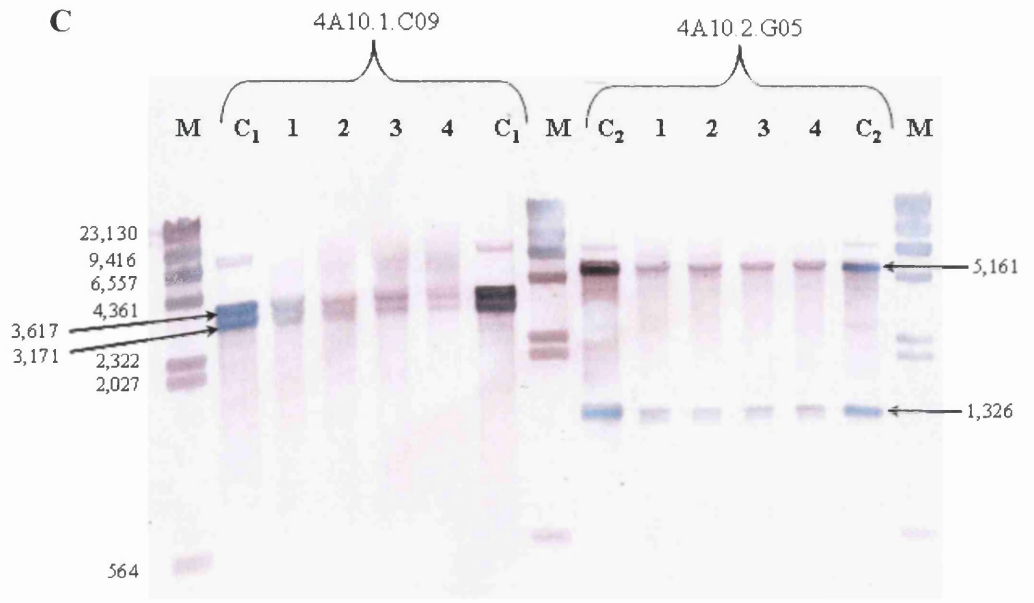

Figure 6.1: Southern Blot (SB) analysis of *ftsI* mutants with 4A10.1.C09 and 4A10.2.G05 insertions each. **(A & B)** Diagrammatic representation of *ftsI* locus with 4A10.1.C09 (A) and 4A10.2.G05 (B) independent insertions showing Tn*5062* position and the corresponding *Kpn*I restriction sites to calculate the size of bands that should be obtained after Southern hybridization. Each cosmid insertion used for *ftsI* mutagenesis is written in blue colour with its respective position in the cosmid. Just under the cosmid name and position, the start and end sites of Tn*5062* are written in square brackets. The position of an important *Kpn*I restriction sites in the *ftsI* region of cosmid are shown in the brackets and in Tn*5062* region is shown in square brackets. Arrows with different colours represent different genes and their directions. Name of each respective gene is shown just under each arrow. *aac(3)IV* – Apramycin resistance; T4 t1,2 – Transcription terminator t1 & 2; *egfp* – Enhanced green fluorescent protein gene; *oriT* – Origin of transfer. Expected size of bands that should be obtained in SB is shown in bold letters with underline. The rectangular box shows the scale of the map. **(C)** SB of *ftsI* mutants (4 clones for each insertion). The size (in bp) of each expected band is shown by arrow. M –*Hin*dIII digested λ DNA marker with the size (in bp) for each band written on the left hand side; C_1 – *Kpn*I digested 4A10.1.C09 cosmid insertion; C_2 – *Kpn*I digested 4A10.2.G05 cosmid insertion; and 1 to 4 – *Kpn*I digested chromosome of each *ftsI* mutant clone with respective insertion. Additional bands other than expected size are due to partial digestion of the DNA. Digoxigenin labelled Tn*5062* was used as a hybridization probe.

6.3 Phenotypic analysis of *ftsI* mutants

To characterize *ftsI* mutants macroscopically, the clones of *ftsI* mutant strains DSCO2090-1 and DSCO2090-2 were plated on sporulation specific SFM medium along with the wild type strain M145. The cultures were grown at 30° C for three days and accessed for sporulation by visualizing the production of grey pigmented spores on

the surface of SFM agar grown culture. Unlike the wild type strain that starts producing grey pigmented spores just after 38 to 40 h of growth, all *ftsI* mutants exhibited a white non-sporulating phenotype similar to that of *ftsW* mutants (Fig. 6.2). The size of the *ftsI* mutant colonies was also similar to wild type. The *ftsI* mutants grown on NMMP

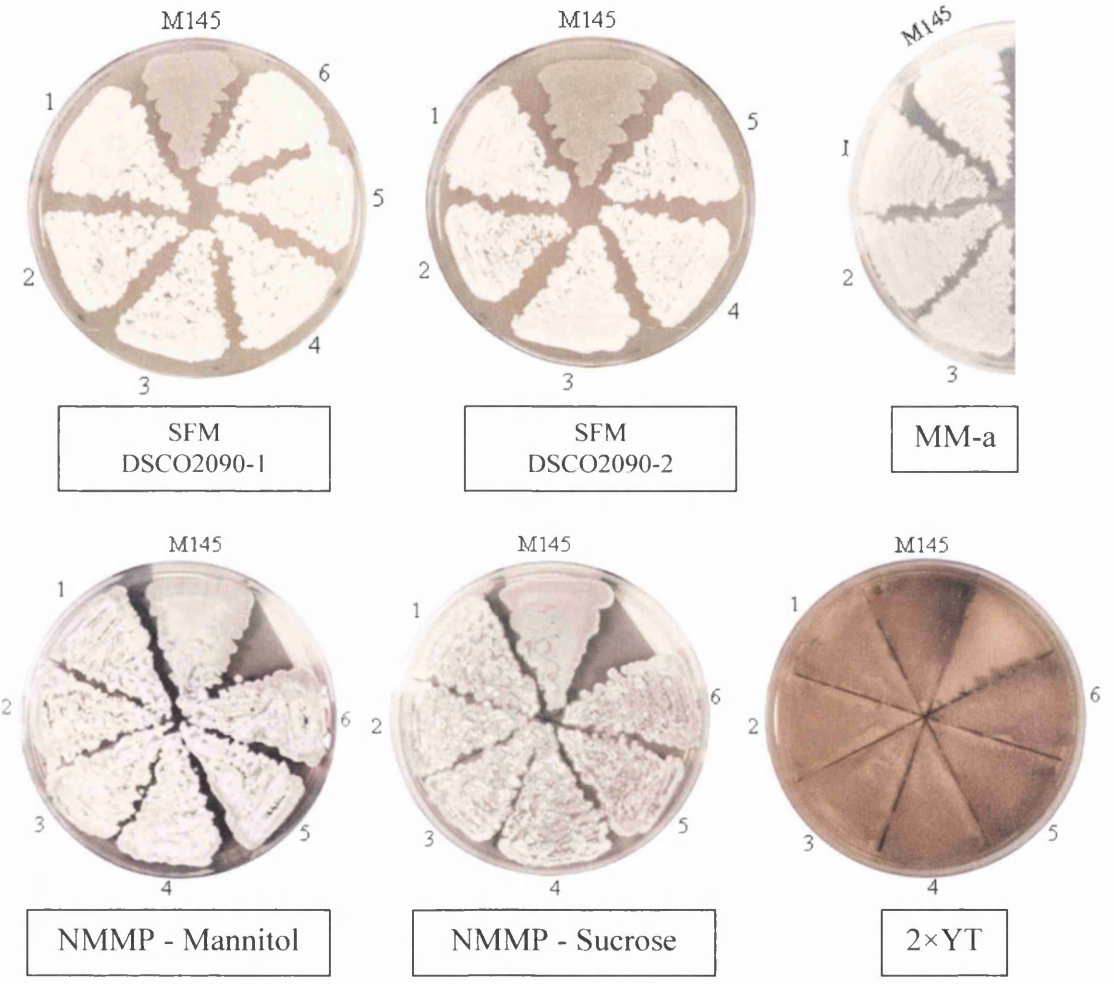

Figure 6.2: Phenotype of *ftsI* mutants and their congenic parental strain *S. coelicolor* M145 on different media. Strains were grown for 4 days (3 days for cultures grown on SFM) at 30° C. Name of the medium used for characterization of the mutants is indicated in a rectangular box just below each picture of the plate. Clones of both the *ftsI* mutant strains were plated on separate SFM plate where number indicates clone of each mutant strain. In the pictures of other media plates the numbers 1-3 represents the clones of DSCO2090-1 mutant strain and 4-6 represents the clones of DSCO2090-2 mutant strain. MM-a, Minimal medium containing L-asparagine agar media. In minimal medium glucose was used as a carbon source.

containing either mannitol or sucrose also showed no significant difference in the phenotype except the mutants were lighter grey than wild type (Fig. 6.2). Also no apparent macroscopic differences between the wild type and *ftsI* mutants were observed when grown on minimal medium or rich complex medium 2×YT (Fig. 6.2). Both wild type and *ftsI* mutants showed a substantial amount of blue and red pigmented antibiotics production on all the media tested (Fig. 6.2).

6.4 Microscopic analysis of *ftsI* mutants

Fluorescence microscopy was performed for cytological characterization of the mutants. To visualize vegetative septa, wild type and *ftsI* mutants were grown on 2×YT agar with coverslips inserted at an acute angle. The cultures were grown for 48 hours at 30° C and stained with FL-vancomycin as described earlier. Upon observation of FL-vancomycin stained samples of wild type and mutants under the microscope, no difference in the pattern of vegetative septation in both the strains was observed (Fig. 6.3 A-D). As in the case of *ftsW* mutants, this observation also suggests that FtsI is not required for vegetative septation. Although not shown, the DSCO2090-2 mutant also showed a similar patter of septation when stained with FL-vancomycin. To further confirm that complete crosswalls were formed in the substrate mycelium of *ftsI* mutant, the DSCO2090-1 mutant strain was sent to John Innes Centre for transmission electron microscopy (TEM). TEM of vegetative hyphae of wild type and mutant revealed that complete crosswalls similar to wild type were formed in *ftsI* mutants further confirming that FtsI does not require for vegetative septation in *S. coelicolor* (Fig. 6.3 E & F).

To check the effect of *ftsI* disruption on non-sporulating aerial hyphae in *ftsI* mutants, cultures of wild type and mutant were grown on the surface of SFM agar plate at 30° C for 38h (wild type) and up to 96h (*ftsI* mutants). Impressions of each culture were taken on coverslips and the samples were observed under the microscope after staining with Fluo-WGA (for cell wall) and propidium iodide (PI) (for chromosomal DNA). As usual, regularly spaced sporulation septa defining pre-spore compartments each containing a single condensed chromosomal DNA were observed in wild type aerial hyphae (Fig. 6.4 A & B). On the other hand, the aerial hyphae of *ftsI* mutants showed no sporulation septa and no apparent chromosome condensation, similar to that of *ftsW* mutant phenotype, even after prolonged incubation (Fig. 6.4 C & D). Such a

similarity in the phenotype of *ftsW* and *ftsI* mutants indicates the functional relationship between FtsW and FtsI, as expected. The image of aerial hyphae of the *ftsI* mutant shown in the Figure 6.4 is of the DSCO2090-1 strain. The DSCO2090-2 mutant strain also showed a similar phenotype (Not shown).

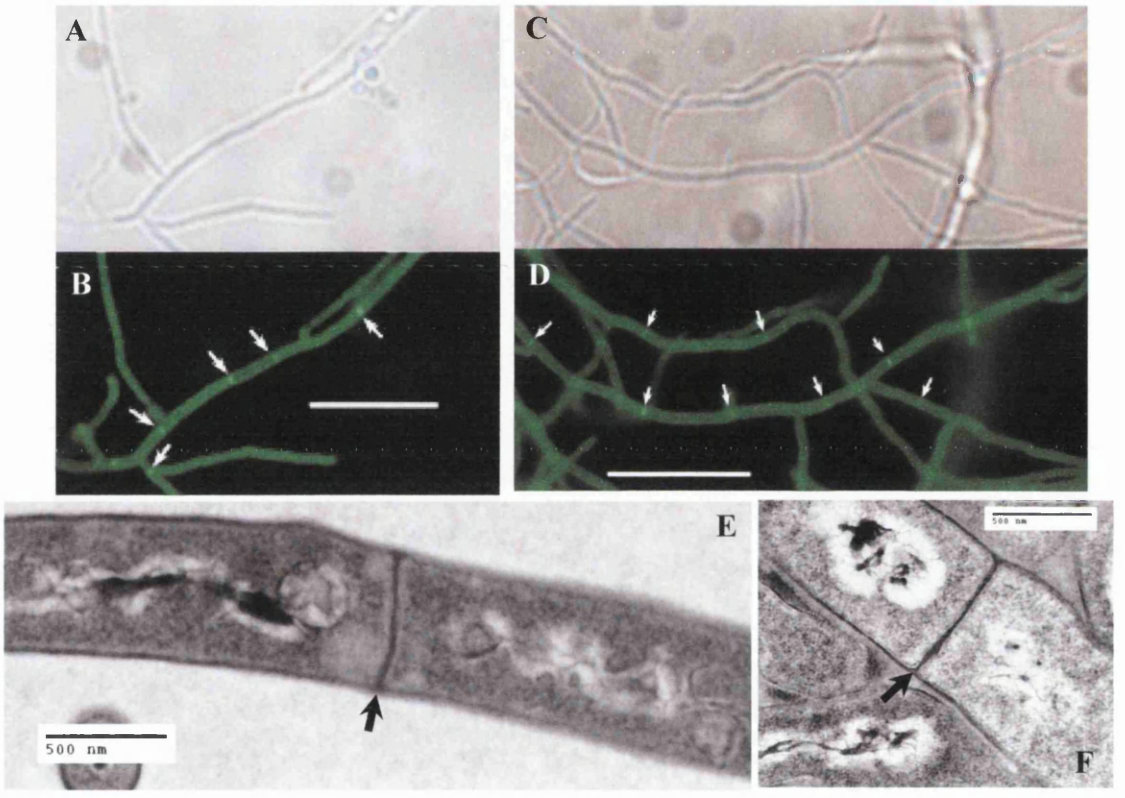

Figure 6.3: Vegetative cross-wall formation in wild type and *ftsW* mutants. Substrate mycelium from 48h grown culture of wild type and mutant strains stained with FL-vancomycin to reveal septa. Phase contrast and fluorescence microscopy (A and B) of wild type M145; (C and D) of DSCO2090-1. Transmission electron microscopy of substrate hyphae of wild type (E) and DSCO2090-1 (F) to reveal complete cross walls. Scale bar = 10 μm for panels A-D, Scale bar = 500 nm for panels E and F. Putative crosswalls in fluorescence microscopic image are shown be white arrows. Complete crosswalls in TEM samples are shown by black arrows.

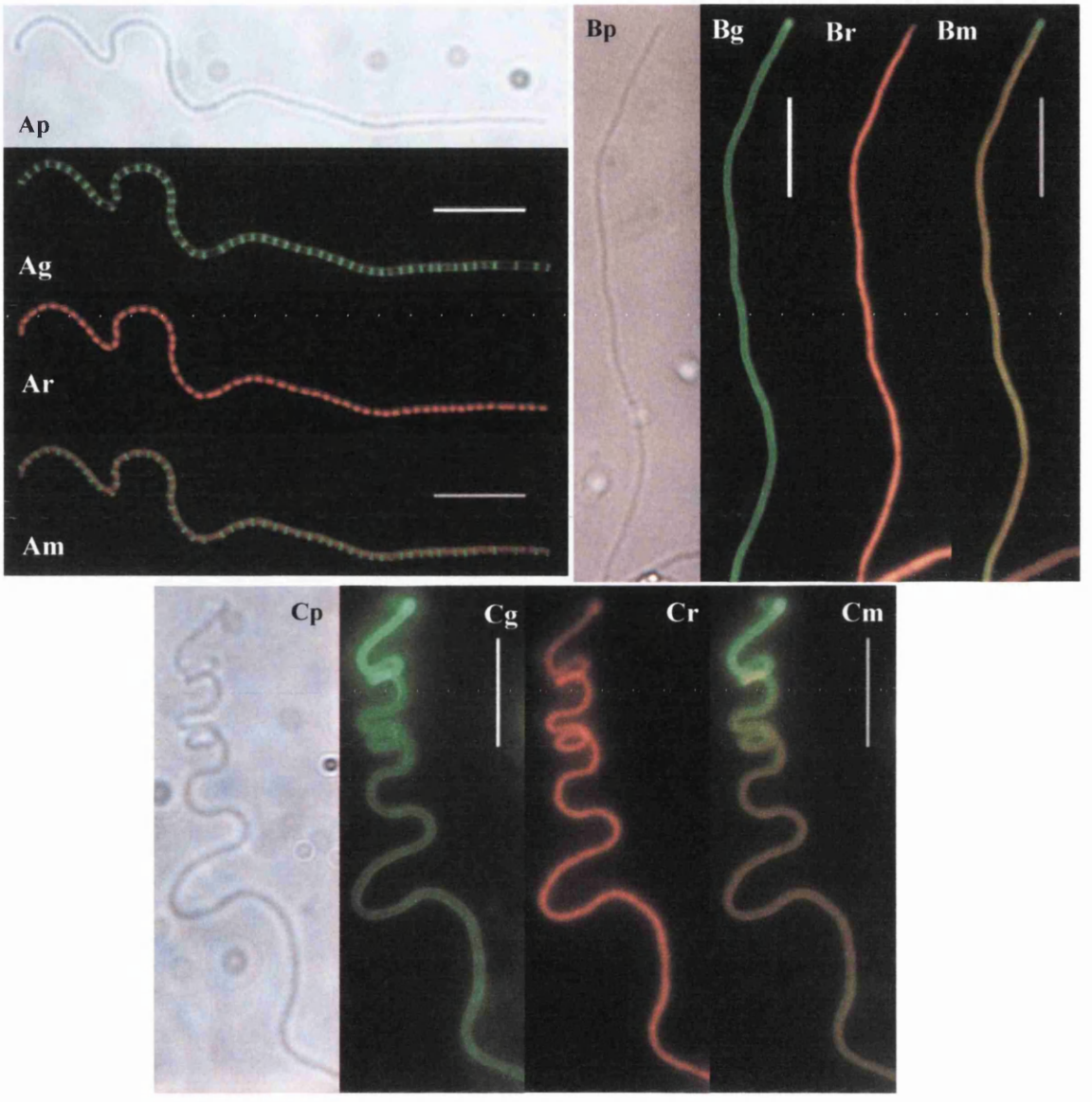

Figure 6.4: Fluorescence microscopy of aerial hyphae of parental strain *S. coelicolor* M145 and DSCO2090-1 mutant using Fluo-WGA (for cell wall) and PI (chromosomal DNA) staining to visualize sporulation septa and chromosome condensation. Impressions of each sample were taken after 38h of growth in case of wild type and after 60h or 84h in case of *ftsI* mutants at 30° C. Panel A - *S. coelicolor* M145 sporulation stage, Panel B- DSCO2090-1 (after 60h); Panel C- DSCO2090-1 (after 96h); Each panel shows phase contrast (p), Fluo-WGA staining (g), PI staining (r) and merged (m) images of Fluo-WGA and PI stained aerial hyphae of respective strains. (Scale bar = 10 μm)

As for *ftsW* mutants, atomic force microscopy (AFM) of the aerial hyphae of the *ftsI* mutant also revealed a smooth, continuous layer of hydrophobic proteins, rodlins and chaplins (Fig. 6.5 B).

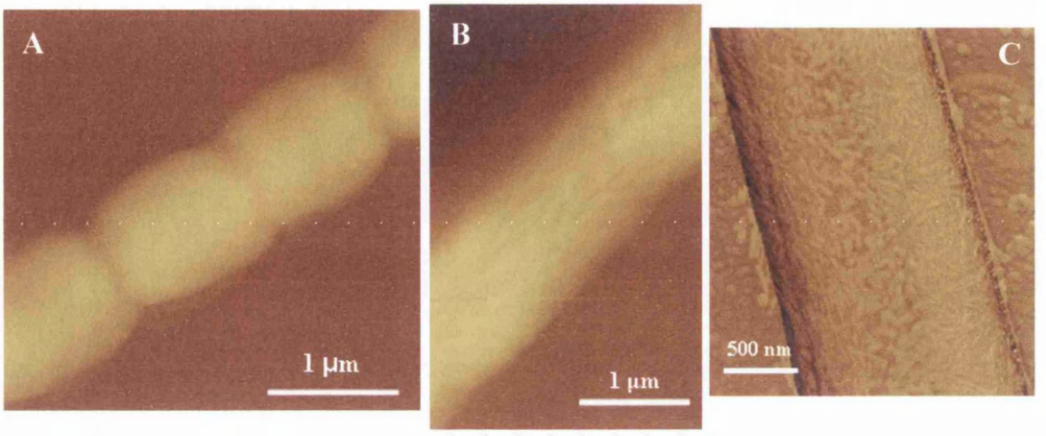

Figure 6.5: Atomic force microscopy of wild type strain M145 (A) and *ftsI* mutant strain DSCO2090-1 (B & C) revealing external features of the hyphae. The 'height' images (A & B) obtained using tapping mode revealed indented hyphae of septating wild-type (A) and smooth hyphae of non-septating *ftsI* mutant (B). Image C is the phase image of *ftsI* mutant showing rodlins and chaplins layer. Cultures were grown on SFM medium at 30° C for four days.

6.5 Analysis of FtsZ-EGFP distribution in *ftsI* mutant

As the *ftsW* mutants were shown to block cell division during the early stage of Z-ring assembly and there is similarity in the microscopic phenotype of *ftsW* and *ftsI* mutants, EGFP-tagged FtsZ was expressed in the *ftsI* mutant and compared with that in the wild type to address the effect of *ftsI* disruption on FtsZ distribution and Z-ring stabilization. The plasmid, pKF41, containing *ftsZ* fused with *egfp* was introduced into *ftsI* mutant strain DSCO2090-1 by applying the same approach as described for FtsZ-EGFP expression in *ftsW* mutant. The *ftsI* mutant strain containing pKF41 was designated as DSCO2090-1/pKF41. To observe the FtsZ-EGFP distribution in the vegetative mycelium of wild type and *ftsI* mutant, respective strains containing pKF41 were grown on either SFM or 2×YT agar medium with an acute angle coverslip for 36-48h at 30° C. Each sample was then directly observed under the microscope. As shown in the previous chapter, normal Z-rings distributed irregularly were observed in the

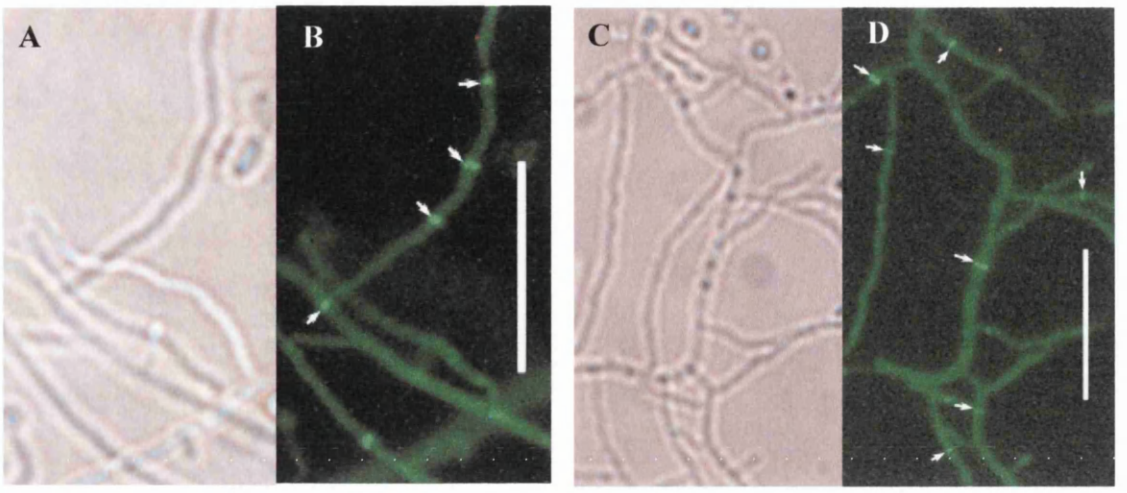

Figure 6.6: Distribution of FtsZ-EGFP in vegetative mycelium of wild type and *ftsI* mutant. Substrate mycelium from 48h old culture of M145/pKF41 and DSCO2090-1/pKF41 grown on SFM or 2×YT agra medium were observed under fluorescence microscope. Phase contrast and fluorescence microscopy (A and B) of M145/pKF41; (C and D) of DSCO2090-1/pKF41 showing FtsZ rings. Some of the FtsZ rings are indicated by white arrows. Scale bar = 10 μm.

vegetative mycelium of M145/pKF41 strain (Fig. 6.6 A). A similar distribution of FtsZ-EGFP was also observed in the vegetative mycelium of the DSCO2090-1/pKF41 strain, confirming that FtsI is not involved in Z-ring stabilization during vegetative septation (Fig. 6.6B).

For the analysis of FtsZ-EGFP distribution in the aerial hyphae of M145/pKF41 and DSCO2090-1/pKF41 strains, the M145/pKF41 strain was grown on the surface of SFM agar for 36h while the DSCO2090-1/pKF41 strain was grown on the same medium for 60h to 96h. Impressions of each sample were taken on coverslips after appropriate incubation period and the samples were directly observed under the microscope. As described earlier, a typical progression of FtsZ-EGFP from being diffuse during an early developmental stage to forming spiral like structures and then multiple regularly spaced Z-rings was observed in aerial hyphae of the wild type strain containing pKF41 (Fig. 6.7 A-B & Fig. 5.10 in chapter 5). In contrast, the aerial hyphae of the DSCO2090-1 mutant containing pKF41 showed only diffuse fluorescence or FtsZ-EGFP spirals, but no Z-rings were observed, similar to *ftsW* mutants, even after extended period of growth up to 96h (Fig. 6.7 C-F). This result and the result of FtsZ-EGFP distribution in the *ftsW* mutant suggest that both FtsW and FtsI are directly or

indirectly involved in the stabilization of Z-ring during the sporulation septation in *S. coelicolor*.

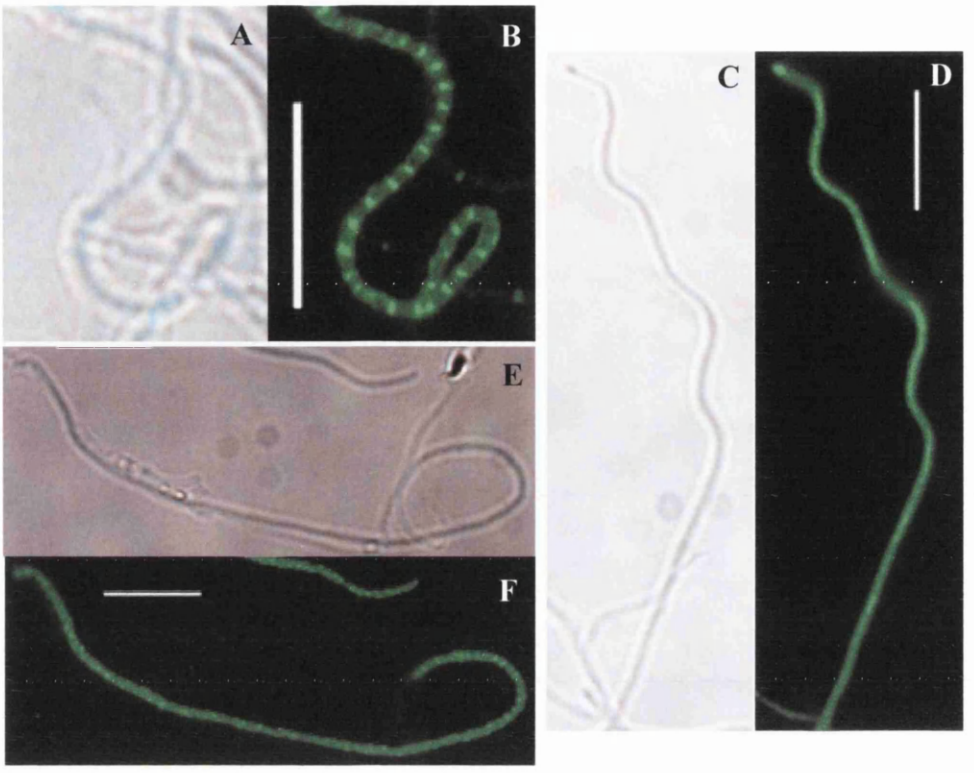

Figure 6.7: Phase contrast and fluorescence microscopy showing the assembly of FtsZ-EGFP in aerial hyphae of wild type and *ftsI* mutant. Regular Z rings could be observed in older aerial hyphae (36h) of M145/pKF41 (A and B). Diffuse fluorescence (C and D) or spiral structures (E and F) were observed, but not Z-ring in the aerial hyphae of DSCO2090-1/pKF41 mutant even after prolonged incubation. Images of DSCO2090-1/pKF41 shown were taken after 60h (C and D) and 84h (E and F). (Scale bar = 10 μm)

6.6 Complementation analysis of *ftsI* mutants

Initially, to complement *ftsI* mutants, pSFTI1 integrating plasmid containing *ftsI, ftsL, SCO2092* and the 449 bp intergenic sequence upstream of the GTG start codon of *SCO2092* was constructed with the likelihood of the possible promoter of *ftsI* being within the region in the fragment that is upstream to the *ftsI* gene (Fig. 6.8). To construct pSFTI1, a 3953 bp *Eco*RI fragment containing *ftsI, ftsL, SCO2092* and 449 bp intergenic was excised from cosmid SC4A10 with a Tn*5062* insertion at position 24916 and cloned into pBluescript II SK (+) creating pBSI1 (Fig. 6.8). The *SCO2092, ftsL* and

ftsI fragment from pBSI1 was subsequently subcloned as a 3987 bp *EcoRV-XbaI* fragment into similarly digested pSH152, to create pSFTI1 (Fig. 6.9).

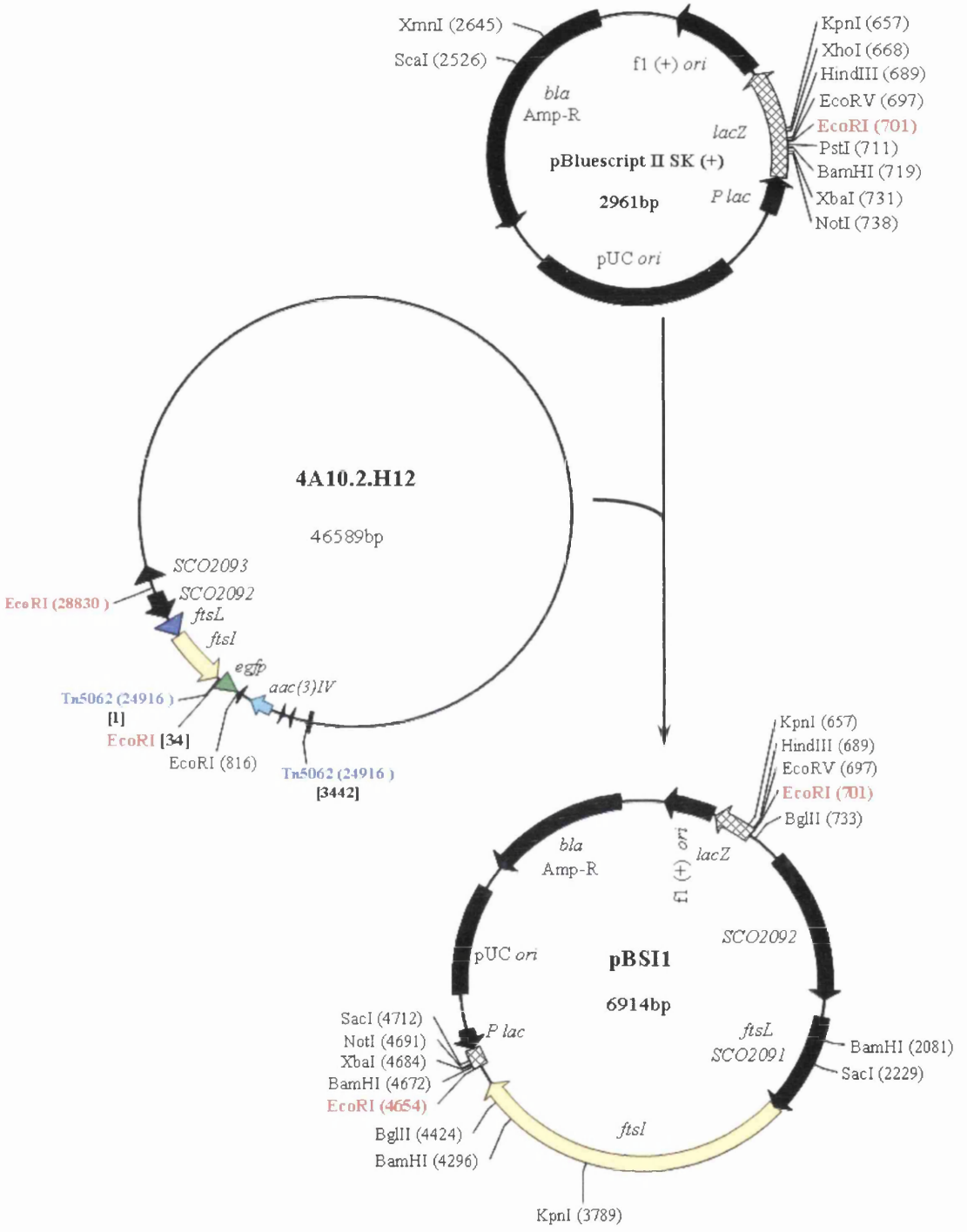

Figure 6.8: Plasmid and cosmid maps used to construct pBSI1 plasmid. An *EcoRI* (red) fragment from 4A10.2.H12 cosmid insertion was cloned into pBluescript II SK (+) at its unique *Eco*RI (red) site to construct pBSI1. Position of cosmid insertion in the map of 4A10.2.H12 cosmid insertion is shown with blue colour. Numbers is the square bracket represents the stare and end site of the Tn*5062* and the position of *Eco*RI site within the Tn*5062*. Maps are not drawn to the scale.

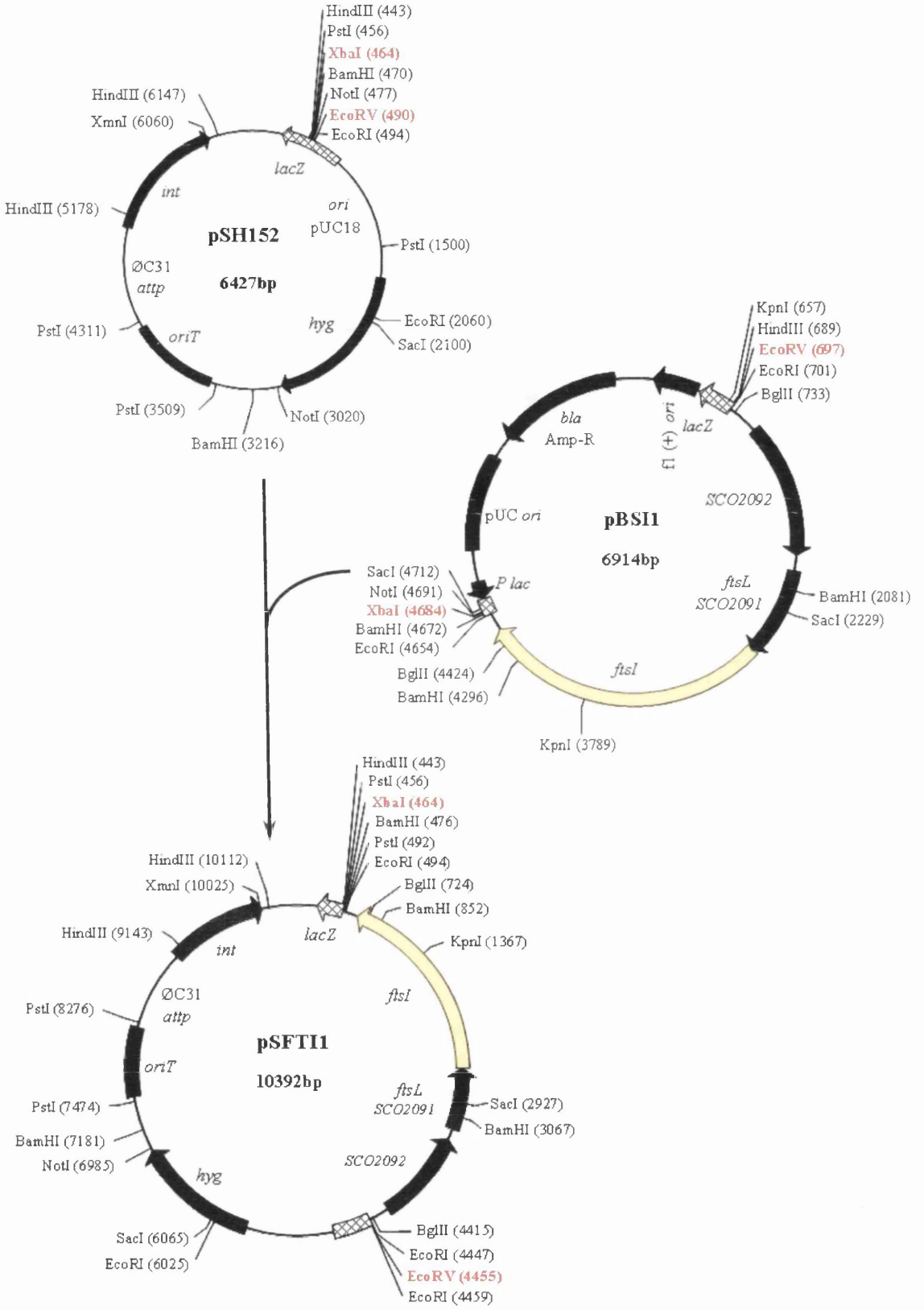

Figure 6.9: Plasmid maps showing the construction of pSFTI1 plasmid. An *Eco*RV-*Xba*I (red) fragment from pBSI1 was cloned into pSH152 digested with same enzymes to construct pSFTI1. Maps are not drawn to the scale.

To complement *ftsI* mutants, pSFTI1 was introduced into *ftsI* mutants by intergeneric conjugal transfer and exconjugants were screened for hygromycin resistance. The resulting strains of *ftsI* mutants with pSFTI1 were designated as CDSCO2090-11 (DSCO2090-1 with pSFTI1) and CDSCO2090-21 (DSCO2090-2 with pSFTI1). The strains were characterized for complementation by growing them on SFM agar along with the wild type, respective *ftsI* mutant and *ftsI* mutant with the empty vector pSH152 for 3 days at 30° C. Introduction of pSFTI1 into *ftsI* mutants did not restore the non-sporulating white phenotype of the mutants (Fig. 6.12 and 6.13 C-D). This could imply that either a critical promoter for the operon containing *ftsI* is located further upstream of the 449 bp intergenic region or there is a polar effect of the Tn*5062* insertion within the *ftsI* gene on the downstream gene *murE,* which encodes an essential enzyme involved in the cytoplasmic synthesis of peptidoglycan monomer. Interestingly, in *E. coli* it was shown that a promoter for the essential gene $ftsI_{Ec}$ (*ftsI* gene of *E.coli*) was precisely localized 1.9 kb upstream from this gene (Hara *et al.*, 1997). As the *dcw* gene cluster is highly conserved among the bacteria, it may be possible that the promoter of *S. coelicolor ftsI* gene is located a similar distance upstream from the *ftsI* gene. If this is true then the region immediately upstream to the *ftsI* gene in a 3953 bp *Eco*RI fragment of pSFTI1 plasmid construct is just 1863 bp long, which is slightly shorter than the possible location of the promoter. Therefore, assuming that the promoter of *S. coelicolor ftsI* gene is also located at least 1.9 kb upstream a new plasmid, pSFTI3, with longer fragment including more than 1.9 kb upstream region of *ftsI* was constructed as follows. A 7081 bp *Xmn*I fragment containing the putative operon of *ftsI*, *ftsL* and *SCO2092* genes, the divergently transcribed *SCO2093* and the apramycin resistance of Tn*5062* was obtained from the same cosmid as mentioned above and cloned into pSH152 digested at its unique *Eco*RV site (Fig. 6.10). The recombinant plasmid was screen for apramycin resistance to obtain pSFTI2 (Fig. 6.10). The Tn*5062* sequence was deleted by digesting pSFTI2 with *Xba*I and religated to create pSFTI3 (Fig. 6.11)

The new recombinant plasmid, pSFTI3, with a larger fragment, was then introduced into *ftsI* mutants by applying the same protocol of intergeneric conjugal transfer. The exconjugants were screened for hygromycin resistance and the resulting strains for *ftsI* mutants containing pSFTI3 were designated as CDSCO2090-13 (DSCO2090-1 with pSFTI3) and CDSCO2090-23 (DSCO2090-2 with pSFTI3).

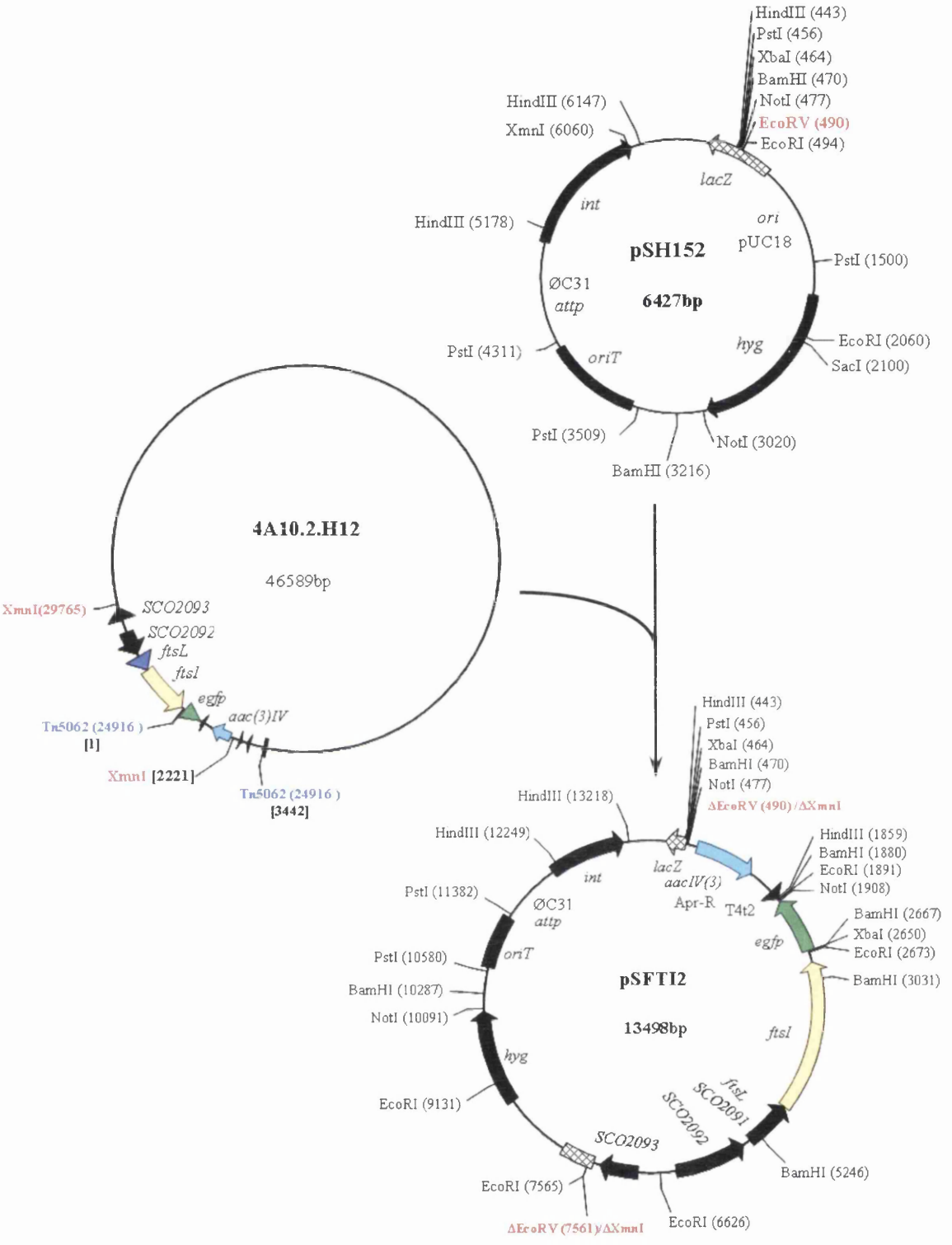

Figure 6.10: Plasmid and cosmid maps used to construct pSFI2. An *Xmn*I (red) fragment from 4A10.2.H12 cosmid insertion was cloned into pSH152 at its unique *Eco*RV (red) site to construct pSFTI2. Position of cosmid insertion in the map of 4A10.2.H12 cosmid insertion is shown with blue colour. Numbers is the square bracket represents the stare and end site of the Tn*5062* and the position of *Xmn*I site within the Tn*5062*. Maps are not drawn to the scale.

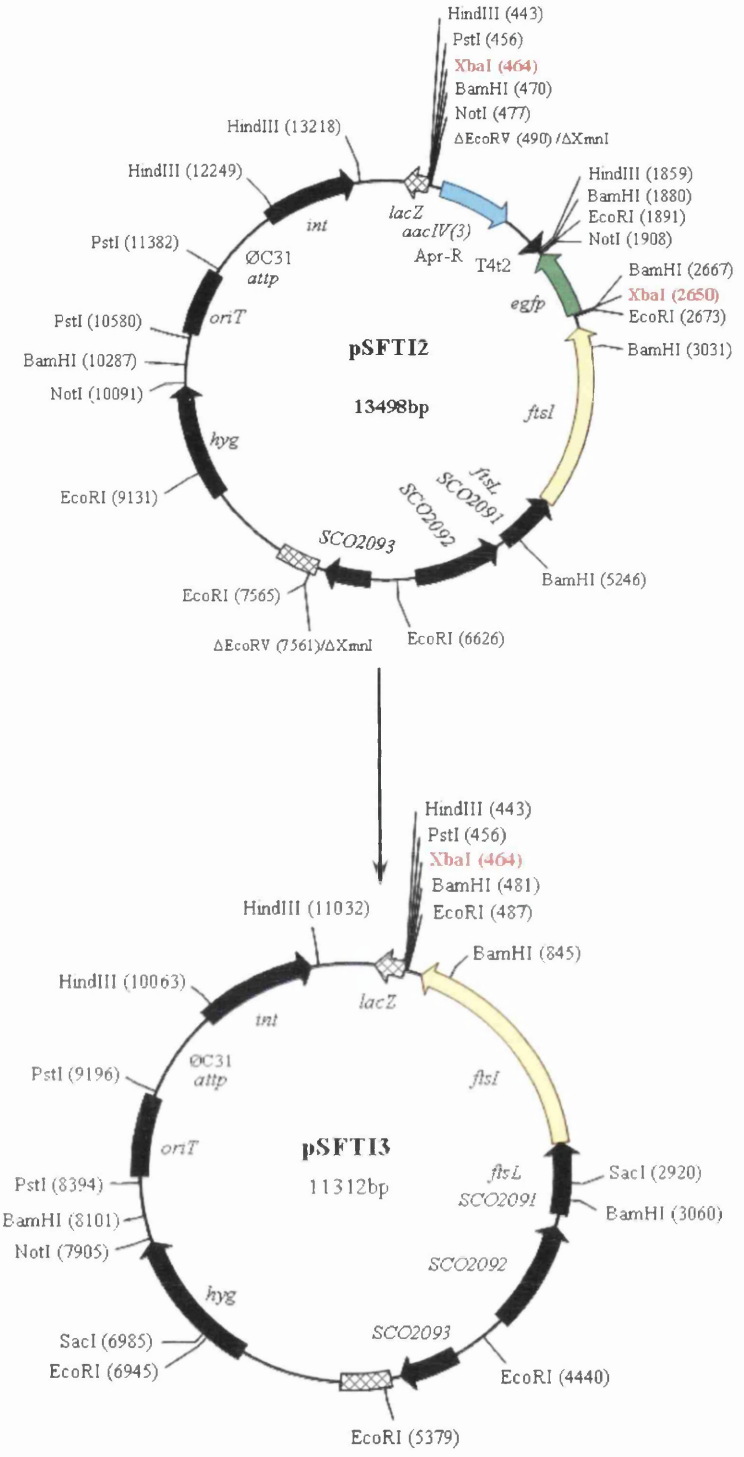

Figure 6.11: Plasmid and cosmid maps showing the construction of pSFTI3 plasmid. pSFTI2 plasmid was digested with *Xba*I (red) and religated to create pSFTI3 by remove apramycin resistance region of Tn*5062*. Maps are not drawn to the scale.

For the complementation analysis of new *ftsI* complementing strains, the cultures were grown on SFM agar medium along with the wild type, respective *ftsI* mutant, *ftsI* mutant with empty vector pSH152 and *ftsI* mutant with pSFTI1. All the cultures were cultivated at 30° C for three days. Introduction of pSFTI3 into *ftsI* mutants restored the white phenotype of the mutants (Fig. 6.12). The phenotype of *ftsI* mutant strains with empty vector, DSCO2090-1v and DSCO2090-2v was same as the mutant alone.

Figure 6.12: Complementation analysis of *ftsI* insertion mutants. Strains were grown on SFM sporulationn media for 3 days at 30° C. Wild type strain is labelled as M145; different *ftsI* mutant strains are labelled as DSCO2090-X, where X represents number (1 or 2) to indicate the respective insertion used to construct the mutants; DSCO2090-Xv, respective mutant strain with empty vector pSH152 (v); CDSCO2090-X1, respective DSCO2090-X mutant strain with pSFTI1 plasmid; CDSCO2090-X3, respective DSCO2090-X mutant strain with pSFTI3 plasmid; All the *ftsI* mutant strains containing either pSFTI3 showed complementation where as pSFTI1 failed to complement any of the *ftsI* mutants.

To check sporulation septation further in the complemented *ftsI* strains, fluorescence microscopy of CDSCO2090-11 and CDSCO2090-13 was performed. Fluorescence microscopy revealed that the CDSCO2090-13 strain formed regular sporulation septa creating pre-spore compartments with a single condensed chromosome, similar to the wild type strain (Fig. 6.13). In contrast, the aerial hyphae of CDSCO2090-11 strain were unseptated with diffuse chromosomes, similar to the mutant phenotype (Fig. 6.13). Microscopy of DSCO2090-1v (DSCO2090-1 with pSH152) was also similar to the DSCO2090-1 alone, suggesting that empty vector does

not have any effect on the phenotype of the mutant. Measurements of the dimensions of pre-spore compartments also revealed normal spore sizes with the majority of the spore lengths falling between 1 to 1.3 μm (Fig. 6.14). The average length calculated for the pre-spore compartments of CDSCO2090-13 strain was 1.1 ± 0.17 μm and the average width was 0.73 ± 0.1 μm, similar to the wild type average dimensions (Table-4.1).

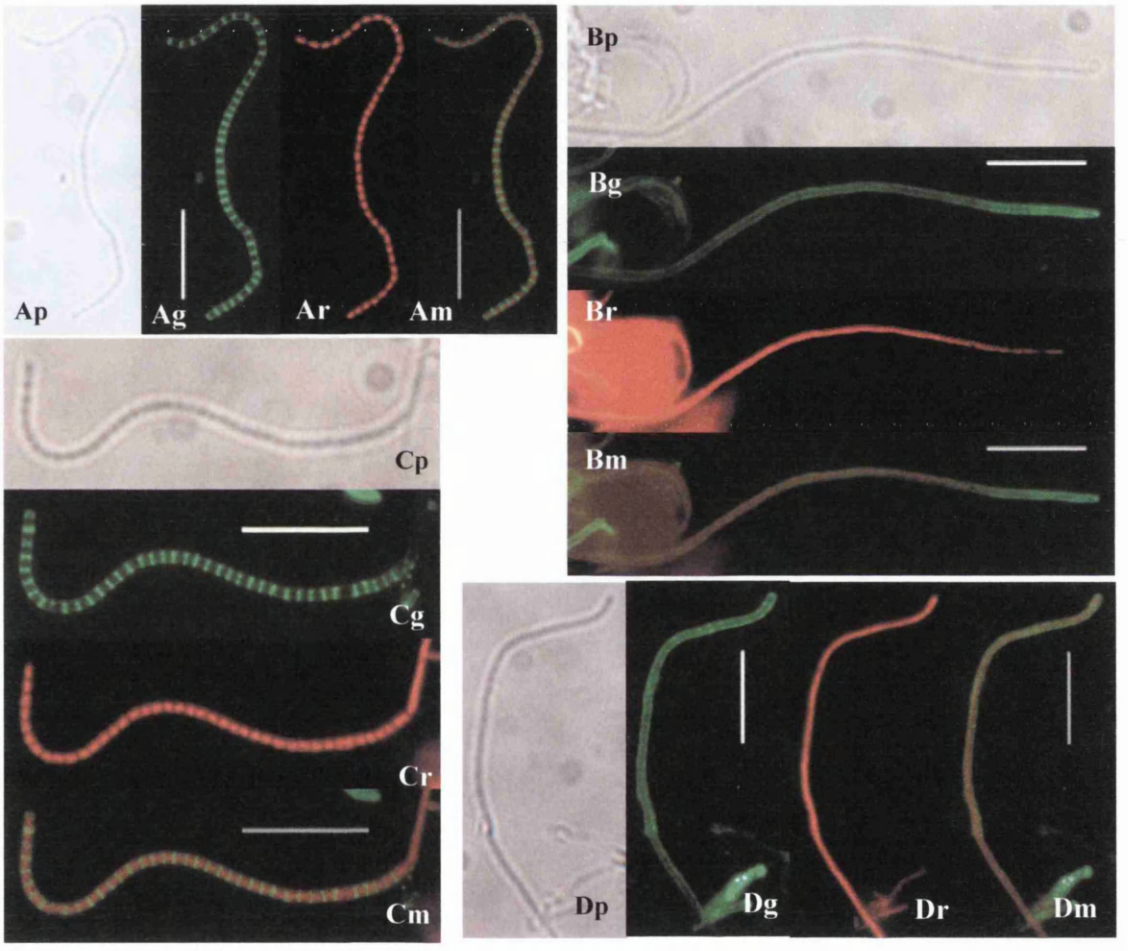

Figure 6.13: Fluorescence microscopy of aerial hyphae of parental strain *S. coelicolor* M145 (A), DSCO2090-1v (DSCO2090-1 with pSH152) (B), CDSCO2090-11 (DSCO2090-1 with pSFTI1) (C) and CDSCO2090-13 (DSCO2090-1 with pSFTI3) (D) strains. Impressions of each sample grown on SFM agar were prepared by staining the samples with Fluo-WGA (for cell wall) and PI (chromosomal DNA) to visualize sporulation septa and chromosome condensation. Wild type and CDSCO2090-13 strains were grown for 38h, whereas CDSCO2090-11 was grown for 75h at 30° C. Each panel shows phase contrast (p), Fluo-WGA staining (g), PI staining (r) and merged (m) images of Fluo-WGA and PI staining of aerial hyphae of respective strains. (Scale bar 10 μm)

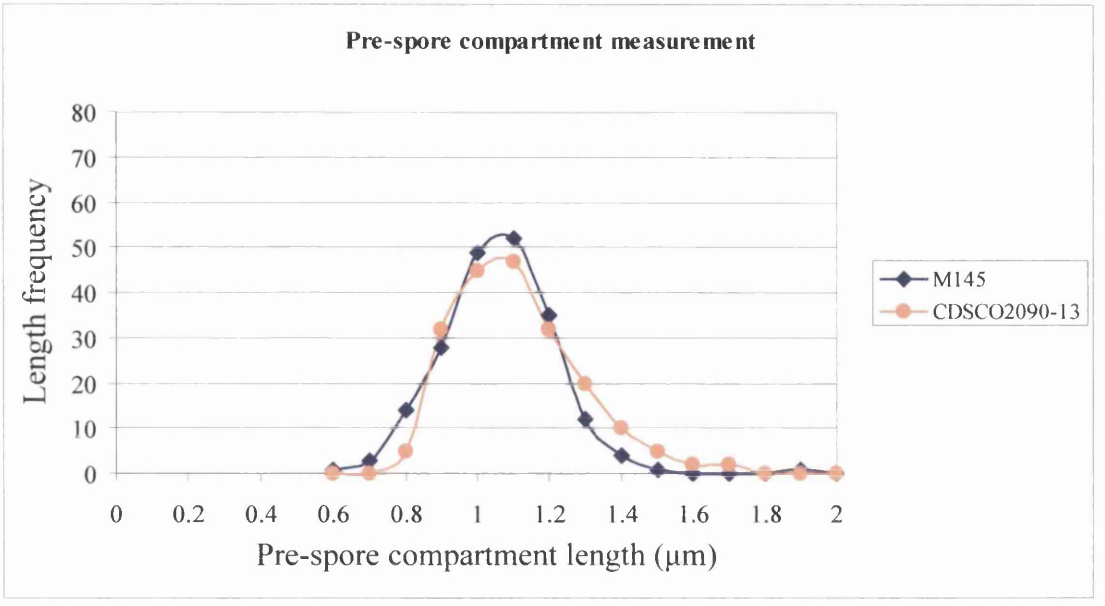

Figure 6.14: Graph of pre-spore compartment length versus frequency of the length of pre-spore compartment in wild type and CDSCO2090-13 strains. The length of randomly selected 200 pre-spore compartments of each strain was measured from the Fluo-WGA stained images using Scion Image software.

6.7 Summary

Inactivation of *ftsI* in *S. coelicolor* resulted in a white non-sporulating phenotype similar to *ftsW* disruption. Microscopic analyses of the *ftsI* mutants revealed that they are defective in synthesis of sporulation septa. The condensation of chromosomes in the aerial hyphae was also affected due to *ftsI* disruption. Vegetative septation was not affected in these mutants suggesting the FtsI is not required for synthesis of vegetative septa. Diffuse or spiral like structures of FtsZ-EGFP were observed in the aerial hyphae of *ftsI* mutants, indicating that FtsI is directly or indirectly required for Z-ring stabilization. Normal Z-rings were observed in the vegetative hyphae of these mutants. To complement the *ftsI* mutant a larger fragment of the *ftsI* locus including *SCO2093* gene was required, suggesting the possible promoter for *ftsI* is located far upstream of the gene itself.

Chapter - 7

Analysis of *ftsQ* function of *Streptomyces coelicolor*

7.1 Introduction

Previously it was shown that *ftsQ* is required for efficient sporulation in *S. coelicolor* (McCormick and Losick, 1996). However, the specific stage of sporulation septation during which it functions is not known. *In situ* localization studies of FtsZ-EGFP in *ftsW* and *ftsI* disruption mutants revealed that the proteins encoded by both the genes have some role in Z-ring stabilization during sporulation septation. The pivotal role of both FtsW and FtsI in stabilising Z-rings in the aerial hyphae could imply that concerted assembly of all or part of the divisome is necessary for Z-ring formation. An obvious component to test if this is indeed the case was FtsQ, encoded by the third and the last gene of the cluster that commences with *ftsW*. Although, *S. coelicolor ftsQ* mutant was previously characterized, more detailed information at the level of FtsZ localization was needed to further understand the multiple septation process during sporulation septation. In an attempt to define the role of FtsQ in sporulation septation, an insertion mutant of *ftsQ* was constructed and characterized. Expression studies of FtsZ-EGFP were also carried out to study the distribution of FtsZ-EGFP in this mutant.

7.2 Construction of an *ftsQ* mutant in *S. coelicolor*

To construct an *ftsQ* disruption mutant in *S. coelicolor*, a Tn*5062* insertion 4A10.2.B05 at the position 2236542 in the chromosome was used. The mutagenesis of *ftsQ* was carried out using intergeneric conjugation as described in Chapter 4. Allelic exchange to replace wild type *ftsQ* with that of the transposon disrupted copy occurred at high frequency of 77% ex-conjugants, indicating no deleterious effects of the mutation on overall growth. To confirm the construction of successful mutants, six exconjugants of double crossover mutants were randomly selected for Southern hybridization analysis. For Southern hybridization, purified chromosomal DNA of selected *ftsQ* mutant clones and the cosmid used for mutagenesis were digested with *Sal*I restriction enzyme to obtain distinct fragments 2966 bp and 945 bp size, as calculated from positions of the transposon and respective restriction enzyme sites (Fig. 7.1A). A digoxigenin labelled Tn*5062* probe was used for hybridization of the blot. A Southern blot of all the *ftsQ* mutant clones tested showed expected sizes of DNA

fragments confirming that all the mutants were true double crossover mutants (Fig. 7.1B). Thus the *ftsQ* mutant strain obtained was designated as DSCO2083.

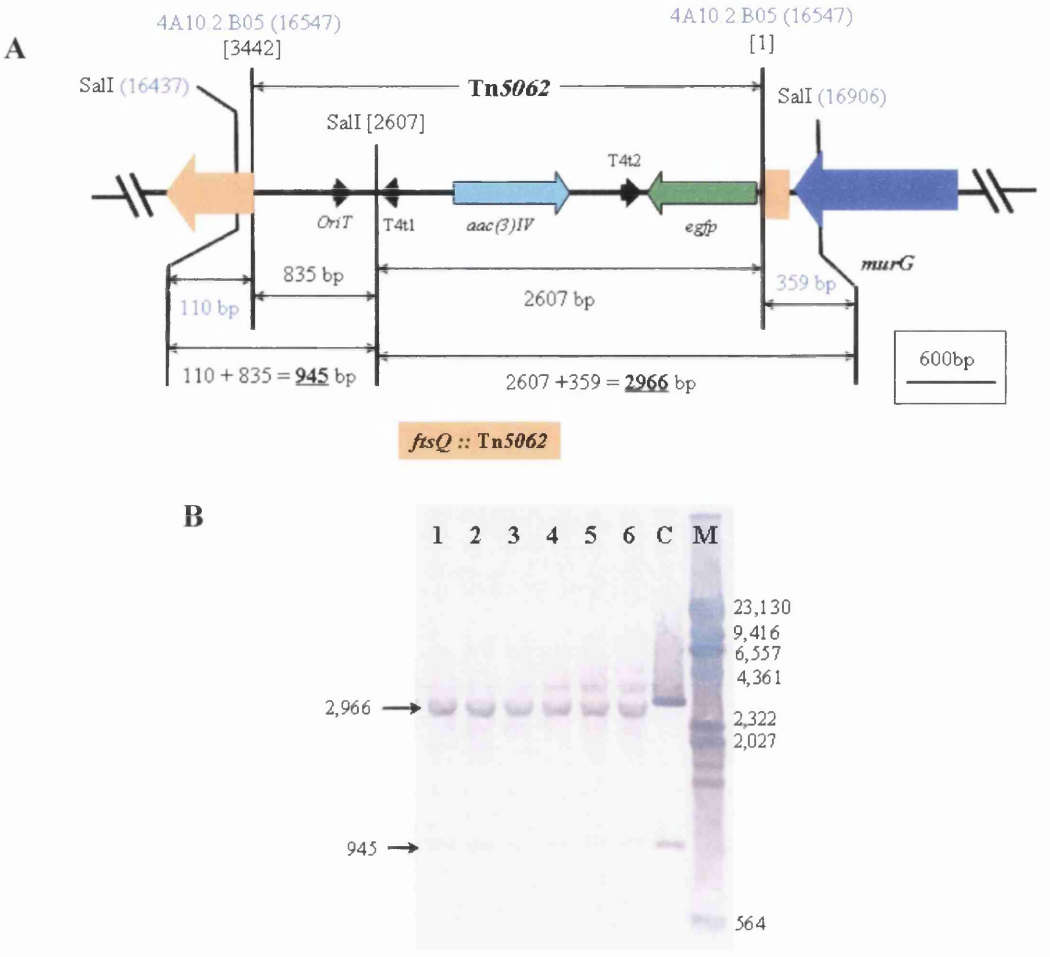

Figure 7.1: Southern Blot (SB) analysis of *ftsQ* mutant clones with 4A10.2.B05 insertion. **(A)** Diagrammatic representation of the *ftsQ* locus showing Tn*5062* insertion and *Sal*I restriction sites to calculate the size of bands that should be obtained after Southern hybridization. The cosmid insertion used for *ftsQ* mutagenesis is written in blue colour with the position of Tn*5062* insertion in the cosmid is presented in brackets. Just under the cosmid name and position, the start and end sites of Tn*5062* are written in square brackets. The position of the important *Sal*I restriction sites in *ftsQ* region of cosmid are shown in the brackets and that of in Tn*5062* region is shown in square brackets. Arrows with different colours represent different genes and their directions. Name of each respective gene is shown just under each arrow. *aac(3)IV* – Apramycin resistance; T4 t1,2 – Transcription terminator t1 & 2; *egfp* – Enhanced green fluorescent protein; *oriT* – Origin of transfer. Expected size of bands that should be obtained in SB is shown in bold letters with underline. The rectangular box shows the scale of the map. **(B)** SB of six *ftsQ* mutant clones. M –HindIII digested λ DNA marker with the size for each band presented on the left hand side; C – *Sal*I digested 4A10.2.B05 cosmid insertion; and 1 to 6 – *Sal*I digested chromosome of each *ftsQ* mutant clone. The size of each expected bands for *ftsQ* mutant is shown by arrow. Digoxigenin labelled Tn*5062* was used as a hybridization probe.

7.3 Phenotypic analysis of *ftsQ* mutant

All *ftsQ* mutant clones when grown on sporulation specific medium SFM for three days at 30° C gave a white non-sporulating phenotype (Fig. 7.2). No apparent difference in the macroscopic phenotype of *ftsQ* mutants from wild type was observed when grown on NMMP containing mannitol or sucrose, rich complex medium 2X YT and minimal medium (MM) for five days at 30° C (Fig. 7.2). There was also no difference in the production of antibiotic when grown on MM even after prolonged incubation.

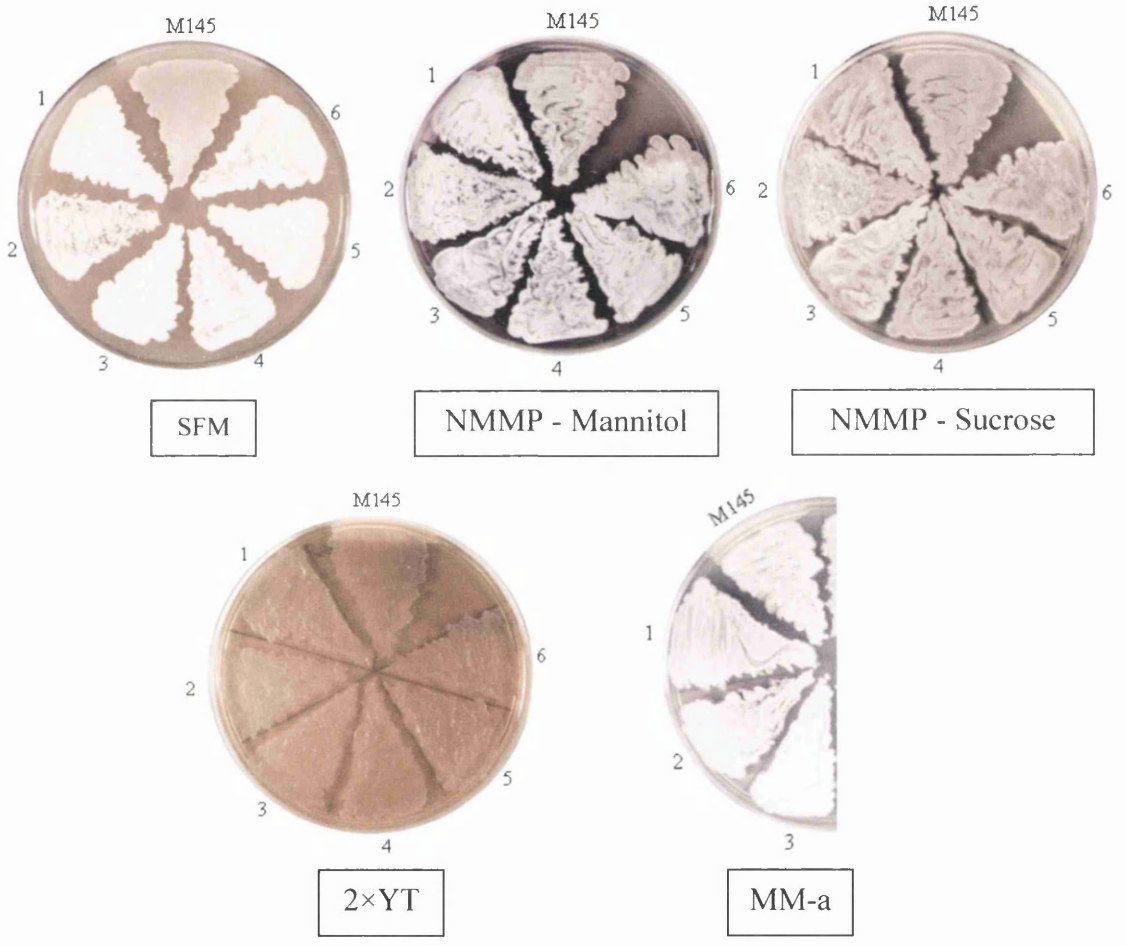

Figure 7.2: Phenotype of *ftsQ* mutant clones and their congenic parental strain *S. coelicolor* M145 on different media. Strains were grown for 5 days (3 days for cultures grown on SFM) at 30° C. Name of the medium used for characterization of the mutants is indicated in a rectangular box just below each picture of the plate. Wild type strain is designated as M145 while clones of DSCO2083 (*ftsQ*⁻) mutant are designated as number 1-6. Only three clones (1-3) are shown on minimal medium. A white non-sporulating phenotype of *ftsQ* mutants is observed on SFM grown cultures. No apparent phenotype is seen on other media tested. MM-a, Minimal medium containing L-asparagine. In minimal medium glucose was used as a carbon source.

7.4 Microscopic analysis of *ftsQ* mutant

For light and fluorescence microscopy of vegetative hyphae of wild type and *ftsQ* mutant, cultures were grown for 48h at 30° C in the acute angle of a sterile coverslips inserted obliquely in 2X YT agar medium that support little or no development of aerial hyphae. Cultures grown on acute angle coverslips were then treated with BODIPY FL vancomycin to stain nascent peptidoglycan as described in Chapter-2. Visualization of the wild type and mutant samples under the fluorescence microscope showed no difference in the pattern of FL vancomycin stained nascent peptidoglycan synthesis at the vegetative septation sites in both the wild type and mutant (Fig. 7.3 A-D).

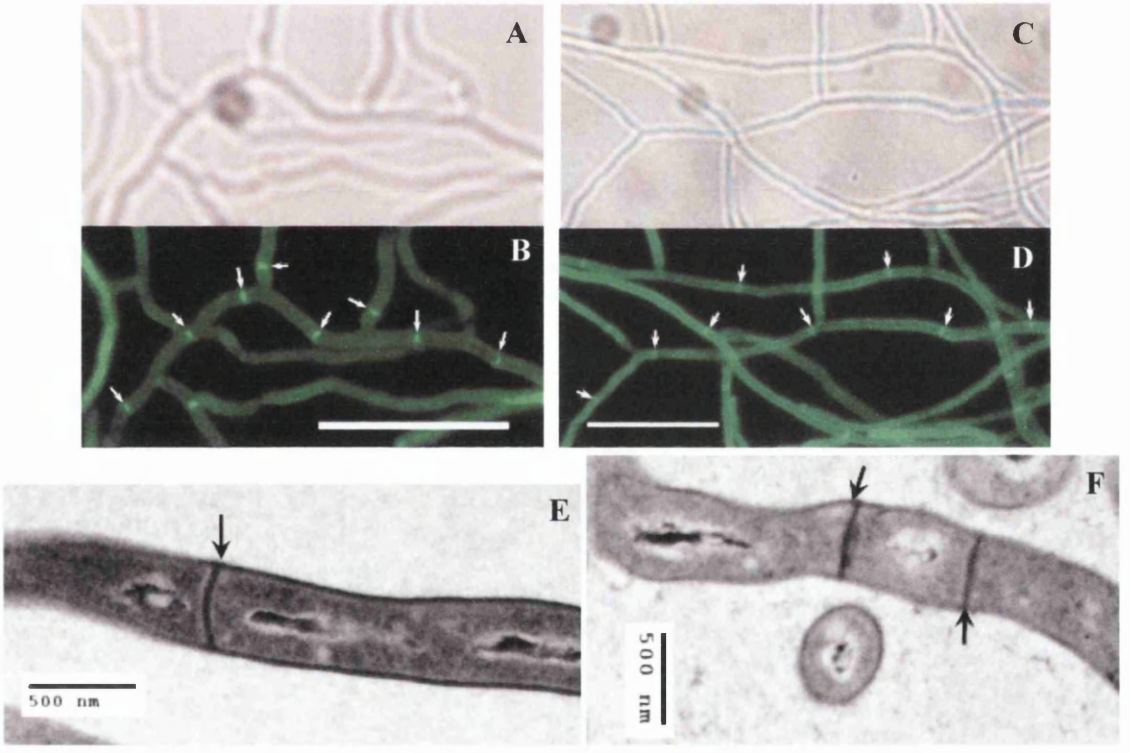

Figure 7.3: Vegetative cross-wall formation in wild type and *ftsQ* mutant. Substrate mycelium from 48h grown culture of wild type and mutant strains stained with FL-vancomycin to reveal septa. Phase contrast and fluorescence microscopy (A and B) of wild type M145; (C and D) of DSCO2083. Transmission electron microscopy of substrate hyphae of wild type (E) and DSCO2083 (F) to reveal complete cross walls. Scale bar = 10 μm for panels A-D, Scale bar = 500 nm for panels E and F. Putative crosswalls in fluorescence microscopic image are shown be white arrows. Complete crosswalls in TEM samples are shown by black arrows.

To confirm further that complete crosswalls were formed in the substrate mycelium of *ftsQ* mutant, the cultures were sent for transmission electron microscopy (TEM). TEM of vegetative hyphae of wild type and mutant revealed that complete crosswalls similar to wild type were formed in *ftsQ* mutants further confirming that FtsQ is not required for vegetative septation in *S. coelicolor* (Fig. 7.3 E & F).

To check the effect of *ftsQ* disruption on aerial hyphae, cultures of wild type and mutant were grown on the surface of SFM agar plates at 30° C for 38h (wild type) and up to 96h (*ftsQ* mutants). An impression of each culture was taken on coverslips and the samples were stained with Fluo-WGA (for peptidoglycan) and Propidium iodide (for chromosomal DNA) as described in Chapter-2. Microscopic observation of the wild type strain showed regularly spaced sporulation septa defining pre-spore compartments each containing a single condensed chromosome (Fig. 7.4 A), as described in previous chapters. On the other hand, the *ftsQ* mutant showed a wide range of atypical morphologies where the majority of aerial hyphae did not produce spores and remained undifferentiated (Fig. 7.4 B-D). Coiled and uncoiled aerial filaments that were blocked in the early stages of sporulation septation were more frequently observed (Fig. 7.4 B). Fluo-WGA staining from 3 days or older cultures also showed regularly spaced septal peptidoglycan synthesis in aerial hyphae of *ftsQ* mutants, indicating a delay in septal peptidoglycan synthesis. However, PI-staining revealed many regions of the hyphae contained diffuse or abnormally condensed nucleoids that were apparently uninterrupted by septa at the position of the Fluo-WGA stained material (Fig. 7.4 C-E). In certain locations along the length of an *ftsQ* mutant aerial hypha, however, it was evident that

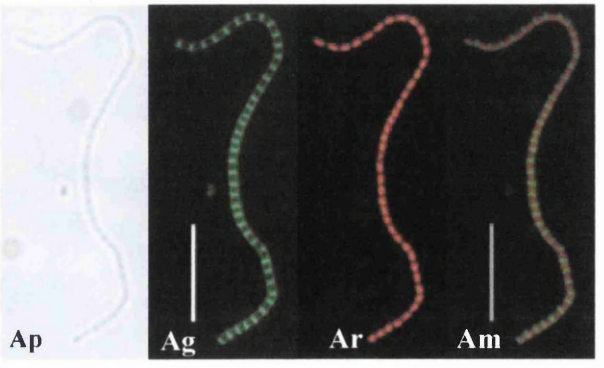

Figure 7.4: Continued on the next page....

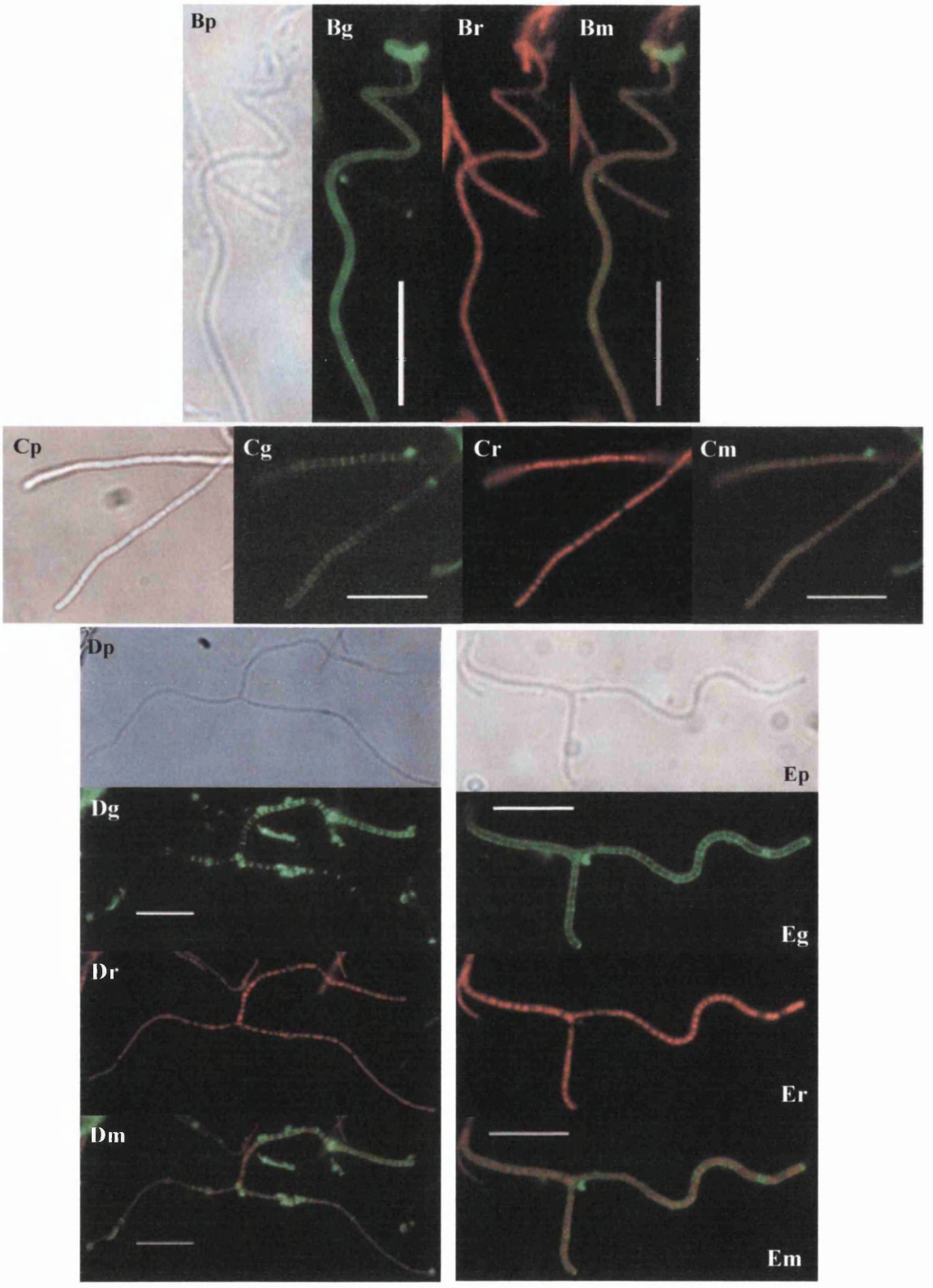

Figure 7.4: Continued on the next page….

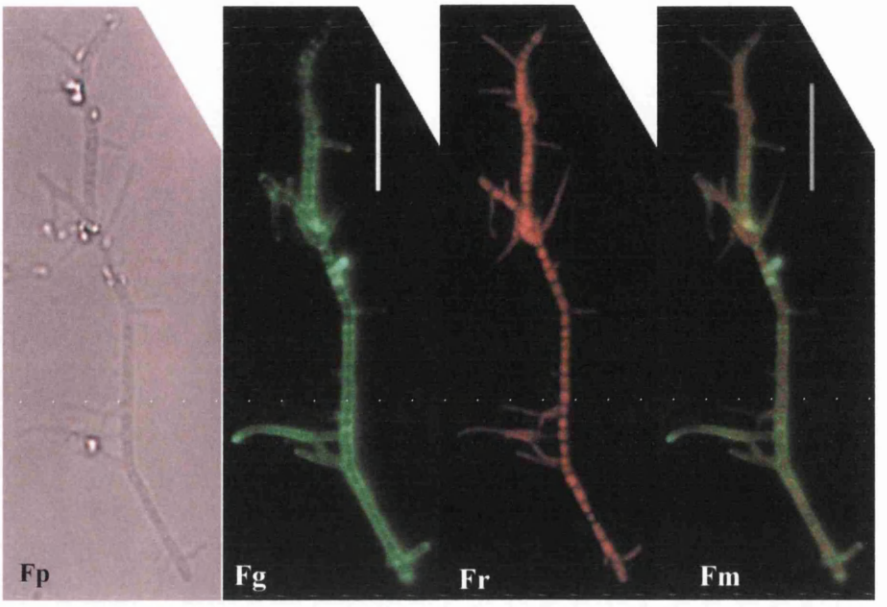

Figure 7.4: Fluorescence microscopy of aerial hyphae of parental strain *S. coelicolor* M145 and DSCO2083 mutant using Fluo-WGA (for cell wall) and PI (chromosomal DNA) staining to visualize sporulation septa and chromosome condensation. Impressions of each sample were taken after 38h of growth in case of wild type and after 60h or 86h in case of *ftsQ* mutants at 30° C. Panel A - *S. coelicolor* M145 sporulation stage, Panel B- DSCO2083 (after 60h); Panel C- DSCO2083 (after 80h); Panel D & E- DSCO2083 (after 84h); Panel F- DSCO2083 (after 96h). Each panel shows phase contrast (p), Fluo-WGA staining (g), PI staining (r) and merged (m) images of Fluo-WGA and PI stained aerial hyphae of respective strains. (Scale bar = 10 μm)

non-PI staining areas coincided with Fluo-WGA staining material, indicative of possible genuine septation in these positions. Occasionally, filaments with condensed nucleoids that are interrupted at the position of septa were also observed in *ftsQ* mutants (Fig. 7.4 E & F). Lateral branching of the aerial hyphae of *ftsQ* mutant was also observed especially after 3 to 4 days of growth. Rarely, structures like completed chains of spores were observed. Surprisingly, pre-mature germination of the pre-spore compartment like structures was also observed (Fig. 7.4 D-F).

To further investigate the aberrant pattern of septation in the *ftsQ* mutant, cultures of wild type and the *ftsQ* mutant were sent to Kim Findlay, John Innes Centre, Norwich, for transmission electron microscopy (TEM). In the TEM of the *ftsQ* mutant

aerial hyphae two types of septal structure were evident (Fig. 7.5 B). There were many incomplete 'thick' sporulation septa formed at regular intervals but not defining separate compartments and these partially formed septa were spanned by nucleoids. A second type was infrequent complete 'thin' septa resembling those of vegetative hyphae. In contrast, the wild type aerial hyphae possessed multiple regularly-placed sporulation septa (Fig. 7.5 A).

Figure 7.5: Transmission electron microscopy of aerial hyphae of *S. coelicolor* M145 (wild type) and *ftsQ* mutant. (A) Wild type strain after 48h growth showing regularly placed thick sporulation septa and condensed nucleoids, and (B) DSCO2083 after 78h growth with frequent incomplete thick sporulation septa (black arrow-head), often spanned by a nucleoid, and infrequent thin cross-wall (white arrow-head). Scale bar = 500 nm

To visualize the topography of the hyphal surfaces of mutant and wild type, atomic force microscopy of the aerial hyphae of both wild type and the *ftsQ* mutant was carried out. In both wild type (Chapter 4, Fig. 4.18) and mutant (Fig. 7.6 C) the aerial hyphae were coated with rodlet layers. Unlike the locally disrupted rodlet layer of wild type aerial hyphae (Fig. 7.6 A) that coincide with indentations at the positions of in-growing septa during sporulation septation, or smooth uninterrupted layers of *ftsW* or *ftsI* mutants (Chapter 5 & 6, respectively), the *ftsQ* mutant showed temporary extruded deformations or annuli, 25-40 nm in height, of the rodlet layers at intervals consistent with the distances between in-growing septa (Fig. 7.6 B & D).

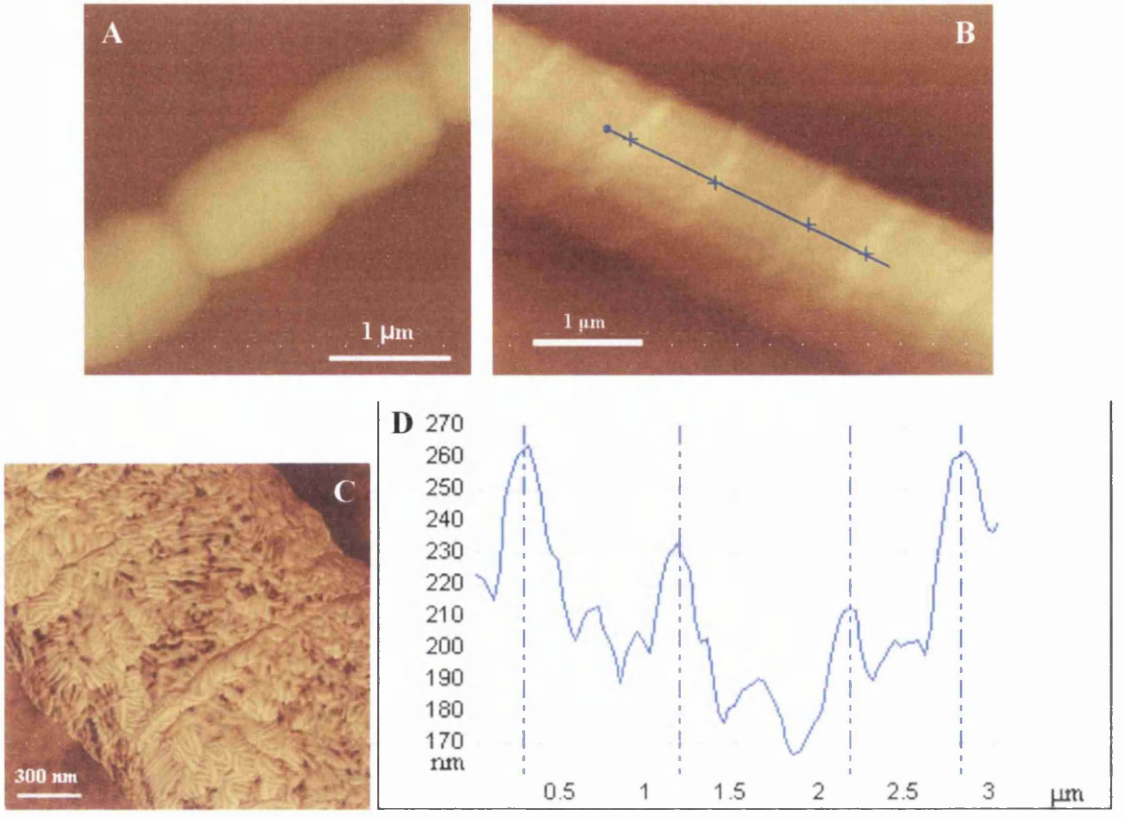

Figure 7.6: Atomic force microscopy of wild type strain M145 (A) and *ftsQ* mutant strain DSCO2083 (B & C) revealing external features of the hyphae. The 'height' images (A & B) obtained using tapping mode revealed indented hyphae of septating wild-type (A) and extruded annuli present on the surface of the *ftsQ* mutant (B). Image C is the phase image of *ftsQ* mutant showing rodlet layer. (D) Graph depicting the height profile of a section along midline of the hypha, indicated by the blue line in panel B. Cultures were grown on SFM medium at 30° C for four days.

7.5 FtsZ-EGFP distribution analysis in *ftsQ* mutant

The white phenotype and range of aberrant microscopic features of *ftsQ* mutants indicated a specific role for FtsQ during sporulation septation. To check the effect of *ftsQ* disruption on FtsZ ring formation in *S. coelicolor*, FtsZ translationally fused with EGFP was expressed in the *ftsQ* mutant as described for FtsZ-EGFP expression in *ftsW* mutant in Chapter 5. The *ftsQ* mutant strain containing pKF41 plasmid (FtsZ-EGFP fusion) was designated as DSCO2083/pKF41. For the visualization of FtsZ rings in vegetative mycelium of wild type (M145/pKF41) and the

ftsQ mutant (DSCO2083/pKF41), both the strains were grown separately at 30° C for 36-48 h on SFM or 2X YT agar medium with acute angle coverslips. The samples were directly observed under the fluorescence microscope. Fluorescence microscopy of vegetative mycelium of both wild type and mutant showed irregularly distributed Z-rings (Fig. 7.7). This observation suggests that FtsQ as well is not required for Z ring formation and subsequent cross wall formation during vegetative growth of *S. coelicolor.*

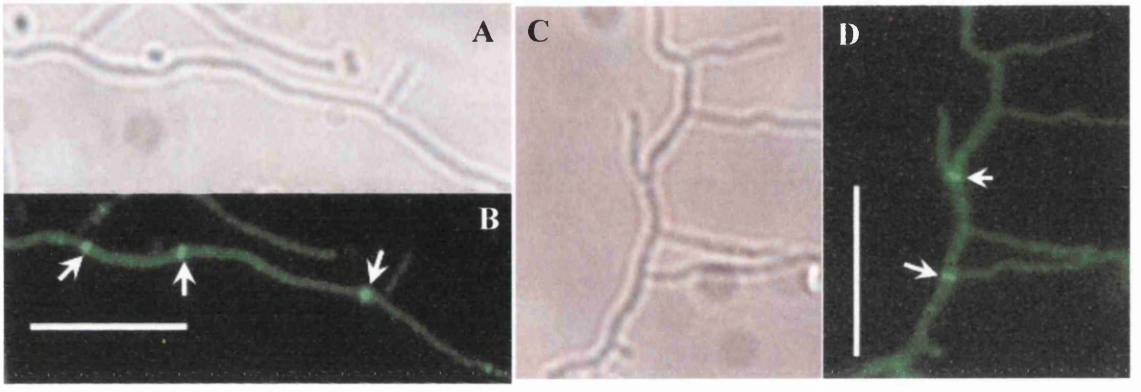

Figure 7.7: Distribution of FtsZ-EGFP in vegetative mycelium of wild type and *ftsQ* mutant. Substrate mycelium from 48h old culture of M145/pKF41 and DSCO2083/pKF41 grown on SFM or 2×YT agar medium were observed under fluorescence microscope. Phase contrast and fluorescence microscopy (A and B) of M145/pKF41; (C and D) of DSCO2083/pKF41 showing irregularly spaced FtsZ rings. The FtsZ rings are indicated by white arrows. Scale bar = 10 μm.

To visualize the distribution of FtsZ-EGFP in aerial hyphae of wild type and mutant strains, impressions of each strain grown on SFM agar at 30° C for 36 h (wild type) or for 60 h to 84h (*ftsQ* mutant) were taken and observed under the fluorescence microscope directly after mounting the samples on slides. As described in the Chapter 5, a typical assembly dynamic of FtsZ-EGFP (from diffuse to spirals to regularly spaced rings) was observed in the aerial hyphae of wild type strain (Fig. 7.8 A & B). On the other hand, Z ring formation was delayed and the assembly of Z rings was less synchronous in the *ftsQ* mutant aerial hyphae (Fig. 7.8). Diffuse fluorescence was observed in the cultures grown for around 60 hours. After around 70 h of growth spiral structures started to appear. Proper Z rings were usually observed in the cultures grown

between 72 to 84 h. Thus, the formation of Z rings in *ftsQ* mutant indicates that FtsQ is not essential for Z ring assembly.

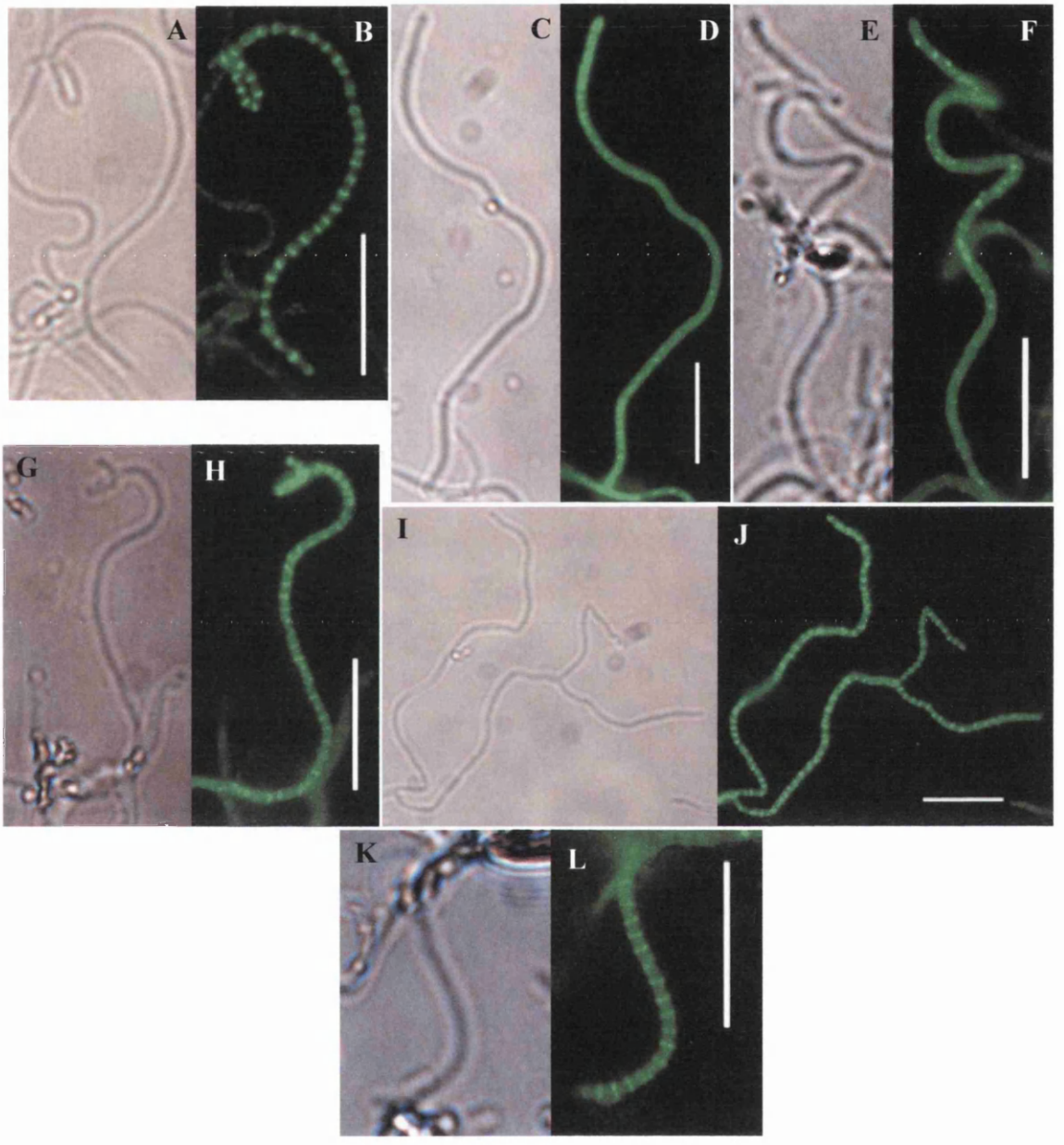

Figure 7.8: Phase contrast and fluorescence microscopy showing the assembly of FtsZ-EGFP in aerial hyphae of wild type and *ftsQ* mutant. Regular Z rings could be observed in older aerial hyphae (36h) of M145/pKF41 (A and B) grown for 38 h. Delayed Z ring formation was apparent in *ftsQ* mutant (DSCO2083/pKF41) grown for 60-78 h. Diffuse fluorescence (C and D) in the *ftsQ* culture grown for 60-66 h; spiral structures (E and F) in the culture grown for 70 h; and spirals or Z rings (G-L) in culture grown for 72-80 h. (Scale bar = 10 μm)

7.6 Complementation of the *ftsQ* mutant

For complementation analysis of the *ftsQ* mutant, pSHBW1, carrying the complete gene cluster consisting of *ftsW*, *murG* and *ftsQ*, and pSHBW12 plasmid with the *ftsW* in-frame deletion were used. Construction of both plasmids is described in Chapter 5 section 5.6. Another complementing plasmid, pSHBW7 containing only the *ftsQ* gene, was also constructed from pSHBW1 for complementation analysis. To generate pSHBW7, pSHBW1 was digested with *Bam*HI and a 4673 bp fragment, containing *ftsQ*, part of *murG*, the origin of plasmid replication and the hygromycin resistance marker, and a 3681 bp fragment, containing *oriT* and the ØC31 attachment site, were purified and re-ligated (Fig. 7.9).

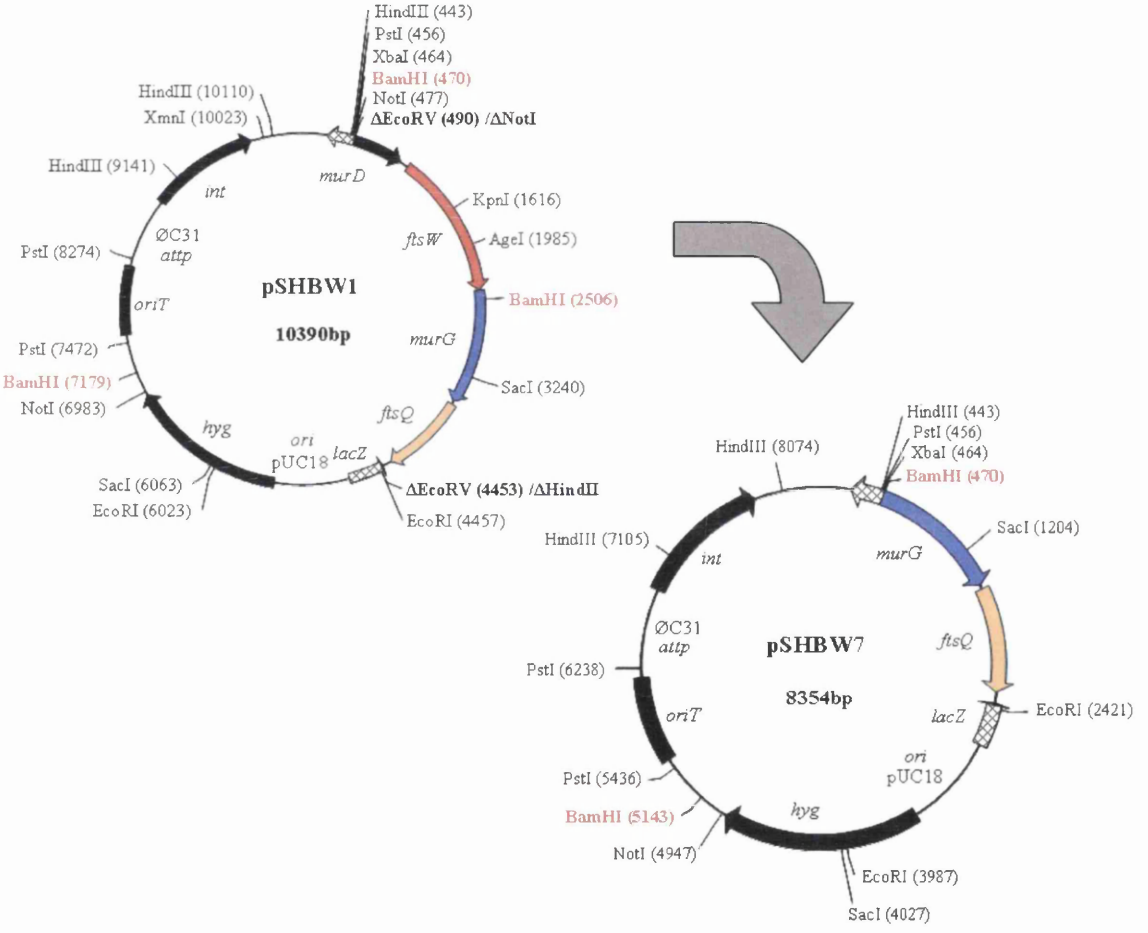

Figure 7.9: Plasmid maps showing the construction of pSHBW7 plasmid. pSHBW1 was digested with *Bam*HI (red) and 4673 bp and 3681 bp fragments were purified and religated to obtain pSHBW7. Maps are not drawn to the scale.

Each of the three complementing plasmids (pSHBW1, pSHBW12 and pSHBW7) was introduced independently into the *ftsQ* mutant using intergeneric conjugation as described earlier. An empty vector pSH152 was also introduced separately as a control. The mutant strain, with pSHBW1 was designated as CDSCO2083-1, with pSHBW12 was designated as CDSCO2083-2, with the pSHBW7 was designated as CDSCO2083-7 and with the empty vector was designated as DSCO2083v. Introduction of pSHBW1 or pSHBW12 into the *ftsQ* mutant restored the wild type phenotype of *ftsQ* mutants (Fig. 7.10). A plasmid, pSHBW7, lacking *ftsW* and part of *murG* could also complement (Fig. 7.10), although the strain developed dark grey spores slightly later than the wild-type or mutant complemented with either pSHBW1 or pSHBW12. This could indicate that expression of *ftsQ* in pSHBW7 is affected due to loss of one or more upstream promoters.

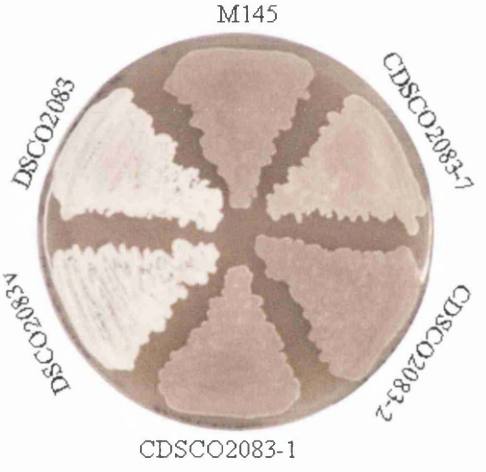

Figure 7.10: Complementation analysis of *ftsQ* mutants. Strains were grown on SFM sporulation media for 3 days at 30° C. Labelling of the plate is: M145, Wild type strain; DSCO2083, *ftsQ* mutant; DSCO2083v, *ftsQ* mutant with empty vector pSH152; CDSCO2083-1, with complementing plasmid pSHBW1; CDSCO2083-2, with complementing plasmid pSHBW12; and CDSCO2083-2, with complementing plasmid pSHBW7. The non-sporulating phenotype of the *ftsQ* mutant was restored by genetic complementation with pSHBW1, pSHBW12 or pSHBW7.

To confirm further the complementation, fluorescence microscopy of CDSCO2083-2 and CDSCO2083-7 strains was carried out using WGA-PI staining as described previously. Microscopic analysis of both the complementing strains showed

normal unigenomic pre-spore compartments defined by the sporulation septa stained green with WGA and each compartment containing a condensed chromosome stained red with PI (Fig. 7.11). The spore dimensions of complementing strains CDSCO2083-2 and CDSCO2083-7 were also similar to those of the wild type with an average spore length 1.16 ± 0.16 μm and 1.12 ± 0.20 μm, respectively (Fig. 7.12). Thus, the complementation analysis of *ftsQ* mutant suggests that the phenotype of the mutant is due to loss of *ftsQ*.

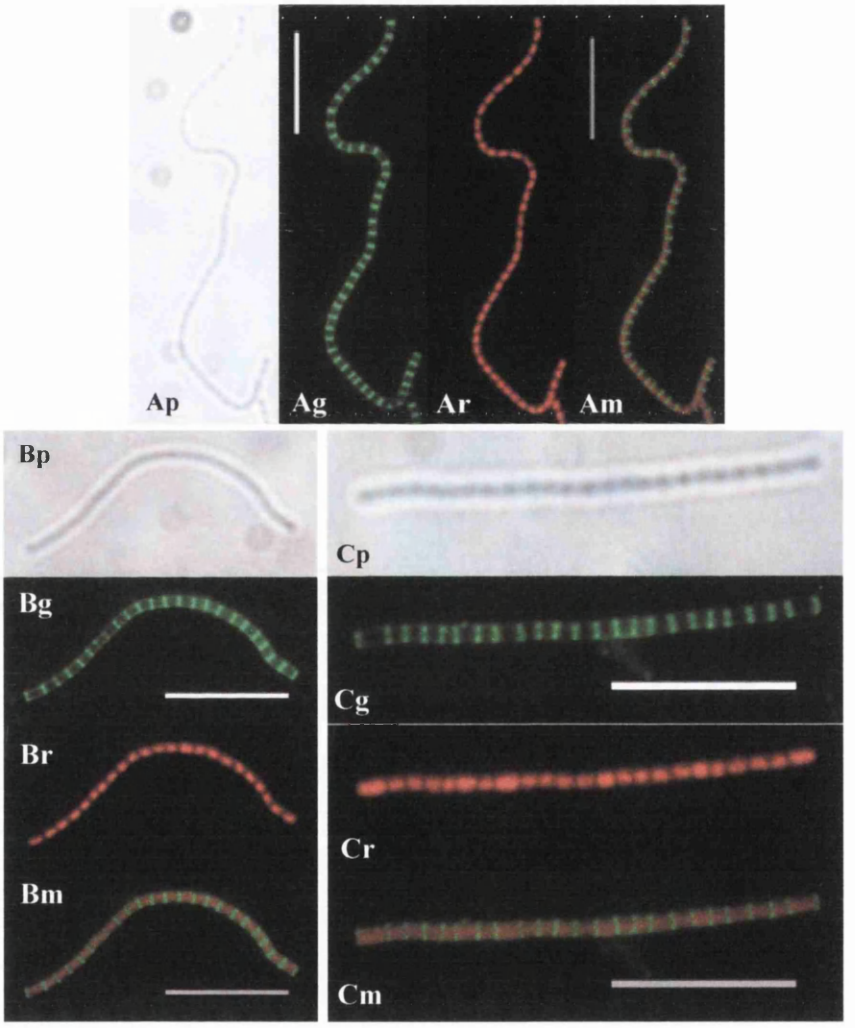

Figure 7.11: Fluorescence microscopy of aerial hyphae of parental strain *S. coelicolor* M145 (A), CDSCO2083-2 (DSCO2083 with pSHBW12) (B) and CDSCO2083-7 (DSCO2083 with pSHBW7) (C) strains. All the strains were grown on SFM agar plates at 30° C for 38 h. Impressions of each culture were taken on sterile coverslip and the samples were stained with Fluo-WAG (for cell wall) and PI (chromosomal DNA) after fixing. Each panel shows phase contrast (p), Fluo-WGA staining (g), PI staining (r) and merged (m) images of Fluo-WGA and PI staining of aerial hyphae of respective strains. (Scale bar 10 μm)

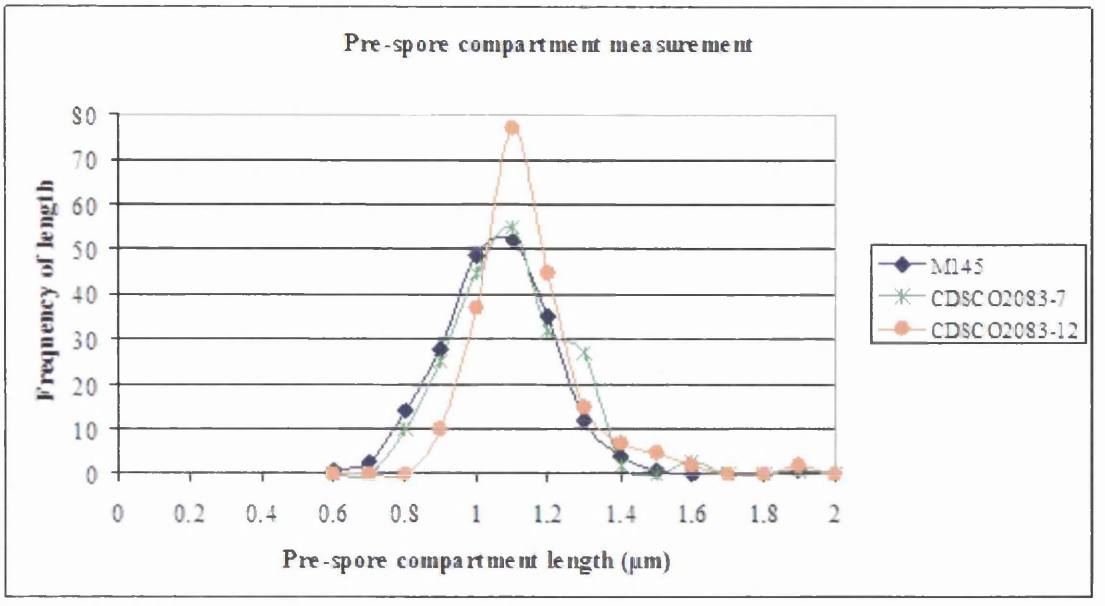

Figure 7.12: Graph of pre-spore compartment length versus frequency of the length of pre-spore compartment in wild type, CDSCO2083-12 and CDSCO2083-7 strains. The length of randomly selected 200 pre-spore compartments of each strain was measured from the Fluo-WGA stained images using Scion Image software.

7.7 Summary

Mutational analysis of *ftsQ* in *S. coelicolor* showed that *ftsQ* is dispensable for growth and viability. The *ftsQ* disrupted mutant was largely blocked in the conversion of the aerial hyphae into spores and was macroscopically similar in appearance to the known developmental *whi* mutants. No effect of *ftsQ* disruption on vegetative septation was observed. Aerial hyphae of the mutant showed a wide range of abnormal morphologies, with unseptated aerial hyphae with diffuse chromosomes, branched aerial hyphae, hyphae with incomplete septa, and infrequent spore chains with possible germinating spores. Although Z ring assembly was delayed and less synchronous, their formation implies that FtsQ is not required for Z ring assembly.

Chapter - 8

Discussion

The results chapters in this thesis describe the effects of the disruption of the genes encoding SEDS family proteins, their cognate penicillin binding proteins (PBPs) and FtsQ, on the growth and development of *S. coelicolor*. The SEDS family proteins have been described as transmembrane proteins that are involved in peptidoglycan synthesis by modulating the activity of high molecular weight penicillin binding proteins (HMW-PBPs) (Harry *et al.*, 2006; Ikeda *et al.*, 1989; Joris *et al.*, 1990; Matsuzawa *et al.*, 1989). Computational analyses allowed the prediction of topology of SEDS proteins and also established the phylogenetic relationship of four *S. coelicolor* SEDS proteins and their cognate PBPs with their respective homologues in other bacterial species. To get a global picture about the roles of the SEDS proteins, their cognate PBPs and FtsQ protein during different stages of the *S. coelicolor* life cycle, all the results are collectively discussed in this chapter. In addition to this, the current knowledge about cell division processes in *Streptomyces* and other bacterial species is also linked with the results of this study to gain some more general understanding about the functions of SEDS proteins, their cognate PBPs and FtsQ during the bacterial cell division. Lastly, possible future experimental approaches that may increase our understanding about the role of SEDS proteins and their cognate PBPs in cell division are proposed.

8.1 Features of gene loci encoding SEDS proteins in *Streptomyces*

A survey of actinomycete genomes revealed that there is a minimum of two and a maximum of four genes per genome encoding SEDS family proteins. At least two genes encoding SEDS proteins, namely *ftsW* and *rodA*, are highly conserved in all the rod shaped and filamentous bacteria (Henriques *et al.*, 1998; Ikeda *et al.*, 1989; Joris *et al.*, 1990). The amino acid sequence analyses and phylogenetic studies of SEDS proteins from different bacteria (specifically actinomycetes) showed distinct clustering of FtsW and RodA proteins according to their specific role in cell wall synthesis during cell division and growth, respectively. Similarity in phylogenetic grouping of SEDS proteins and their cognate PBPs suggests their co-evolution. Streptomycete genomes

contain four SEDS genes. In *S. coelicolor* these four genes are *SCO2085 (ftsW), SCO2067 (sfr), SCO3846 (rodA)* and *SCO5302 (rodA2).* All the four genes are located in the central core region of the *S. coelicolor* chromosome, suggesting possible indispensable roles of these genes during the life cycle. Analysis of each gene locus showed that each gene is a part of an operon like structure and they are located close to their cognate HMW-PBP genes [In *S. coelicolor*, the cognate *pbp* genes are *SCO2090 (ftsI), SCO2608 (pbp2), SCO3847* and *SCO5301,* respectively]. Genomic comparison of the *ftsW*-like gene locus of *S. coelicolor* with other actinobacterial genomes and some well characterized non-actinobacterial genomes such as *E. coli* revealed that *ftsW* is a part of highly conserved *dcw* cluster, which encodes genes involved in cell wall synthesis and cell division, suggesting the probable role of *ftsW* gene product in cell division in actinobacteria.

The second SEDS gene of actinomycetes, *rodA* (*SCO3846* in *S. coelicolor*), is a part of a conserved actinomycete gene cluster located close to the origin of replication, *oriC* in all respective chromosomes. The location of the cluster close to the *oriC* is a good indicator of essential functions of the genes in the cluster. The cluster includes genes encoding probable signal transduction proteins (serine/threonine kinase, phosphatase and forkhead associated proteins), a penicillin binding protein and CrgA, which is implicated in coordinating growth and cell division in streptomycete aerial hyphae (Del Sol *et al.*, 2003; Del Sol *et al.*, 2006). The presence of regulatory genes and cell wall synthesis genes together in an operon-like organization indicates some functional relationship among the products of these genes. In *M. tuberculosis,* the PBPA (class B PBP) encoding gene of this conserved cluster has been shown to play an important role in cell division and cell shape maintenance. The positioning of the PBPA protein at the septum was regulated by the serine/threonine kinase (PknB) and phosphatase (PstP) proteins that are involved in signal transduction (Dasgupta *et al.*, 2006). Thus, the conservation of such gene cluster among actinobacterial genomes suggests some unknown signalling mechanism that regulates cell wall synthesis during growth and division.

The sfr_{Sc} gene is a less conserved gene among the actinomycetes and is a part of the *mreBCD* operon, which consists of five genes *mreBCD, pbp2* and *sfr* in *S. coelicolor* genome. Comparative analysis of the *mreBCD* operon revealed that it is only found in strains having a multicellular complex life cycle among the actinobacterial

group. Most of the non mycelial actinomycetes such as *Mycobacterium* species do not have an equivalent *mreBCD* operon. An exception to this are rod shaped *Nocardioides* species, which have a simple life cycle and do not produce spores. The *mreBCD* operon is also present in *E. coli* and *B. subtilis*, however, there are no genes encoding SEDS protein and PBP in it. The Sfr_{Sc} protein shows a high degree of similarity to the RodA protein of *E. coli* and *B. subtilis* (34% and 31%, respectively). The RodA of *E. coli* and *B. subtilis* is reported to be involved in lateral cell wall synthesis, thereby maintaining the cell shape (Henriques *et al.*, 1998; Tamaki *et al.*, 1980). The *mreBCD* genes in *E. coli* and *B. subtilis* are also reported to be responsible for determining cell shape (Formstone and Errington, 2005; Kruse *et al.*, 2005; Leaver and Errington, 2005). Recently, it has been shown that the *mreBCD* genes in *S. coelicolor* play an important role in spore wall synthesis and are not required for vegetative growth (Mazza *et al.*, 2006; Noens, 2007). The location of the SEDS protein gene and PBP gene (in *S. coelicolor, sfr* and *pbp2,* respectively) in the *mreBCD* operon of some mycelial actinomycetes and the role of *mreBCD* genes in spore wall synthesis in *S. coelicolor* suggest that SEDS gene and *pbp* gene (equivalent to *sfr* and *pbp2* of *S. coelicolor,* respectively) may also play some important role in the spore wall synthesis.

The fourth SEDS gene (in *S. coelicolor, rodA2*) is also less conserved and only found in *Streptomyces* species and *Thermobifida fusca.* This SEDS gene locus in *Streptomyces* contains genes encoding a PBP, a probable histidine kinase, a probable phosphatase, a probable lipoprotein, a probable DNA ligase and some unidentified proteins. These genes are organized in a possible operon like structure, suggesting some kind of coordinated expression of them.

The topologies of FtsW proteins of *S. pneumoniae, E. coli* and *M. tuberculosis* have been shown to have ten transmembrane helices (TMHs), with both N- and C-termini in the cytoplasm (Datta *et al.*, 2006; Gerard *et al.*, 2002; Lara and Ayala, 2002). The FtsW homologue, SpoVE in *B. subtilis* has also been shown to have ten TMHs (Real *et al.*, 2008). The results of hydropathy analyses and topology predictions of the four SEDS proteins of *S. coelicolor* using different programs showed that they are polytopic membrane proteins containing eight to twelve transmembrane domains with, in each case, both N- and C- termini being located in the cytoplasm. For $FtsW_{Sc}$, different topology prediction programs predicted eight to ten TMHs. The topological model of FtsW of *S. pneumoniae* and *E. coli* predict a large extracytoplasmic loop

(approximately 70 amino acid residues) between transmembrane segments 7 and 8 (Gerard *et al.*, 2002; Lara and Ayala, 2002; Real *et al.*, 2008). The equivalent loop in FtsW of *M. tuberculosis* is shorter (20 amino acid residues) (Datta *et al.*, 2006). All the verified topological models of SEDS proteins in different bacteria mentioned above predict ten TMHs suggesting that the $FtsW_{Sc}$ may also have 10 TMHs. The phylogenetic relationship of *S. coelicolor* and *M. tuberculosis* also suggests that the topology of $FtsW_{Sc}$ could be more similar to that of *M. tuberculosis* FtsW. Sfr of *S. coelicolor* is predicted to have 10 TMHs, while RodA and RodA2 each are predicted to possess 12 TMHs. To validate these predictions further experiments such as gene fusions with reporter enzymes, protease protection assays and cysteine scanning are necessary to be performed.

8.2 *ftsW, sfr* and *rodA2* are dispensable for growth and survival in *S. coelicolor*

The SEDS proteins and their cognate PBP function as part of essential elongation and division complexes for peptidoglycan synthesis (den Blaauwen *et al.*, 2008). Construction of successful Tn*5062* insertion mutants of three SEDS genes, *ftsW, sfr* and *rodA2,* in *S. coelicolor* showed that three of the four *S. coelicolor* SEDS genes are not essential for growth and viability of this organism. The *sfr*, *rodA2, pbp2* and *rodA2/sfr* double mutants showed no apparent phenotypic difference from the wild strain of *S. coelicolor* with the growth conditions tested. Lack of any macroscopic phenotypic difference in these mutants indicates that these genes do not have any major effect on growth and cell division of *S. coelicolor*. In contrast, mutants of *ftsW* and its cognate PBP gene, *ftsI,* exhibited a white phenotype similar to other developmental mutants like *whiG, whiI* etc. when grown on sporulation specific media. The white phenotype of these mutants indicates that the mutants are defective in differentiation of aerial hyphae and the products of these genes play some important role in spore formation. As attempts to construct a successful *rodA* (*SCO3846*) mutant failed unless a second copy of this gene was introduced, this demonstrates that *rodA* is essential for growth and viability of *S. coelicolor. rodA* in other eubacteria, such as *E. coli* and *B. subtilis,* has been shown to be essential and is involved in elongation by lateral cell wall

synthesis (Henriques *et al.*, 1998; Tamaki *et al.*, 1980). In contrast to *E. coli* and *B. subtilis*, growth in actinomycetes occurs primarily by *de novo* synthesis of peptidoglycan at the pole (or hyphal tips in filamentous actinomycetes) (Flardh, 2003a; Hett and Rubin, 2008). Hence it is predicted that RodA may form part of an apical protein complex, along with another essential protein DivIVA, that has been shown to be involved directly in the cell wall synthesis at the cell poles (or hyphal tips in filamentous actinomycetes) (Flardh, 2003b; Kang *et al.*, 2008; Letek *et al.*, 2008).

8.3 *sfr* and *pbp2* are required for spore wall integrity in *S. coelicolor*

Disruption of *rodA2, sfr*, *pbp2* or simultaneously both *rodA2/sfr* did not give any abnormal phenotype of septation during vegetative as well as aerial growth. FL-vancomycin staining of vegetative mycelium showed normal cross-wall formation in vegetative hyphae. Normal sporulation septa and chromosome condensation were observed in the aerial hyphae of all the mutants stained with Fluo-WGA/PI. The size of the pre-spore compartments of the mutants was also normal. These observations suggested that *rodA2, sfr* and *pbp2* genes are not required for any kind of septation in *S. coelicolor*. However, the spores of *sfr* and *pbp2* mutants were susceptible to heat and SDS treatment. In addition to the susceptibility of *sfr* and *pbp2* mutant spores to heat and SDS treatment, they also showed susceptibility to the cell wall specific antibiotics, such as vancomycin and ampicillin that function during late stages of cell wall synthesis. In *B. subtilis*, *spoVE* and *spoVD* mutants were shown to be defective in spore cortex formation (Daniel *et al.*, 1994; Piggot and Coote, 1976; Real *et al.*, 2008). The *spoVE* and *spoVD* are homologues of *rodA* and *pbp*, respectively, and are not essential for growth and survival of *B. subtilis* (Daniel *et al.*, 1994; Ikeda *et al.*, 1989). The spores of an *spoVE* mutant of *B. subtilis* have been shown to be susceptible to heat treatment (Real *et al.*, 2008). The *mreB* disruption mutant constructed during this study also showed a similar phenotype to that of *sfr* and *pbp2* mutants. That is the *mreB* mutant spores were also susceptible to heat, SDS and cell wall specific antibiotics. These results are consistent with heat and SDS susceptibility of the spores of *mreB* deletion

mutants in *S. coelicolor* constructed by Mazza *et al.*, 2006. The susceptibility of the spores of *sfr, pbp2* and *mreB* mutants to physical and chemical stress, as well as to the cell wall specific antibiotics suggests the importance of *sfr, pbp2* and *mreB* genes in spore wall synthesis during spore maturation and maybe also during spore germination. In *E. coli,* the membrane-bound complex of MreB, MreC and MreD was proposed to interact with PBP2 and RodA during lateral cell wall synthesis (Kruse *et al.*, 2005). Localization of PBP2 in spiral-shaped structures in *C. crescentus* was shown to be dependent on MreB (Figge *et al.*, 2004). The *sfr* and *pbp2* genes in *S. coelicolor* are part of *mre* gene cluster and are shown to be physically linked to *mreBCD* genes forming an operon like structure (Burger *et al.*, 2000). MreB was shown to be localized at the cytoplasmic membrane of the spores in *S. coelicolor* (Mazza *et al.*, 2006). Taken together, these results indicate that Sfr, PBP2, MreB, MreC and MreD in *Streptomyces* are linked and they may form a part of a putative peptidoglycan synthesis complex specific for spore wall synthesis. Localization studies and protein-protein interaction studies of these proteins will be important to further understand the interdependency and the specific role of these proteins during sporulation.

The spores of *mreB, mreC, mreD* and *mreBCD* deletion mutants were shown to be swollen and larger in size (Mazza *et al.*, 2006; Noens, 2007). In contrast, the Tn*5062* disruption mutants of *sfr, pbp,* and *mreB* constructed during this study did not show any major effect on spore shape and size. Such a difference in the phenotype of the mutants may be due to strain differences and the way the respective mutants were constructed.

A lack of any apparent phenotype of *rodA2* disruption mutants or of a *rodA2/sfr* double mutant suggest that the *rodA2* gene does not play any major role in cell wall synthesis during the life cycle of *S. coelicolor.*

8.4 FtsW and FtsI are required for Z-ring formation during sporulation septation in *S. coelicolor*

Sporulation septation in *Streptomycetes* is a non-essential and a developmentally programmed type of cell division which effectively transforms multi-nucleoid filamentous aerial hyphae into unigenomic spores (Chater, 1993; Flardh *et al.*,

1999). The typical white phenotype of *ftsW* and *ftsI* disruption mutants of *S. coelicolor* suggests that both the mutants are defective in developmental differentiation of aerial hyphae into spores. Fluorescence microscopy of Fluo-WGA/PI stained aerial hyphae of both the mutants revealed that *ftsW* and *ftsI* mutants were unable to form sporulation septa, suggesting some important role of both the genes in sporulation septation. The hyphae of both the mutants were also defective in chromosomal condensation, implying that this process is linked with septation. FtsW and FtsI in *E. coli* have been shown to localize to the septum and act in a concerted manner to carry out septal peptidoglycan biosynthesis (Mercer and Weiss, 2002; Wang *et al.*, 1998). In *S. griseus*, an 85 kDa PBP was shown to function specifically during sporulation septation, as the binding of Cefoxitin to this protein prevented sporulation septation but not vegetative septation (Hao and Kendrick, 1998). The characterization of *ftsW* and *ftsI* mutants of *S. coelicolor* supports the likely role of FtsW in recruitment of the cognate penicillin binding protein FtsI to the sporulation septa. The complementation analysis of the *ftsI* mutant suggests that the promoter of *ftsI* is located upstream of the *Eco*RI site that is located 1.8 kb upstream of the *ftsI* gene, in the intergenic region between *SCO2092* and *SCO2093* genes. This is consistent with the dependence of expression of *E. coli ftsI* on a promoter located 1.9 kb upstream of the *ftsI* gene (Hara *et al.*, 1997).

In contrast to the ladder like organization of Z-rings in the aerial hyphae of the wild type strain during early stages of sporulation septation, *in situ* localization analysis of FtsZ-EGFP in *ftsW* and *ftsI* mutants revealed diffuse fluorescence or FtsZ-EGFP spirals, but no Z-rings. These data imply that formation of a complex between FtsW and FtsI of *S. coelicolor* either directly provides a membrane anchor to stabilise FtsZ rings or has an indirect role in this process in the absence of FtsA, ZipA or ZapA. In *E. coli,* FtsW and FtsI are believed to be recruited late to the divisome in a quasi-linear assembly sequence involving, first, stabilisation of the Z-ring with FtsA and the membrane anchor ZipA, then subsequently recruitment of FtsK and a trimeric complex involving FtsL, FtsB and FtsQ (Buddelmeijer and Beckwith, 2002, 2004; Goehring and Beckwith, 2005; Goehring *et al.*, 2005; Goehring *et al.*, 2006). Systematic bacterial two-hybrid assays support subsequent recruitment of FtsW and FtsI, which both interact with FtsQ (Di Lallo *et al.*, 2003). In contrast, the late division proteins appear to be recruited in a concerted manner in *B. subtilis,* where mutation or depletion of any one prevents all the others assembling after formation of the Z-ring and, consequently there

is no peptidoglycan synthesis at the division site (Errington *et al.*, 2003; Harry *et al.*, 2006). Unlike late recruited FtsW and FtsI proteins of *E. coli* and *B. subtilis*, the data from this study suggests that FtsW and FtsI are recruited early in the divisome during sporulation septation in *S. coelicolor.*

Using a combination of genetic and cytological approaches, a role for FtsW in stabilization of Z-rings has been reported in *E. coli* (Boyle *et al.*, 1997). However, subsequent biochemical analysis has not provided evidence for a direct interaction between these proteins. Interestingly, interaction between C-terminal tails of mycobacterial FtsW and FtsZ has been demonstrated (Datta *et al.*, 2002). Indeed, in merodiploids expressing both wild-type and fluorophore-tagged versions of both proteins, this interaction helps to direct co-localization of both the proteins to the septum in *M. smegmatis* (Rajagopalan *et al.*, 2005). Due to the proportion of septal Z-rings scoring positive for either tagged protein, it was interpreted that, just as in *E. coli,* FtsW is recruited late to the divisome in mycobacteria. This interpretation is inconsistent with our observations implicating an earlier pivotal role for FtsW in stabilization of Z-rings in the aerial hyphae of *S. coelicolor.* This could imply a fundamental difference in assembly of divisomes in these related actionmycetes, or alternatively may be due to dissimilarity in the experimental approaches needed to study cell division in both organisms. Both *ftsW* and *ftsZ* are essential for cell viability in mycobacterium, necessitating construction of merodiploid strains to examine localization of fluorophore-tagged proteins that may not retain full biological function. Antisense depletion of FtsW in *M. smegmatis* leads to irregular Z-ring assembly and prevents septation (Datta *et al.*, 2006), which is more consistent with the pivotal role of FtsW protein in actinomycete cell division. The interaction between the mycobacterial proteins is believed to depend on a cluster of four aspartate residues located at the C-terminus of FtsZ and an oppositely-charged arginine-rich region in the cytoplasmic C-terminus of FtsW (Datta *et al.*, 2002). A cluster of aspartates is not present in the C-terminus of FtsZ of *S. coelicolor.* Moreover, the C-terminal 18 amino acid region of *S. coelicolor* FtsW containing several arginine residues could be replaced with no affect on Z-ring stabilization, indicating that the nature of any direct or indirect interaction between the streptomycete proteins is unlike that described for the mycobacterial proteins. In contrast, two proline residues in two extracytoplasmic loops of mycobacterial FtsW, Pro^{306} and Pro^{386}, that are required for interaction with

mycobacterial FtsI, are also conserved in *S. coelicolor* FtsW (Pro^{302} and Pro^{382}). It has been suggested that the interaction between mycobacterial FtsZ and FtsW may modulate the latter's interaction with FtsI (Datta *et al.*, 2006). This study implies that formation of a complex between FtsW and FtsI proteins of *S. coelicolor* is required to stabilize Z-rings at division sites. Further investigation is required to understand the role of FtsW and FtsI proteins in *S. ceolicolor*.

8.5 FtsQ functions during a later stage in sporulation septation

Disruption of *ftsQ* in *S. coelicolor* also resulted in a white phenotype when grown on sporulation specific medium. Fluorescence microscopic analysis of aerial hyphae showed a range of abnormal morphologies from coiled unseptated filaments with diffuse chromosomes to hyphae divided into probable pre-spore compartments with abnormally condensed nucleoids, and also branching aerial hyphae. Such variations in morphologies of *ftsQ* mutant aerial hyphae suggest some specific role of FtsQ during sporulation septation. A similar phenotype of an *ftsQ* deletion mutant was also reported previously (McCormick and Losick, 1996). However, the *ftsQ* mutant described in this study differs in some respects from the previously described *ftsQ* deletion mutant. The *ftsQ* deletion mutant was reported to produce copious amounts of actinorhodin compared to the wild type and it exhibit reduced vegetative septation (McCormick and Losick, 1996). On the other hand, the *ftsQ* disruption mutant constructed during this study produced a normal level of actinorhodin and there was no significant difference in the vegetative septation in the mutant from the wild type. These discrepancies may be due to strain differences and the way the respective mutants were constructed. The phenotype of the *ftsQ* deletion mutant, created by deleting the majority of the *ftsQ* coding sequence (McCormick and Losick, 1996) could be in part due to the result of polarity on expression of the downstream *ftsZ*. Although, the complementation analysis of this mutant showed that the defect in sporulation septation was 'substantially' restored by *ftsQ* and 4 kb of upstream sequence. In this regard it is interesting to note that in addition to three putative *ftsZ* promoters detected in the

intergenic region between *ftsQ* and *ftsZ*, some read-through from upstream promoter(s) also contributes to *ftsZ* expression in *S. coelicolor* (Flardh *et al.*, 2000). Out of three *ftsZ* promoters, one is specifically expressed during sporulation septation. It is also interesting to note that complementation of an *ftsZ* null mutant with a plasmid carrying *ftsZ,* in which the sporulation specific *ftsZ* promoter was inactivated by deletion, restored vegetative septation as well as normal production of actinorhodin (Flardh *et al.*, 2000). This complemented *ftsZ* mutant was defective in sporulation septation only. The *fts* mutants characterized in this study also showed a similar macroscopic phenotype. These observations suggest that the small colony size, reduced vegetative septation and overproduction of blue pigment in the *ftsQ* deletion mutant constructed by McCormick and Losick in 1996 may be due to a polar effect on expression of *ftsZ* specifically required for vegetative septation. In *S. griseus*, one of the four *ftsZ* promoters is shown to be located within the *ftsQ* coding region (Kwak *et al.*, 2001), while in *C. glutamicum*, a related actinomycete, *ftsZ* expression is controlled by at least five promoters, three of which are located in the coding region of the upstream *ftsQ* gene (Letek *et al.*, 2007).

Formation of FtsZ rings in the aerial hyphae of the *ftsQ* mutant and visualization of regularly spaced septal peptidoglycan and abnormally condensed nucleoids in three days or older samples of the mutant hyphae stained with Fluo-WGA/PI suggest that *ftsQ* mutants are blocked at a more advanced stage of septation than *ftsW* and *ftsI* mutants, which do not show any sign of cell wall synthesis or chromosomal condensation even after prolonged incubation. Further, the transmission electron microscopic (TEM) analysis showed that sporulation septal peptidoglycan synthesis begins at the division sites at regular intervals in *ftsQ* mutant, but these septa failed to complete their centripetal growth and are spanned by nucleoids. This suggests a critical role of FtsQ in linking constriction of the cytosolic Z-ring with invagination of newly synthesized murein. In the absence of this function, new peptidoglycan synthesis at division sites may cause localized temporary outward deformations of surface rodlet layers, as observed using atomic force microscopy (AFM). The temporary localized breakage of the rodlet layer at the sites of in-growing septa in sporulating aerial hyphae of wild type was observed during AFM. Such a breakage of the rodlet layer in *ftsQ* mutant aerial hyphae was not observed, suggesting that this is a late event, presumably occurring after completion of septal ingrowth. The formation of occasional vegetative septa in the aerial hyphae may trigger branch formation in the aerial hyphae. In *E. coli*

FtsQ is recruited to the divisome after forming a trimeric complex with FtsL and FtsB (Buddelmeijer and Beckwith, 2004). Recently, the *ftsL* and *divIC* mutants of *S. coelicolor* have been shown to be conditionally defective in completion of septal closure in the aerial hyphae, with the phenotype being apparent when grown on the medium containing osmolyte (Bennett *et al.*, 2007). This may indicate some interaction between FtsQ, FtsL and DivIC at least under certain growth conditions. The absolute phenotype of the *ftsQ* mutant in contrast to the conditional phenotype of *ftsL* and *divIC* mutants implies a more critical role of FtsQ in septum closure.

From the characterization of *ftsW*, *ftsI* and *ftsQ* mutants and the FtsZ localization studies in *S. coelicolor*, it appears that FtsW and FtsI are recruited early to the sporulation divisome while FtsQ is recruited after localization of FtsW and FtsI. This is in contrast to that of well characterized divisome assembly in *E. coli* and *B. subtilis* (Harry *et al.*, 2006). Thus, it implies that in *S. coelicolor* the order of recruiting divisome proteins to the septal ring is different from that in *E. coli* and *B. subtilis.* The diffuse nucleoids in the aerial hyphae of *ftsW* and *ftsI* mutants and abnormally condensed chromosomes in the *ftsQ* mutant suggest that chromosome condensation and sporulation septation are taking place simultaneously. Further, these also suggest that the condensation of chromosomes advances simultaneously with the advancement of septation stages. In *Streptomyces* sporulation division, the invagination at the septation site occurs after complete septum formation. On the other hand in *E. coli* and *B. subtilis*, chromosome condensation happens before the start of divisome assembly and the invagivation takes place during septum synthesis (Errington *et al.*, 2003; Harry *et al.*, 2006). For a proper understanding of the cell division events in bacteria especially in *Streptomyces* further investigation is needed.

8.6 Vegetative septation in *S. coelicolor* occurs by a different mechanism

FtsZ is required for both (vegetative and sporulation) types of septation in *S. coelicolor,* as is evident from the *ftsZ* mutant that is unable to form vegetative cross walls and produce spores (McCormick *et al.*, 1994). The overall growth of this mutant is also affected, as it only attains small colony sizes, and it produces copious amounts of

actinorhodin. In contrast, the *ftsW, ftsI* and *ftsQ* mutants constructed during this study grew well forming aerial hyphae with no apparent increase in antibiotic production compared to the wild type. The *sfr* and *rodA2* mutants also underwent normal developmental differentiation producing spores similar to wild type. Microscopic analyses of the mutants of three non-essential SEDS genes (*ftsW, sfr* and *rodA2*), *ftsI* and *ftsQ* showed that the process of cross-wall formation in vegetative hyphae was not affected in all these mutants. Disruption of *ftsW, ftsI* or *ftsQ* specifically affected sporulation septation. The vegetative cross-wall formation observed in mutants of three different *fts* genes confirms that the two types of septation in streptomycetes are mechanically very distinct, as originally suggested from the functions of different forms of FtsZ (Grantcharova *et al.*, 2003). Normal Z ring formation in the vegetative hyphae of *ftsW, ftsI* and *ftsQ* mutants further suggests that the proteins encoded by these *fts* genes are not required for Z ring stabilization in vegetative hyphae. These *fts* genes have been shown to play indispensable role in cell division of all the bacteria studied (Errington *et al.*, 2003; Harry *et al.*, 2006). The formation of normal Z rings and complete vegetative septa in *ftsW, ftsI* and *ftsQ* mutants of *S. coelicolor* imply that vegetation septation in *Streptomyces* occurs by a different mechanism and is mechanically distinct from sporulation septation and vegetative septation in non-filamentous bacteria. The observation of normal vegetative septation in three non-essential SEDS genes mutants may be due to functional redundancy of the proteins encoded by these genes. To exclude functional redundancy, three double mutants, one with the insertions in both *ftsW* and *sfr*, the second with disrupted copies of both *rodA2* and *sfr* and the third with mutations in *ftsW* and *rodA2* were constructed. Normal *de novo* synthesis of septal peptidoglycan was observed in all the double mutants suggesting that the vegetative septation is not affected in these double mutants as well. These observations are very likely to rule out the possibility of functional redundancy among the three non-essential SEDS proteins. However, to rule out the functional redundancy completely, a triple mutant of the three non-essential SEDS gene (*ftsW, sfr* and *rodA2*) needs to be constructed.

8.7 Conclusion

Computational analysis of the four SEDS proteins (FtsW, Sfr, RodA and RodA2) of *S. coelicolor* showed that the gene encoding each SEDS protein is located in a distinct gene cluster. Two of these gene clusters are highly conserved among the actinomycetes. Genetic and cytological data show that three of the four SEDS proteins are not essential for growth and survival of *S. coelicolor.* Sfr and its cognate PBP has specific role in spore wall synthesis and perhaps in spore germination. The mutational analysis of *ftsW, ftsI* and *ftsQ* genes, members of the highly conserved *dcw* cluster, indicates that they primarily function during sporulation septation. FtsW and FtsI are recruited early during the divisome assembly and both are required for Z ring stabilization. FtsQ is recruited late in the divisome after stabilization of Z rings. Thus, the order of recuitement of divisome protein during sporulation septation in *Streptomyces* is different from that typically found in *E. coli* and *B. subtilis.* The FtsW, FtsI and FtsQ proteins are not required for vegetative septation in *S. coelicolor* and this occurs by some unknown mechanism.

8.8 Future perspectives

The work presented in this thesis provides an insight into the functions of SEDS proteins (especially FtsW and Sfr) and their cognate PBPs (especially FtsI and PBP2). It also sheds some light on interesting mechanisms of cell division during the developmental cycle of *Streptomyces.*

This study can be the starting point for future research to understand the interesting mechanisms of cell wall synthesis during growth and division in bacteria. A few suggestions that would be interesting to pursue are:

- *In situ* localization and expression studies of four SEDS proteins and their cognate PBPs will provide more insight in to the specific functions of these proteins.
- *sfr* and *pbp2* are part of *mre* gene cluster and MreB is shown to be involved in spore wall synthesis. Protein-protein interaction studies among the members of

mre genes cluster using bacterial two hybrid system can be useful to understand interdependency of the proteins encoded by this cluster.

- To understand the functions of the SEDS proteins and their relationship with other proteins, topological characterization of the four *S. coelicolor* SEDS proteins using different techniques such as gene fusions with reporter enzymes, protease protection assays and cysteine scanning will be useful.
- To investigate the function of the essential SEDS protein, RodA, in *S. coelicolor*, a conditional mutant of *rodA* needs to be constructed.
- To investigate the order of recruitment of divisome proteins during sporulation septation, localization studies of these proteins in wild type as well as in different mutant background and their interaction analysis using a bacterial two hybrid system need to be performed.
- The relation between chromosome condensation and septation during sporulation in *S. coelicolor* can be investigated by visualization of the proteins involved in the chromosome partitioning, such as ParA and ParB, in the background of different *fts* mutants.

References

Aarsman, M.E., Piette, A., Fraipont, C., Vinkenvleugel, T.M., Nguyen-Disteche, M., and den Blaauwen, T. (2005) Maturation of the *Escherichia coli* divisome occurs in two steps. *Mol Microbiol* **55**: 1631-1645.

Addinall, S.G., Cao, C., and Lutkenhaus, J. (1997) FtsN, a late recruit to the septum in *Escherichia coli*. *Mol Microbiol* **25**: 303-309.

Ainsa, J.A., Parry, H.D., and Chater, K.F. (1999) A response regulator-like protein that functions at an intermediate stage of sporulation in *Streptomyces coelicolor* A3(2). *Mol Microbiol* **34**: 607-619.

Ainsa, J.A., Ryding, N.J., Hartley, N., Findlay, K.C., Bruton, C.J., and Chater, K.F. (2000) WhiA, a protein of unknown function conserved among gram-positive bacteria, is essential for sporulation in *Streptomyces coelicolor* A3(2). *J Bacteriol* **182**: 5470-5478.

Alexander, M. (1997) *Introduction to Soil Microbiology*: John Wiley and Sons, New York.

Ali, N., Herron, P.R., Evans, M.C., and Dyson, P.J. (2002) Osmotic regulation of the *Streptomyces lividans* thiostrepton-inducible promoter, *ptipA*. *Microbiology* **148**: 381-390.

Alting-Mees, M.A., and Short, J.M. (1989) pBluescript II: gene mapping vectors. *Nucleic Acids Res* **17**: 9494.

Altschul, S.F., Madden, T.L., Schaffer, A.A., Zhang, J., Zhang, Z., Miller, W., and Lipman, D.J. (1997) Gapped BLAST and PSI-BLAST: a new generation of protein database search programs. *Nucleic Acids Res* **25**: 3389-3402.

Anderson, A.S., and Wellington, E.M. (2001) The taxonomy of *Streptomyces* and related genera. *Int J Syst Evol Microbiol* **51**: 797-814.

Anderson, D.E., Gueiros-Filho, F.J., and Erickson, H.P. (2004) Assembly dynamics of FtsZ rings in *Bacillus subtilis* and *Escherichia coli* and effects of FtsZ-regulating proteins. *J Bacteriol* **186**: 5775-5781.

Angell, S., Lewis, C.G., Buttner, M.J., and Bibb, M.J. (1994) Glucose repression in *Streptomyces coelicolor* A3(2): a likely regulatory role for glucose kinase. *Mol Gen Genet* **244**: 135-143.

Arigoni, F., Pogliano, K., Webb, C.D., Stragier, P., and Losick, R. (1995) Localization of protein implicated in establishment of cell type to sites of asymmetric division. *Science* **270**: 637-640.

Ausmees, N., Wahlstedt, H., Bagchi, S., Elliot, M.A., Buttner, M.J., and Flardh, K. (2007) SmeA, a small membrane protein with multiple functions in *Streptomyces* sporulation including targeting of a SpoIIIE/FtsK-like protein to cell division septa. *Mol Microbiol* **65**: 1458-1473.

Av-Gay, Y., Jamil, S., and Drews, S.J. (1999) Expression and characterization of the *Mycobacterium tuberculosis* serine/threonine protein kinase PknB. *Infect Immun* **67**: 5676-5682.

Ayala, J.A., Garrido, T., de Pedro, M.A., and Vicente, M. (1994) *Molecular biology of bacterial septation.* In Bacterial Cell Wall, Ghuysen, JM., Habenbeck R (eds). Elsevier Science: Amsterdam.

Bao, K., and Cohen, S.N. (2001) Terminal proteins essential for the replication of linear plasmids and chromosomes in *Streptomyces*. *Genes Dev* **15**: 1518-1527.

Barak, I., and Youngman, P. (1996) SpoIIE mutants of *Bacillus subtilis* comprise two distinct phenotypic classes consistent with a dual functional role for the SpoIIE protein. *J Bacteriol* **178**: 4984-4989.

Barak, I., and Wilkinson, A.J. (2007) Division site recognition in *Escherichia coli* and *Bacillus subtilis*. *FEMS Microbiol Rev* **31**: 311-326.

Beall, B., and Lutkenhaus, J. (1989) Nucleotide sequence and insertional inactivation of a *Bacillus subtilis* gene that affects cell division, sporulation, and temperature sensitivity. *J Bacteriol* **171**: 6821-6834.

Begg, K.J., Dewar, S.J., and Donachie, W.D. (1995) A new *Escherichia coli* cell division gene, *ftsK*. *J Bacteriol* **177**: 6211-6222.

Ben-Yehuda, S., and Losick, R. (2002) Asymmetric cell division in *B. subtilis* involves a spiral-like intermediate of the cytokinetic protein FtsZ. *Cell* **109**: 257-266.

Bennett, J.A., and McCormick, J.R. (2001) Two new loci affecting cell division identified as suppressors of an *ftsQ*-null mutation in *Streptomyces coelicolor* A3(2). *FEMS Microbiol Lett* **202**: 251-256.

Bennett, J.A., Aimino, R.M., and McCormick, J.R. (2007) *Streptomyces coelicolor* genes *ftsL* and *divIC* play a role in cell division but are dispensable for colony formation. *J Bacteriol* **189**: 8982-8992.

Bentley, S.D., Chater, K.F., Cerdeno-Tarraga, A.M., Challis, G.L., Thomson, N.R., James, K.D., Harris, D.E., Quail, M.A., Kieser, H., Harper, D., Bateman, A., Brown, S., Chandra, G., Chen, C.W., Collins, M., Cronin, A., Fraser, A., Goble, A., Hidalgo, J., Hornsby, T., Howarth, S., Huang, C.H., Kieser, T., Larke, L., Murphy, L., Oliver, K., O'Neil, S., Rabbinowitsch, E., Rajandream, M.A., Rutherford, K., Rutter, S., Seeger, K., Saunders, D., Sharp, S., Squares, R., Squares, S., Taylor, K., Warren, T., Wietzorrek, A., Woodward, J., Barrell, B.G., Parkhill, J., and Hopwood, D.A. (2002) Complete genome sequence of the model actinomycete *Streptomyces coelicolor* A3(2). *Nature* **417**: 141-147.

Berdy, J. (2005) Bioactive microbial metabolites. *J Antibiot (Tokyo)* **58**: 1-26.

Bernhardt, T.G., and de Boer, P.A. (2003) The *Escherichia coli* amidase AmiC is a periplasmic septal ring component exported via the twin-arginine transport pathway. *Mol Microbiol* **48**: 1171-1182.

Bernhardt, T.G., and de Boer, P.A. (2004) Screening for synthetic lethal mutants in *Escherichia coli* and identification of EnvC (YibP) as a periplasmic septal ring factor with murein hydrolase activity. *Mol Microbiol* **52**: 1255-1269.

Bernhardt, T.G., and de Boer, P.A. (2005) SlmA, a nucleoid-associated, FtsZ binding protein required for blocking septal ring assembly over Chromosomes in *E. coli*. *Mol Cell* **18**: 555-564.

Betts, J.C., Lukey, P.T., Robb, L.C., McAdam, R.A., and Duncan, K. (2002) Evaluation of a nutrient starvation model of Mycobacterium tuberculosis persistence by gene and protein expression profiling. *Mol Microbiol* **43**: 717-731.

Bibb, M.J., Molle, V., and Buttner, M.J. (2000) sigma(BldN), an extracytoplasmic function RNA polymerase sigma factor required for aerial mycelium formation in *Streptomyces coelicolor* A3(2). *J Bacteriol* **182**: 4606-4616.

Bibb, M.J. (2005) Regulation of secondary metabolism in streptomycetes. *Curr Opin Microbiol* **8**: 208-215.

Bignell, D.R., Warawa, J.L., Strap, J.L., Chater, K.F., and Leskiw, B.K. (2000) Study of the bldG locus suggests that an anti-anti-sigma factor and an anti-sigma factor may be involved in *Streptomyces coelicolor* antibiotic production and sporulation. *Microbiology* **146**: 2161-2173.

Bignell, D.R., Lau, L.H., Colvin, K.R., and Leskiw, B.K. (2003) The putative anti-anti-sigma factor BldG is post-translationally modified by phosphorylation in *Streptomyces coelicolor*. *FEMS Microbiol Lett* **225**: 93-99.

Bigot, S., Corre, J., Louarn, J.M., Cornet, F., and Barre, F.X. (2004) FtsK activities in Xer recombination, DNA mobilization and cell division involve overlapping and separate domains of the protein. *Mol Microbiol* **54**: 876-886.

Bishop, A., Fielding, S., Dyson, P., and Herron, P. (2004) Systematic insertional mutagenesis of a streptomycete genome: a link between osmoadaptation and antibiotic production. *Genome Res* **14**: 893-900.

Boitel, B., Ortiz-Lombardia, M., Duran, R., Pompeo, F., Cole, S.T., Cervenansky, C., and Alzari, P.M. (2003) PknB kinase activity is regulated by phosphorylation in two Thr residues and dephosphorylation by PstP, the cognate phospho-Ser/Thr phosphatase, in Mycobacterium tuberculosis. *Mol Microbiol* **49**: 1493-1508.

Bork, P., Sander, C., and Valencia, A. (1992) An ATPase domain common to prokaryotic cell cycle proteins, sugar kinases, actin, and hsp70 heat shock proteins. *Proc Natl Acad Sci U S A* **89**: 7290-7294.

Boyle, D.S., Khattar, M.M., Addinall, S.G., Lutkenhaus, J., and Donachie, W.D. (1997) *ftsW* is an essential cell-division gene in *Escherichia coli*. *Mol Microbiol* **24**: 1263-1273.

Brock, T.D., Madigan, M.T., Martinko, J.M., and Parker, J. (1994) *Biology of Microorganisms*: Prentice-Hall International, Inc.

Buddelmeijer, N., Aarsman, M.E., Kolk, A.H., Vicente, M., and Nanninga, N. (1998) Localization of cell division protein FtsQ by immunofluorescence microscopy in dividing and nondividing cells of *Escherichia coli*. *J Bacteriol* **180**: 6107-6116.

Buddelmeijer, N., and Beckwith, J. (2002) Assembly of cell division proteins at the *E. coli* cell center. *Curr Opin Microbiol* **5**: 553-557.

Buddelmeijer, N., Judson, N., Boyd, D., Mekalanos, J.J., and Beckwith, J. (2002) YgbQ, a cell division protein in *Escherichia coli* and *Vibrio cholerae*, localizes in codependent fashion with FtsL to the division site. *Proc Natl Acad Sci U S A* **99**: 6316-6321.

Buddelmeijer, N., and Beckwith, J. (2004) A complex of the *Escherichia coli* cell division proteins FtsL, FtsB and FtsQ forms independently of its localization to the septal region. *Mol Microbiol* **52**: 1315-1327.

Burger, A., Sichler, K., Kelemen, G., Buttner, M., and Wohlleben, W. (2000) Identification and characterization of the *mre* gene region of *Streptomyces coelicolor* A3(2). *Mol Gen Genet* **263**: 1053-1060.

Cabeen, M.T., and Jacobs-Wagner, C. (2005) Bacterial cell shape. *Nat Rev Microbiol* **3**: 601-610.

Callaway, E. (2008) Cell biology. Bacteria's new bones. *Nature* **451**: 124-126.

Capstick, D.S., Willey, J.M., Buttner, M.J., and Elliot, M.A. (2007) SapB and the chaplins: connections between morphogenetic proteins in *Streptomyces coelicolor*. *Mol Microbiol* **64**: 602-613.

Carballido-Lopez, R., and Errington, J. (2003) A dynamic bacterial cytoskeleton. *Trends Cell Biol* **13**: 577-583.

Carballido-Lopez, R. (2006) The bacterial actin-like cytoskeleton. *Microbiol Mol Biol Rev* **70**: 888-909.

Carballido-Lopez, R., Formstone, A., Li, Y., Ehrlich, S.D., Noirot, P., and Errington, J. (2006) Actin homolog MreBH governs cell morphogenesis by localization of the cell wall hydrolase LytE. *Dev Cell* **11**: 399-409.

Carballido-Lopez, R., and Formstone, A. (2007) Shape determination in *Bacillus subtilis*. *Curr Opin Microbiol* **10**: 611-616.

Castillo, U.F., Strobel, G.A., Ford, E.J., Hess, W.M., Porter, H., Jensen, J.B., Albert, H., Robison, R., Condron, M.A., Teplow, D.B., Stevens, D., and Yaver, D. (2002) Munumbicins, wide-spectrum antibiotics produced by *Streptomyces* NRRL 30562, endophytic on Kennedia nigriscans. *Microbiology* **148**: 2675-2685.

Cha, J.H., and Stewart, G.C. (1997) The divIVA minicell locus of Bacillus subtilis. *J Bacteriol* **179**: 1671-1683.

Chaba, R., Raje, M., and Chakraborti, P.K. (2002) Evidence that a eukaryotic-type serine/threonine protein kinase from *Mycobacterium tuberculosis* regulates morphological changes associated with cell division. *Eur J Biochem* **269**: 1078-1085.

Chakraburtty, R., and Bibb, M. (1997) The ppGpp synthetase gene (relA) of *Streptomyces coelicolor* A3(2) plays a conditional role in antibiotic production and morphological differentiation. *J Bacteriol* **179**: 5854-5861.

Challis, G.L., and Hopwood, D.A. (2003) Synergy and contingency as driving forces for the evolution of multiple secondary metabolite production by *Streptomyces* species. *Proc Natl Acad Sci U S A* **2**: 14555-14561.

Champness, W.C. (1988) New loci required for *Streptomyces coelicolor* morphological and physiological differentiation. *J Bacteriol* **170**: 1168-1174.

Chater, K.F. (1972) A morphological and genetic mapping study of white colony mutants of *Streptomyces coelicolor*. *J Gen Microbiol* **72**: 9-28.

Chater, K.F. (1975) Construction and phenotypes of double sporulation deficient mutants in *Streptomyces coelicolor* A3(2). *J Gen Microbiol* **87**: 312-325.

Chater, K.F. (1989) Multilevel regulation of *Streptomyces* differentiation. *Trends Genet* **5**: 372-377.

Chater, K.F. (1993) Genetics of differentiation in *Streptomyces*. *Annu Rev Microbiol* **47**: 685-713.

Chater, K.F. (1998) Taking a genetic scalpel to the *Streptomyces* colony. *Microbiology* **144**: 1465-1478.

Chater, K.F. (2000) Developmental decisions during sporulation in the aerial mycelium in *Streptomyces*. In *Prokaryotic Development*. Brun, Y.V., Shimkets, L.J. and Chater, K.F. (eds): American Society for Microbiology press, pp. 33-48.

Chater, K.F. (2001) Regulation of sporulation in *Streptomyces coelicolor* A3(2): a checkpoint multiplex? *Curr Opin Microbiol* **4**: 667-673.

Chater, K.F., and Horinouchi, S. (2003) Signalling early developmental events in two highly diverged *Streptomyces* species. *Mol Microbiol* **48**: 9-15.

Chater, K.F. (2006) *Streptomyces* inside-out: a new perspective on the bacteria that provide us with antibiotics. *Philos Trans R Soc Lond B Biol Sci* **361**: 761-768.

Chater, K.F., and Chandra, G. (2006) The evolution of development in *Streptomyces* analysed by genome comparisons. *FEMS Microbiol Rev* **30**: 651-672.

Chater, K.F., and Chandra, G. (2008) The use of the rare UUA codon to define "expression space" for genes involved in secondary metabolism, development and environmental adaptation in *Streptomyces*. *J Microbiol* **46**: 1-11.

Chen, J.C., Weiss, D.S., Ghigo, J.M., and Beckwith, J. (1999) Septal localization of FtsQ, an essential cell division protein in *Escherichia coli*. *J Bacteriol* **181**: 521-530.

Chen, J.C., and Beckwith, J. (2001) FtsQ, FtsL and FtsI require FtsK, but not FtsN, for co-localization with FtsZ during *Escherichia coli* cell division. *Mol Microbiol* **42**: 395-413.

Chopra, P., Singh, B., Singh, R., Vohra, R., Koul, A., Meena, L.S., Koduri, H., Ghildiyal, M., Deol, P., Das, T.K., Tyagi, A.K., and Singh, Y. (2003) Phosphoprotein phosphatase of *Mycobacterium tuberculosis* dephosphorylates serine-threonine kinases PknA and PknB. *Biochem Biophys Res Commun* **311**: 112-120.

Chung, K.M., Hsu, H.H., Govindan, S., and Chang, B.Y. (2004) Transcription regulation of *ezrA* and its effect on cell division of *Bacillus subtilis*. *J Bacteriol* **186**: 5926-5932.

Chung, K.M., Hsu, H.H., Yeh, H.Y., and Chang, B.Y. (2007) Mechanism of regulation of prokaryotic tubulin-like GTPase FtsZ by membrane protein EzrA. *J Biol Chem* **282**: 14891-14897.

Claessen, D., Rink, R., de Jong, W., Siebring, J., de Vreugd, P., Boersma, F.G., Dijkhuizen, L., and Wosten, H.A. (2003) A novel class of secreted hydrophobic

proteins is involved in aerial hyphae formation in *Streptomyces coelicolor* by forming amyloid-like fibrils. *Genes Dev* **17**: 1714-1726.

Claessen, D., Stokroos, I., Deelstra, H.J., Penninga, N.A., Bormann, C., Salas, J.A., Dijkhuizen, L., and Wosten, H.A. (2004) The formation of the rodlet layer of streptomycetes is the result of the interplay between rodlins and chaplins. *Mol Microbiol* **53**: 433-443.

Claessen, D., de Jong, W., Dijkhuizen, L., and Wosten, H.A. (2006) Regulation of *Streptomyces* development: reach for the sky! *Trends Microbiol* **14**: 313-319.

Claros, M.G., and von Heijne, G. (1994) TopPred II: an improved software for membrane protein structure predictions. *Comput Appl Biosci* **10**: 685-686.

Colquhoun, J.A., Heald, S.C., Li, L., Tamaoka, J., Kato, C., Horikoshi, K., and Bull, A.T. (1998) Taxonomy and biotransformation activities of some deep-sea actinomycetes. *Extremophiles* **2**: 269-277.

Colquhoun, J.A., Zulu, J., Goodfellow, M., Horikoshi, K., Ward, A.C., and Bull, A.T. (2000) Rapid characterisation of deep-sea actinomycetes for biotechnology screening programmes. *Antonie Van Leeuwenhoek* **77**: 359-367.

Combes, P., Till, R., Bee, S., and Smith, M.C. (2002) The streptomyces genome contains multiple pseudo-*attB* sites for the (phi)C31-encoded site-specific recombination system. *J Bacteriol* **184**: 5746-5752.

D'Ulisse, V., Fagioli, M., Ghelardini, P., and Paolozzi, L. (2007) Three functional subdomains of the *Escherichia coli* FtsQ protein are involved in its interaction with the other division proteins. *Microbiology* **153**: 124-138.

Daniel, R.A., Drake, S., Buchanan, C.E., Scholle, R., and Errington, J. (1994) The *Bacillus subtilis spoVD* gene encodes a mother-cell-specific penicillin-binding protein required for spore morphogenesis. *J Mol Biol* **235**: 209-220.

Daniel, R.A., Harry, E.J., Katis, V.L., Wake, R.G., and Errington, J. (1998) Characterization of the essential cell division gene *ftsL(yIID)* of *Bacillus subtilis* and its role in the assembly of the division apparatus. *Mol Microbiol* **29**: 593-604.

Daniel, R.A., and Errington, J. (2000) Intrinsic instability of the essential cell division protein FtsL of *Bacillus subtilis* and a role for DivIB protein in FtsL turnover. *Mol Microbiol* **36**: 278-289.

Daniel, R.A., Harry, E.J., and Errington, J. (2000) Role of penicillin-binding protein PBP 2B in assembly and functioning of the division machinery of *Bacillus subtilis*. *Mol Microbiol* **35**: 299-311.

Daniel, R.A., and Errington, J. (2003) Control of cell morphogenesis in bacteria: two distinct ways to make a rod-shaped cell. *Cell* **113**: 767-776.

Daniel, R.A., Noirot-Gros, M.F., Noirot, P., and Errington, J. (2006) Multiple interactions between the transmembrane division proteins of *Bacillus subtilis* and the role of FtsL instability in divisome assembly. *J Bacteriol* **188**: 7396-7404.

Dasgupta, A., Datta, P., Kundu, M., and Basu, J. (2006) The serine/threonine kinase PknB of *Mycobacterium tuberculosis* phosphorylates PBPA, a penicillin-binding protein required for cell division. *Microbiology* **152**: 493-504.

Datsenko, K.A., and Wanner, B.L. (2000) One-step inactivation of chromosomal genes in *Escherichia coli* K-12 using PCR products. *Proc Natl Acad Sci U S A* **97**: 6640-6645.

Datta, P., Dasgupta, A., Bhakta, S., and Basu, J. (2002) Interaction between FtsZ and FtsW of *Mycobacterium tuberculosis*. *J Biol Chem* **277**: 24983-24987.

Datta, P., Dasgupta, A., Singh, A.K., Mukherjee, P., Kundu, M., and Basu, J. (2006) Interaction between FtsW and penicillin-binding protein 3 (PBP3) directs PBP3 to mid-cell, controls cell septation and mediates the formation of a trimeric complex involving FtsZ, FtsW and PBP3 in mycobacteria. *Mol Microbiol* **62**: 1655-1673.

Davis, N.K., and Chater, K.F. (1990) Spore colour in *Streptomyces coelicolor* A3(2) involves the developmentally regulated synthesis of a compound biosynthetically related to polyketide antibiotics. *Mol Microbiol* **4**: 1679-1691.

de Boer, P.A., Crossley, R.E., and Rothfield, L.I. (1989) A division inhibitor and a topological specificity factor coded for by the minicell locus determine proper placement of the division septum in E. coli. *Cell* **56**: 641-649.

de la Fuente, A., Palacios, P., and Vicente, M. (2001) Transcription of the *Escherichia coli* dcw cluster: evidence for distal upstream transcripts being involved in the expression of the downstream *ftsZ* gene. *Biochimie* **83**: 109-115.

de Pedro, M.A., Quintela, J.C., Holtje, J.V., and Schwarz, H. (1997) Murein segregation in *Escherichia coli*. *J Bacteriol* **179**: 2823-2834.

De Pedro, M.A., Schwarz, H., and Koch, A.L. (2003) Patchiness of murein insertion into the sidewall of *Escherichia coli*. *Microbiology* **149**: 1753-1761.

Defeu Soufo, H.J., and Graumann, P.L. (2006) Dynamic localization and interaction with other *Bacillus subtilis* actin-like proteins are important for the function of MreB. *Mol Microbiol* **62**: 1340-1356.

Del Sol, R., Pitman, A., Herron, P., and Dyson, P. (2003) The product of a developmental gene, *crgA*, that coordinates reproductive growth in *Streptomyces* belongs to a novel family of small actinomycete-specific proteins. *J Bacteriol* **185**: 6678-6685.

Del Sol, R. (2004) Functional analysis of a gene involved in coordinating reproductive growth of the model actinomycete *Streptomyces coelicolor*. In *School of Biological Sciences*. Vol. Ph.D. Swansea: University of Wales Swansea.

Del Sol, R., Mullins, J.G., Grantcharova, N., Flardh, K., and Dyson, P. (2006) Influence of CrgA on assembly of the cell division protein FtsZ during development of *Streptomyces coelicolor*. *J Bacteriol* **188**: 1540-1550.

Del Sol, R., Armstrong, I., Wright, C., and Dyson, P. (2007) Characterization of changes to the cell surface during the life cycle of *Streptomyces coelicolor*: atomic force microscopy of living cells. *J Bacteriol* **189**: 2219-2225.

Demerec, M., and Hartman, P.E. (1959) Complex Loci in Microorganisms. *Annual Review of Microbiology* **13**: 377-406.

Den Blaauwen, T., Buddelmeijer, N., Aarsman, M.E., Hameete, C.M., and Nanninga, N. (1999) Timing of FtsZ assembly in *Escherichia coli*. *J Bacteriol* **181**: 5167-5175.

Den Blaauwen, T., Aarsman, M.E., Vischer, N.O., and Nanninga, N. (2003) Penicillin-binding protein PBP2 of *Escherichia coli* localizes preferentially in the lateral wall and at mid-cell in comparison with the old cell pole. *Mol Microbiol* **47**: 539-547.

den Blaauwen, T., de Pedro, M.A., Nguyen-Disteche, M., and Ayala, J.A. (2008) Morphogenesis of rod-shaped sacculi. *FEMS Microbiol Rev* **32**: 321-344.

Denome, S.A., Elf, P.K., Henderson, T.A., Nelson, D.E., and Young, K.D. (1999) *Escherichia coli* mutants lacking all possible combinations of eight penicillin binding proteins: viability, characteristics, and implications for peptidoglycan synthesis. *J Bacteriol* **181**: 3981-3993.

Dharmatilake, A.J., and Kendrick, K.E. (1994) Expression of the division-controlling gene *ftsZ* during growth and sporulation of the filamentous bacterium *Streptomyces griseus*. *Gene* **147**: 21-28.

Di Lallo, G., Fagioli, M., Barionovi, D., Ghelardini, P., and Paolozzi, L. (2003) Use of a two-hybrid assay to study the assembly of a complex multicomponent protein machinery: bacterial septosome differentiation. *Microbiology* **149**: 3353-3359.

Din, N., Quardokus, E.M., Sackett, M.J., and Brun, Y.V. (1998) Dominant C-terminal deletions of FtsZ that affect its ability to localize in *Caulobacter* and its interaction with FtsA. *Mol Microbiol* **27**: 1051-1063.

Distler, J., Mansouri, K., Mayer, G., Stockmann, M., and Piepersberg, W. (1992) Streptomycin biosynthesis and its regulation in *Streptomycetes*. *Gene* **115**: 105-111.

Divakaruni, A.V., Loo, R.R., Xie, Y., Loo, J.A., and Gober, J.W. (2005) The cell-shape protein MreC interacts with extracytoplasmic proteins including cell wall assembly complexes in *Caulobacter crescentus*. *Proc Natl Acad Sci U S A* **102**: 18602-18607.

Dobrowolski, A., Sobczak-Elbourne, I., and Lolkema, J.S. (2007) Membrane topology prediction by hydropathy profile alignment: membrane topology of the Na(+)-glutamate transporter GltS. *Biochemistry* **46**: 2326-2332.

Doering-Saad, C., Kampfer, P., Manulis, S., Kritzman, G., Schneider, J., Zakrzewska-Czerwinska, J., Schrempf, H., and Barash, I. (1992) Diversity among *Streptomyces* Strains Causing Potato Scab. *Appl Environ Microbiol* **58**: 3932-3940.

Dye, N.A., Pincus, Z., Theriot, J.A., Shapiro, L., and Gitai, Z. (2005) Two independent spiral structures control cell shape in *Caulobacter*. *Proc Natl Acad Sci U S A* **102**: 18608-18613.

Ebersbach, G., Galli, E., Moller-Jensen, J., Lowe, J., and Gerdes, K. (2008) Novel coiled-coil cell division factor ZapB stimulates Z ring assembly and cell division. *Mol Microbiol* **68**: 720-735.

Eccleston, M., Ali, R.A., Seyler, R., Westpheling, J., and Nodwell, J. (2002) Structural and genetic analysis of the BldB protein of *Streptomyces coelicolor*. *J Bacteriol* **184**: 4270-4276.

Edwards, D.H., and Errington, J. (1997) The Bacillus subtilis DivIVA protein targets to the division septum and controls the site specificity of cell division. *Mol Microbiol* **24**: 905-915.

Elliot, M., Damji, F., Passantino, R., Chater, K., and Leskiw, B. (1998) The *bldD* gene of *Streptomyces coelicolor* A3(2): a regulatory gene involved in morphogenesis and antibiotic production. *J Bacteriol* **180**: 1549-1555.

Elliot, M.A., and Leskiw, B.K. (1999) The BldD protein from *Streptomyces coelicolor* is a DNA-binding protein. *J Bacteriol* **181**: 6832-6835.

Elliot, M.A., Bibb, M.J., Buttner, M.J., and Leskiw, B.K. (2001) BldD is a direct regulator of key developmental genes in *Streptomyces coelicolor* A3(2). *Mol Microbiol* **40**: 257-269.

Elliot, M.A., Karoonuthaisiri, N., Huang, J., Bibb, M.J., Cohen, S.N., Kao, C.M., and Buttner, M.J. (2003) The chaplins: a family of hydrophobic cell-surface proteins involved in aerial mycelium formation in *Streptomyces coelicolor*. *Genes Dev* **17**: 1727-1740.

Elliot, M.A., and Talbot, N.J. (2004) Building filaments in the air: aerial morphogenesis in bacteria and fungi. *Curr Opin Microbiol* **7**: 594-601.

Embley, T.M., and Stackebrandt, E. (1994) The molecular phylogeny and systematics of the actinomycetes. *Annu Rev Microbiol* **48**: 257-289.

Erickson, H.P. (1995) FtsZ, a prokaryotic homolog of tubulin? *Cell* **80**: 367-370.

Erickson, H.P., Taylor, D.W., Taylor, K.A., and Bramhill, D. (1996) Bacterial cell division protein FtsZ assembles into protofilament sheets and minirings, structural homologs of tubulin polymers. *Proc Natl Acad Sci U S A* **93**: 519-523.

Eritt, I., Grafe, U., and Fleck, W.F. (1982) A screening method for autoregulators of anthracycline-producing streptomycetes. *Z Allg Mikrobiol* **22**: 91-96.

Errington, J. (2001) Septation and chromosome segregation during sporulation in *Bacillus subtilis*. *Curr Opin Microbiol* **4**: 660-666.

Errington, J., Daniel, R.A., and Scheffers, D.J. (2003) Cytokinesis in bacteria. *Microbiol Mol Biol Rev* **67**: 52-65.

Fahal, A.H., and Hassan, M.A. (1992) Mycetoma. *Br J Surg* **79**: 1138-1141.

Fernandez-Moreno, M.A., Caballero, J.L., Hopwood, D.A., and Malpartida, F. (1991) The act cluster contains regulatory and antibiotic export genes, direct targets for translational control by the *bldA* tRNA gene of *Streptomyces*. *Cell* **66**: 769-780.

Figge, R.M., Divakaruni, A.V., and Gober, J.W. (2004) MreB, the cell shape-determining bacterial actin homologue, co-ordinates cell wall morphogenesis in Caulobacter crescentus. *Mol Microbiol* **51**: 1321-1332.

Fisher, S.H. (1992) Glutamine synthesis in *Streptomyces*--a review. *Gene* **115**: 13-17.

Flardh, K., Findlay, K.C., and Chater, K.F. (1999) Association of early sporulation genes with suggested developmental decision points in *Streptomyces coelicolor* A3(2). *Microbiology* **145**: 2229-2243.

Flardh, K., Leibovitz, E., Buttner, M.J., and Chater, K.F. (2000) Generation of a non-sporulating strain of *Streptomyces coelicolor* A3(2) by the manipulation of a developmentally controlled *ftsZ* promoter. *Mol Microbiol* **38**: 737-749.

Flardh, K. (2003a) Essential role of DivIVA in polar growth and morphogenesis in *Streptomyces coelicolor* A3(2). *Mol Microbiol* **49**: 1523-1536.

Flardh, K. (2003b) Growth polarity and cell division in *Streptomyces*. *Curr Opin Microbiol* **6**: 564-571.

Flett, F., Mersinias, V., and Smith, C.P. (1997) High efficiency intergeneric conjugal transfer of plasmid DNA from *Escherichia coli* to methyl DNA-restricting streptomycetes. *FEMS Microbiol Lett* **155**: 223-229.

Formstone, A., and Errington, J. (2005) A magnesium-dependent *mreB* null mutant: implications for the role of *mreB* in *Bacillus subtilis*. *Mol Microbiol* **55**: 1646-1657.

Fox, G.E., Pechman, J., and Woese, C.R. (1977) Comparative cataloguing of 16S ribosomal rinonucleic acid: molecular approach to prokaryotic systematics. *J Syst Bacteriol* **27**: 44-57.

Francis, F., Ramirez-Arcos, S., Salimnia, H., Victor, C., and Dillon, J.R. (2000) Organization and transcription of the division cell wall (dcw) cluster in *Neisseria gonorrhoeae*. *Gene* **251**: 141-151.

Frobisher, M., Hinsdill, R.D., Crabtree, K.T., and Goodheart, C.R. (1974) *Fundamentals of Microbiology*: W. B. Saunders Company.

Fujibuchi, W., Ogata, H., Matsuda, H., and Kanehisa, M. (2000) Automatic detection of conserved gene clusters in multiple genomes by graph comparison and P-quasi grouping. *Nucleic Acids Res* **28**: 4029-4036.

Gerard, P., Vernet, T., and Zapun, A. (2002) Membrane topology of the *Streptococcus pneumoniae* FtsW division protein. *J Bacteriol* **184**: 1925-1931.

Gerber, N.N., and Lechevalier, H.A. (1965) Geosmin, an earthly-smelling substance isolated from actinomycetes. *Appl Microbiol* **13**: 935-938.

Ghigo, J.M., and Beckwith, J. (2000) Cell division in *Escherichia coli*: role of FtsL domains in septal localization, function, and oligomerization. *J Bacteriol* **182**: 116-129.

Gitai, Z., Dye, N.A., Reisenauer, A., Wachi, M., and Shapiro, L. (2005) MreB actin-mediated segregation of a specific region of a bacterial chromosome. *Cell* **120**: 329-341.

Goehring, N.W., and Beckwith, J. (2005) Diverse paths to midcell: assembly of the bacterial cell division machinery. *Curr Biol* **15**: R514-526.

Goehring, N.W., Gueiros-Filho, F., and Beckwith, J. (2005) Premature targeting of a cell division protein to midcell allows dissection of divisome assembly in *Escherichia coli*. *Genes Dev* **19**: 127-137.

Goehring, N.W., Gonzalez, M.D., and Beckwith, J. (2006) Premature targeting of cell division proteins to midcell reveals hierarchies of protein interactions involved in divisome assembly. *Mol Microbiol* **61**: 33-45.

Goffin, C., and Ghuysen, J.M. (1998) Multimodular penicillin-binding proteins: an enigmatic family of orthologs and paralogs. *Microbiol Mol Biol Rev* **62**: 1079-1093.

Gomez, J.E., and Bishai, W.R. (2000) *whmD* is an essential mycobacterial gene required for proper septation and cell division. *Proc Natl Acad Sci U S A* **97**: 8554-8559.

Grantcharova, N., Ubhayasekera, W., Mowbray, S.L., McCormick, J.R., and Flardh, K. (2003) A missense mutation in *ftsZ* differentially affects vegetative and developmentally controlled cell division in *Streptomyces coelicolor* A3(2). *Mol Microbiol* **47**: 645-656.

Grantcharova, N., Lustig, U., and Flardh, K. (2005) Dynamics of FtsZ assembly during sporulation in *Streptomyces coelicolor* A3(2). *J Bacteriol* **187**: 3227-3237.

Gray, D.I., Gooday, G.W., and Prosser, J.I. (1990) Apical hyphal extension in *Streptomyces coelicolor* A3(2). *J Gen Microbiol* **136**: 1077-1084.

Greenwood, D., and Whitley, R. (2003) Modes of action. In *Antibiotic and Chemotheraphy*, Finch, R., Greenwood, D., Norrby, RS. and Whitley, R. (8^{th} eds). Edinburgh, UK: Churchill Livingstone, pp. 11-24.

Grund, A.D., and Ensign, J.C. (1982) Activation of *Streptomyces viridochromogenes* spores by detergents. *Curr Microbiol* **7**: 223–228.

Grundner, C., Gay, L.M., and Alber, T. (2005) *Mycobacterium tuberculosis* serine/threonine kinases PknB, PknD, PknE, and PknF phosphorylate multiple FHA domains. *Protein Sci* **14**: 1918-1921.

Gueiros-Filho, F.J., and Losick, R. (2002) A widely conserved bacterial cell division protein that promotes assembly of the tubulin-like protein FtsZ. *Genes Dev* **16**: 2544-2556.

Gust, B., Challis, G.L., Fowler, K., Kieser, T., and Chater, K.F. (2003) PCR-targeted *Streptomyces* gene replacement identifies a protein domain needed for biosynthesis of the sesquiterpene soil odor geosmin. *Proc Natl Acad Sci U S A* **100**: 1541-1546.

Guzman, L.M., Barondess, J.J., and Beckwith, J. (1992) FtsL, an essential cytoplasmic membrane protein involved in cell division in *Escherichia coli*. *J Bacteriol* **174**: 7716-7728.

Haeusser, D.P., Schwartz, R.L., Smith, A.M., Oates, M.E., and Levin, P.A. (2004) EzrA prevents aberrant cell division by modulating assembly of the cytoskeletal protein FtsZ. *Mol Microbiol* **52**: 801-814.

Hale, C.A., and de Boer, P.A. (1997) Direct binding of FtsZ to ZipA, an essential component of the septal ring structure that mediates cell division in *E. coli*. *Cell* **88**: 175-185.

Hale, C.A., and de Boer, P.A. (1999) Recruitment of ZipA to the septal ring of *Escherichia coli* is dependent on FtsZ and independent of FtsA. *J Bacteriol* **181**: 167-176.

Hale, C.A., and de Boer, P.A. (2002) ZipA is required for recruitment of FtsK, FtsQ, FtsL, and FtsN to the septal ring in *Escherichia coli*. *J Bacteriol* **184**: 2552-2556.

Hamoen, L.W., Meile, J.C., de Jong, W., Noirot, P., and Errington, J. (2006) SepF, a novel FtsZ-interacting protein required for a late step in cell division. *Mol Microbiol* **59**: 989-999.

Hao, J., and Kendrick, K.E. (1998) Visualization of penicillin-binding proteins during sporulation of *Streptomyces griseus*. *J Bacteriol* **180**: 2125-2132.

Hara, H., Yasuda, S., Horiuchi, K., and Park, J.T. (1997) A promoter for the first nine genes of the *Escherichia coli mra* cluster of cell division and cell envelope biosynthesis genes, including *ftsI* and *ftsW*. *J Bacteriol* **179**: 5802-5811.

Harasym, M., Zhang, L.H., Chater, K., and Piret, J. (1990) The *Streptomyces coelicolor* A3(2) *bldB* region contains at least two genes involved in morphological development. *J Gen Microbiol* **136**: 1543-1550.

Harry, E., Monahan, L., and Thompson, L. (2006) Bacterial cell division: the mechanism and its precison. *Int Rev Cytol* **253**: 27-94.

Harry, E.J., and Wake, R.G. (1989) Cloning and expression of a *Bacillus subtilis* division initiation gene for which a homolog has not been identified in another organism. *J Bacteriol* **171**: 6835-6839.

Harry, E.J. (2001) Bacterial cell division: regulating Z-ring formation. *Mol Microbiol* **40**: 795-803.

Henriques, A.O., de Lencastre, H., and Piggot, P.J. (1992) A *Bacillus subtilis* morphogene cluster that includes *spoVE* is homologous to the mra region of *Escherichia coli*. *Biochimie* **74**: 735-748.

Henriques, A.O., Glaser, P., Piggot, P.J., and Moran, C.P., Jr. (1998) Control of cell shape and elongation by the *rodA* gene in *Bacillus subtilis*. *Mol Microbiol* **28**: 235-247.

Hett, E.C., and Rubin, E.J. (2008) Bacterial growth and cell division: a mycobacterial perspective. *Microbiol Mol Biol Rev* **72**: 126-156.

Hodgson, D.A. (2000) Primary metabolism and its control in streptomycetes: a most unusual group of bacteria. *Adv Microb Physiol* **42**: 47-238.

Hofmann, K., and Stoffel, W. (1993) TMBASE - A database of membrane spanning protein segments. *Biol. Chem. Hoppe-Seyler* **374**: 166.

Hong, H.J., Paget, M.S., and Buttner, M.J. (2002) A signal transduction system in *Streptomyces coelicolor* that activates the expression of a putative cell wall

glycan operon in response to vancomycin and other cell wall-specific antibiotics. *Mol Microbiol* **44**: 1199-1211.

Hong, H.J., Hutchings, M.I., Neu, J.M., Wright, G.D., Paget, M.S., and Buttner, M.J. (2004) Characterization of an inducible vancomycin resistance system in *Streptomyces coelicolor* reveals a novel gene *(vanK)* required for drug resistance. *Mol Microbiol* **52**: 1107-1121.

Hong, H.J., Hutchings, M.I., Hill, L.M., and Buttner, M.J. (2005) The role of the novel Fem protein VanK in vancomycin resistance in *Streptomyces coelicolor*. *J Biol Chem* **280**: 13055-13061.

Hood, D.W., Heidstra, R., Swoboda, U.K., and Hodgson, D.A. (1992) Molecular genetic analysis of proline and tryptophan biosynthesis in *Streptomyces coelicolor* A3(2): interaction between primary and secondary metabolism--a review. *Gene* **115**: 5-12.

Hopwood, D.A., Wildermuth, H., and Palmer, H.M. (1970) Mutants of *Streptomyces coelicolor* defective in sporulation. *J Gen Microbiol* **61**: 397-408.

Hopwood, D.A. (1999) Forty years of genetics with *Streptomyces*: from in vivo through in vitro to in silico. *Microbiology* **145**: 2183-2202.

Horinouchi, S., and Beppu, T. (1992a) Regulation of secondary metabolism and cell differentiation in *Streptomyces*: A-factor as a microbial hormone and the AfsR protein as a component of a two-component regulatory system. *Gene* **115**: 167-172.

Horinouchi, S., and Beppu, T. (1992b) Autoregulatory factors and communication in actinomycetes. *Annu Rev Microbiol* **46**: 377-398.

Horinouchi, S. (2002) A microbial hormone, A-factor, as a master switch for morphological differentiation and secondary metabolism in *Streptomyces griseus*. *Front Biosci* **7**: d2045-2057.

Hu, D.S., Hood, D.W., Heidstra, R., and Hodgson, D.A. (1999a) The expression of the *trpD*, *trpC* and *trpBA* genes of *Streptomyces coelicolor* A3(2) is regulated by growth rate and growth phase but not by feedback repression. *Mol Microbiol* **32**: 869-880.

Hu, Z., and Lutkenhaus, J. (1999) Topological regulation of cell division in *Escherichia coli* involves rapid pole to pole oscillation of the division inhibitor MinC under the control of MinD and MinE. *Mol Microbiol* **34**: 82-90.

Hu, Z., Mukherjee, A., Pichoff, S., and Lutkenhaus, J. (1999b) The MinC component of the division site selection system in *Escherichia coli* interacts with FtsZ to prevent polymerization. *Proc Natl Acad Sci U S A* **96**: 14819-14824.

Hudson, M.E., Zhang, D., and Nodwell, J.R. (2002) Membrane association and kinase-like motifs of the RamC protein of *Streptomyces coelicolor*. *J Bacteriol* **184**: 4920-4924.

Hunt, A.C., Servin-Gonzalez, L., Kelemen, G.H., and Buttner, M.J. (2005) The *bldC* developmental locus of *Streptomyces coelicolor* encodes a member of a family of small DNA-binding proteins related to the DNA-binding domains of the MerR family. *J Bacteriol* **187**: 716-728.

Ikeda, H., Ishikawa, J., Hanamoto, A., Shinose, M., Kikuchi, H., Shiba, T., Sakaki, Y., Hattori, M., and Omura, S. (2003) Complete genome sequence and comparative analysis of the industrial microorganism Streptomyces avermitilis. *Nat Biotechnol* **21**: 526-531.

Ikeda, M., Sato, T., Wachi, M., Jung, H.K., Ishino, F., Kobayashi, Y., and Matsuhashi, M. (1989) Structural similarity among *Escherichia coli* FtsW and RodA proteins and *Bacillus subtilis* SpoVE protein, which function in cell division, cell elongation, and spore formation, respectively. *J Bacteriol* **171**: 6375-6378.

Ishikawa, S., Kawai, Y., Hiramatsu, K., Kuwano, M., and Ogasawara, N. (2006) A new FtsZ-interacting protein, YlmF, complements the activity of FtsA during progression of cell division in *Bacillus subtilis*. *Mol Microbiol* **60**: 1364-1380.

Jakimowicz, P., Cheesman, M.R., Bishai, W.R., Chater, K.F., Thomson, A.J., and Buttner, M.J. (2005) Evidence that the *Streptomyces* developmental protein WhiD, a member of the WhiB family, binds a [4Fe-4S] cluster. *J Biol Chem* **280**: 8309-8315.

Jiang, H., and Kendrick, K.E. (2000) Characterization of *ssfR* and *ssgA*, two genes involved in sporulation of *Streptomyces griseus*. *J Bacteriol* **182**: 5521-5529.

Jiang, J., He, X., and Cane, D.E. (2006) Geosmin biosynthesis. *Streptomyces coelicolor* germacradienol/germacrene D synthase converts farnesyl diphosphate to geosmin. *J Am Chem Soc* **128**: 8128-8129.

Johnston, D.W., and Cross, T. (1976) The occurrence and distribution of actinomycetes in lakes of the English Lake District. *Freshwater Biology* **6**: 457-463.

Jones, G., and Dyson, P. (2006) Evolution of transmembrane protein kinases implicated in coordinating remodeling of gram-positive peptidoglycan: inside versus outside. *J Bacteriol* **188**: 7470-7476.

Jones, L.J., Carballido-Lopez, R., and Errington, J. (2001) Control of cell shape in bacteria: helical, actin-like filaments in *Bacillus subtilis*. *Cell* **104**: 913-922.

Joris, B., Dive, G., Henriques, A., Piggot, P.J., and Ghuysen, J.M. (1990) The life-cycle proteins RodA of *Escherichia coli* and SpoVE of *Bacillus subtilis* have very similar primary structures. *Mol Microbiol* **4**: 513-517.

Kampfer, P., Kroppenstedt, R.M., and Dott, W. (1991) A numerical classification of the genera *Streptomyces* and *Streptoverticillium* using miniaturized physiological tests. *J Gen Microbiol* **137**: 1831-1891.

Kang, C.M., Nyayapathy, S., Lee, J.Y., Suh, J.W., and Husson, R.N. (2008) Wag31, a homologue of the cell division protein DivIVA, regulates growth, morphology and polar cell wall synthesis in mycobacteria. *Microbiology* **154**: 725-735.

Kataoka, M., Ueda, K., Kudo, T., Seki, T., and Yoshida, T. (1997) Application of the variable region in 16S rDNA to create an index for rapid species identification in the genus *Streptomyces*. *FEMS Microbiol Lett* **151**: 249-255.

Kataoka, M., Kosono, S., and Tsujimoto, G. (1999) Spatial and temporal regulation of protein expression by *bldA* within a *Streptomyces lividans* colony. *FEBS Lett* **462**: 425-429.

Katis, V.L., Wake, R.G., and Harry, E.J. (2000) Septal localization of the membrane-bound division proteins of *Bacillus subtilis* DivIB and DivIC is codependent only at high temperatures and requires FtsZ. *J Bacteriol* **182**: 3607-3611.

Kato, J.Y., Ohnishi, Y., and Horinouchi, S. (2005) Autorepression of AdpA of the AraC/XylS family, a key transcriptional activator in the A-factor regulatory cascade in *Streptomyces griseus*. *J Mol Biol* **350**: 12-26.

Kawamoto, S., and Ensign, J.C. (1995) Cloning and characterization of a gene involved in regulation of sporulation and cell division in *Streptomyces griseus*. *Actinomycetologica* **9**: 136-151.

Kawamoto, S., Watanabe, H., Hesketh, A., Ensign, J.C., and Ochi, K. (1997) Expression analysis of the *ssgA* gene product, associated with sporulation and cell division in *Streptomyces griseus*. *Microbiology* **143**: 1077-1086.

Keijser, B.J., Noens, E.E., Kraal, B., Koerten, H.K., and van Wezel, G.P. (2003) The Streptomyces coelicolor *ssgB* gene is required for early stages of sporulation. *FEMS Microbiol Lett* **225**: 59-67.

Kelemen, G.H., Brown, G.L., Kormanec, J., Potuckova, L., Chater, K.F., and Buttner, M.J. (1996) The positions of the sigma-factor genes, *whiG* and *sigF*, in the hierarchy controlling the development of spore chains in the aerial hyphae of *Streptomyces coelicolor* A3(2). *Mol Microbiol* **21**: 593-603.

Kelemen, G.H., Brian, P., Flardh, K., Chamberlin, L., Chater, K.F., and Buttner, M.J. (1998) Developmental regulation of transcription of *whiE*, a locus specifying the polyketide spore pigment in *Streptomyces coelicolor* A3 (2). *J Bacteriol* **180**: 2515-2521.

Kelemen, G.H., and Buttner, M.J. (1998) Initiation of aerial mycelium formation in *Streptomyces*. *Curr Opin Microbiol* **1**: 656-662.

Keller, U., Krengel, U., and Haese, A. (1985) Genetic analysis in *Streptomyces chrysomallus*. *J Gen Microbiol* **131**: 1181-1191.

Kendrick, K.E., and Wheelis, M.L. (1982) Histidine dissimilation in *Streptomyces coelicolor*. *J Gen Microbiol* **128**: 2029-2040.

Khattar, M.M., Begg, K.J., and Donachie, W.D. (1994) Identification of FtsW and characterization of a new *ftsW* division mutant of *Escherichia coli*. *J Bacteriol* **176**: 7140-7147.

Khattar, M.M., Addinall, S.G., Stedul, K.H., Boyle, D.S., Lutkenhaus, J., and Donachie, W.D. (1997) Two polypeptide products of the *Escherichia coli* cell division gene *ftsW* and a possible role for FtsW in FtsZ function. *J Bacteriol* **179**: 784-793.

Khvorova, A., Zhang, L., Higgins, M.L., and Piggot, P.J. (1998) The *spoIIE* locus is involved in the Spo0A-dependent switch in the location of FtsZ rings in *Bacillus subtilis*. *J Bacteriol* **180**: 1256-1260.

Kieser, H.M., Kieser, T., and Hopwood, D.A. (1992) A combined genetic and physical map of the *Streptomyces coelicolor* A3(2) chromosome. *J Bacteriol* **174**: 5496-5507.

Kieser, T., Bibb, M.J., Buttner, M.J., Chater, K.F., and Hopwood, D.A. (2000) *Practical Streptomyces genetics*: John Innes Foundation, Norwich, United Kingdom.

Kihara, D., and Kanehisa, M. (2000) Tandem clusters of membrane proteins in complete genome sequences. *Genome Res* **10**: 731-743.

Kim, H.J., Calcutt, M.J., Schmidt, F.J., and Chater, K.F. (2000) Partitioning of the linear chromosome during sporulation of *Streptomyces coelicolor* A3(2) involves an *oriC*-linked *parAB* locus. *J Bacteriol* **182**: 1313-1320.

Kodani, S., Hudson, M.E., Durrant, M.C., Buttner, M.J., Nodwell, J.R., and Willey, J.M. (2004) The SapB morphogen is a lantibiotic-like peptide derived from the product of the developmental gene *ramS* in *Streptomyces coelicolor*. *Proc Natl Acad Sci U S A* **101**: 11448-11453.

Kormanec, J., Potuckova, L., and Rezuchova, B. (1994) The *Streptomyces aureofaciens* homologue of the *whiG* gene encoding a putative sigma factor essential for sporulation. *Gene* **143**: 101-103.

Kormanec, J., and Sevcikova, B. (2002) The stress-response sigma factor sigma(H) controls the expression of *ssgB*, a homologue of the sporulation-specific cell division gene *ssgA*, in *Streptomyces coelicolor* A3(2). *Mol Genet Genomics* **267**: 536-543.

Kroening, T.A., and Kendrick, K.E. (1987) In vivo regulation of histidine ammonia-lyase activity from *Streptomyces griseus*. *J Bacteriol* **169**: 823-829.

Kruse, T., Moller-Jensen, J., Lobner-Olesen, A., and Gerdes, K. (2003) Dysfunctional MreB inhibits chromosome segregation in *Escherichia coli*. *Embo J* **22**: 5283-5292.

Kruse, T., Bork-Jensen, J., and Gerdes, K. (2005) The morphogenetic MreBCD proteins of *Escherichia coli* form an essential membrane-bound complex. *Mol Microbiol* **55**: 78-89.

Kumar, S., Tamura, K., and Nei, M. (1994) MEGA: Molecular Evolutionary Genetics Analysis software for microcomputers. *Comput Appl Biosci* **10**: 189-191.

Kwak, J., McCue, L.A., and Kendrick, K.E. (1996) Identification of *bldA* mutants of *Streptomyces griseus*. *Gene* **171**: 75-78.

Kwak, J., Dharmatilake, A.J., Jiang, H., and Kendrick, K.E. (2001) Differential regulation of *ftsZ* transcription during septation of *Streptomyces griseus*. *J Bacteriol* **183**: 5092-5101.

Kwakman, J.H., and Postma, P.W. (1994) Glucose kinase has a regulatory role in carbon catabolite repression in *Streptomyces coelicolor*. *J Bacteriol* **176**: 2694-2698.

Kyte, J., and Doolittle, R.F. (1982) A simple method for displaying the hydropathic character of a protein. *J Mol Biol* **157**: 105-132.

Lacey, J. (1973) Actinomycetes in soils, composts and fodders. *Soc Appl Bacteriol Symp Ser* **2**: 231-251.

Lara, B., and Ayala, J.A. (2002) Topological characterization of the essential *Escherichia coli* cell division protein FtsW. *FEMS Microbiol Lett* **216**: 23-32.

Lawlor, E.J., Baylis, H.A., and Chater, K.F. (1987) Pleiotropic morphological and antibiotic deficiencies result from mutations in a gene encoding a tRNA-like product in *Streptomyces coelicolor* A3(2). *Genes Dev* **1**: 1305-1310.

Leaver, M., and Errington, J. (2005) Roles for MreC and MreD proteins in helical growth of the cylindrical cell wall in *Bacillus subtilis*. *Mol Microbiol* **57**: 1196-1209.

Leblond, P., Redenbach, M., and Cullum, J. (1993) Physical map of the *Streptomyces lividans* 66 genome and comparison with that of the related strain *Streptomyces coelicolor* A3(2). *J Bacteriol* **175**: 3422-3429.

Lechevalier, M.P., and Lechevalier, H. (1970) Chemical composition as a criterion in the classification of aerobic actinomycetes. *Int J Syst Bacteriol* **20**: 435-443.

Lee, J.C., and Stewart, G.C. (2003) Essential nature of the *mreC* determinant of *Bacillus subtilis*. *J Bacteriol* **185**: 4490-4498.

Leskiw, B.K., Bibb, M.J., and Chater, K.F. (1991a) The use of a rare codon specifically during development? *Mol Microbiol* **5**: 2861-2867.

Leskiw, B.K., Lawlor, E.J., Fernandez-Abalos, J.M., and Chater, K.F. (1991b) TTA codons in some genes prevent their expression in a class of developmental, antibiotic-negative, Streptomyces mutants. *Proc Natl Acad Sci U S A* **88**: 2461-2465.

Leskiw, B.K., Mah, R., Lawlor, E.J., and Chater, K.F. (1993) Accumulation of *bldA*-specified tRNA is temporally regulated in *Streptomyces coelicolor* A3(2). *J Bacteriol* **175**: 1995-2005.

Leskiw, B.K., and Mah, R. (1995) The *bldA*-encoded tRNA is poorly expressed in the *bldI* mutant of *Streptomyces coelicolor* A3(2). *Microbiology* **141**: 1921-1926.

Letek, M., Ordonez, E., Fiuza, M., Honrubia-Marcos, P., Vaquera, J., Gil, J.A., Castro, D., and Mateos, L.M. (2007) Characterization of the promoter region of *ftsZ* from *Corynebacterium glutamicum* and controlled overexpression of FtsZ. *Int Microbiol* **10**: 271-282.

Letek, M., Ordonez, E., Vaquera, J., Margolin, W., Flardh, K., Mateos, L.M., and Gil, J.A. (2008) DivIVA is required for polar growth in the MreB-lacking rod-shaped actinomycete Corynebacterium glutamicum. *J Bacteriol* **190**: 3283-3292.

Levin, P.A., Margolis, P.S., Setlow, P., Losick, R., and Sun, D. (1992) Identification of *Bacillus subtilis* genes for septum placement and shape determination. *J Bacteriol* **174**: 6717-6728.

Levin, P.A., and Losick, R. (1994) Characterization of a cell division gene from *Bacillus subtilis* that is required for vegetative and sporulation septum formation. *J Bacteriol* **176**: 1451-1459.

Levin, P.A., and Grossman, A.D. (1998) Cell cycle and sporulation in *Bacillus subtilis*. *Curr Opin Microbiol* **1**: 630-635.

Levin, P.A., Kurtser, I.G., and Grossman, A.D. (1999) Identification and characterization of a negative regulator of FtsZ ring formation in *Bacillus subtilis*. *Proc Natl Acad Sci U S A* **96**: 9642-9647.

Li, J., Lee, G.I., Van Doren, S.R., and Walker, J.C. (2000) The FHA domain mediates phosphoprotein interactions. *J Cell Sci* **113**: 4143-4149.

Liu, N.J., Dutton, R.J., and Pogliano, K. (2006) Evidence that the SpoIIIE DNA translocase participates in membrane fusion during cytokinesis and engulfment. *Mol Microbiol* **59**: 1097-1113.

Lu, Z., Takeuchi, M., and Sato, T. (2007) The LysR-type transcriptional regulator YofA controls cell division through the regulation of expression of *ftsW* in *Bacillus subtilis*. *J Bacteriol* **189**: 5642-5651.

Lucet, I., Feucht, A., Yudkin, M.D., and Errington, J. (2000) Direct interaction between the cell division protein FtsZ and the cell differentiation protein SpoIIE. *Embo J* **19**: 1467-1475.

Ma, H., and Kendall, K. (1994) Cloning and analysis of a gene cluster from *Streptomyces coelicolor* that causes accelerated aerial mycelium formation in *Streptomyces lividans*. *J Bacteriol* **176**: 3800-3811.

Ma, X., Ehrhardt, D.W., and Margolin, W. (1996) Colocalization of cell division proteins FtsZ and FtsA to cytoskeletal structures in living *Escherichia coli* cells by using green fluorescent protein. *Proc Natl Acad Sci U S A* **93**: 12998-13003.

Macheboeuf, P., Contreras-Martel, C., Job, V., Dideberg, O., and Dessen, A. (2006) Penicillin binding proteins: key players in bacterial cell cycle and drug resistance processes. *FEMS Microbiol Rev* **30**: 673-691.

Margolin, W. (2000) Themes and variations in prokaryotic cell division. *FEMS Microbiol Rev* **24**: 531-548.

Margolin, W. (2001) Spatial regulation of cytokinesis in bacteria. *Curr Opin Microbiol* **4**: 647-652.

Margolis, P.S., Driks, A., and Losick, R. (1993) Sporulation gene *spoIIB* from *Bacillus subtilis*. *J Bacteriol* **175**: 528-540.

Marston, A.L., and Errington, J. (1999) Selection of the midcell division site in *Bacillus subtilis* through MinD-dependent polar localization and activation of MinC. *Mol Microbiol* **33**: 84-96.

Martin, J.F. (2004) Phosphate control of the biosynthesis of antibiotics and other secondary metabolites is mediated by the PhoR-PhoP system: an unfinished story. *J Bacteriol* **186**: 5197-5201.

Matsuzawa, H., Asoh, S., Kunai, K., Muraiso, K., Takasuga, A., and Ohta, T. (1989) Nucleotide sequence of the *rodA* gene, responsible for the rod shape of *Escherichia coli*: *rodA* and the *pbpA* gene, encoding penicillin-binding protein 2, constitute the *rodA* operon. *J Bacteriol* **171**: 558-560.

Mazodier, P., Petter, R., and Thompson, C. (1989) Intergeneric conjugation between *Escherichia coli* and *Streptomyces* species. *J Bacteriol* **171**: 3583-3585.

Mazza, P., Noens, E.E., Schirner, K., Grantcharova, N., Mommaas, A.M., Koerten, H.K., Muth, G., Flardh, K., van Wezel, G.P., and Wohlleben, W. (2006) MreB of *Streptomyces coelicolor* is not essential for vegetative growth but is required for the integrity of aerial hyphae and spores. *Mol Microbiol* **60**: 838-852.

McBride, M.J., and Ensign, J.C. (1987) Effects of intracellular trehalose content on *Streptomyces griseus* spores. *J Bacteriol* **169**: 4995-5001.

McCarthy, A.J., and Williams, S.T. (1992) Actinomycetes as agents of biodegradation in the environment--a review. *Gene* **115**: 189-192.

McCormick, J.R., Su, E.P., Driks, A., and Losick, R. (1994) Growth and viability of *Streptomyces coelicolor* mutant for the cell division gene *ftsZ*. *Mol Microbiol* **14**: 243-254.

McCormick, J.R., and Losick, R. (1996) Cell division gene *ftsQ* is required for efficient sporulation but not growth and viability in *Streptomyces coelicolor* A3(2). *J Bacteriol* **178**: 5295-5301.

McNeil, M.M., and Brown, J.M. (1994) The medically important aerobic actinomycetes: epidemiology and microbiology. *Clin Microbiol Rev* **7**: 357-417.

McVittie, A. (1974) Ultrastructural studies on sporulation in wild-type and white colony mutants of *Streptomyces coelicolor*. *J Gen Microbiol* **81**: 291-302.

Mendez, C., Brana, A.F., Manzanal, M.B., and Hardisson, C. (1985) Role of substrate mycelium in colony development in *Streptomyces*. *Can J Microbiol* **31**: 446-450.

Mengin-Lecreulx, D., Texier, L., Rousseau, M., and van Heijenoort, J. (1991) The *murG* gene of *Escherichia coli* codes for the UDP-N-acetylglucosamine: N-acetylmuramyl-(pentapeptide) pyrophosphoryl-undecaprenol N-acetylglucosamine transferase involved in the membrane steps of peptidoglycan synthesis. *J Bacteriol* **173**: 4625-4636.

Mengin-Lecreulx, D., Ayala, J., Bouhss, A., van Heijenoort, J., Parquet, C., and Hara, H. (1998) Contribution of the *Pmra* promoter to expression of genes in the *Escherichia coli mra* cluster of cell envelope biosynthesis and cell division genes. *J Bacteriol* **180**: 4406-4412.

Mercer, K.L., and Weiss, D.S. (2002) The *Escherichia coli* cell division protein FtsW is required to recruit its cognate transpeptidase, FtsI (PBP3), to the division site. *J Bacteriol* **184**: 904-912.

Merrick, M.J. (1976) A morphological and genetic mapping study of bald colony mutants of *Streptomyces coelicolor*. *J Gen Microbiol* **96**: 299-315.

Miguelez, E.M., Hardisson, C., and Manzanal, M.B. (1999) Hyphal death during colony development in *Streptomyces antibioticus*: morphological evidence for the existence of a process of cell deletion in a multicellular prokaryote. *J Cell Biol* **145**: 515-525.

Miguelez, E.M., Hardisson, C., and Manzanal, M.B. (2000) Streptomycetes: a new model to study cell death. *Int Microbiol* **3**: 153-158.

Mikulik, K., Zhulanova, E., Kratky, M., Kofronova, O., and Benada, O. (2000) Isolation and characterization of dcw cluster from *Streptomyces collinus* producing kirromycin. *Biochem Biophys Res Commun* **268**: 282-288.

Mingorance, J., Tamames, J., and Vicente, M. (2004) Genomic channeling in bacterial cell division. *J Mol Recognit* **17**: 481-487.

Molle, V., and Buttner, M.J. (2000) Different alleles of the response regulator gene *bldM* arrest *Streptomyces coelicolor* development at distinct stages. *Mol Microbiol* **36**: 1265-1278.

Molle, V., Palframan, W.J., Findlay, K.C., and Buttner, M.J. (2000) WhiD and WhiB, homologous proteins required for different stages of sporulation in *Streptomyces coelicolor* A3(2). *J Bacteriol* **182**: 1286-1295.

Moller-Jensen, J., and Lowe, J. (2005) Increasing complexity of the bacterial cytoskeleton. *Curr Opin Cell Biol* **17**: 75-81.

Moran, M.A., Rutherford, L.T., and Hodson, R.E. (1995) Evidence for indigenous *Streptomyces* populations in a marine environment determined with a 16S rRNA probe. *Appl Environ Microbiol* **61**: 3695-3700.

Muchova, K., Kutejova, E., Scott, D.J., Brannigan, J.A., Lewis, R.J., Wilkinson, A.J., and Barak, I. (2002) Oligomerization of the *Bacillus subtilis* division protein DivIVA. *Microbiology* **148**: 807-813.

Mukherjee, A., Dai, K., and Lutkenhaus, J. (1993) *Escherichia coli* cell division protein FtsZ is a guanine nucleotide binding protein. *Proc Natl Acad Sci U S A* **90**: 1053-1057.

Mukherjee, A., and Lutkenhaus, J. (1998) Dynamic assembly of FtsZ regulated by GTP hydrolysis. *Embo J* **17**: 462-469.

Nanninga, N. (1998) Morphogenesis of *Escherichia coli*. *Microbiol Mol Biol Rev* **62**: 110-129.

Narayan, A., Sachdeva, P., Sharma, K., Saini, A.K., Tyagi, A.K., and Singh, Y. (2007) Serine threonine protein kinases of mycobacterial genus: phylogeny to function. *Physiol Genomics* **29**: 66-75.

Nelson, D.E., and Young, K.D. (2001) Contributions of PBP 5 and DD-carboxypeptidase penicillin binding proteins to maintenance of cell shape in *Escherichia coli*. *J Bacteriol* **183**: 3055-3064.

Nguyen, K.T., Willey, J.M., Nguyen, L.D., Nguyen, L.T., Viollier, P.H., and Thompson, C.J. (2002) A central regulator of morphological differentiation in the multicellular bacterium *Streptomyces coelicolor*. *Mol Microbiol* **46**: 1223-1238.

Nguyen, K.T., Tenor, J., Stettler, H., Nguyen, L.T., Nguyen, L.D., and Thompson, C.J. (2003) Colonial differentiation in *Streptomyces coelicolor* depends on translation of a specific codon within the *adpA* gene. *J Bacteriol* **185**: 7291-7296.

Nicieza, R.G., Huergo, J., Connolly, B.A., and Sanchez, J. (1999) Purification, characterization, and role of nucleases and serine proteases in *Streptomyces* differentiation. Analogies with the biochemical processes described in late steps of eukaryotic apoptosis. *J Biol Chem* **274**: 20366-20375.

Nikolaichik, Y.A., and Donachie, W.D. (2000) Conservation of gene order amongst cell wall and cell division genes in Eubacteria, and ribosomal genes in Eubacteria and Eukaryotic organelles. *Genetica* **108**: 1-7.

Nodwell, J.R., McGovern, K., and Losick, R. (1996) An oligopeptide permease responsible for the import of an extracellular signal governing aerial mycelium formation in *Streptomyces coelicolor*. *Mol Microbiol* **22**: 881-893.

Nodwell, J.R., and Losick, R. (1998) Purification of an extracellular signaling molecule involved in production of aerial mycelium by *Streptomyces coelicolor*. *J Bacteriol* **180**: 1334-1337.

Nodwell, J.R., Yang, M., Kuo, D., and Losick, R. (1999) Extracellular complementation and the identification of additional genes involved in aerial mycelium formation in *Streptomyces coelicolor*. *Genetics* **151**: 569-584.

Noens, E.E., Mersinias, V., Traag, B.A., Smith, C.P., Koerten, H.K., and van Wezel, G.P. (2005) SsgA-like proteins determine the fate of peptidoglycan during sporulation of *Streptomyces coelicolor*. *Mol Microbiol* **58**: 929-944.

Noens, E.E. (2007) Control of sporulation-specific cell division in *Streptomyces coelicolor*. In *Department of Molecular Cell Biology*. Vol. Ph.D. Leiden: Leiden University.

Noens, E.E., Mersinias, V., Willemse, J., Traag, B.A., Laing, E., Chater, K.F., Smith, C.P., Koerten, H.K., and van Wezel, G.P. (2007) Loss of the controlled localization of growth stage-specific cell-wall synthesis pleiotropically affects developmental gene expression in an *ssgA* mutant of *Streptomyces coelicolor*. *Mol Microbiol* **64**: 1244-1259.

Noirclerc-Savoye, M., Morlot, C., Gerard, P., Vernet, T., and Zapun, A. (2003) Expression and purification of FtsW and RodA from *Streptococcus pneumoniae*, two membrane proteins involved in cell division and cell growth, respectively. *Protein Expr Purif* **30**: 18-25.

Norris, V., den Blaauwen, T., Doi, R.H., Harshey, R.M., Janniere, L., Jimenez-Sanchez, A., Jin, D.J., Levin, P.A., Mileykovskaya, E., Minsky, A., Misevic, G., Ripoll, C., Saier, M., Jr., Skarstad, K., and Thellier, M. (2007) Toward a hyperstructure taxonomy. *Annu Rev Microbiol* **61**: 309-329.

Ogawara, H. (1981) Antibiotic resistance in pathogenic and producing bacteria, with special reference to beta-lactam antibiotics. *Microbiol Rev* **45**: 591-619.

Ohnishi, Y., Ishikawa, J., Hara, H., Suzuki, H., Ikenoya, M., Ikeda, H., Yamashita, A., Hattori, M., and Horinouchi, S. (2008) Genome sequence of the streptomycin-producing microorganism *Streptomyces griseus* IFO 13350. *J Bacteriol* **190**: 4050-4060.

Omura, S., Ikeda, H., Ishikawa, J., Hanamoto, A., Takahashi, C., Shinose, M., Takahashi, Y., Horikawa, H., Nakazawa, H., Osonoe, T., Kikuchi, H., Shiba, T., Sakaki, Y., and Hattori, M. (2001) Genome sequence of an industrial microorganism *Streptomyces avermitilis*: deducing the ability of producing secondary metabolites. *Proc Natl Acad Sci U S A* **98**: 12215-12220.

Osborn, M.J., and Rothfield, L. (2007) Cell shape determination in Escherichia coli. *Curr Opin Microbiol* **10**: 606-610.

Overbeek, R., Fonstein, M., D'Souza, M., Pusch, G.D., and Maltsev, N. (1999) The use of gene clusters to infer functional coupling. *Proc Natl Acad Sci U S A* **96**: 2896-2901.

Paradkar, A., Trefzer, A., Chakraburtty, R., and Stassi, D. (2003) Streptomyces genetics: a genomic perspective. *Crit Rev Biotechnol* **23**: 1-27.

Pastoret, S., Fraipont, C., den Blaauwen, T., Wolf, B., Aarsman, M.E., Piette, A., Thomas, A., Brasseur, R., and Nguyen-Disteche, M. (2004) Functional analysis of the cell division protein FtsW of *Escherichia coli*. *J Bacteriol* **186**: 8370-8379.

Persson, B., and Argos, P. (1994) Prediction of transmembrane segments in proteins utilising multiple sequence alignments. *J Mol Biol* **237**: 182-192.

Pichoff, S., and Lutkenhaus, J. (2002) Unique and overlapping roles for ZipA and FtsA in septal ring assembly in *Escherichia coli*. *Embo J* **21**: 685-693.

Piggot, P.J., and Coote, J.G. (1976) Genetic aspects of bacterial endospore formation. *Bacteriol Rev* **40**: 908-962.

Piggot, P.J., and Hilbert, D.W. (2004) Sporulation of *Bacillus subtilis*. *Curr Opin Microbiol* **7**: 579-586.

Pope, M.K., Green, B.D., and Westpheling, J. (1996) The *bld* mutants of *Streptomyces coelicolor* are defective in the regulation of carbon utilization, morphogenesis and cell--cell signalling. *Mol Microbiol* **19**: 747-756.

Pope, M.K., Green, B., and Westpheling, J. (1998) The *bldB* gene encodes a small protein required for morphogenesis, antibiotic production, and catabolite control in *Streptomyces coelicolor*. *J Bacteriol* **180**: 1556-1562.

Potuckova, L., Kelemen, G.H., Findlay, K.C., Lonetto, M.A., Buttner, M.J., and Kormanec, J. (1995) A new RNA polymerase sigma factor, sigma F, is required for the late stages of morphological differentiation in *Streptomyces* spp. *Mol Microbiol* **17**: 37-48.

Quintana, E.T., Wierzbicka, K., Mackiewicz, P., Osman, A., Fahal, A.H., Hamid, M.E., Zakrzewska-Czerwinska, J., Maldonado, L.A., and Goodfellow, M. (2008) Streptomyces sudanensis sp. nov., a new pathogen isolated from patients with actinomycetoma. *Antonie Van Leeuwenhoek* **93**: 305-313.

Rajagopalan, M., Maloney, E., Dziadek, J., Poplawska, M., Lofton, H., Chauhan, A., and Madiraju, M.V. (2005) Genetic evidence that mycobacterial FtsZ and FtsW proteins interact, and colocalize to the division site in *Mycobacterium smegmatis*. *FEMS Microbiol Lett* **250**: 9-17.

Ramos, A., Honrubia, M.P., Valbuena, N., Vaquera, J., Mateos, L.M., and Gil, J.A. (2003) Involvement of DivIVA in the morphology of the rod-shaped actinomycete *Brevibacterium lactofermentum*. *Microbiology* **149**: 3531-3542.

Ramos, A., Honrubia, M.P., Vega, D., Ayala, J.A., Bouhss, A., Mengin-Lecreulx, D., and Gil, J.A. (2004) Characterization and chromosomal organization of the *murD-murC-ftsQ* region of *Corynebacterium glutamicum* ATCC 13869. *Res Microbiol* **155**: 174-184.

Raskin, D.M., and de Boer, P.A. (1997) The MinE ring: an FtsZ-independent cell structure required for selection of the correct division site in *E. coli*. *Cell* **91**: 685-694.

Raskin, D.M., and de Boer, P.A. (1999) MinDE-dependent pole-to-pole oscillation of division inhibitor MinC in *Escherichia coli*. *J Bacteriol* **181**: 6419-6424.

Rausch, H., and Lehmann, M. (1991) Structural analysis of the actinophage phi C31 attachment site. *Nucleic Acids Res* **19**: 5187-5189.

Real, G., Fay, A., Eldar, A., Pinto, S.M., Henriques, A.O., and Dworkin, J. (2008) Determinants for the subcellular localization and function of a nonessential SEDS protein. *J Bacteriol* **190**: 363-376.

Redenbach, M., Kieser, H.M., Denapaite, D., Eichner, A., Cullum, J., Kinashi, H., and Hopwood, D.A. (1996) A set of ordered cosmids and a detailed genetic and physical map for the 8 Mb *Streptomyces coelicolor* A3(2) chromosome. *Mol Microbiol* **21**: 77-96.

Reynolds, P.E. (1989) Structure, biochemistry and mechanism of action of glycopeptide antibiotics. *Eur J Clin Microbiol Infect Dis* **8**: 943-950.

Rigden, M.D., Baier, C., Ramirez-Arcos, S., Liao, M., Wang, M., and Dillon, J.A. (2008) Identification of the coiled-coil domains of Enterococcus faecalis DivIVA that mediate oligomerization and their importance for biological function. *J Biochem* **144**: 63-76.

Robson, S.A., and King, G.F. (2006) Domain architecture and structure of the bacterial cell division protein DivIB. *Proc Natl Acad Sci U S A* **103**: 6700-6705.

Romberg, L., and Levin, P.A. (2003) Assembly dynamics of the bacterial cell division protein FTSZ: poised at the edge of stability. *Annu Rev Microbiol* **57**: 125-154.

Rothfield, L., Taghbalout, A., and Shih, Y.L. (2005) Spatial control of bacterial division-site placement. *Nat Rev Microbiol* **3**: 959-968.

Ryding, N.J., Kelemen, G.H., Whatling, C.A., Flardh, K., Buttner, M.J., and Chater, K.F. (1998) A developmentally regulated gene encoding a repressor-like protein is essential for sporulation in *Streptomyces coelicolor* A3(2). *Mol Microbiol* **29**: 343-357.

Ryding, N.J., Bibb, M.J., Molle, V., Findlay, K.C., Chater, K.F., and Buttner, M.J. (1999) New sporulation loci in *Streptomyces coelicolor* A3(2). *J Bacteriol* **181**: 5419-5425.

Saitou, N., and Nei, M. (1987) The neighbor-joining method: a new method for reconstructing phylogenetic trees. *Mol Biol Evol* **4**: 406-425.

Sambrook, J., Fritsch, F.E., and Maniatis, T. (1989) *Molecular Cloning: A Laboratory Manual.* Cold Spring Harbor, New York: Cold Spring Harbor Laboratory Press.

San Paolo, S., Huang, J., Cohen, S.N., and Thompson, C.J. (2006) *rag* genes: novel components of the RamR regulon that trigger morphological differentiation in *Streptomyces coelicolor*. *Mol Microbiol* **61**: 1167-1186.

Sanglier, J.J., Haag, H., Huck, T.A., and Fehr, T. (1993a) Novel bioactive compounds from Actinomycetes: a short review (1988-1992). *Res Microbiol* **144**: 633-642.

Sanglier, J.J., Wellington, E.M., Behal, V., Fiedler, H.P., Ellouz Ghorbel, R., Finance, C., Hacene, M., Kamoun, A., Kelly, C., Mercer, D.K., and et al. (1993b) Novel bioactive compounds from actinomycetes. *Res Microbiol* **144**: 661-663.

Sauvage, E., Kerff, F., Terrak, M., Ayala, J.A., and Charlier, P. (2008) The penicillin-binding proteins: structure and role in peptidoglycan biosynthesis. *FEMS Microbiol Rev* **32**: 234-258.

Scheffers, D.J., and Pinho, M.G. (2005) Bacterial cell wall synthesis: new insights from localization studies. *Microbiol Mol Biol Rev* **69**: 585-607.

Schmidt, K.L., Peterson, N.D., Kustusch, R.J., Wissel, M.C., Graham, B., Phillips, G.J., and Weiss, D.S. (2004) A predicted ABC transporter, FtsEX, is needed for cell division in *Escherichia coli*. *J Bacteriol* **186**: 785-793.

Schwedock, J., McCormick, J.R., Angert, E.R., Nodwell, J.R., and Losick, R. (1997) Assembly of the cell division protein FtsZ into ladder-like structures in the aerial hyphae of *Streptomyces coelicolor*. *Mol Microbiol* **25**: 847-858.

Sharp, M.D., and Pogliano, K. (2003) The membrane domain of SpoIIIE is required for membrane fusion during *Bacillus subtilis* sporulation. *J Bacteriol* **185**: 2005-2008.

Shen, Y., Yoon, P., Yu, T.W., Floss, H.G., Hopwood, D., and Moore, B.S. (1999) Ectopic expression of the minimal *whiE* polyketide synthase generates a library of aromatic polyketides of diverse sizes and shapes. *Proc Natl Acad Sci U S A* **96**: 3622-3627.

Shih, Y.L., Le, T., and Rothfield, L. (2003) Division site selection in *Escherichia coli* involves dynamic redistribution of Min proteins within coiled structures that extend between the two cell poles. *Proc Natl Acad Sci U S A* **100**: 7865-7870.

Shih, Y.L., and Rothfield, L. (2006) The bacterial cytoskeleton. *Microbiol Mol Biol Rev* **70**: 729-754.

Sizemore, R.K., Caldwell, J.J., and Kendrick, A.S. (1990) Alternate gram staining technique using a fluorescent lectin. *Appl Environ Microbiol* **56**: 2245-2247.

Soliveri, J., Brown, K.L., Buttner, M.J., and Chater, K.F. (1992) Two promoters for the *whiB* sporulation gene of *Streptomyces coelicolor* A3(2) and their activities in relation to development. *J Bacteriol* **174**: 6215-6220.

Soliveri, J., Vijgenboom, E., Granozzi, C., Plaskitt, K.A., and Chater, K.F. (1993) Functional and evolutionary implications of a survey of various actinomycetes for homologues of two *Streptomyces coelicolor* sporulation genes. *J Gen Microbiol* **139**: 2569-2578.

Sonnhammer, E.L., von Heijne, G., and Krogh, A. (1998) A hidden Markov model for predicting transmembrane helices in protein sequences. *Proc Int Conf Intell Syst Mol Biol* **6**: 175-182.

Spratt, B.G. (1975) Distinct penicillin binding proteins involved in the division, elongation, and shape of *Escherichia coli* K12. *Proc Natl Acad Sci U S A* **72**: 2999-3003.

Stackebrandt, E., Rainey, F.A., and Ward-Rainey, N.L. (1997) Proposal for a New Hierarchic Classification System, *Actinobacteria* classis nov. *Int J Syst Bacteriol* **47**: 479-491.

Stockman, G. (2007) Expression analysis of *bldN*-gene in *Streptomyces levoris* DSM40202. In *Department of Genetics*. Vol. Diploma Kaiserslautern, Germany: Technological University of Kaiserslautern.

Stricker, J., Maddox, P., Salmon, E.D., and Erickson, H.P. (2002) Rapid assembly dynamics of the *Escherichia coli* FtsZ-ring demonstrated by fluorescence recovery after photobleaching. *Proc Natl Acad Sci U S A* **99**: 3171-3175.

Sun, J., Kelemen, G.H., Fernandez-Abalos, J.M., and Bibb, M.J. (1999) Green fluorescent protein as a reporter for spatial and temporal gene expression in *Streptomyces coelicolor* A3(2). *Microbiology* **145**: 2221-2227.

Takano, E., Tao, M., Long, F., Bibb, M.J., Wang, L., Li, W., Buttner, M.J., Bibb, M.J., Deng, Z.X., and Chater, K.F. (2003) A rare leucine codon in *adpA* is implicated in the morphological defect of *bldA* mutants of *Streptomyces coelicolor*. *Mol Microbiol* **50**: 475-486.

Takano, E. (2006) Gamma-butyrolactones: Streptomyces signalling molecules regulating antibiotic production and differentiation. *Curr Opin Microbiol* **9**: 287-294.

Tamaki, S., Matsuzawa, H., and Matsuhashi, M. (1980) Cluster of *mrdA* and *mrdB* genes responsible for the rod shape and mecillinam sensitivity of *Escherichia coli*. *J Bacteriol* **141**: 52-57.

Tamames, J., Gonzalez-Moreno, M., Mingorance, J., Valencia, A., and Vicente, M. (2001) Bringing gene order into bacterial shape. *Trends Genet* **17**: 124-126.

Tamura, K., Dudley, J., Nei, M., and Kumar, S. (2007) MEGA4: Molecular Evolutionary Genetics Analysis (MEGA) software version 4.0. *Mol Biol Evol* **24**: 1596-1599.

Tan, H., Yang, H., Tian, Y., Wu, W., Whatling, C.A., Chamberlin, L.C., Buttner, M.J., Nodwell, J., and Chater, K.F. (1998) The *Streptomyces coelicolor* sporulation-specific sigma WhiG form of RNA polymerase transcribes a gene encoding a ProX-like protein that is dispensable for sporulation. *Gene* **212**: 137-146.

Thanedar, S., and Margolin, W. (2004) FtsZ exhibits rapid movement and oscillation waves in helix-like patterns in *Escherichia coli*. *Curr Biol* **14**: 1167-1173.

Thomaides, H.B., Freeman, M., El Karoui, M., and Errington, J. (2001) Division site selection protein DivIVA of *Bacillus subtilis* has a second distinct function in chromosome segregation during sporulation. *Genes Dev* **15**: 1662-1673.

Thomas, D.P. (2001) Soya induced gene regulation in *Streptomyces lividans*. In *School of Biological Sciences*. Vol. Ph.D. Swansea: University of Wales Swansea.

Thompson, J.D., Higgins, D.G., and Gibson, T.J. (1994) CLUSTAL W: improving the sensitivity of progressive multiple sequence alignment through sequence weighting, position-specific gap penalties and weight matrix choice. *Nucleic Acids Res* **22**: 4673-4680.

Tian, Y., Fowler, K., Findlay, K., Tan, H., and Chater, K.F. (2007) An unusual response regulator influences sporulation at early and late stages in Streptomyces coelicolor. *J Bacteriol* **189**: 2873-2885.

Tillotson, R.D., Wosten, H.A., Richter, M., and Willey, J.M. (1998) A surface active protein involved in aerial hyphae formation in the filamentous fungus *Schizophillum* commune restores the capacity of a bald mutant of the filamentous bacterium *Streptomyces coelicolor* to erect aerial structures. *Mol Microbiol* **30**: 595-602.

Tiyanont, K., Doan, T., Lazarus, M.B., Fang, X., Rudner, D.Z., and Walker, S. (2006) Imaging peptidoglycan biosynthesis in *Bacillus subtilis* with fluorescent antibiotics. *Proc Natl Acad Sci U S A* **103**: 11033-11038.

Tokala, R.K., Strap, J.L., Jung, C.M., Crawford, D.L., Salove, M.H., Deobald, L.A., Bailey, J.F., and Morra, M.J. (2002) Novel plant-microbe rhizosphere interaction involving *Streptomyces lydicus* WYEC108 and the pea plant (Pisum sativum). *Appl Environ Microbiol* **68**: 2161-2171.

Tomii, K., and Kanehisa, M. (1998) A comparative analysis of ABC transporters in complete microbial genomes. *Genome Res* **8**: 1048-1059.

Traag, B.A., Kelemen, G.H., and Van Wezel, G.P. (2004) Transcription of the sporulation gene *ssgA* is activated by the IclR-type regulator SsgR in a whi-independent manner in *Streptomyces coelicolor* A3(2). *Mol Microbiol* **53**: 985-1000.

Trepanier, N.K., Nguyen, G.D., Leedell, P.J., and Leskiw, B.K. (1997) Use of polymerase chain reaction to identify a leucyl tRNA in *Streptomyces coelicolor*. *Gene* **193**: 59-63.

Tusnady, G.E., and Simon, I. (1998) Principles governing amino acid composition of integral membrane proteins: application to topology prediction. *J Mol Biol* **283**: 489-506.

Uchida, K., and Seino, A. (1997) Intra- and intergeneric relationships of various actinomycete strains based on the acyl types of the muramyl residue in cell wall peptidoglycans examined in a glycolate test. *Int J Syst Bacteriol* **47**: 182-190.

Ueda, K., Miyake, K., Horinouchi, S., and Beppu, T. (1993) A gene cluster involved in aerial mycelium formation in *Streptomyces griseus* encodes proteins similar to the response regulators of two-component regulatory systems and membrane translocators. *J Bacteriol* **175**: 2006-2016.

Valbuena, N., Letek, M., Ordonez, E., Ayala, J., Daniel, R.A., Gil, J.A., and Mateos, L.M. (2007) Characterization of HMW-PBPs from the rod-shaped actinomycete *Corynebacterium glutamicum*: peptidoglycan synthesis in cells lacking actin-like cytoskeletal structures. *Mol Microbiol* **66**: 643-657.

van den Ent, F., Amos, L.A., and Lowe, J. (2001) Prokaryotic origin of the actin cytoskeleton. *Nature* **413**: 39-44.

van den Ent, F., Vinkenvleugel, T.M., Ind, A., West, P., Veprintsev, D., Nanninga, N., den Blaauwen, T., and Lowe, J. (2008) Structural and mutational analysis of the cell division protein FtsQ. *Mol Microbiol* **68**: 110-123.

van Wezel, G.P., van der Meulen, J., Kawamoto, S., Luiten, R.G., Koerten, H.K., and Kraal, B. (2000a) *ssgA* is essential for sporulation of *Streptomyces coelicolor* A3(2) and affects hyphal development by stimulating septum formation. *J Bacteriol* **182**: 5653-5662.

van Wezel, G.P., van der Meulen, J., Taal, E., Koerten, H., and Kraal, B. (2000b) Effects of increased and deregulated expression of cell division genes on the morphology and on antibiotic production of streptomycetes. *Antonie Van Leeuwenhoek* **78**: 269-276.

van Wezel, G.P., and Vijgenboom, E. (2004) Novel aspects of signaling in *Streptomyces* development. *Adv Appl Microbiol* **56**: 65-88.

Varley, A.W., and Stewart, G.C. (1992) The *divIVB* region of the *Bacillus subtilis* chromosome encodes homologs of *Escherichia coli* septum placement *(minCD)* and cell shape *(mreBCD)* determinants. *J Bacteriol* **174**: 6729-6742.

Ventura, M., Canchaya, C., Tauch, A., Chandra, G., Fitzgerald, G.F., Chater, K.F., and van Sinderen, D. (2007) Genomics of Actinobacteria: tracing the evolutionary history of an ancient phylum. *Microbiol Mol Biol Rev* **71**: 495-548.

Vicente, M., and Errington, J. (1996) Structure, function and controls in microbial division. *Mol Microbiol* **20**: 1-7.

Vicente, M., Gomez, M.J., and Ayala, J.A. (1998) Regulation of transcription of cell division genes in the *Escherichia coli* dcw cluster. *Cell Mol Life Sci* **54**: 317-324.

Vicente, M., and Rico, A.I. (2006) The order of the ring: assembly of *Escherichia coli* cell division components. *Mol Microbiol* **61**: 5-8.

Vicente, M., Rico, A.I., Martinez-Arteaga, R., and Mingorance, J. (2006) Septum enlightenment: assembly of bacterial division proteins. *J Bacteriol* **188**: 19-27.

Volff, J.N., and Altenbuchner, J. (1998) Genetic instability of the *Streptomyces* chromosome. *Mol Microbiol* **27**: 239-246.

von Heijne, G. (1989) Control of topology and mode of assembly of a polytopic membrane protein by positively charged residues. *Nature* **341**: 456-458.

Vujaklija, D., Ueda, K., Hong, S.K., Beppu, T., and Horinouchi, S. (1991) Identification of an A-factor-dependent promoter in the streptomycin biosynthetic gene cluster of *Streptomyces griseus*. *Mol Gen Genet* **229**: 119-128.

Wachi, M., Doi, M., Tamaki, S., Park, W., Nakajima-Iijima, S., and Matsuhashi, M. (1987) Mutant isolation and molecular cloning of *mre* genes, which determine cell shape, sensitivity to mecillinam, and amount of penicillin-binding proteins in *Escherichia coli*. *J Bacteriol* **169**: 4935-4940.

Wachi, M., Doi, M., Okada, Y., and Matsuhashi, M. (1989) New *mre* genes *mreC* and *mreD*, responsible for formation of the rod shape of *Escherichia coli* cells. *J Bacteriol* **171**: 6511-6516.

Wadsworth, K.D., Rowland, S.L., Harry, E.J., and King, G.F. (2008) The divisomal protein DivIB contains multiple epitopes that mediate its recruitment to incipient division sites. *Mol Microbiol* **67**: 1143-1155.

Waksman, S.A., and Henrici, A.T. (1943) The nomenclature and classification of the actinomycetes. *J Bacteriol* **46**: 337-341.

Wang, L., Khattar, M.K., Donachie, W.D., and Lutkenhaus, J. (1998) FtsI and FtsW are localized to the septum in *Escherichia coli*. *J Bacteriol* **180**: 2810-2816.

Wang, L., Yu, Y., He, X., Zhou, X., Deng, Z., Chater, K.F., and Tao, M. (2007) Role of an FtsK-like protein in genetic stability in *Streptomyces coelicolor* A3(2). *J Bacteriol* **189**: 2310-2318.

Wang, S.J., Chang, H.M., Lin, Y.S., Huang, C.H., and Chen, C.W. (1999) *Streptomyces* genomes: circular genetic maps from the linear chromosomes. *Microbiology* **145**: 2209-2220.

Watve, M.G., Tickoo, R., Jog, M.M., and Bhole, B.D. (2001) How many antibiotics are produced by the genus *Streptomyces*? *Arch Microbiol* **176**: 386-390.

Weiss, D.S., Chen, J.C., Ghigo, J.M., Boyd, D., and Beckwith, J. (1999) Localization of FtsI (PBP3) to the septal ring requires its membrane anchor, the Z ring, FtsA, FtsQ, and FtsL. *J Bacteriol* **181**: 508-520.

Weiss, D.S. (2004) Bacterial cell division and the septal ring. *Mol Microbiol* **54**: 588-597.

White, J., and Bibb, M. (1997) *bldA* dependence of undecylprodigiosin production in *Streptomyces coelicolor* A3(2) involves a pathway-specific regulatory cascade. *J Bacteriol* **179**: 627-633.

Wildermuth, H., Wehrli, E., and Horne, R.W. (1971) The surface structure of spores and aerial mycelium in *Streptomyces coelicolor*. *J Ultrastruct Res* **35**: 168-180.

Willey, J., Santamaria, R., Guijarro, J., Geistlich, M., and Losick, R. (1991) Extracellular complementation of a developmental mutation implicates a small sporulation protein in aerial mycelium formation by *S. coelicolor*. *Cell* **65**: 641-650.

Willey, J., Schwedock, J., and Losick, R. (1993) Multiple extracellular signals govern the production of a morphogenetic protein involved in aerial mycelium formation by *Streptomyces coelicolor*. *Genes Dev* **7**: 895-903.

Willey, J.M., Willems, A., Kodani, S., and Nodwell, J.R. (2006) Morphogenetic surfactants and their role in the formation of aerial hyphae in *Streptomyces coelicolor*. *Mol Microbiol* **59**: 731-742.

Williams, R.R., Goodfellow, M., Alderson, G., Wellington, E.M.H., Sheath, P.H.A., Sackin, M.J., and Mortimer, A.M. (1983) Numerical classification of *Streptomyces* and related genera. *J Gen Microbiol* **129**: 1743-1813.

Woldringh, C.L., Mulder, E., Huls, P.G., and Vischer, N. (1991) Toporegulation of bacterial division according to the nucleoid occlusion model. *Res Microbiol* **142**: 309-320.

Wosten, H.A., Richter, M., and Willey, J.M. (1999) Structural proteins involved in emergence of microbial aerial hyphae. *Fungal Genet Biol* **27**: 153-160.

Wu, L.J., and Errington, J. (1997) Septal localization of the SpoIIIE chromosome partitioning protein in *Bacillus subtilis*. *Embo J* **16**: 2161-2169.

Wu, L.J., and Errington, J. (2004) Coordination of cell division and chromosome segregation by a nucleoid occlusion protein in *Bacillus subtilis*. *Cell* **117**: 915-925.

Yamazaki, H., Ohnishi, Y., and Horinouchi, S. (2003a) Transcriptional switch on of *ssgA* by A-factor, which is essential for spore septum formation in *Streptomyces griseus*. *J Bacteriol* **185**: 1273-1283.

Yamazaki, H., Takano, Y., Ohnishi, Y., and Horinouchi, S. (2003b) *amfR*, an essential gene for aerial mycelium formation, is a member of the AdpA regulon in the A-factor regulatory cascade in *Streptomyces griseus*. *Mol Microbiol* **50**: 1173-1187.

Yan, K., Pearce, K.H., and Payne, D.J. (2000) A conserved residue at the extreme C-terminus of FtsZ is critical for the FtsA-FtsZ interaction in *Staphylococcus aureus*. *Biochem Biophys Res Commun* **270**: 387-392.

Yan, K., Sossong, T.M., and Payne, D.J. (2001) Regions of FtsZ important for self-interaction in *Staphylococcus aureus*. *Biochem Biophys Res Commun* **284**: 515-518.

Yang, M.C., and Losick, R. (2001) Cytological evidence for association of the ends of the linear chromosome in *Streptomyces coelicolor*. *J Bacteriol* **183**: 5180-5186.

Zhang, X., Clark, C.A., and Pettis, G.S. (2003) Interstrain inhibition in the sweet potato pathogen *Streptomyces ipomoeae*: purification and characterization of a highly specific bacteriocin and cloning of its structural gene. *Appl Environ Microbiol* **69**: 2201-2208.

Publication

Mistry, B.V., Del Sol, R., Wright, C., Findlay, K., and Dyson, P. (2008) FtsW is a dispensable cell division protein required for Z-ring stabilization during sporulation septation in *Streptomyces coelicolor*. *J Bacteriol* **190**: 5555-5566.